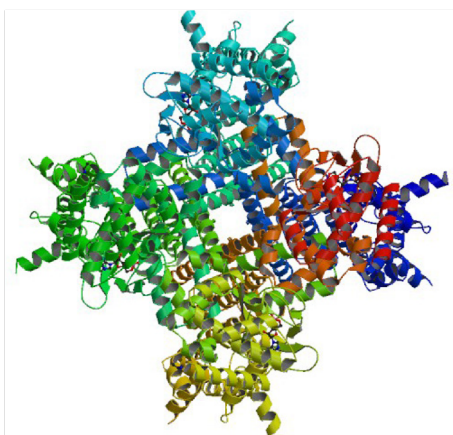# Weill Cornell Medicine
Anesthesiology

14th Annual
Research Exposition

Thursday
November 21, 2019

Oral Presentations
3:00–3:45 pm in M309

Special Research Seminar
4:00-4:30 pm in M309

Reception
4:30-5:00 pm outside P300

Poster Presentations
5:00-6:00 pm in P300

3:00-3:45 pm
Oral Presentations

"HCN1 channels as targets for treating neuropathic pain; where are we and how did we get here?"

Peter Goldstein, MD
Professor of Anesthesiology
Associate Professor of Medical Ethics in Medicine
Professor of Anesthesiology in Neuroscience
Weill Cornell Medicine

"Use of novel imaging techniques and hemodynamic parameters to predict outcomes in cardiac surgery."

Lisa Qia Rong, MD
Assistant Professor of Clinical Anesthesiology
Cardiothoracic Division
Weill Cornell Medicine

4:00-4:30 pm
Special Research Seminar

"ERAS and the Opioid Crisis"

Christopher L. Wu, MD
Attending Anesthesiologist, Department of
  Anesthesiology, Critical Care & Pain Management
Hospital for Special Surgery
Director of Clinical Research
Clinical Professor of Anesthesiology
Weill Cornell Medicine

Department of Anesthesiology • 525 East 68th Street, P3
For more information contact: **Michele Steinkamp, RN**
212-746-2953 or mls9004@med.cornell.edu

WELCOME TO THE 14TH ANESTHESIOLOGY RESEARCH EXPOSITION
November 21st 2019

Oral Presentations

"HCN1 Channels as Targets for Treating Neuropathic Pain; Where are we and how did we get here?"

Peter Goldstein, MD
Professor of Anesthesiology
Associate Professor Medical Ethics in Medicine
Professor of Anesthesiology in Neuroscience
Weill Cornell Medicine

"Use of Novel Imaging Techniques and Hemodynamic Parameters to Predict Outcomes in Cardiac Surgery"

Lisa Qia Rong, MD
Assistant Professor Clinical Anesthesiology
Cardiothoracic Division
Weill Cornell Medicine

3:00- 3:45pm, M309

Special Research Seminar

"ERAS and the Opioid Crisis"
Christopher L. Wu, MD
Attending Anesthesiologist, Department of Anesthesiology, Critical Care & Pain Management
Hospital for Special Surgery
Directory of Clinical Research
Clinical Professor of Anesthesiology
Weill Cornell Medicine

4:00pm – 4:30pm, M309

Reception
4:30pm – 5:00pm
Outside P300

Poster Presentations
5:00pm – 6:00pm
P300

Table of Contents

Department of Anesthesiology Research Divisions

Hugh C. Hemmings, Jr, MD, PhD, FRCA
Senior Associate Dean of Research
Joseph F. Artusio Professor
Chair of Anesthesiology

Kane O. Pryor, MD
Vice Chair for Academic Affairs
Director of Clinical Research
Director of Education

Zachary A. Turnbull, MD, MBA, MS
Director of the Center for Perioperative Outcomes
Medical Director of Performance Improvement

Anesthesiology Clinical Research

Kane O. Pryor, MD	Michele Steinkamp, RN
Jade Basem, BA	Alexandra Lopes, BA
Alexandra Hohmann, BS	Christina Rao, BA
Samantha Huynh, BS	Kaitlyn Sbrollini, BS
Anita Jegarl, BS	Andrew Virgile, BA

Center for Perioperative Outcomes

Zachary A. Turnbull, MD, MBA, MS

Silis Jiang, PhD	Kane O. Pryor, MD
Lauren Buck, BA	Robert White, MD, MS
Victoria Jimenez, BS	Virginia Tangel, MA
Briana Lui, BS	Samson Obembe, BS
Melissa Sanchez, BS	Andre Volel, BS

High-Speed Atomic Force Microscopy Laboratory

Simon Scheuring, PhD

James Goodchild, PhD	Grigory Tagiltsev, *Specialist*
Motonori Imamura, PhD	Nebojsa Jukic, MS
Yi-Chih Lin, PhD	Yining Jiang, BA
Tina Matin, PhD	Raghavendar Gari, PhD
Atsushi Miyagi, PhD	Viktor Belay, BS
Alma Perez Perrino, PhD	Vishnu Ghani, BS
Raghu Sanganna Gari, PhD	

Neuromuscular Relaxant Research

John Savarese, MD

Laboratory of Molecular Anesthesiology

Hugh C. Hemmings, Jr, MD, PhD, FRCA

Karl Herold, MD, PhD	Vanessa Osman, BS
Jimcy Platholi, PhD	Kishan Patel, BS
Iris Speigel, PhD	Riley Williams, BS
Bela Zimmer, PhD	

CV Starr Laboratory for Molecular NeuroPharmacology

Latrice Goss, BS	Quetanya Brown, BS

Alessio Accardi, Ph.D.

Maria Falzone, BA	Eva Verdejo, MS

Diany Paola Calderon, MD, PhD

Md Safiqul Islam, PhD	Jasmine Gamboa, BA
Sijia Gao, MS	

Peter A. Goldstein, MD

Kelly Aromolaran, PhD	Gareth Tibbs, PhD

Crina Nimigean, PhD

Chen Fan, PhD	Philipp Schmidpeter, PhD
Xiaolong Gao, PhD	Nattakan Sukomon, PhD
Elizabeth Kim, PhD	

Paul Riegelhaupt, PhD

Aboubacar Wague, BS

Department of Anesthesiology Research Devisions

General Clinical Research
Noemi Balogh, MD
Farida Gadalla, MD
Peter Goldstein, MD
Marcus Gutzler, MD
Shreyajit Kumar, MD
Christine Lennon, MD
Jaideep Malhotra, MD
Vinod Malhotra, MD
Danielle McCullough, MD
Matthew Murrell, MD, PhD

Nathan Painter, MD
Rohan Panchamia, MD
Anup Pamnani, MD
Kane Pryor, MD
Lori Rubin, MD
Seyed A. Safavynia, MD, PhD
Mahendra Samaru, MD
Jon Samuels, MD
Jacques Scharoun, MD
Kevin Walsh, MD

Cardiac Clinical Research
Daryl Banton, MD
June Chan, MD
Meghann Fitzgerald, MD
Shanna Sykes Hill, MD
Natalia Ivascu, MD
Adam D. Lichtman, MD
Bessie Kachulis, MD
Diana Khatib, MD

Shreyajit Kumar, MD
James Littlejohn, MD, PhD
James Osorio, MD
Lisa Q. Rong, MD
Liang Shen, MD
Irene Stadnyk, MD
Christopher Tam, MD
Fun-Sun Yao, MD

Global Health Research
Gunisha Kaur, MD, MA
Eric D. Brumberger, MD
Sheida Tabaie, MD
Roniel Weinberg, MD
Sonny Sabhlok, MD

Andrew Milewski, PhD
Alessandra Weidman, MPH
Kevin Ackerman, BS
Anna Cai, BS
Samantha Huynh, BS

Obstetrics/Gynecological Clinical Research
Jamie Aaronson, MD
Sharon Abramovitz, MD
Alaeldin Darwich, MD
Farida Gadalla, MD, ChB
Klaus Kjaer, MD, MBA

Jennifer Wagner, MD
Roniel Weinberg, MD
Jill Fong, MD
Robert White, MD, MS
Laura Burey, MD

Pain Clinical Research
Neel Mehta, MD
Shakil Ahmed, MD
Elena Christ, MD
Amitabh Gulati, MD
Jatin Joshi, MD

Mohammad Piracha, MD
Sadiah Siddiqui, MD
Mary So, MD
Abhilasha Solanki, MD
Lisa R. Witkin, MD

Regional Anesthesia Clinical Research
Tiffany Tedore, MD
Michael Akerman, MD
Eric D. Brumberger, MD
Ryan Lippell, MD

Milica Markovic, MD
Roniel Weinberg, MD
Hannah Liu, MD

Pediatrics Clinical Research
Aarti Sharma, MD
Veronica Carullo, MD
Jennifer Lee, MD
Yang Long, MD

Jasmine Patel, MD
Jayanth Swathirajan, MD
Casey Chai, MD

Department of Healthcare Policy & Research Division of Biostatistics and Epidemiology
Paul Christos, DrPH, MS
Linda Gerber, PhD
Imaani Easthausen, MS

Elizabeth Mauer, MS
Xiaoyue Ma, MS

P-03 Poster Map

Center for Perioperative Outcomes
Current Studies Wall

Clinical Research Upcoming Studies

Clinical Research Completed Studies

Clinical Research
Current Studies

P-03-300 Conference Room
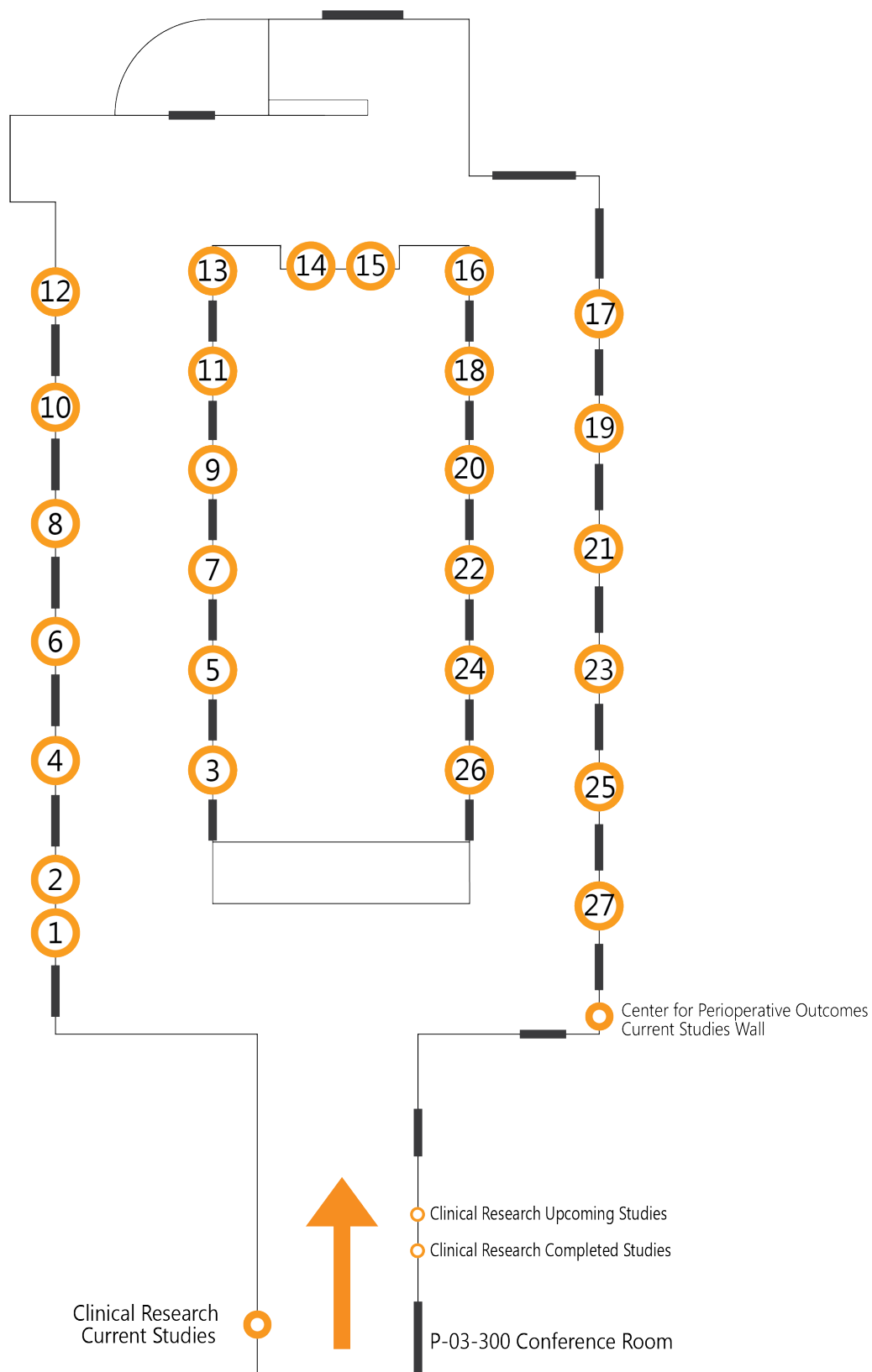
P-03 Poster Map Key

1. **Anaesthetic Depth and Complications After Major Surgery: An International, Randomised Controlled Trial**
   Timothy Short MD, Douglas Campbel BM, Christopher Frampton PhD, et al.
   WCM Investigators: Kane Pryor MD, Michele Steinkamp RN, Farrell Cooke BS, Rachel Friedlander BS, Jaideep Malhotra MD, Lori A. Rubin MD

2. **Protective Intraoperative Ventilation with Higher versus Lower Levels of Positive End-Expiratory Pressure in Obese Patients (PROBESE)**
   Lead author: Thomas Bluth MD for the PROBESE Writing Committee
   WCM co-authors: Peter A. Goldstein MD, Zachary A. Turnbull MD
   WCM co-investigators: Jon D. Samuels MD, Farida Gadalla MD, Matthew T. Murrell MD PhD, Farrell E. Cooke BS, Michele L. Steinkamp RN, Cheguevara Afaneh MD, Gregory F. Dakin MD, Kelly A. Garrett MD, Alfons Pomp MD, Douglas S. Scherr MD

3. **Chronic Pain in Refugee Torture Survivors**
   Gunisha Kaur MD MA, Roniel Weinberg MD, Andrew Milewski PhD, Samantha Huynh BS, Elizabeth Mauer MS, Hugh Hemmings MD PhD, Kane Pryor MD

4. **Characteristics and Anatomic Distribution of Early vs. Late Stroke After Cardiac Surgery**
   Natalia S. Ivascu MD, Faiza M. Khan MD, Mohammed Rahouma MD, Irbaz Hameed MD, Ahmed Abouarab MD, Alan Z. Segal MD, Mario F. L. Gaudino, Leonard N. Girardi MD

5. **Medical Mission Location as Compared to Country Need: A Systematic Review**
   Keerteshwrya Mishra BS, Sonal Jessel MPH, Jacob Lurie MPH, Kane O. Pryor MD, Gunisha Kaur MD MA

6. **Female genital mutilation/cutting: a systematic review and meta-analysis of somatic pain and obstetric sequelae**
   Jacob Lurie MPH, Alessandra Weidman MPH, Samantha Huynh BS, Diana Delgado MLS, Imaani Easthausen, MS, Gunisha Kaur MD MA

7. **Application of Mastery Learning Principles to Anesthesiology Intern Intubation Training**
   Liang Shen MD MPH, Lori Rubin MD, Eric Brumberger MD, Kane Pryor MD

8. **Echocardiographic Predictors of Intraoperative Right Ventricular Dysfunction: A 2D and Speckle Tracking Echocardiography Study**
   Lisa Q. Rong MD, Brian Yum MD, Christiane Abouzeid MD, Maria Chiara Palumbo MS, Jonathan W. Weinsaft MD, Jiwon Kim MD

9. **Can echo-derived cardiac output replace pulmonary artery catheter derived cardiac output in cardiac surgery?**
   Lisa Q. Rong,, Gabriel Arguelles, Elizabeth Mauer, Lillye Anderson, Kane O. Pryor

10. **Female Authorship in Anesthesiology in 2008 – 2018: A Bibliometric Study**
    Lisa Q. Rong, Lillye P. Anderson, Mohamed M. Rahouma, Samantha Huynh, Jacqueline Emerson, Faiza Khan, Kane O. Pryor, Mario Gaudino

11. **Three-dimensional echocardiography for transcatheter aortic valve replacement – A systematic review and meta-analysis**
    Lisa Q. Rong MD, Irbaz Hameed MD, Arash Salemi MD, Mohamed Rahouma MD, Faiza M. Khan MD, Linda Shore-Lesserson MD, Mario Gaudino MD

12. **Use of Auricular Acupuncture for Intraoperative Sedation in a Patient with Multiple Medication Sensitivities**
    Deirdre C. Kelleher MD & Stephanie I. Cheng MD

13. **Lessons learned from Pediatric Difficult Intubation Cases: A Single Institution Experience**
    Casey Chai MD, Jimmy Lin MD, Hannah Oden-Brunson BA, Aarti Sharma MD

14. **ESCRT-III Assembles Simultaneously and Without Preference on Supported Lipid Bilayers of**

M Corridor Poster Map

13

12

M312 Clinical Research

11

10

9

8

M309 Conference Room

7

6

5

4

M304 Education Suite

3

2

1

M Corridor Poster Map Key

1. **Determining the Contribution of Ryanodine Receptors to Action Potentialdriven Calcium Efflux from the Endoplasmic Reticulum in Cortical Neurons**
   Daniel Cook, Ryan Farrell, Timothy Ryan

2. **Anesthestics-Induced Burst Suppression Unconvers Rapid Widespread Alterations in Network Excitability Cuased By An Acute Seizure Focus**
   Jyun-you Liou, Eliza Baird-Daniel, Mingrui Zhao, Andy Daniel, Catherine A Svhevon, Hongtao Ma, Theodore H Schwartz

3. **Force-Induced Conformational Changes In PIEZO1**
   Yi-Chih Lin, Yusong R Guo, Atsushi Miyagi, Jesper Levring, Roderick MacKinnon, and Simon Scheuring

4. **The Effect of Isoflurane on Axonal Endoplasmic Reticulum Ca^{2+} Dynamics in Hippocampal Neurons**
   Vanessa Osman and Hugh C. Hemmings Jr. MD PhD

5. **Optical measurements of anesthetic action on GABA exocytosis**
   I.A. Seigel, H.C. Hemmings JR.

6. **Reduced brain-derived neurotrophic factor signaling exacerbates synaptic dysfunction following isoflurane exposure**
   KW Johnson, RA Williams, FS Lee, HC Hemmings Jr., J Platholi

7. **Lipid-modulation of SthK, a cylic nucleotide-gated channel**
   Philipp AM Schmidpeter, Di Wu, Jan Rheinberger, Haiping Tang, Carol V. Robinson, Crina M. Nimigean

8. **ESCRT-III spirals are loaded springs that govern spontaneous membrane deformation**
   Alma P. Perrino, Nebojsa Jukic, Simon Scheuring

9. **Native-state prolyl isomerization regulates activation kinetics of a CNH channel**
   Philipp AM Schmidpeter, Crina M. Nimigean

10. **Cortical features predict movement dynamics during emergence from anesthesia**
    Sijia Gao, Vikram Krishnamurthy, Diany Paola Calderon

11. **Milisecond time resolution of GltPh dynamics by HS-AFM line scanning**
    Tina R. Matin, George R. Heath, Gerard Huysmans, Olga Boudker, Simon Scheuring

12. **Backbone amides are conserved determinants of inter-anion selectivity in CLCs**
    Eva Fortea, Lilia Leisle, Kin Lam, Tao Jiang, Alessandra Picollo, Jason D. Galpin, Emad Tajkhorshid, Christopher A. Ahern & Alessio Accardi

13. **Structural basis of lipid and ion transport by TMEM16 scramblases**
    Maria Falzone, George Khelashvili, Xiaolu Cheng, Byoung-Cheol Lee, Jan Rheinberger, Ashleigh Raczkowski, Edward Eng, Crina Nimigean, Harel Weinstein, Alessio Accardi

American Pain Society (APS)

1. Drug Toxicology Screening in Cancer Pain
   Dustin Liebling MD, Neel Mehta MD, Ruth Eisenberg MS, Amitabh Gulati MD

American Society of Anesthesiologists (ASA)

1. Black Race As A Social Determinant Of Health And Outcomes After Lumbar Spinal Fusion Surgery: A Multistate Analysis, 2007 - 2014
   Dima El Halawani Aladdin MD, Virginia Tangel MA, Briana Lui BS, Lisa R. Witkin MD, Kane O. Pryor MD, Robert S. White MD MS

2. Use of Auricular Acupuncture for Intraoperative Sedation in a Patient with Multiple Medication Sensitivities
   Deirdre C. Kelleher MD & Stephanie I. Cheng MD

3. Can echo-derived cardiac output replace pulmonary artery catheter derived cardiac output in cardiac surgery?
   Lisa Q. Rong MD, Gabriel Arguelles BA, Elizabeth Mauer MS, Lillye Anderson BA, Kane O. Pryor MD

4. Female Authorship in Anesthesiology in 2008 – 2018: A Bibliometric Study
   Lisa Q. Rong MD, Lillye P. Anderson BA, Mohamed M. Rahouma MD, Samantha Huynh BA, Jacqueline Emerson BA, Faiza Khan MD, Kane O. Pryor MD, Mario Gaudino MD

5. Use of Pulmonary Artery Pulsatility Index in Cardiac Surgery
   Lisa Q. Rong MD, Mohamed M. Rahouma MD, Peter J. Neuburger MD, Gabriel Arguelles BA, Jacqueline Emerson BS, Elizabeth Mauer MS, Linda Shore-Lesserson MD, Kane O. Pryor MD, Mario Gaudino MD

6. In Monkeys, Recovery Time Remains Constant Following Bolus Doses of 1-10x ED95 or Infusions of Up To 3 Hours in Length of Both the Ultra-short Acting NMBA CW 1759-50 and the Intermediate-Acting Compound CW 002
   John J. Savarese MD, Hiroshi Sunaga MD, Jeff D. McGilvra PhD, Anita Jegarl BS, Paul M Heerdt MD PhD

7. Validity of Population-Based Comorbidity Adjustment Scores in Estimating In-Hospital Mortality in Individual Subgroups of Race/Ethnicity
   Virginia Tangel MA, Dima El Halawani Aladdin MD, Kane O. Pryor MD, Robert S. White MD MS

8. Long-term mortality, hospital length of stay, and discharge disposition in patients classified as American Society of Anesthesiology Physical Status 5 or 5E
   Zachary A. Turnbull MD MBA/MS, Virginia Tangel MA, Matthew Alexander BS, Peter A. Goldstein MD
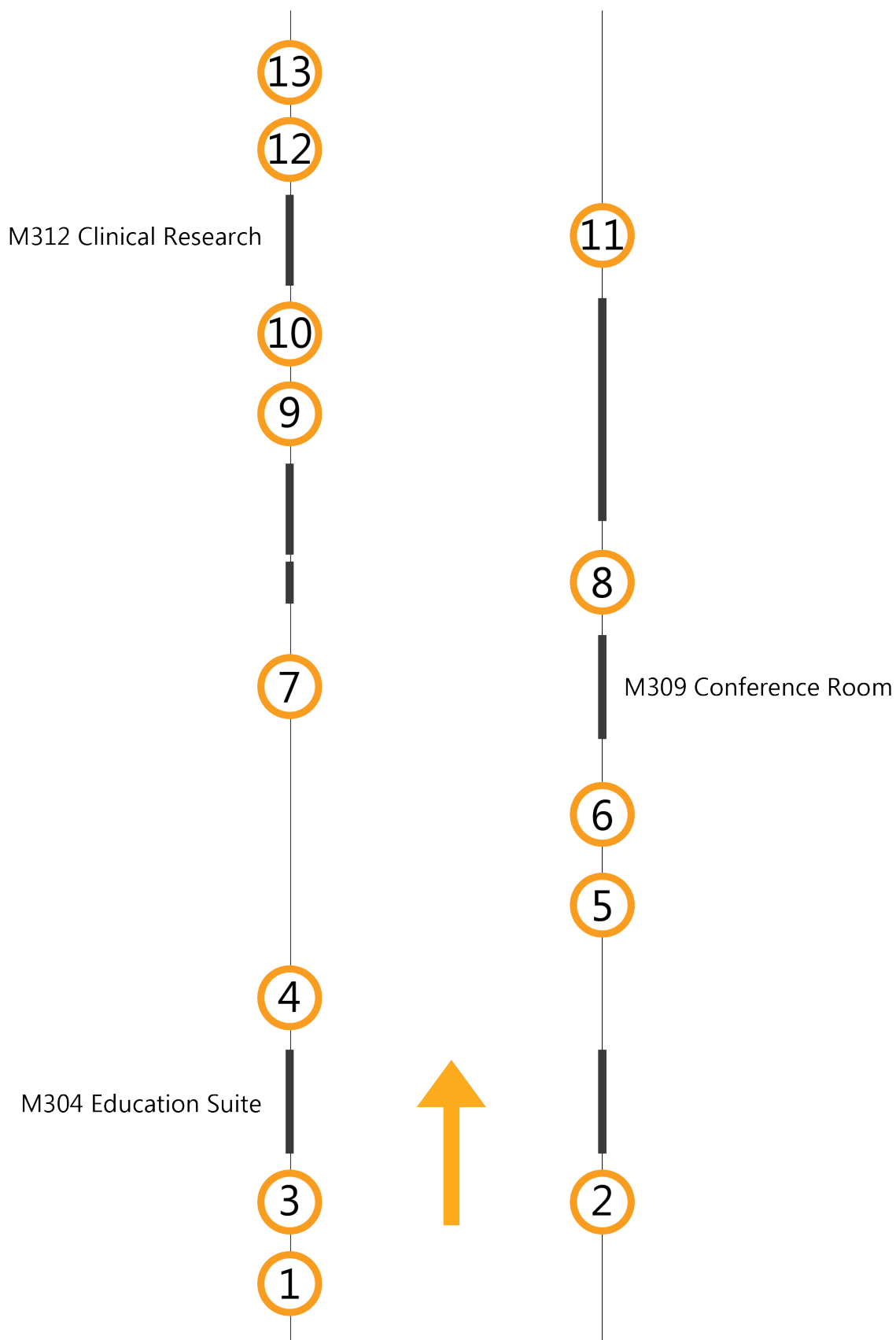
9. Hospital safety-net burden is associated with increased inpatient mortality and postoperative complications after colectomy
   Wendy Wang PhD, Robert S. White MD MS, Virginia Tangel MA, Anna S. Nachamie MBA, Kane O. Pryor MB BS

10. The Association of Race with Utilization of Antiemetic Prophylaxis in the Multicenter Perioperative Outcomes Group (MPOG)
    Robert S. White MD MS, Michael H. Andreae MD, Xiaoyue Ma MS, Zachary A. Turnbull MD, Anna S. Nachamie BS, Julia M. Rosenbloom MD, Kane O. Pryor MD

American Society of Regional Anesthesia (ASRA)

1. Preexisting Opioid Use Disorder and Postoperative Outcomes After Appendectomy or Cholecystectomy: A Multi-State Analysis, 2007-2014
   Alina Boltunova MD, Robert S. White MD, Selaiman Noori MD, Stephanie A. Chen BA, Licia K. Gaber-Baylis BA, Roniel Weinberg MD

2. **Hospital Safety Net Burden Is Associated with Increased Inpatient Mortality and Postoperative Morbidity after Total Hip Arthroplasty: A Retrospective Multistate Review, 2007-2014**
   Melvin La MD, Virginia Tangel MA, Soham Gupta BA, Tiffany R. Tedore MD, and Robert S. White MD MS

3. **Ultrasound-Guided Caudal Epidural Steroid Injection for Successful Treatment of Radiculopathy During Pregnancy**
   Danielle Nadav MD, Timothy M. Connolly MD, Mohammad Piracha MD, Semih Gungor MD

European Society for Paediatric Anaesthesiology (ESPA)
1. **Lessons learned from Pediatric Difficult Intubation Cases: A Single Institution Experience**
   Casey Chai MD, Jimmy Lin MD, Hannah Oden-Brunson BA, Aarti Sharma MD

International Anesthesia Research Society (IARS)
1. **One lung ventilation in a pediatric patient in a resource limited setting in Rwanda**
   Harmandeep Singh MD, Zachary Adam Turnbull MD, Eric Brumberger MD and Stephanie Vecino MD

2. **Studies of the New Neuromuscular Blocking Agent CW 1759-50 in the Cat, as in Monkeys, Predict Short-to Ultra-short Duration in Humans, Reflecting Rapid Degradation by L-Cysteine Adduction in Vitro**
   John J. Savarese MD, Hiroshi Sunaga MD, Jeff D. McGilvra PhD, Paul M Heerdt MD PhD, Anita Jegarl BS, Farrell E Cooke BS, Stewart McCallum MD, and Randy Mack MS

New York Academy of Medicine (NYAM)
1. **The Non-Intubatable Pediatric Patient**
   Angelica M. Delgado MD & Jennifer K. Lee MD

2. **Enhanced Recovery After Surgery For Cesarean Delivery: Standardizing Protocols And Reducing Variability**
   Rohan Jotwani MD MBA. Ojas Mainkar MD, Lisa Lee MD, Justin Chung MD, Kathy Matthews MD, Robin Kalish MD, Sharon Abramovitz MD

3. **The Weekend Add-Ons Quality Improvement Initiative**
   Olga Rozental MD PhD, Joel Ehrenfeld MD DPT, Margo Hoyler MD, Michael Kim MD, Jyun-You Liou MD PhD, Vanessa Ng MD, Patricia Fogarty Mack MD, Rohan Panchamia MD

4. **Improving Adherence to a PONV Prevention Protocol**
   Javier Sanchez MD, Jimmy Lin MD, Camille Roberts MD, Maria Quincy MD, Jolie Shosfy MD, Patricia Fogarty Mack MD, Douglas Carras MD

New York Simulation Center for the Health Sciences (NYSIM)
1. **Application of Mastery Learning Principles to Anesthesiology Intern Intubation Training**
   Liang Shen MD MPH, Lori Rubin MD, Eric Brumberger MD, Kane Pryor MD

New York State Conference for Anesthesiology Residents and Fellows (NYSCARF)
1. **Correcting Arterial Hypotension with a Beta-Blocker: A Case Report**
   Larry Wineland MD, Gregory Fischer MD GASA, Alexis Lewis MD

PostGraduate Assembly in Anesthesiology (PGA)
1. **The Effect of Obstructive Sleep Apnea on Readmissions and Atrial Fibrillation after Cardiac Surgery**
   T. Robert Feng MD, Robert S. White MD, Gulce Askin MPH, Kane Pryor MD

2. **Perioperative Outcomes for Liver Transplant or Hepatectomy Based on Race, Insurance Status, and Socioeconomic Status**
   John E. Rubin MD, Iris Chu MD, Robert S. White MD, Gulce Askin MPH, Zachary A. Turnbull MD, Christine M. Lennon MD

Society of Cardiovascular Anesthesiologists (SCA)

1. **Anesthetic Management Of A Parturient With Repaired Anomalous Left Coronary Artery From The Pulmonary Artery After Takeuchi Procedure**
   Cindy Cheung MD, Danielle McCullough MD, Robert White MD, Farida Gadalla MD

2. **Anesthetic Management of Congenital Long QT Syndrome in Labor and Delivery**
   Meghan Daly MD, Robert White MD, Danielle McCullough MD

3. **Insurance Status and Socioeconomic Markers Affect Readmission Rates after Cardiac Valve Surgery**
   T. Robert Feng MD, Marguerite M. Hoyler MD, Xiaoyue Ma MS, Robert S. White MD MS

4. **Mitral Stenosis In The Parturient**
   Jenessa K. Job MD, Sharon Abramovitz MD, Robert White MD, Nathan Liu MD

5. **Reporting the First Transcatheter Tricuspid Valve in Valve for Severe Bioprosthetic Tricuspid Stenosis in a Pregnant Woman**
   Mudit Kaushal MD, Shanna Hill MD

6. **Pulsus Bisferiens in a Patient with a Contained Rupture of a Thoracoabdominal Aortic Aneurysm**
   Christina Lee MD, John E. Rubin MD, June M. Chan MBBS FANZCA, Adam D. Lichtman MD FASE

7. **High-Grade Intracardiac Sarcoma Causing Right Ventricular Outflow Tract Obstruction**
   Christina Lee MD, Sankalp Sehgal MD

8. **Peripartum Management of a Patient with Repaired Transposition of the Great Arteries**
   Abdullah Rasheed MD, Robert White MD, Danielle McCullough MD

9. **Three-dimensional echocardiography for transcatheter aortic valve replacement – A systematic review and meta-analysis**
   Lisa Q. Rong MD, Irbaz Hameed MD, Arash Salemi MD, Mohamed Rahouma MD, Faiza M. Khan MD, Linda Shore-Lesserson MD, Mario Gaudino MD

10. **Evaluation of Right Ventricular Systolic Function acutely after Elective Cardiac Surgery: A 3D echocardiography feasibility study**
    Lisa Q. Rong MD, Robert Sickeler MD, Maria Chiara Palumbo MS, Jiwon Kim MD, Jonathan W. Weinsaft MD

11. **Echocardiographic Predictors of Intraoperative Right Ventricular Dysfunction: A 2D and Speckle Tracking Echocardiography Study**
    Lisa Q. Rong MD, Brian Yum MD, Christiane Abouzeid MD, Maria Chiara Palumbo MS, Jonathan W. Weinsaft MD, Jiwon Kim MD

Society for Obstetric Anesthesia and Perinatology (SOAP)

1. **Postpartum Readmission Rates and Inpatient Mortality In Pregnancies Complicated By Sickle Cell Disease: A Multistate Analysis 2007-2014**
   Evelyn E. Bae MD, Virginia Tangel MA, Robert S. White MD, Anna S. Nachamie BS, Sharon E. Abramovitz MD, Nathan A. Liu MD

2. **Opioid Use Disorder and Maternal Outcomes Following Cesarean Section, A Multistate Analysis 2007 - 2014**
   Maria M. Quincy MD, Roniel Weinberg MD, Virginia Tangel MA, Sharon Abramovitz MD, Jaime Aaronson MD, Robert S. White MD MS

3. **Racial and Ethnic Disparities in Obstetric Complications: A Retrospective Analysis, 2007-2014**
   Virginia Tangel MD, Anne Budnick RN, Sharon Abramovitz MD, Robert S. White MD MS

World Airway Management Meeting (WAMM)

1. **Close the Bag: A Project to Methodically Improve the Quality of the Emergency Airway Bag**
   Jon D. Samuels MD, Brian Like MD, Patricia Mack MD, Vinod Malhotra MD, M. Spiegel MD

2. **Emergent Airway Management in a Patient with in situ Tracheobronchial Stents**
   Jon D. Samuels MD, John Rubin MD, Christina Lee MD, Erin Adams MD, Rohan Panchamia MD

Departmental Posters

1. **Protective Intraoperative Ventilation with Higher versus Lower Levels of Positive End-Expiratory Pressure in Obese Patients (PROBESE)**
   Lead author: Thomas Bluth MD for the PROBESE Writing Committee
   WCM co-authors: Peter A. Goldstein MD, Zachary A. Turnbull MD
   WCM co-investigators: Jon D. Samuels MD, Farida Gadalla MD, Matthew T. Murrell MD PhD, Farrell E. Cooke BS, Michele L. Steinkamp RN, Cheguevara Afaneh MD, Gregory F. Dakin MD, Kelly A. Garrett MD, Alfons Pomp MD, Douglas S. Scherr MD

2. **Enhanced Recovery after Ambulatory Orthopedic Surgery**
   Elizabeth Fouts-Palmer MD, Nathan Painter MD, Sarah Wu BA, Sabrina Petrillo CRNA, Roniel Weinberg MD

3. **Characteristics and Anatomic Distribution of Early vs. Late Stroke After Cardiac Surgery**
   Natalia S. Ivascu MD, Faiza M. Khan MD, Mohammed Rahouma MD, Irbaz Hameed MD, Ahmed Abouarab MD, Alan Z. Segal MD, Mario F. L. Gaudino, Leonard N. Girardi MD

4. **Chronic Pain in Refugee Torture Survivors**
   Gunisha Kaur MD MA, Roniel Weinberg MD, Andrew Milewski PhD, Samantha Huynh BS, Elizabeth Mauer MS, Hugh Hemmings MD PhD, Kane Pryor MD

5. **Female Genital Mutilation/Cutting: A Sreview and Meta-Analysis of Somatic Pain and Obstetric Sequelae**
   Jacob Lurie MPH, Alessandra Weidman MPH, Samantha Huynh BS, Diana Delgado MLS., Imaani Easthausen MS, Gunisha Kaur MD MA

6. **Medical Mission Location as Compared to Country Need: A Systematic Review**
   Keerteshwrya Mishra BS, Sonal Jessel MPH, Jacob Lurie MPH, Kane O. Pryor MD, Gunisha Kaur MD MA

7. **Anaesthetic Depth and Complications After Major Surgery: An International, Randomised Controlled Trial**
   Timothy Short MD, Douglas Campbel, BM, Christopher Frampton PhD, et al.
   WCM Investigators: Kane Pryor MD, Michele Steinkamp RN, Farrell Cooke BS, Rachel Friedlander BS, Jaideep Malhotra MD, Lori A. Rubin MD

American Pain Society (APS)

Drug Toxicology Screening in Cancer Pain

Dustin Liebling MD[1], Neel Mehta MD[2], Ruth Eisenberg MS[1], Amitabh Gulati MD[3]

[1]Montefiore Medical Center – Albert Einstein College of Medicine, [2]Weill Cornell School of Medicine, [3]Memorial Sloan Kettering Cancer Center

INTRODUCTION

- Despite the risk of opioid abuse and the growing use of opioids to treat cancer pain, no clear guidelines currently exist when monitoring opioid compliance in the cancer setting.
- While the use of urine drug screening as a diagnostic tool to guide physicians' therapeutic decisions has been described in chronic non-cancer pain, the use of urine drug screening in patients with cancer pain has not been appropriately discussed.
- Prior to considering the development of clinical practice guidelines for the vigilant monitoring of opioids in the cancer setting, this study was created to evaluate the current practices and attitudes physicians have towards screening, monitoring and prescribing opioids in patients with active cancer and in cancer survivors.

METHODS

A 24-item survey was completed by 106 pain management physicians (54.4% response rate) to assess how clinicians screen, monitor and prescribe opioids to patients with active cancer, cancer survivors, and patients with no history of cancer.

RESULTS

Demographics (N = 106)

Gender: Male (72.5%); Female (27.5%)

Years in pain management practice:
1-4 (29.7%); 5-9 (18.7%); 10-19 (19.8%); 20+ (31.8%)

Formal training in treating cancer pain:
Yes (76.9%); No (23.1%)

How frequently do you treat cancer pain:
0% of patients (1.1%); 1-9% of patients (52.8%);
10-19% of patients (22.0%); 20-49% (11.0%);
50% or more of patients (13.1%)

TABLE II: Survey Questions with Statistical Significance

Which toxicology screen do you use in your practice?

Urine; Saliva; Blood; More than 1
P-values > 0.05

None:
Active cancer: 8.6%
Cancer survivor: 2.9%
No history of cancer: 0.0%
P-value = 0.003

*Do you require a **baseline** toxicology screen before initiating opioids?*

Always:
Active cancer: 43.8%
Cancer survivor: 61.0%
No history of cancer: 64.4%

Sometimes:
Active cancer: 34.3%
Cancer survivor: 27.6%
No history of cancer: 27.0%

Rarely:
Active cancer: 12.4%
Cancer survivor: 5.7%
No history of cancer: 3.9%

Never:
Active cancer: 9.5%
Cancer survivor: 5.7%
No history of cancer: 4.8%
P-value = 0.04

*For patients who **refuse** a toxicology screen, I:*

Discuss the importance of a urine toxicology screen and **prescribe refill** without a completed screen:
Active cancer: 18.3%
Cancer survivor: 9.6%
No history of cancer: 5.8%

Do not refill prescription until the urine toxicology screen is completed:
Active cancer: 68.3%
Cancer survivor: 87.5%
No history of cancer: 92.3%
P-value < 0.001

*For patients who **fail** a toxicology screen*, I*

Discuss importance of urine toxicology screen and prescribe refill:
Active cancer: 63.7%
Cancer survivor: 32.6%
No history of cancer: 26.3%
P-value < 0.0001

Eliminate opioids from treatment regimen:
Active cancer: 30.8%
Cancer survivor: 55.8%
No history of cancer: 53.7%
P-value = 0.0006

Dismiss patient from practice P-value > 0.05
Refer patient to addiction medicine P-value > 0.05
*A toxicology screen is failed if the patient either (a) tested negative for the prescribed opioid, (b) tested positive for an opioid that was not prescribed, or (c) tested positive for other illicit substance(s)

DISCUSSION

Pain management physicians generally require similar toxicology screening for cancer patients, cancer survivors and patients with chronic non-cancer pain. However, cancer status plays a role in the clinicians' decision-making in the following scenarios:

- Prior to initiating opioid therapy, baseline toxicology screening is more often required in patients with no history of cancer and cancer survivors; similarly, clinicians are almost twice as likely to report "never" using a baseline screen in patients with active cancer as compared to patients with no history of cancer
- For active cancer patients who refuse a toxicology screen, clinicians are more likely to refill an opioid prescription.
- For patients with no cancer history who fail a toxicology screen, clinicians are more likely to refuse a prescription refill, and are almost twice as likely to eliminate opioids from the treatment regimen.

CONCLUSION

- For patients with active cancer, clinicians are more likely to prescribe opioids despite patient refusal for toxicology screen as well as history of substance abuse.
- For patients with no history of cancer, clinicians are more likely to refuse a prescription refill and eliminate opioids from treatment regimen.
- Further discussion and consensus is needed to ensure the safe monitoring of opioids when treating cancer pain.

REFERENCES

1. Goudas LC, Bloch R, Gialeli-Goudas M, Lau J, Carr DB. The epidemiology of cancer pain. Cancer Invest. 2005;23(2):182-9.
2. Carmichael AN, Morgan L, Del Fabbro. Identifying and assessing the risk of opioid abuse in patients with cancer: an integrative review. Subst Abuse Rehabil. 2016 Jun 2;7:71-9.
3. Kwon JH, Tanco K, Park JC et al. Frequency, Predictors, and Medical Record Documentation of Chemical Coping Among Advanced Cancer. Oncologist. 2015 Jun;20(6):692-7

American Society of Anesthesiologists (ASA)

Poster 1

Weill Cornell Medicine **NewYork-Presbyterian**

Black Race As A Social Determinant Of Health And Outcomes After Lumbar Spinal Fusion Surgery: A Multistate Analysis, 2007 - 2014

Dima El Halawani Aladdin, MD, Virginia Tangel, MA, Briana Lui, BS, Lisa R. Witkin, MD, Kane O. Pryor, MD, Robert S. White, MD, MS | October 2019

American Society of Anesthesiologists®

Introduction

- Disparities in healthcare have been demonstrated across a range of surgical procedures and remain a major determinant of outcomes for racial, ethnic, and socioeconomically vulnerable populations[1,2].

- Spinal fusions were the sixth most common operating room procedure in 2014[3,4].

- Previous research has identified black patients to be more likely than white to experience increased postoperative length of stay (LOS), major complications, mortality, 30- and 90- day readmissions, and surgical costs following lumbar spinal fusion surgery[5,6]. These studies are outdated, contain data from a single institution, or analyze small limited samples.

- No major study to date has comprehensively analyzed the impact of race on post-lumbar spine surgical complications, LOS, charges, and readmissions after adjusting for pertinent hospital-, patient-, and surgical-level factors.

- We hypothesize that black patients, compared to white patients, are more likely to have increased unadjusted rates and adjusted odds of postoperative complications, longer LOS, higher total hospital charges, and increased readmissions.

References

1. LaPar DJ, Bhamidipati CM, Mery CM, Stukenborg GJ, Jones DR, Schirmer BD, et al. Primary payer status affects mortality for major surgical operations. Ann Surg. 2010;252(3):544-50; discussion 50-1.
2. Andreae MH, Gabry JS, Goodrich B, White RS, Hall CJA, analgesia. Antiemetic Prophylaxis as a Marker of Health Care Disparities in the National Anesthesia Clinical Outcomes Registry. 2018;129(2):588-99.
3. Lad SP, Bagley JH, Kenney KT, Ugiliweneza B, Kong M, Bagley CA, et al. Racial disparities in outcomes of spinal surgery for lumbar stenosis. Spine (Phila Pa 1976). 2013;38(11):927-35.
4. Chen SA, White RS, Tangel V, Nachamie AS, Witkin LR. Sociodemographic Characteristics Predict Readmission Rates After Lumbar Spinal Fusion Surgery. Pain Med. 2019.
5. Seicean A, Seicean S, Neuhauser D, Benzel EC, Weil RJ. The Influence of Race on Short-term Outcomes After Laminectomy and/or Fusion Spine Surgery. Spine (Phila Pa 1976).2017;42(1):34-41.
6. Poorman GW, Moon JY, Wang C, Horn SR, Beautruin BM, Bono OJ, et al. Rates of Mortality in Lumbar Spine Surgery and Factors Associated With Its Occurrence Over a 10-Year Period: A Study of 803,949 Patients in the Nationwide Inpatient Sample. Int J Spine Surg. 2018;12(5):617-23.
7. White RS, Matthews KC, Tangel V, Abramovitz SJ.obNMA. Enhanced Recovery After Surgery (ERAS) Programs for Cesarean Delivery Can Potentially Reduce Healthcare and Racial Disparities. 2019.

Table 1. Patient demographics and medical/hospital characteristics according to race and ethnicity.

Characteristic	White	Black	Hispanic	Other	Missing	Total	P-value
Total	208,088 (77.7)	17,326 (6.5)	24,454 (9.1)	13,573 (5.1)	4,535 (1.7)	267,976 (100.0)	
Median household income state quartile for patient ZIP code							< .0001
First quartile	35,949 (17.3)	7,264 (41.9)	7,461 (30.5)	2,786 (20.5)	1,023 (22.6)	54,483 (20.3)	
Second quartile	54,542 (26.2)	3,699 (21.3)	6,257 (25.6)	3,094 (22.8)	1,127 (24.9)	68,719 (25.6)	
Third quartile	56,112 (27)	3,704 (21.4)	5,952 (24.3)	3,467 (25.5)	1,190 (26.2)	70,425 (26.3)	
Fourth quartile	57,712 (27.7)	2,148 (12.4)	4,169 (17)	3,798 (28)	1,090 (24)	68,917 (25.7)	
Missing	3,773 (1.8)	511 (2.9)	615 (2.5)	428 (3.2)	105 (2.3)	5,432 (2)	
Relevant comorbidities							< .0001
Obesity	26,307 (12.6)	3,480 (20.1)	3,550 (14.5)	1,410 (10.4)	653 (14.4)	35,400 (13.2)	
Diabetes, uncomplicated	29,101 (14)	3,944 (22.8)	4,703 (19.2)	2,412 (17.8)	677 (14.9)	40,837 (15.2)	
Hypertension, uncomplicated	97,667 (46.9)	9,748 (56.3)	10,459 (42.8)	6,188 (45.6)	1,913 (42.2)	125,975 (47)	
Elective Operation Status							< .0001
Emergency	6,345 (3)	1,167 (6.7)	1,240 (5.1)	650 (4.8)	72 (1.6)	9,474 (3.5)	
Urgent	7,150 (3.4)	659 (3.8)	1,147 (4.7)	283 (2.1)	116 (2.6)	9,355 (3.5)	
Hospital spine surgery volume							< .0001
First quartile	45,793 (22)	5,155 (29.8)	8,416 (34.4)	3,376 (24.9)	2,362 (52.1)	65,102 (24.3)	
Fourth quartile	60,790 (29.2)	4,108 (23.7)	3,186 (13)	3,037 (22.4)	320 (7.1)	71,544 (26.7)	
Hospital safety net burden							< .0001
Low burden	66,578 (32)	4,383 (25.3)	5,401 (22.1)	5,102 (37.6)	1,608 (35.5)	83,072 (31)	
Medium burden	109,456 (52.6)	8,144 (47)	10,825 (44.3)	4,839 (35.7)	1,950 (43)	135,214 (50.5)	
High burden	32,054 (15.4)	4,799 (27.7)	8,228 (33.6)	3,632 (26.8)	977 (21.5)	49,690 (18.5)	

Table 2. Risk-adjusted outcomes according to race and ethnicity.

Outcome	White (reference)	Black	Hispanic	Other	Missing	N
Spine Surgery complications	1.00	1.08 (1.03-1.13)**	0.93 (0.89,0.97)***	1.08 (1.02,1.13)**	1.01 (0.92,1.10)	267,976
General surgical complications	1.00	1.15 (1.09,1.21)***	1.04 (0.99,1.10)	1.07 (1.01,1.14)*	1.05 (0.94,1.17)	267,976
Length of stay (logged days)	1.00	1.16 (1.15,1.17)***	1.08 (1.08,1.09)***	1.07 (1.06,1.08)***	1.02 (1.01,1.04)**	267,976
Total charges (logged 2017 US $)	1.00	1.09 (1.08,1.09)***^^^	1.05 (1.05,1.06)***	1.12 (1.11,1.13)***	1.02 (1.00,1.03)*	267,976
30 day readmission	1.00	1.13 (1.07,1.20)***	0.94 (0.89,1.00)*	0.88 (0.82,0.95)**	0.74 (0.64,0.85)***	267,976
90 day readmission	1.00	1.07 (1.02,1.13)**	0.94 (0.90,0.99)*	0.85 (0.79,0.90)***	0.79 (0.71,0.88)***	267,976

* $p < 0.05$, ** $p < 0.01$, *** $p < 0.001$.
All numbers reported are odds ratios (95% CI) unless noted otherwise.

Methods

- Data source: State Inpatient Databases, Healthcare Cost and Utilization Project, Agency for Health Research and Quality) from California (2007-2011); Florida, Kentucky, Maryland, New York (2007-2014)
- Patients aged ≥18 years undergoing Lumbar spine surgery (International Classification of Diseases, Ninth Revision)
- Outcomes: complications related to spinal surgery, general surgical complications, LOS, total charges, 30- and 90- day readmission.
- Unadjusted bivariate analyses, adjusted multivariable, and stratified analysis to compare patient demographics, present-on-admission comorbidities, hospital characteristics, and complications by categories of race/ethnicity (Our primary variable of interest).
- Model covariates included patient's age, gender, comorbidities, quartile of median income of patient's residence, and primary insurance payer.

Results

- Black patients were 8% and 15% more likely than white patients to experience spine surgery specific complications (OR: 1.08, 95% CI: 1.03-1.13) and general postoperative complications (aOR: 1.15, 95% CI: 1.07-1.20), respectively. Black patients, compared to white patients, also had increased adjusted odds of 30-day readmissions (aOR: 1.13, 95% CI: 1.07-1.20), 90-day readmissions (aOR: 1.07, 95% CI: 1.02-1.13, longer LOS (aIRR: 1.16, 95% CI: 1.15-1.17), and higher total charges (aIRR: 1.09, 95% CI: 1.08-1.09).

Discussion

Our findings could be related to:
- *Hospital-related factors:* Black patients being more likely to undergo surgery at low surgical volume and high safety net burden hospitals.
- *Patient-related factors:* Black patients had poorer preoperative baseline health.
- Differences in presurgical optimization and timing of surgery.

Conclusion

- Black race remains a social determinant of health impacting equity in surgical outcomes with black patients experiencing a significantly poorer postoperative course following lumbar spinal fusion surgery even in models controlling for confounding patient demographics and comorbidities, hospital characteristics, surgical approach, and year and state of surgery.
- Hospital systems and providers should adopt methods to promote equity in care, including employee educational programs focusing on healthcare disparities and the impact of unequal care, and through the utilization of standardized protocol based care, such as ERAS programs, that can reduce the impact of implicit bias on post-surgical outcomes[7].

Poster 2

HOSPITAL FOR SPECIAL SURGERY

Use of Auricular Acupuncture for Intraoperative Sedation in a Patient with Multiple Medication Sensitivities

Deirdre C. Kelleher, MD[1] and Stephanie I. Cheng, MD[1-2]
[1]Weill Cornell Medicine, Dept of Anesthesiology, NY, NY   [2]Hospital for Special Surgery, Dept of Anesthesiology, Critical Care & Pain Management, NY, NY

Weill Cornell Medicine Anesthesiology

BACKGROUND

- Auricular acupuncture (AA) is a subset of acupuncture where needles are placed only in the ear, but affect the entire body
- AA can be implemented perioperatively to reduce pain and anxiety. Needles may be placed for a short duration (< 30 min) or semi-permanent needles may be placed for up to a week.
- In meta-analysis, periop AA has been shown to reduce post-op VAS pain scores.[1] Single RCT report decreased intraoperative anesthetic use and postoperative opioid use.[2-3]
- In RCTs, use of complementary and alternative medicine techniques have been shown to improve overall patient satisfaction scores regardless of changes in other outcomes.[4]

CASE

A 49-year-old female with mild intermittent asthma and multiple drug allergies presented preoperatively to discuss her anesthetic options for her upcoming elective hip arthroscopy and labral repair. She reported history of poor tolerance to anesthesia in the past with slow emergence and substantial post-op nausea and vomiting. She was eager to minimize pharmacologic agents (especially opioids) so as to avoid any adverse reactions and allow herself to return to her baseline mental status quickly. After a discussion of her anesthetic options, the patient agreed to have a bupivacaine spinal and acupuncture as her main anesthetics.

ANESTHESIOLOGY 2019
OCTOBER 19-23 | ORLANDO

INTRAOP

On the day of surgery, the patient underwent the procedure with the planned anesthetic plus soothing music by headphones. Her induction included:

- Spinal anesthesia: 2.5 mL bupivacaine 0.5%
- Auricular acupuncture: 8 left ear points (Auricular Trauma Protocol)
  - DBC 0.20 x 30mm needles: Amygdala, Hippocampus, Prefrontal Cortex, Point Zero, Insula
  - Seirin 0.20 x 30mm needles: Hypothalamus and Vagus
- Body acupuncture: GV20, Yin Tang (Seirin 0.20 x 40 mm)
- Soothing music (patient choice) via one earbud to right ear

IV medications included standard ambulatory surgery prophylaxis medications: cefazolin 1 g, dexamethasone 8 mg, acetaminophen 850 mg, ketorolac 30 mg.

Needles were removed at the end of the procedure. Minor heme was noted at Shen Men and Point Zero. The patient reported some abdominal fullness postoperatively but was otherwise very pleased with her perioperative experience. She was discharged following resolution of her spinal anesthetic.

Auricular Trauma Protocol

SHEN MEN
POINT ZERO
VAGUS
HYPOTHALAMUS
HIPPOCAMPUS
INSULA   AMYGDALA   PREFRONTAL CORTEX

DISCUSSION

- As demonstrated in this case, AA may be used in conjunction with regional anesthesia to maintain an opioid-free anesthetic for orthopedic procedures. Standard prophylactic medications such as acetaminophen and ketorolac were given, but no stronger pain medication was required during her recovery.
- AA may also be combined with other complementary and alternative medicine techniques (e.g., aromatherapy, music therapy, hypnotherapy) to limit pharmacologic agents used during the perioperative period. In this case, music therapy assisted in keeping the patient calm during the procedure.
- Offering complementary medicine in ambulatory surgery may help improve patient satisfaction during the perioperative period. This patient was displeased with her previous experiences with anesthesia and was grateful that efforts were made to provide her with an anesthetic that was tailored to her needs.
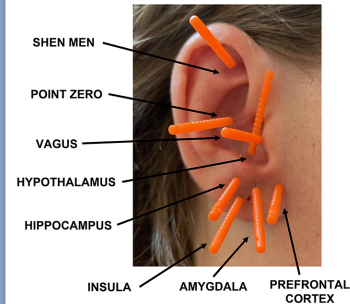
[1]He BJ, et al. Auricular acupressure for analgesia in perioperative period of total knee arthroplasty. Pain Med 2013;14(10):1608-13. [2]Zhong Q., et al. Effectiveness of auricular acupressure for acute postoperative pain after surgery: a systematic review and meta-analysis. Chin J Integr Med 2019;25(3):225-32. [3]Ye X, et al. Effectiveness of perioperative auricular therapy on postoperative pain after total hip arthroplasty: a systematic review and meta-analysis of randomised controlled trials. eCAM 2019; doi: 10.1155/2019/2979780. [4]Rice KL, et al. Bundling interventions to enhance pain care quality (BITE Pain) in medical surgical patients. Ochsner J 2019;19:77-95. doi: 10.31486/toj.18.0164.eCollection 2019

Female Authorship in Anesthesiology in 2008 – 2018: A Bibliometric Study

Lisa Q. Rong[1], Lillye P. Anderson[1], Mohamed M. Rahouma[2], Samantha Huynh[1], Jacqueline Emerson[1], Faiza Khan[2], Kane O. Pryor[1], Mario Gaudino[2]
1 Department of Anesthesiology, Weill Cornell Medicine/New-York-Presbyterian Hospital, New York, NY
2 Department of Cardiothoracic Surgery, Weill Cornell Medicine/New-York-Presbyterian Hospital, New York, NY

Introduction

- Women represent 36% of all practicing physicians in the United States in 2019 but remain underrepresented in leadership roles, editorial boards of academic journals, and as speakers in national and international conferences.
- Identifying gender disparities in authorship is important for future strategies to promote women in academics.
- We examined the prevalence of female first and last authors in original research articles published from 2008 to 2018 in the five anesthesia journals with the highest impact factor.
- We sought to quantify the gender gap, examine changes of the gap over time, and evaluate factors associated with female authorship.

Methods

Selection of journals and articles:
- Five highest impact journals in anesthesia were identified: Anesthesiology, BJA, EJA, A&A and Anaesthesia **(Figure 1).**
- All original research articles, systematic reviews, and meta-analyses published in 2008, 2010, 2012, 2014, 2016, and 2018.

Extraction of data and study classification
- Year of publication, origin of study, departmental affiliations, number of authors, gender, academic degrees and titles of the first and last authors, type of study, country of origin, and source of funding.
- Articles with first or last female author were classified as "female-authored". Others were classified as "male-authored".

Table 1: Multivariate regression of variables associated with female-authored studies in anesthesia.

	OR (95% CI) and p-value
Year of publication	1.02 (0.99-1.04) p=0.19
Academic degree of first author (reference: MD degree only)	
• MD and Others	0.65 (0.53-0.80) p<0.001*
• Others	1.71 (1.21-2.41) p<0.01*
• PhD	1.64 (1.20-2.24) p<0.01*
Academic degree of last author (reference: MD degree only)	
• MD and others	1.09 (0.90-1.32) p=0.36
• Others	3.28 (1.87-5.79) p<0.001*
• PhD	1.17 (0.88-1.55) p=0.28
Number of female co-authors per study	2.08 (1.94-2.23) p<0.001*
Study origin (reference: North America)	
• Africa	1.15 (0.49-2.71) p=0.75
• Asia	1.17 (0.90-1.52) p=0.25
• Australia	0.85 (0.56-1.29) p=0.44
• Europe	1.28 (1.05-1.55) p=0.01*
• South America	0.48 (0.23-1.00) p=0.05
• Multi-continental	0.55 (0.28-1.06) p=0.07

References
1. Young A, et al.. FSMB Census of Licensed Physicians in the United States, 2018. J Med Regul. 2019 Jul;105(2):7–23.
2. Professionally Active Physicians by Gender [Internet]. The Henry J. Kaiser Family Foundation. 2019 [cited 2019 Aug 28]. https://www.kff.org/other/state-indicator/physicians-by-gender/
3. Jagsi R et al. The "gender gap" in authorship of academic medical literature--a 35-year perspective. N Engl J Med. 2006 Jul 20;355(3):281–7.

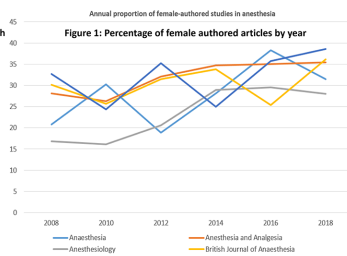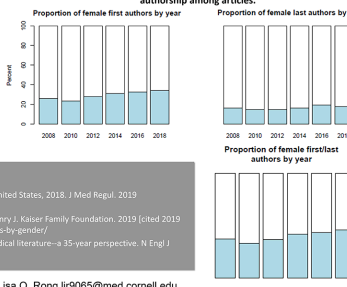Contact: Lisa Q. Rong lir9065@med.cornell.edu

Figure 1: Percentage of female authored articles by year

Figure 2: Annual proportion of female first (FA), last (LA) and first or last (FA/LA) authorship among articles.
Proportion of female first authors by year
Proportion of female last authors by year
Proportion of female first/last authors by year

Statistical analysis

- Descriptive analyses were performed to compare male- and female-authored studies. Logistic regression was used to determine factors associated with female authorship.

Results

- Median of authors: 6 [IQR 5, 8] of which 4 [IQR 3, 6] were male and 1 [IQR 1, 2] female.
- 4720 total articles: 39.6% were female-authored.
  - 22.9% female first author, 10.1% female last author, 6.6% female first and last author.
- Female-authored articles increased from **37.3% in 2008 to 45.7% in 2018 (p <0.001)** while female last-authorship plateaued. (**Figure 2**)
- Female authorship was significantly associated with:
  - first author holding a PhD (OR 1.64, 95%CI 1.20-2.24, p<0.01)or non-medical academic degree (OR 1.71, 95%CI 1.21-2.41, p<0.01)
  - last author holding a non-medical academic degree (OR 3.28, 95%CI 1.87-5.79, p<0.001 **(Table 1).**
  - number of female co-authors (OR 2.08, 95%CI 1.94-2.23, p<0.01)
- Compared to articles originating from North America, articles from Europe were more likely to be female-authored. (OR 1.28, 95%CI 1.05-1.55, p=0.01) **(Table 1)**

Conclusions

- Women tend to be first rather than last author.
- Female first & last authors are more likely to hold a PhD or non-medical academic degree.
- Significant geographic variations exist in female authorship.
- The gender difference in authorship in anesthesia has reduced significantly over the last decade; proportion of women first and last authors in the current anesthesia literature seems consistent with the percentage of practicing women in the field.

Can echo-derived cardiac output replace pulmonary artery catheter derived cardiac output in cardiac surgery?

Lisa Q. Rong, Gabriel Arguelles, Elizabeth Mauer, Lillye Anderson, Kane O. Pryor
Department of Anesthesiology, Weill Cornell Medicine/New-York-Presbyterian Hospital, New York, NY

Introduction

- Estimation of cardiac output (CO) by thermodilution using pulmonary artery catheter (PAC) is used in cardiac surgery to guide intraoperative management.
- While PAC is considered the gold standard, CO can be measured using transesophageal echo (TEE) by multiplying stroke volume by heart rate. **(Figures 1, 2)**
- Three-dimensional (3D) TEE has been shown to be more accurate than two-dimensional (2D) TEE in evaluation of left ventricular outflow tract (LVOT) area. **(Figure 3)**
- We hypothesize that 3D echo-derived CO should be more accurate than 2D echo-derived CO as compared to the reference standard of PAC.

Methods

- PAC-derived CO with 2D and 3D Doppler-derived CO measurements were collected as part of a prospective observational echo protocol.
- Measurements were obtained pre-sternotomy and post-chest closure (within 5 minutes of each other).
- Exclusion criteria included atrial fibrillation; tricuspid, mitral, and aortic regurgitation greater than mild; and any intracardiac shunts.
- Pairwise relationships between PAC CO measurements and echo CO measurements were examined by scatterplots and Pearson's correlation coefficients.
- Bland-Altman plots were also constructed to assess agreement between measurement methods, defined by bias (mean difference between measurements) and limits of agreement (bias ± 1.96 standard deviations of the bias). Confidence intervals were constructed for both bias and limits of agreement.
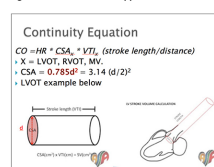

Figure 1: Calculation of Doppler-derived CO

Continuity Equation

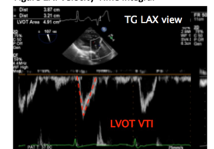$CO = HR * CSA_a * VTI_a$ (stroke length/distance)
- X = LVOT, RVOT, MV.
- $CSA = 0.785 d^2 = 3.14 (d/2)^2$
- LVOT example below

Figure 2A: Velocity-Time integral
TG LAX view
LVOT VTI

Figure 2B: Estimation of LVOT area
ME AV SAX view

Figure 4: Scatter plots for comparison of cardiac output (CO)
A
r = 0.56
r = 0.50
r = 0.49
Pre-CPB
B
r = 0.33
r = 0.53
r = 0.42
Post-CPB
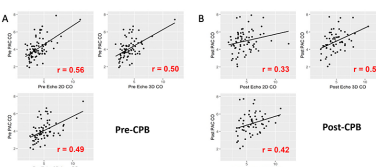
Figure 5: Bland-Altman plots for comparison of cardiac output (CO)
A Bias (-0.01) L/min LOA (-2.75 to 2.73) L/min
B Bias (0.14) L/min LOA (-2.99 to 2.27) L/min
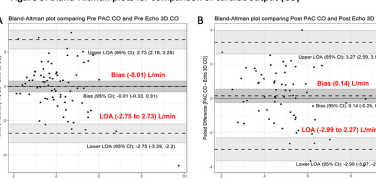
Figure 3: Anatomy of the LVOT
Proximal LVOT Major Axis > Minor Axis
Distal LVOT Equal Major Axis and Minor Axes
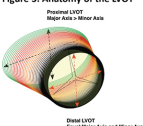
Results

- A total of 83 subjects were analyzed.
- Procedures included: Coronary artery bypass surgery (CABG) 36.2%, aortic valve (AV) replacement 20.3%, aortic surgery 21.7%, and combination AV/CABG/Aortic surgery 21.8% patients.
- Echo derived 2D, 3D diameter, and 3D area CO values pre-cardiopulmonary bypass (CPB) were highly correlated with one another (all Pearson's correlations r > 0.90) while less correlated post-CPB (0.70 ≤ r ≤ 0.90).
- The echo-derived measurements correlated with PAC derived CO measurements pre-CPB (r= 0.56, 0.50, 0.49 respectively) but less post-CPB (0.33, 0.53, 0.42 respectively) **(Figure 4).**
- Among the pre-CPB measurements, echo-derived 3D CO had the most agreement with PAC-derived CO in terms of bias (-0.01, 95% CI: -0.33 to 0.31) L/min.
- However, the limits of agreement (LOA) were wide (-2.75 to 2.73) L/min **(Figure 5A).**
- Similarly, among post-CPB measurements, echo-derived 3D CO had the most agreement with PAC-derived CO in terms of bias (0.14, 95% CI: -0.25 to 0.54) L/min but with wide limits of agreement (-2.99 to 3.27) L/min **(Figure 5B)**.

Conclusions

- 3D echo-derived CO measurements were only modestly correlated with PAC-derived CO pre-CBP.
- Despite low bias, the wide limits of agreement from echo-derived CO by 3D in comparison to PAC-derived CO suggest that the two methods are not interchangeable.

Contact: Lisa Q. Rong lir9065@med.cornell.edu

Use of Pulmonary Artery Pulsatility Index in Cardiac Surgery

Lisa Q. Rong[1], Mohamed M. Rahouma MD[2], Peter J. Neuburger[3], Gabriel Arguelles BA[1], Jacqueline Emerson BS[1], Elizabeth Mauer MS[1], Linda Shore-Lesserson MD[4], Kane O. Pryor MD[1], Mario Gaudino[1]
- [1]Department of Anesthesiology, Weill Cornell Medicine, New York, NY, USA. [2]Department of Cardiothoracic Surgery, Weill Cornell Medicine, New York, NY, USA.
- [3]Department of Anesthesiology, New York University Hospital, New York, NY, USA. [4]Department of Anesthesiology, North Shore University Hospital, Manhasset, NY, USA.

Introduction

- **Pulmonary artery pulsatility index (PAPI),** defined as pulmonary artery pulse pressure [pulmonary artery systolic pressure (PASP)-pulmonary artery diastolic pressure (PADP)], divided by central venous pressure (CVP) is a novel hemodynamic measure that has been used to predict RV failure.
- It has yet to be prospectively applied to the elective cardiac surgical population to predict right ventricular dysfunction. We aim to study this novel index to determine if it is a more sensitive marker of RV dysfunction than traditional hemodynamic parameters and if it can be used to predict intraoperative RV dysfunction.
- In this study, we evaluate whether pulmonary artery pulsatility index (PAPi) collected before and after cardiopulmonary bypass (CPB) is predictive and diagnostic of new onset right ventricular (RV) failure in the elective cardiac surgical population.

Methods

- This was a prospective observational study of patients who had cardiac surgery between March 2017 and January 2019 at Weill Cornell Medical Center in New York, NY.
- Echo and hemodynamic data were collected at two specified timepoints: pre-sternotomy and post chest-closure.
- Intraoperative RV dysfunction was defined as fractional area of change (FAC) < 35% after chest closure.
- Exclusion criteria included patients with greater than mild [1+] tricuspid regurgitation, and significant mitral or aortic regurgitation.
- Patients with and without post-CPB RV dysfunction fractional area of change (FAC) < 35% were compared and receiver operating characteristic curve was constructed.

Table 1: Demographic Characteristics

	Overall (N=119)	RV Function post-CPB		
		Normal (N Total=62)	Abnormal (N Total=57)	P
	N (%) or Mean (SD)	N (%) or Mean (SD)	N (%) or Mean (SD)	
Age (years)	63.3±12.6	66.7±11.4	59.7±13	0.003
Male Gender	76 (64.4)	39 (51.3)	37 (48.7)	1.00
Height (cm)	174 (19)	172 (10.3)	176 (18.5)	0.13
Weight (kg)	86.5 (20)	84.1(18.4)	87.3 (16.8)	0.33
BMI	29 (6.3)	28.2 (5.2)	28.8 (5.6)	0.59
CV Risk Factors				
HTN	80 (67.8)	42 (52.5)	38 (47.5)	0.96
HLD	66 (56.4)	34 (51.5)	32 (48.5)	1.00
DM	21 (17.8)	8 (38.1)	13 (61.9)	0.27
Prior MI	16 (13.6)	7 (43.8)	9 (56.2)	0.69
CAD	50 (42.7)	27 (54.0)	23 (46.0)	0.87
Operation				
AVR	25 (21.2)	16 (64.0)	9 (36.0)	
CABG	27 (22.9)	16 (59.3)	11 (40.7)	0.16
AORTIC	22 (18.6)	12 (54.5)	10 (45.5)	
Combination	44 (37.3)	17 (38.6)	27 (61.4)	
NYHA Class (I/II/III/IV)	77 (65.3)/ 25 (21.2)/ 16 (13.6)/0	41 (53.2)/10 (40.0)/10 (62.5)/0	36 (46.8)/15 (60.0)/6 (37.5)/0	0.33

Table legend: CPB, cardiopulmonary bypass; BMI, body mass index; HTN, hypertension; HLD, hyperlipidemia, DM; diabetes mellitus; MI, myocardial infarction; CAD, coronary artery disease
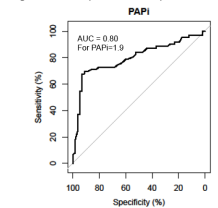
Figure: Receiver operator curve of post-CPB PAPi

PAPi

AUC = 0.80
For PAPi=1.9

Table 2: Echocardiographic and Hemodynamic Characteristics

		Overall (N=119)	RV Function		
			Normal (N=62)	Abnormal (N=57)	P
		N (%) or Mean (±SD)	N (%) or Mean (SD)	N (%) or Mean (SD)	
Pre- CPB	ESA	12.2±4.7	11.9±4.3	12.6±5.2	0.40
	EDA	20.0±6.0	19.8±5.6	20.3±6.5	0.70
	FAC	39±10	40±10	38±11	0.24
	PAPi	2.3±1.3	2.5±1.2	2.0±1.0	0.003
	MPAP	16.5±5.0	16.1±25.1	16.9±4.8	0.4
	PASP	26.0±6.8	25.9±6.9	26.0±6.9	1.0
	PADP	11.1±4.2	10.6±4.3	11.7±4.1	0.2
	CVP	7.7±3.2	6.9±2.7	8.3±3.6	0.02
	SBP	112.2±14.0	114.5±13.6	109.8±14.2	0.07
	DBP	57.6±10.0	57.1±11.2	58.2±8.5	0.50
	MAP	77.3±10.0	77.5±10.3	77.1±9.8	0.90
	LVEF	60.7±9.7	62.0±9.6	59.2±9.7	0.12
	CO	4.3±1.5	4.3±1.1	4.4±1.9	0.47
	PAPi				
	≤1.9	50 (42.0%)	20 (32.3%)	30 (52.6%)	0.04
	>1.9	69 (58.0%)	42 (67.7%)	27 (47.4%)	
Post- CPB	ESA	11.1±3.4	10.2±3.2	12.1±3.3	0.003
	EDA	17.6±4.9	18.4±5.1	16.7±4.6	0.05
	FAC	36.0±11.0	45.0±7.3	26.8±5.6	<0.001
	PAPi	1.9±1.0	2.4±1.1	1.4±0.6	<0.001
	MPAP	18.1±7.1	18.1±8.9	18.1±4.6	0.93
	PASP	27.4±6.3	27.8±6.9	26.9±5.6	0.49
	PADP	11.8±4.0	10.8±3.7	12.9±4.0	0.006
	CVP	9.4±3.6	8.2±3.5	10.8±3.2	<0.001
	SBP	110.4±14	111.2±12.5	109.8±14.2	0.32
	DBP	57.5±8.4	56.1±8.0	59.1±8.5	0.09
	MAP	75.3±9.7	74.3±9.0	76.4±10.5	0.25
	LVEF	63.4±9.5	63.9±10.1	63.0±8.8	0.61
	CO	5.2±1.3	5.4±1.3	5.0±1.3	0.09
	PAPi				
	≤1.9	74 (62.2%)	21 (33.9%)	53 (93.0%)	<0.001
	>1.9	45 (37.8%)	41 (66.1%)	4 (7.0%)	

Table legend: ESA, end systolic area; EDA, end diastolic area; FAC, fractional area of change; PAPi, pulmonary artery pulsatility index; MPAP, mean pulmonary artery pressure; PASP, pulmonary artery systolic blood pressure; PADP, pulmonary artery diastolic pressure; SBP, systolic blood

Table 3. Multivariable Regression for predictors of RV Dysfunction

Parameter	Exp(B) (95% CI)	P-value
Pre EDA	1.009 (1.001-1.017)	0.026
Pre ESA	0.985 (0.976-0.995)	0.004
Pre PAPI	0.981 (0.962-0.999)	0.048
Pre PADP	0.996 (0.991-1.002)	0.226
Age	1.001 (0.999-1.003)	0.300

Results

- One hundred and nineteen patients undergoing elective surgery: coronary artery bypass graft (23%), aortic valve replacement (21%), aortic surgery (19%) and combined surgery (37%) were evaluated. **(Table 1)**
- Post-CPB RV dysfunction was associated with lower pre-CPB PAPi values (2.0±1.0 vs 2.5±1.2, p=0.001 and p=0.03) and higher pre-CPB central venous pressure (8.3±3.6 and 6.9±2.7, p=0.003 and p=0.02 respectively). **(Table 2)**
- Pre-CPB PAPi [(0.98 (95%CI 0.96-0.99)], end systolic area [0.99 (95%CI 0.98-0.99)], and end diastolic area [1.01 (95%CI 1.001-1.02)] were independently associated with RV dysfunction in multivariable modelling, with a lower PAPi and end systolic area, and higher end diastolic area. **(Table 3)**
- Post-CPB area under the curve for PAPi 0.80 (95%CI: 0.71-0.88; sensitivity = 0.68, specificity = 0.93, optimal cutoff = 1.9). **(Figure).**

Conclusions

- PAPi measured pre-CPB is a potential predictor and marker of post-CPB RV dysfunction and may have diagnostic utility in cardiac surgery.
- Further, large scale studies are needed to confirm this finding.

References

- Korabathina R, et al. The pulmonary artery pulsatility index identifies severe right ventricular dysfunction in acute inferior myocardial infarction. Catheter Cardiovasc Interv 2012;80:593-600.
- Kochav SM, et al. Prognostic Impact of Pulmonary Artery Pulsatility Index (PAPi) in Patients With Advanced Heart Failure: Insights Assist Device Implantation: The Tale of EFrom the ESCAPE Trial. J Card Fail 2018;24:453-9.
- Alfirevic A, Sale S, Soltesz E. Foretelling Right Ventricular Failure After Left Ventricular he Pulmonary Artery Pulsatility Index. Anesth Analg 2019;128:8-10.

Contact: Lisa Q. Rong lir9065@med.cornell.edu

In Monkeys, Recovery Time Remains Constant Following Bolus Doses of 1-10x ED95 or Infusions of Up To 3 Hours in Length of Both the Ultra-short Acting NMBA CW 1759-50 and the Intermediate-Acting Compound CW 002

John J. Savarese MD*, Hiroshi Sunaga MD**, Jeff D. McGilvra PhD+, Anita Jegarl BS*, Paul M Heerdt MD PhD***

*Department of Anesthesiology, Weill Cornell Medical College, New York, NY
**Ikei University School of Medicine, Tokyo, Japan
*** Yale School of Medicine, New Haven, CT
+Cedarbury- Hauser Pharmaceuticals, Grafton WI, a Division of Albany Molecular Research, Albany, NY

Introduction

CW 1759-50 and CW 002 are nondepolarizing NMBAs (esters of fumaric or maleic acids) which are degraded in a chemical (adduction) reaction with L-cysteine. In Rhesus monkeys, which are a good model of the anticipated properties of such materials in humans, we have focused on the rate of recovery from NMB in this species after a wide range of bolus doses and of continuous infusions of various lengths. This was done to evaluate whether increasing dosage or duration of administration might affect the rate of recovery from NMB.

Methods

With IACUC approval, we studied adult male Rhesus monkeys (10-18 kg) under isoflurane anesthesia, during experiments lasting 6-10 hours. Twitch (0.15 Hz) and TOF (2 Hz x 2 sec) were recorded. MAP and HR, EKG, and T were monitored continuously and kept WNL.

Only one compound (either CW 1759-50 or CW 002) was evaluated during any experiment. Bolus doses of 1x-10x ED95 were given, and spontaneous recovery of twitch from 5% to 95% of baseline was measured. Continuous infusions of 20-180 min duration were given, maintaining 99% twitch suppression. After discontinuation of infusion, spontaneous recovery (5-95% twitch) was measured. Recovery times for each compound were compared separately by ANOVA.

Results

Recovery intervals did not differ significantly among either doses of CW 1759-50 or doses of CW 002

Table 1. 5-95% Twitch Recovery Intervals Following Bolus or Infusion

| CW 1759-50 | | CW 002 | |
Dose (mg/kg)	5-95% Interval (mins ± SD)	Dose (mg/kg)	5-95% Interval (mins ± SD)
0.10 (n = 52)	6.1 ± 1.6	0.05* (n = 6)	15.3 ± 7.5
0.20 (n = 80)	6.4 ± 1.9	0.10 (n = 8)	14.3 ± 6.5
0.50 (n = 48)	6.7 ± 2.4	0.20 (n = 9)	13.3 ± 4.4
Infusion (n = 48)	6.2 ± 1.4	0.40 (n = 13)	15.5 ± 5.1
		Infusion (n = 26)	13.1 ± 3.7

* ED 95 (approx)
NS Differences not significant by ANOVA

Conclusion

Recovery times were not significantly affected by size of bolus or by infusion. We hypothesize that this feature may be due to the inactivation of the compounds by the adduction reaction with L-cysteine.

An unvarying rate of recovery from NMB under most clinical circumstances would most likely allow prediction of time of spontaneous recovery from any depth of NMB, a characteristic seemingly unique to this type of NMBA.

CW 1759-50

Figure 1. 5-95% Recovery Interval Following Boluses or Infusions of CW 1759-50 in the *Rhesus* Money

CW 002

Figure 2. 5-95% Recovery Interval Following Boluses or Infusions of CW 002 in the *Rhesus* Money

Validity of Population-Based Comorbidity Adjustment Scores in Estimating In-Hospital Mortality in Individual Subgroups of Race/Ethnicity
ANESTHESIOLOGY 2019
Virginia Tangel, MA, Dima El Halawani Aladdin, MD, Kane O. Pryor, MD, Robert S. White, MD, MS | October 22, 2019
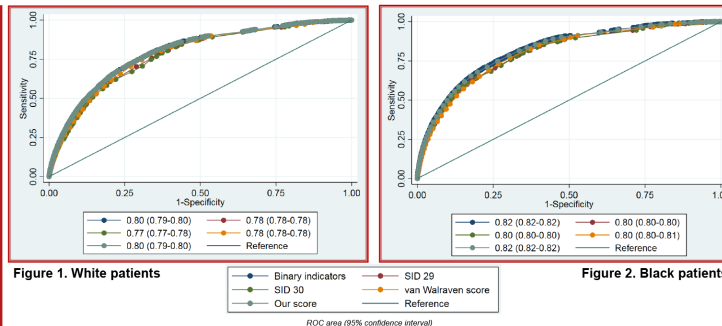
American Society of **Anesthesiologists**®

Introduction

- Weighted composite comorbidity indexes are commonly used to adjust for patient comorbidities in administrative database research
- In spite of their widespread population-based use, composite comorbidity measures were created without accounting for the heterogeneity of comorbidity prevalence within individual demographic categories
- We hypothesized that there are differences by race/ethnicity in the validity of comorbidity adjustment scores, and that race/ethnicity-specific comorbidity indexes will perform better than overall composite measures when analyzed in these subpopulations

References

Elixhauser, A, et al. *Medical care (1998)*
van Walraven, C, et al. *Medical care (2009)*
Thompson, NR, et al. *Medical care* (2015)

Figure 1. White patients

White patients ROC legend:
- 0.80 (0.79-0.80) — 0.78 (0.78-0.78)
- 0.77 (0.77-0.78) — 0.78 (0.78-0.78)
- 0.80 (0.79-0.80) — Reference

Figure 2. Black patients

Black patients ROC legend:
- 0.82 (0.82-0.82) — 0.80 (0.80-0.80)
- 0.80 (0.80-0.80) — 0.80 (0.80-0.81)
- 0.82 (0.82-0.82) — Reference

Legend:
- Binary indicators
- SID 30
- Our score
- SID 29
- van Walraven score
- Reference

ROC area (95% confidence interval)

Methods:

- State Inpatient Databases for CA, FL, NY, MD, and KY, Healthcare Cost and Utilization Project, Agency for Healthcare Research and Quality (2007-2014)
- Divided sample into a randomly-chosen training and testing data sample
- Using the testing data, we re-derived Elixhauser comorbidity summary measures by categories of race/ethnicity (binary indicators, SID 29, SID 30, van Walraven score)
- For each population, we created logistic regression models to predict in-hospital mortality, including as covariates the 29 Elixhauser comorbidities
- We retained variables in subsequent logistic regression models with a P value of < 0.05. In models, the comorbidities that were not retained received a comorbidity weight of 0; retained covariates were assigned weights by taking the covariate's coefficient divided by the absolute value of the smallest coefficient. To create a summary comorbidity measure, each coefficient was multiplied by its weight.
- In models stratified by category of race/ethnicity, we modeled our category-specific comorbidity score on the outcome of in-hospital mortality in our testing sample

Results

- In the overall sample (N = 9,564,277), our index (c = 0.80, 95% CI: 0.80 – 0.80) discriminated better than the van Walraven score (VW) (c = 0.79, 95% CI 0.79-0.79), SID 29 (c = 0.78, 95% CI 0.78 - 0.79), and SID 30 (c = 0.78, 95% CI 0.78-0.78), but was not superior to the binary indicators (c = 0.80, 95% CI 0.80 – 0.80)
- In populations of white patients (N = 5,867,762), our index performed slightly better than the VW, SID 29, and SID 30, but had no difference in discriminatory power with the binary indicators **(Figure 1)**
- Among black patients (N = 1,563,454), our index again performed slightly better than the VW, SID 29, and SID 30, but was not different than the binary indicators **(Figure 2)**
- Our index also performed well in Hispanic patients and in patients of other races/ethnicities

Conclusions

- In a large, demographically diverse sample, we found that our race/ethnicity-specific comorbidity adjustment scores performed slightly better than the overall VW score, SID 29, and SID 30 at modeling in-hospital mortality. However, including the individual Elixhauser comorbidities in multivariable models are robust to category of race/ethnicity
- Future research should examine if differences in comorbidity indexes exist according to other social determinants of health

Question/Comments? Please contact:
Virginia Tangel, MA (vit2010@med.cornell.edu)

Long-term mortality, hospital length of stay, and discharge disposition in patients classified as American Society of Anesthesiology Physical Status 5 or 5E
ANESTHESIOLOGY 2019
Zachary A. Turnbull, MD, MBA/MS, Virginia Tangel, MA, Matthew Alexander, BS, Peter A. Goldstein, MD | October 20, 2019

American Society of **Anesthesiologists**®

Introduction

- Given that end-of-life healthcare costs are continuing to rise, it is imperative that anesthesiologists and surgeons understand and present the full range of likely outcomes of putative lifesaving measures when offering moribund patients and their families the option of surgical intervention
- Longer-term outcomes (beyond 48 hours) in ASA PS 5 or 5E patients are unknown
- **Primary objective:** identify the difference in mortality rate of ASA PS 5 and 5E patients 30 and 90 days postoperatively
- **Secondary objectives:** identify the distribution of these patients across discharge dispositions and length of stay (LOS) based on emergency status

References

- Hopkins TJ, Raghunathan K, Barbeito A, et al. Associations between ASA Physical Status and postoperative mortality at 48 h: a contemporary dataset analysis compared to a historical cohort. *Perioper Med (Lond)* 2016; **5**: 29
- Dalton JE, Kurz A, Turan A, Mascha EJ, Sessler DI, Saager L. Development and validation of a risk quantification index for 30-day postoperative mortality and morbidity in noncardiac surgical patients. *Anesthesiology* 2011; **114**: 1336-44
- Sidi A, Lobato EB, Cohen JA. The American Society of Anesthesiologists' Physical Status: category V revisited. *J Clin Anesth* 2000; **12**: 328-34

Figure 1. Kaplan-Meier survival curves for ASA PS 5 at 30 and 90 days postoperatively, by emergency status.
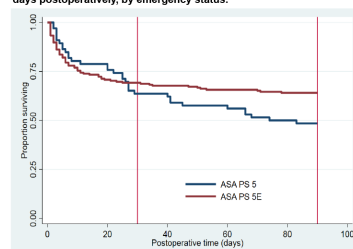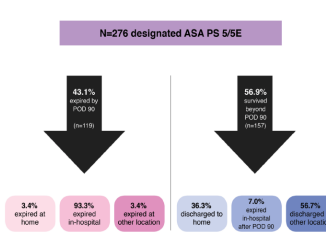

Legend:
- ASA PS 5
- ASA PS 5E

Figure 2. Discharge disposition of all ASA PS 5/5E patients.

N=276 designated ASA PS 5/5E

43.1% expired by POD 90 (n=119)

56.9% survived beyond POD 90 (n=157)

- 3.4% expired at home
- 93.3% expired in-hospital
- 3.4% expired at other location
- 36.3% discharged to home
- 7.0% expired in-hospital after POD 90
- 56.7% discharged to other location

Table 1. Length of stay (LOS) in days, by emergency status.

LOS (MEDIAN, IQR)	49 HOURS - 30 DAYS (P=0.08)	N	31+ DAYS (P=0.79)	N
ASA PS 5	9.5 [5-25]	22	16 [4-43]	42
ASA PS 5E	6.5 [4-11]	40	14 [7-34]	135
All ASA PS 5s	7 [4-17]	62	15 [7-36]	177

P values represent comparison between non-emergency and emergency status populations at each interval.

Methods:

- Patient population was of cases >= 18 years with anesthesia records at our hospital between 1/1/2013 and 12/31/2017
- Parametric and non-parametric methods to test difference in mortality rate between ASA PS 5/5E cases at 30 and 90 days; LOS; discharge dispositions
  - Discharge dispositions: in-hospital death, home, and other: hospice, long-term care facility, inpatient rehabilitation facility, or self-discharge
- Kaplan-Meier survival analysis to test the independent effect of E classification 30 and 90 day all-cause mortality in ASA PS 5/5E
- All analyses were performed in Stata SE, Version 16 (College Station, TX), and significance was assessed at the 0.05 level
- The Institutional Review Board at Weill Cornell Medical College approved all study activities

Results

- N=276 ASA PS 5/5E, 25% ASA PS 5 and 207 (75.0%) 5E
- 35.9% of 5/5E expired in <= 30 days; 98% in-hospital
- Overall, ASA PS 5/5E patients had a significantly higher mortality rate at 30 days than at 48 hours (25.9% vs. 13.4%, respectively, p < 0.01)
- No significant difference of the survivor functions at 30 and 90 days between 5 and 5E classifications (p = 0.63, p = 0.09, respectively; Figure 1)
- Of the 62 ASA PS 5 patients who survived beyond 48 hours but expired on or before postoperative day 30, 40 (64.5%) had an emergency designation
- Of the 177 ASA PS 5 patients surviving beyond 30 days postoperatively, 135 (76.3%) had an emergency designation
- Median LOS not significantly different between elective and emergent groups (Table 1)
- 157 of 276 (56.9%) patients survived beyond 90 days; 79.6% had the emergency designation
- No significant differences in discharge disposition for patients who survived 0-48 hours, 49 hours-30 days, and 31-90 days postoperatively (p = 0.18)

Conclusions

- The E designation on moribund cases does not offer any meaningful difference in terms of predicting long-term mortality, nor hospital LOS
- Most 5/5E patients are not discharged to home
- These results should be considered in the informed consent process

Question/Comments? Please contact:
Zachary A. Turnbull, MD, MBA/MS (zat2002@med.cornell.edu)

Hospital safety-net burden is associated with increased inpatient mortality and postoperative complications after colectomy

ANESTHESIOLOGY 2019 | October 19, 2019

Wendy Wang, PhD, Robert S. White, MD, MS, Virginia Tangel, MA, Anna S. Nachamie, MBA, Kane O. Pryor, MB, BS

American Society of Anesthesiologists®

Introduction

- Safety-net hospitals (SNHs) treat vulnerable populations and carry a high safety-net burden (SNB, proportion of uninsured or Medicaid-insured patients).
- Colectomies are common (275,000 in the US) with high surgical site infections (SSI) rates, up to 26%.
- Few studies have examined the relationship between hospital SNB and colectomy outcomes.

Hypothesis

Among colectomy patients:

- **SNHs have worse outcomes (higher in-hospital mortality and complications).**
- SSIs are associated with worse outcomes.
- SSI patients at SNHs have even worse outcomes.

Methods

- Data: State Inpatient Databases, Healthcare Cost and Utilization Project
  - CA (2009-2011), FL, NY, MD, and KY (2009-2014)
- Colectomies for patients ≥ 18 years
  - Except rectal or transverse colon cancer cases
- Variables
  - Patient (demographics, present-on-admission comorbidities), Procedure, Hospital
  - **Primary covariates**
    - SNB category   – SSI status
  - **Outcomes**
    - In-hospital mortality
    - Any complications (CV, pulmonary, intraoperative)
- Bivariate and multivariable logistic regression analyses (generalized linear mixed models, with interaction term between SNB and SSI)

Table 1. Unadjusted SSIs and outcomes for colectomy patients by hospital SNB.

	Hospital SNB		
	Low (%)	Medium (%)	High (%)
Total	125,042 (28.2)	214,882 (48.5)	103,149 (23.3)
SSI present	7,183 (5.7)	11,944 (5.6)	7,681 (7.4)
In-hospital mortality	2,588 (2.1)	5,258 (2.4)	3,320 (3.2)
Complications	23,135 (18.5)	43,066 (20.0)	23,230 (22.5)

All P values < 0.0001

Table 2. Unadjusted SNB category and outcomes by SSI category.

	No SSI (%)	SSI (%)
Total	416,265 (93.9)	26,808 (6.1)
SNB		
Low	117,859 (28.3)	7,183 (26.8)
Medium	202,938 (48.8)	11,944 (44.6)
High	95,468 (22.9)	7,681 (28.7)
In-hospital mortality	8,733 (2.1)	2,433 (9.1)
Complications	70,926 (17.0)	18,505 (69.0)

All P values < 0.0001

Table 3. Risk-adjusted outcomes by hospital SNB or SSI category.

	In-hospital mortality	Complications
Hospital SNB		
Low (reference)	1.00	1.00
Medium	1.17*** (1.07, 1.27)	1.04 (0.97, 1.11)
High	1.37*** (1.24, 1.50)	1.11** (1.04, 1.19)
SSI		
No SSI (reference)	1.00	1.00
SSI	1.92*** (1.82, 2.02)	3.63*** (3.52, 3.73)

*P < 0.05, **P < 0.01, ***P < 0.001

Results

- 457,794 colectomies total
  - Mean age: 61.3y (SD 14.9y)
  - ~51.7% female
  - 38.4% robotic, 21.8% laparoscopic, 39.8% open, 0.1% converted
- **Colectomy patients were more likely to die in-hospital and experience postoperative complications at SNHs.**
- Colectomy patients with SSIs also had greater odds of in-hospital mortality and complications.
- **Patients treated at SNHs who developed an SSI were even more likely to have a postoperative complication.**
  - aOR: 4.29, 95% CI: 3.94-3.68, P<0.001

Conclusions

- Colectomy patients at SNHs have poorer outcomes.
- For patients with SSIs, the effect of treatment at a SNH was even more pronounced in the likelihood for a postoperative complication.

References

1. Aimaq R, Akopian G, Kaufman HS. Surgical site infection rates in laparoscopic versus open colorectal surgery. *Am Surg*. 2011;77(10):1290-1294.
2. Institute of Medicine. 2000. America's Health Care Safety Net: Intact but Endangered. Washington, DC: The National Academies Press. https://doi.org/10.17226/9612.
3. Sastow DL, White RS, Mauer E, et al. The disparity of care and outcomes for Medicaid patients undergoing colectomy. *J Surg Res*. 2019;235:190-201.

Question/Comments? Please contact:
Wendy Wang, PhD (wew2006@med.cornell.edu)

The Association of Race with Utilization of Antiemetic Prophylaxis in the Multicenter Perioperative Outcomes Group (MPOG)

Robert S. White MD, MS, Michael H. Andreae, MD, Xiaoyue Ma, MS, Zachary A. Turnbull, MD, Anna S. Nachamie, BS, Julia M. Rosenbloom, MD, Kane O. Pryor, MD | ANESTHESIOLOGY 2019 October 21, 2019

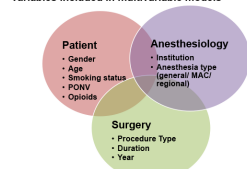**American Society of Anesthesiologists®**

BACKGROUND

- Healthcare disparities persist and are evolving in the United States.
- Anesthesiology is not immune, as evidenced by research demonstrating differences in both perioperative health services and health outcomes based on social determinants of health such as race/ethnicity and socioeconomic status.
- Our prior research using a national anesthesia information management systems' data showed a large significant association between socioeconomic markers, Medicaid insured versus commercially insured patients and lower versus higher median income, and reduced administration of antiemetic prophylaxis (ondansetron and dexamethasone).
- We chose antiemetic prophylaxis administration as our outcome of interest because it serves as a measure of anesthesia quality.
- In this study, using data from the Multicenter Perioperative Outcomes Group (MPOG) we examined whether a patient's race is associated with the utilization of antiemetic prophylaxis. We hypothesized that Black race, as compared to White race, is associated with reduced receipt of intraoperative antiemetic prophylaxis.

REFERENCES

- Andreae MH, Gabry JS, Goodrich B, White RS, Hall C Antiemetic Prophylaxis as a Marker of Health Care Disparities in the National Anesthesia Clinical Outcomes Registry. *Anesthesia and Analgesia* 2018.
- Dutton, R.P., *Disparities in Anesthesia Care*. Anesthesia & Analgesia 2018.
- LaPar DJ, Bhamidipati CM, Mery CM, et al. Primary Payer Status Affects Mortality for Major Surgical Operations. *Annals of Surgery* 2010.
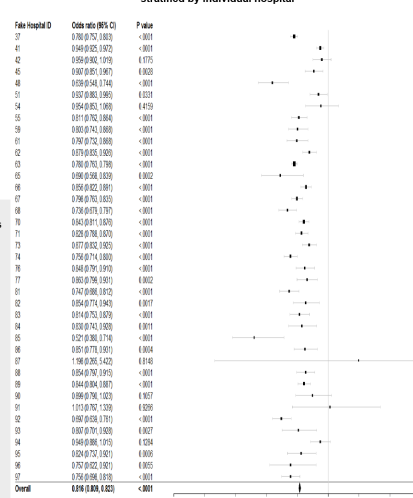
Figure 1. Patient-, anesthesiology-, surgery- specific variables included in multivariable models

Patient
- Gender
- Age
- Smoking status
- PONV
- Opioids

Anesthesiology
- Institution
- Anesthesia type (general MAC/ regional)

Surgery
- Procedure Type
- Duration
- Year

METHODS

- We performed a focused analyses of the MPOG data (years 2004 - 2018), using the Prevention of Post-Operative Nausea and Vomiting (PONV 01) ASPIRE Measure Specification sample procedure population.
- Exclusion criteria included patients aged <18 years and patients who underwent obstetric non-operative procedures (labor and delivery; labor epidurals).
- Variables extracted included race (variable of interest; unordered – Black, White, Other, Unknown), sex, age, ASA status, procedure, year, hospital, anesthesia staffing, anesthesia administered, and PONV risk factors (inhalational general anesthetic use, female sex, PONV/motion sickness history, non-smoker, intended post-operative opioid administration).
- Our outcome of interest was administration of ondansetron, dexamethasone, or either.
- We tested our hypothesis fitting bivariate, multivariate logistic regression, and sensitivity analyses.
- Statistical significance was established a priori, at alpha <0.01. Analyses were conducted in SAS Version 9.4 (Cary, NC, USA).

Figure 2. aOR for black race receiving PONV prophylaxis stratified by individual hospital

Fake Hospital ID	Odds ratio (95% CI)	P value
37	0.788 (0.757, 0.883)	<.0001
41	0.949 (0.925, 0.972)	<.0001
42	0.996 (0.902, 1.019)	0.1775
45	0.907 (0.851, 0.967)	0.0028
48	0.938 (0.543, 0.744)	<.0001
51	0.930 (0.863, 0.966)	0.0331
54	0.954 (0.853, 1.068)	0.4159
55	0.611 (0.762, 0.884)	<.0001
59	0.800 (0.743, 0.868)	<.0001
61	0.790 (0.732, 0.868)	<.0001
62	0.879 (0.659, 0.920)	<.0001
63	0.786 (0.763, 0.798)	<.0001
65	0.690 (0.566, 0.830)	0.0002
66	0.856 (0.822, 0.891)	<.0001
67	0.796 (0.763, 0.835)	<.0001
68	0.736 (0.673, 0.787)	<.0001
70	0.643 (0.611, 0.670)	<.0001
71	0.028 (0.788, 0.670)	<.0001
73	0.677 (0.632, 0.905)	<.0001
74	0.756 (0.714, 0.800)	<.0001
76	0.648 (0.791, 0.910)	<.0001
77	0.863 (0.796, 0.931)	0.0002
81	0.747 (0.988, 0.812)	<.0001
82	0.854 (0.774, 0.940)	0.0017
83	0.614 (0.753, 0.929)	<.0001
84	0.630 (0.743, 0.920)	0.0011
85	0.521 (0.360, 3.714)	<.0001
86	0.851 (0.773, 0.931)	0.0004
87	1.198 (0.950, 5.422)	0.0140
88	0.854 (0.797, 0.915)	<.0001
89	0.644 (0.804, 0.887)	<.0001
90	0.699 (0.796, 1.023)	0.1057
91	1.013 (0.767, 1.539)	0.9299
92	0.697 (0.658, 0.731)	<.0001
93	0.650 (0.701, 0.909)	0.0027
94	0.949 (0.886, 1.015)	0.1284
95	0.624 (0.757, 0.982)	0.0008
96	0.757 (0.922, 0.921)	0.0055
97	0.756 (0.956, 0.918)	<.0001
Overall	0.816 (0.809, 0.823)	<.0001

RESULTS

- MPOG (2004-2018) contained 5.1 million relevant cases from 40 institutions.
- Bivariate analysis showed that Black patients, compared to White patients, received ondansetron (52.4 vs 55.9%), dexamethasone (28.1 vs 36.7%), or either (58.0 vs 63.9%) at reduced rates.
- Multivariable logistic regression showed that Black patients, compared to White patients, had reduced adjusted odds ratios (aOR) of receiving ondansetron (aOR 0.86, 95% CI 0.86-0.87), dexamethasone (aOR 0.79, 95% CI 0.78-0.79), or either (aOR 0.82, 95% CI 0.81-0.82).
- Sensitivity analysis for most frequent procedures performed or stratified by hospital confirmed our main model findings (Fig 2).

DISCUSSION

- Our analyses of MPOG anesthesia records provides evidence that Black patients may receive inferior anesthesia care compared to White patients as evidenced by reduced rates and adjusted odds of receiving antiemetic prophylaxis.
- Possible solutions include anesthesiologists continuing their role as patient advocates by actively promoting health equity, the routine elicitation of PONV risk factors, and the inclusion of antiemetic medication in Enhanced Recovery After Surgery (ERAS) protocols.
- Future directives should study the effect of individual practitioners and hospital systems; and the impact of ERAS and clinical decision support as interventional approaches to close the gap in provided care.

Question/Comments? Please contact:
Robert S. White MD, MS (rsw9006@med.cornell.edu)

American Society of Regional Anesthesia (ASRA)

Preexisting opioid use disorder and postoperative outcomes after appendectomy or cholecystectomy: a multi-state analysis, 2007-2014

Alina Boltunova, MD,[1] Robert S. White, MD,[1] Selaiman Noori, MD,[1] Stephanie A. Chen, BA,[1] Licia K. Gaber-Baylis, BA,[2] Roniel Weinberg, MD[1]
[1] Department of Anesthesiology, New York Presbyterian Hospital-Weill Cornell Medicine, New York, New York
[2] Center for Perioperative Outcomes, Department of Anesthesiology, New York Presbyterian Hospital-Weill Cornell Medicine, New York, New York

Introduction

- Opioid use disorder has emerged as a significant public health issue as opioid use and opioid-related deaths have reached epidemic proportions in recent years (1).
- Previous studies have shown that patients with opioid dependence undergoing orthopedic, elective abdominopelvic, and cardiac procedures have poorer postoperative outcomes (2-5).
- The aim of this study was to examine the effect of preexisting opioid use disorder on postoperative outcomes including in-hospital mortality, hospital length of stay (LOS), hospital readmission, and postoperative complications in patients undergoing appendectomy or cholecystectomy.

Materials and Methods

- We used administrative data from the State Inpatient Databases (SID), a component of the Healthcare Cost and Utilization Project (HCUP), for the years 2007-2014 from California, Florida, Kentucky, Maryland, and New York.
- The SID contains all-payer inpatient care data from non-federal, non-psychiatric hospitals.
- Cases of opioid use disorder were identified through International Classification of Diseases, Ninth Revision, Clinical Modification (ICD-9-CM) codes used by HCUP to identify opioid dependence or abuse.
- Unadjusted rates of in-hospital mortality, postoperative complications, LOS, and 30-day and 90-day readmission status were compared between opioid use and no opioid use groups
- Adjusted odds ratios (ORs) for our outcomes of interest were calculated using logistic regression models

Table 1: Demographic and clinical characteristics according to opioid use status.

	Opioid use (n = 5200)	%	No opioid use (n = 1,274,272)	%	p-value
Age in years					<.0001
Mean (SD)	44.34 (14.08)		49.43 (19.11)		
Gender					<.0001
Male	2,457	47.3	513,783	40.3	
Female	2,743	52.8	760,469	59.7	
Race					<.0001
White	3,310	63.7	729,986	57.3	
Black	814	15.7	114,349	9	
Hispanic	733	14.1	281,981	22.1	
Other	228	4.4	96,284	7.6	
Missing	115	2.2	51,672	4.1	
Year of surgery					<.0001
2007	568	10.9	191,181	15	
2008	626	12	191,981	15.1	
2009	698	13.4	196,274	15.4	
2010	756	14.5	195,836	15.4	
2011	815	15.7	191,413	15	
2012	530	10.2	108,975	8.6	
2013	595	11.4	102,047	8	
2014	612	11.8	96,565	7.6	
Payer					<.0001
Medicare	1,099	21.1	332,677	26.1	
Medicaid	1,628	37.1	213,857	16.8	
Private insurance	1,092	21	547,314	43	
Other	285	5.5	50,836	4	
Self-pay / No charge	796	15.3	129,468	10.2	
State					<.0001
California	1,339	25.8	389,119	30.5	
Florida	1,344	25.8	406,512	31.9	
Kentucky	292	5.6	77,438	6.1	
Maryland	902	17.3	90,508	7.1	
New York	1,323	25.4	310,695	24.4	
Disposition at discharge					<.0001
Routine	4,329	83.3	1,119,028	87.8	
Short-term hospital	47	0.9	5,692	0.4	
Home health care	360	6.9	79,555	6.2	
Died	44	0.8	9,426	0.7	
Other	420	8.1	60,571	4.8	
Elective Operation Status					<.0001
Emergency	3,208	61.7	672,635	52.8	
Non-Emergent	650	12.5	212,171	16.7	
Missing	1,342	25.8	389,466	30.6	
Procedure					<.0001
Appendectomy	1,342	25.8	487,639	38.3	
Cholecystectomy	3,858	74.2	786,633	61.7	

Table 2: Risk-adjusted outcomes according to opioid use status.

Outcome	Both procedures	Appendectomy only	Cholecystectomy only
In-hospital death	1.58 (1.13 - 2.21)**	2.26 (1.15 - 4.45)*	1.43 (0.98 - 2.08)
Any complication	1.46 (1.35 - 1.58)***	1.46 (1.27 - 1.68)***	1.45 (1.33 - 1.59)***
Pulmonary complications	1.53 (1.39 - 1.69)***	1.58 (1.31 - 1.89)***	1.52 (1.35 - 1.71)***
Infectious complications	1.47 (1.26 - 1.69)***	1.55 (1.21 - 1.98)***	1.44 (1.22 - 1.71)***
GI complications	1.21 (1.04 - 1.41)*	1.34 (1.07 - 1.66)**	1.12 (0.93 - 1.36)
30-day readmission	1.80 (1.63 - 1.98)***	1.94 (1.64 - 2.31)***	1.75 (1.56 - 1.97)***
90-day readmission	1.98 (1.83 - 2.14)***	1.99 (1.70 - 2.34)***	1.97 (1.79 - 2.16)***
Length of stay	1.37 (1.33 - 1.41)***	1.34 (1.28 - 1.41)***	1.36 (1.32 - 1.40)***
Total charges	1.21 (1.19 - 1.24)***	1.19 (1.15 - 1.24)***	1.21 (1.19 - 1.24)***

*** denotes where $p < .005$, ** $p < .01$, * $p < .05$. 95% CI.

Analysis

- Categorical variables were compared using chi square test or Fisher's exact test analysis and continuous variables were compared using analysis of variance (ANOVA).
- Logistic regression models were fit to the data to examine the effect of opioid use status on postoperative outcomes while adjusting for potential confounders such as demographic factors and medical comorbidities.
- Odds ratios were reported with 95% confidence intervals (CIs).

References

1. SAMHSA. Key substance use and mental health indicators in the United States: Results from the 2016 National Survey on Drug Use and Health. 2017; https://www.samhsa.gov/data/https://www.samhsa.gov/data/sites/default/files/NSDUH-FFR1-2016/NSDUH-FFR1-2016.htm - opioid.
2. Sadeghian S, Karimi A, Dowlatshahi S, et al. The association of opium dependence and postoperative complications following coronary artery bypass graft surgery: a propensity-matched study. J Opioid Manag. 2009;5(6):365-372.
3. Sayal P, Bateman BT, Menendez M, et al. Opioid Use Disorders and the Risk of Postoperative Pulmonary Complications. Anesth Analg. 2018.
4. Summers S, Grau L, Massel D, et al. Opioid Use Disorders Are Associated With Perioperative Morbidity and Mortality in the Hip Fracture Population. J Orthop Trauma. 2018;32(5):238-244.
5. Waljee JF, Cron DC, Steiger RM, et al. Effect of Preoperative Opioid Exposure on Healthcare Utilization and Expenditures Following Elective Abdominal Surgery. Ann Surg. 2017;265(4):715-721.

Results

- A total of 488,981 appendectomy patients and 790,491 cholecystectomy patients (age ≥ 18 years) were included in the analysis.
- **Table 1** shows the demographic characteristics, surgical factors, and hospital-related characteristics of patients undergoing appendectomy or cholecystectomy
- Appendectomy patients with opioid use disorder incurred a 126% increase in odds of in-hospital death (**Table 2**)
- Cholecystectomy patients with opioid use disorder had a non-significant increased trend (OR 1.43) of in-hospital death, as shown in **Table 2**
- Patients with opioid use disorder (overall reported, and by each procedure separately) had higher adjusted odds of postoperative complication (OR 1.46), 30-day readmission (OR 1.80), 90-day readmission (OR 1.98), and longer LOS (OR 1.37), as shown in **Table 2**

Discussion

- Our retrospective, multi-state analysis found increased odds of in-patient mortality, hospital readmission, and postoperative complications in patients with opioid use disorder undergoing common abdominal surgeries between 2007 and 2014.
- To our knowledge, this study presents the most up-to-date and extensive data on postoperative outcomes of patients with opioid use disorder.
- Our results suggest that opioid use disorder may be used as a risk factor for poor postoperative outcomes in this surgical patient population.

Hospital Safety Net Burden Is Associated with Increased Inpatient Mortality and Postoperative Morbidity after Total Hip Arthroplasty: A Retrospective Multistate Review, 2007-2014

Melvin La, MD, Virginia Tangel, MA, Soham Gupta, BA, Tiffany R. Tedore, MD, and Robert S. White, MD, MS
Department of Anesthesiology, Center for Perioperative Outcomes, Weill Cornell Medicine
New York-Presbyterian Hospital, New York, NY, USA

Introduction

Total hip arthroplasty (THA) is one of the most widely performed surgical procedures in the United States. Safety net hospitals, defined as hospitals with a high proportion of cases billed to Medicaid or without insurance, deliver a significant portion of their care to vulnerable populations; but little is known about the effects of a hospital's safety net burden and its role in healthcare disparities and outcomes following THA. We quantified safety net burden and examined its impact on in-hospital mortality, complications, length of stay (LOS) in patients who underwent THA.

Methods

We analyzed 500,189 patient discharge records for inpatient primary THA using data from the Healthcare Cost and Utilization Project's State Inpatient Databases (SID) for California, Florida, New York, Maryland, and Kentucky from 2007 through 2014. We compared patient demographics, present-on-admission comorbidities, and hospital characteristics by hospital safety net burden status. We estimated multilevel mixed-effect multivariate logistic regression models and generalized linear models to assess hospital safety burden status' effect on in-hospital mortality, patient complications, and LOS; models controlled for patient and hospital characteristics. All study activities were approved by the Weill Cornell Medicine Institutional Review Board.

Results

Patients undergoing THA at a hospital with a high or medium safety net burden were 38% and 30% more likely, respectively, to die in-hospital compared to those in a low safety net burden hospital (high adjusted OR: 1.38, 95% CI: 1.10-1.73; medium adjusted OR: 1.30, 95% CI: 1.07-1.57). Compared to patients treated in hospitals with low safety-net burden, patients treated in high safety net hospitals had increased likelihoods of developing any postoperative complication and were expected to have a longer LOS.
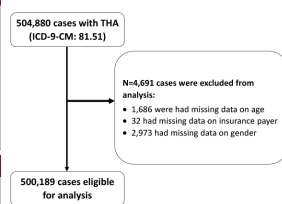
504,880 cases with THA (ICD-9-CM: 81.51)

N=4,691 cases were excluded from analysis:
- 1,686 were had missing data on age
- 32 had missing data on insurance payer
- 2,973 had missing data on gender

500,189 cases eligible for analysis

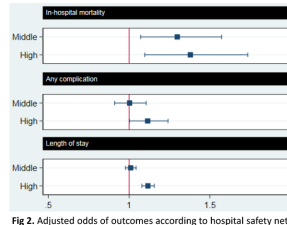**Fig 1.** STROBE figure of included THA patients

Fig 2. Adjusted odds of outcomes according to hospital safety net burden status

Outcome	Low burden (%)	Low burden (OR, CI, reference)	Medium burden (%)	Medium burden (OR, CI)	High burden (%)	High burden (OR, CI)
In-hospital mortality	241 (0.1)	1.00 (1.00,1.00)	367 (0.2)	1.30** (1.07,1.57)	783 (0.2)	1.38** (1.10,1.73)
Any complication	10,475 (5.2)	1.00 (1.00,1.00)	12,387 (5.9)	1.00 (0.91,1.11)	28,782 (5.8)	1.11* (1.00,1.24)
Cardiovascular complication	2,815 (1.4)	1.00 (1.00,1.00)	3,082 (1.5)	0.99 (0.89,1.09)	7,302 (1.5)	1.15* (1.02,1.29)
Pulmonary complication	4,571 (2.3)	1.00 (1.00,1.00)	5,331 (2.5)	1.04 (0.92,1.18)	12,579 (2.5)	1.13 (0.99,1.30)
Infectious complication	2,812 (1.4)	1.00 (1.00,1.00)	3,599 (1.7)	1.07 (0.94,1.22)	8,066 (1.6)	1.24** (1.07,1.43)
Intraoperative complication	845 (0.4)	1.00 (1.00,1.00)	1,081 (0.5)	1.03 (0.83,1.28)	2,444 (0.5)	1.11 (0.87,1.42)
Length of stay	3 (3; 4)^^	1.00^^^ (1.00,1.00)	3 (3; 4)^^	1.01^^^ (0.98,1.04)	3 (3; 4)^^	1.12***^^^^ (1.08,1.16)

Fig 3. Unadjusted rates and risk-adjusted odds of outcome measures for patients undergoing THA according to hospital safety net burden category. * $p < 0.05$, ** $p < 0.01$, *** $p < 0.001$
^^Median (interquartile range), ^^^ Incidence rate ratio (IRR), 95% confidence interval (CI)

Discussion

Our study supports our hypothesis that patients that underwent THA at hospitals with higher safety-net burden have worse outcomes than patients at hospitals with lower safety net burden. These results support growing literature aiming at the importance of understanding hospital level characteristics and their contribution to outcomes disparities. There are likely intrinsic characteristics of safety net hospitals that may contribute to disparities in quality such as staffing, organizational culture, and lack of resources for quality improvement. Specific to anesthesia, recent studies have demonstrated that there are hospital level variations in anesthesia technique, neuraxial anesthesia use, availability of preoperative clinics, and inpatient pain management protocols. Evidence-based interventions, such as enhanced recovery pathways, to reduce unnecessary variation in care could potentially improve disparities. Studies need to investigate if protocol based strategies to improve outcomes, which are currently used in low burden/ financially secure hospitals, are applicable for use in high safety net burden institutions.

References

1. Xu HF, White RS, Sastow DL, Andreae MH, Gaber-Baylis LK, Turnbull ZA. Medicaid insurance as primary payer predicts increased mortality after total hip replacement in the state inpatient databases of California, Florida and New York. J Clin Anesth 2017;43:24-32.
2. LaPar DJ, Bhamidipati CM, Mery CM et al. Primary payer status affects mortality for major surgical operations. Ann Surg 2010;252:544-50; discussion 550-1.
3. Hoehn RS, Wima K, Vestal MA et al. Effect of hospital safety-net burden on cost and outcomes after surgery. JAMA surgery 2016;151:120-8.
4. Jergesen HE, Yi PH. Early complications in hip and knee arthroplasties in a safety net hospital vs a university center. J Arthroplasty 2016;31:754-8.
5. Mouch CA, Regenbogen SE, Revels SL, Wong SL, Lemak CH, Morris AM. The quality of surgical care in safety net hospitals: A systematic review. Surgery 2014;155:826-38.

@RobertWhiteMD

Ultrasound-Guided Caudal Epidural Steroid Injection
for Successful Treatment of Radiculopathy During Pregnancy

Danielle Nadav MD[1], Timothy M. Connolly MD[1,2], Mohammad Piracha MD[1], Semih Gungor MD[1,2]

1 – Department of Anesthesiology, New York Presbyterian - Weill Cornell Medicine
2 – Division of Pain Medicine, Department of Anesthesiology, Hospital for Special Surgery

INTRODUCTION

Lower back pain is reported by nearly 75% of all pregnant women during the course of pregnancy, most frequently encountered in the second and third trimesters. Lumbar disc herniation as an underlying source of pregnancy-related lower back pain is a known yet often underdiagnosed cause. We present the management of a radicular lumbar spinal pain resulting from a herniated nucleus pulposus (HNP) during pregnancy by utilization of an ultrasound-guided epidural steroid injection via caudal approach.

CASE REPORT

A 29-year-old primagravid 32 weeks gestation presented with a 3-day history of acute lower back pain (LBP) with radiation to bilateral lower extremities. The patient had no history of spinal deformity, trauma or surgery. MRI demonstrated a large disc extrusion at L5-S1 level with compression of the bilateral S1 nerve roots (Figure 1). She was referred to interventional pain medicine after failing conservative measures. The LBP was 10/10 in severity, radiating to bilateral gluteal area with paresthesia down both legs posteriorly to her feet. Pain was worse with activity, and mildly improved with rest. There was no numbness or weakness, nor bladder or bowel incontinence. Neurological examination demonstrated normal motor function, diminished sensation along the S1 distribution bilaterally, and absent ankle reflexes bilaterally. Straight leg test was positive to reproduce the leg pain bilaterally. After discussion with the patient and her obstetrician over treatment options, the decision was made to proceed with a caudal epidural steroid injection using ultrasound guidance. Patient was positioned in left lateral decubitus position, and area was prepped with sterile technique. A sterile 12 MHz linear ultrasound initially was placed in transverse view, demonstrating the sacral cornua and sacrococcygeal ligament. The skin was anesthetized with lidocaine, and the ultrasound rotated 90 degrees to a longitudinal view of the caudal canal. A 3.5 inch 22-gauge Tuohy needle was advanced under continuous visualization until passing just beyond the sacral hiatus (Figure 2). After negative aspiration, a mixture containing 6 mL saline and 80 mg triamcinolone was administered. The procedure was tolerated well without complications. The patient reported over 90% relief, with an uneventful subsequent pregnancy course. She underwent elective cesarean section to minimize the risks of intrathecal pressure elevations, and following uneventful delivery, there were no further recurrences of pain.
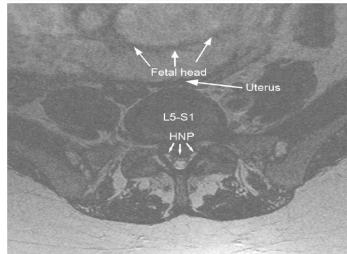
Figure 1: Axial T2 weighted MRI image demonstrating a HNP at L5-S1 level with a marked compression of the proximal S1 nerve roots bilaterally (small arrows), and gravid uterus (big arrows) in close proximity to the L5-S1 disc.
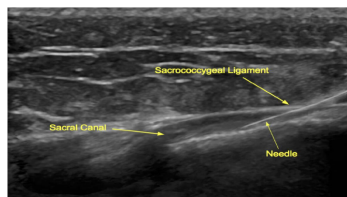
Figure 2: Ultrasound image using a linear array transducer in the in-plane view, demonstrating the epidural needle penetrating through the sacrococcygeal ligament into the caudal canal.

DISCUSSION

The incidence of HNP underlying pregnancy-associated LBP is largely unknown. The limited number of studies lack standardization in both methods and definitions. Prior to magnetic resonance imaging (MRI), the clinically-diagnosed incidence of HNP was 1 in 10,000 parturients. Various lumbosacral pains are common in pregnancy, affecting as many as 62% of patients by 12 to 18 weeks gestation and confounding clinical diagnoses. The initial management of LBP due to herniated discs includes physical therapy and limited analgesics, considering risk of fetal transmission. Nonsteroidal anti-inflammatory medications (NSAIDs) are associated with premature closure of the patent ductus arteriosus (PDA), and opioids can result in neonatal respiratory depression. Acetaminophen is the primary analgesic during pregnancy, but may provide limited relief with severe symptoms. Epidural steroid injections (ESIs) are reserved for parturients with acute symptoms consistent with lumbar nerve root compression. While steroids at any dose are controversial in pregnancy, a single ESI dose appears to have minimal risk to the fetus. Fetal exposure to high-doses of ionizing radiation has been linked to potential spontaneous abortion, growth restriction, and mental retardation. While these adverse events have not been demonstrated at exposures less than 5 rad, minimizing elective radiation exposure during pregnancy is preferred. Ultrasound is safe during pregnancy and has increasingly been utilized to image axial structures and guide procedures. Positioning the patient for such a procedure is also an important consideration. After the second trimester, the left lateral decubitus position avoids uterine aortocaval compression and can prevent hypotension associated with lying supine. Ultrasound guidance is real-time imaging modality that is safe during pregnancy, and may help to increase the margin of safety and accuracy of caudal epidural injections. Therefore, in feasible cases such as lumbosacral disc pathologies refractory to conservative therapy, ultrasound guidance should be considered during performance of caudal epidural injections.

REFERENCES

1. Kristiansson P, Svardsudd K, von Schoultz B. Back pain during pregnancy: a prospective study. Spine 1996; 21(6): 702–709
2. Ireland ML, Ott SM: The effects of pregnancy on the musculoskeletal system. Clin Orthop Relat Res 2000;372:169–179.
3. LaBan MM, Perrin JC, Latimer FR (1983) Pregnancy and the herniated lumbar disc. Arch Phys Med Rehabil 64:319–321
4. Rathmell JP, Viscomi CM, Ashburn MA: Management of nonobstetric pain during pregnancy and lactation. Anesth Analg 1997;85(5):1074–1087.
5. Williams PM, Fletcher S. Health Effects of Prenatal Radiation Exposure. Am Fam Physician. 2010 Sep 1;82(5):488–93

HOSPITAL FOR SPECIAL SURGERY

Weill Cornell Medicine Anesthesiology

ASPA 18th Annual Pain Medicine Meeting
November 14-16, 2019 | New Orleans, LA | Stronger Together

European Society for Paediatric Anaesthesiology (ESPA)

Weill Cornell Medicine   **NewYork-Presbyterian**

Lessons learned from Pediatric Difficult Intubation Cases: A Single Institution Experience

European Society For Paediatric Anaesthesiology

Casey Chai, MD [1], Jimmy Lin, MD [1], Hannah Oden-Brunson, BA [1], Aarti Sharma, MD [1]

[1] Department of Anesthesiology, Weill Cornell Medical College, New York, NY 10021, USA

Introduction:

This study aims to examine the characteristics of pediatric patients with difficult intubation in this institution, and to **reveal potential ways to improve intubating conditions in the future.**

Methods:

Observational data was collected retrospectively from our institution from **2016-2018** for management of pediatric difficult intubations. Data was logged onto a standardized research database. IRB approved retrospective analysis was performed with de-identified cases from our institution.

Discussion:

The first intubation attempt was most commonly performed by pediatric anesthesiologist (32%), reflecting the fact that most difficult airway cases were anticipated. The pediatric anesthesiologist had most successful attempts (61%), followed by ENT attendings (21%). This reflects the importance of having pediatric anesthesiologist and otolaryngologists available for patients with critical airways.

Take home points:

1. Most of the pediatric difficult intubations were **anticipated**
2. **Glidescope** was the most successful intubation tool
3. **Pediatric anesthesiologists** had the most successful attempts
4. Secretions were a major hindrance in visualization. Use of **anti-sialogogue** is highly recommended.

Patient Characteristics	
Median Age	7.5 months
Median Weight	5.85 kg
Physical Exam Findings	
Normal	6/34 (25%)
Micrognathia	12/24 (50%)
Facial dysmorphism	9/24 (37.5%)
Cleft palate	9/24 (37.5%)
Limited Mouth opening	7/24 (29%)
Glossoptosis	6/24(25%)

Difficult Intubation Case Characteristics	
Anticipated difficult airway	24/28 (86%)
Unanticipated difficult airway	4/28 (14%)
Induction method for intubation	
Mask	10/28 (36%)
IV	12/28 (43%)
NA/Awake	6/28 (21%)
Ventilation technique	
Spontaneous ventilation	11/28 (39%)
Controlled ventilation with paralysis	11/28 (39%)
Controlled ventilation without paralysis	6/28 (21%)
Ease of Mask Ventilation	
Not attempted	6/28 (21%)
Grade 1- easy ventilation	11/28 (39%)
Grade 2- required oral airway or 2 hands	10/28 (36%)
Grade 3- 2 provider and still inadequate	1/28 (4%)
Intubation attempts	
1	6/28 (21%)
2	5/28 (18%)
3	7/28 (25%)
4	4/28 (14%)
>/=5	6/28 (21%)

Successful intubation tools	
Glidescope	6/28 (21%)
Miller	5/28 (18%)
Fiberoptic (oral)	4/28 (14%)
Fiberoptic (nasal)	4/28 (14%)
Glidescope+Fiberoptic	3/28 (11%)
McGrath	3/28 (11%)
Miller + Rigid bronchoscope	2/28 (7%)
Fiberoptic via LMA	1/28 (4%)
Technical difficulties	
Secretions	6
Difficulty directing ETT despite good view	5
Difficulty directing fiberoptic	5
Airway activation	3
Abnormal anatomy	3
Device malfunction	3
Device of inappropriate size	2
Complications	
Hypoxia	5
Laryngospasm	2
Bronchospasm	1
Esophageal intubation	1
Bradycardia	1

International Anesthesia Research Society (IARS)

Studies of the New Neuromuscular Blocking Agent CW 1759-50 in the Cat, as in Monkeys, Predict Short- to Ultra-short Duration in Humans, Reflecting Rapid Degradation by L-Cysteine Adduction in Vitro

Weill Cornell Medicine
New York-Presbyterian

John J. Savarese MD*, Hiroshi Sunaga MD, Jeff D. McGilvra PhD+, Paul M Heerdt MD PhD***, Anita Jegarl BS*, Farrell E Cooke BS*, Stewart McCallum MD++, and Randy Mack MS++**

*Department of Anesthesiology, Weill Cornell Medical College, New York, NY
**Jikei University School of Medicine, Tokyo, Japan
*** Yale School of Medicine, New Haven, CT

*Cedarbury- Hauser Pharmaceuticals, Grafton WI, a Division of Albany Molecular Research, Albany, NY
++Recro Pharma Inc., Malvern, PA

Introduction

CW 1759-50 is an ultra-short acting nondepolarizing neuromuscular blocking agent (NMBA) in the monkey, most likely due primarily to its rapid degradation by L-cysteine adduction (1). Dose-duration comparisons in the monkey show a pharmacodynamic half-time of 2.7 min over a wide dose range consonant with its degradation half-time in vitro of 2.3 min (1). In this presentation we report the results of similar work done in the cat.

Methods

In IACUC-approved experiments in male cats (4-6kg) under isoflurane, twitch (at 0.15 Hz) and TOF (2Hz for 2 sec) of the Achilles tendon were recorded, together with EKG, MAP and HR.

A dose-response (DR) curve was plotted by nonlinear regression (NLR) and the ED95 was derived. Duration was measured from IV injection to recovery of twitch to 95% of baseline.

A dose vs duration comparison was made over the dose range [0.01 to 0.50 mg/kg]. An approximate pharmacodynamic half-time ($T_{1/2}$) was derived from the slope of the regression

Results

The ED95 is 0.032 mg/kg (Fig 1). The mean duration at 0.03 mg/kg is 14.6 min and at 0.04 mg/kg it is 15.2 min. At 0.20 mg/kg, or roughly 7X ED95, the duration increases to 23.4 min. The dose-duration regression (Fig 2) estimates a pharmacodynamic half-time in the cat of approximately 1.5 min.
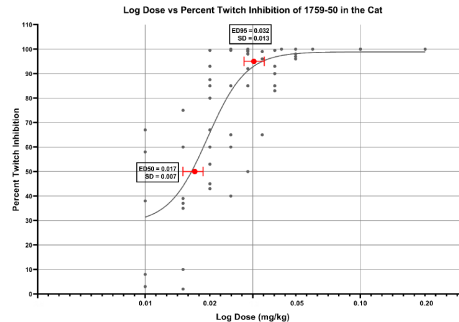
Figure 1. The DR curve (nonlinear regression of twitch inhibition vs log dose) of CW 1759-50 in the cat. ED95 is 0.032 mg/kg
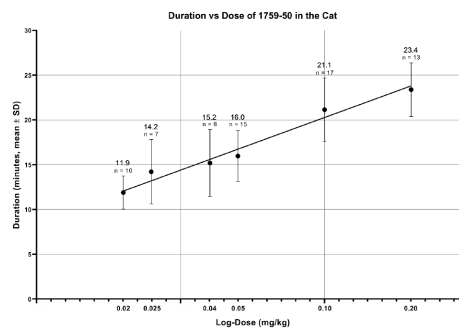
Figure 2. A linear regression of duration of block vs dose (log scale) of CW 1759-50 in the cat. The duration increases by an average of about 3 min as dosage is doubled, yielding a pharmacodynamics half-life of roughly 1.5min in this species, compared to 2.7 min in the monkey (1). These figures are strikingly similar to T1/2 of degradation of CW 1759-50 in vitro of 2.3 min, suggesting that the L-cysteine adduction reaction should be a major determinant of duration of effect in both species, as it should also be in humans

Conclusion

Studies in both the cat and monkey have yielded similar estimates of the pharmacodynamic half-time (2 to 3 min) which are close to the measured $T_{1/2}$ of 2.3 min for the rate of chemical breakdown by the cysteine adduction reaction in vitro, suggesting that the adduction reaction should be a major determinant of clearance and duration of block in vivo. The monkey and cat are generally accepted as the most useful predictive preclinical models of the dynamics of NMBAs in humans. The similar dynamic half-times of about 2 to 3 min found in these two species, together with the measured half-time in vitro of 2.3 min predict a likely short to ultra-short duration of CW 1759-50 in humans. For example, we may estimate from the above results that the duration in humans should be about 20 min at 2 to 3X ED95. Increasing or decreasing dosage by a factor of 2 (doubling or halving the dose) should increase (or decrease) the duration by about 2 to 3 min

References

1. John J. Savarese, Hiroshi Sunaga, Jeff D. McGilvra, Matthew R. Belmont, Matthew T. Murrell, Erin Jeannotte, Farrell E. Cooke, William B. Wastila, Paul M. Heerdt; Preclinical Pharmacology in the Rhesus Monkey of CW 1759-50, a New Ultra-short Acting Nondepolarizing Neuromuscular Blocking Agent, Degraded and Antagonized by L-Cysteine. *Anesthesiology* 2018;129(5):970-988.

Weill Cornell Medicine · **NewYork-Presbyterian**

One lung ventilation in a pediatric patient in a resource limited setting in Rwanda

Harmandeep Singh, MD, Zachary Adam Turnbull, MD, Eric Brumberger, MD and Stephanie Vecino, MD; May 19, 2019

IARS
International Anesthesia Research Society

Introduction

- One lung ventilation (OLV) is necessary for various clinical scenarios, but it can be challenging in countries with limited resources and equipment.
- This case report describes the successful use of a left endobronchial intubation without fiberoptic guidance for a pediatric patient in Rwanda.

Case Report

- An otherwise healthy nine year old male, who aspirated the metallic tip of a ballpoint pen two years prior to presentation and developed recurrent productive cough associated with halitosis, presented for a right lower lobectomy for severe bronchiectasis.
- Patient was initially misdiagnosed with chronic bronchitis and went on to develop recurrent fevers, pneumonias, dyspnea on exertion, muscle wasting, and right pectoral muscle atrophy.
- He ultimately had a chest CT scan which was significant for right pulmonary cavitations with basal loculated empyema and collapse and consolidation of right lower lobe. Patient was placed on broad spectrum antibiotics in preparation for surgical intervention.
- Repeat chest CT prior to surgery revealed improved empyema and a foreign body impacted in the inferior lobe bronchus of right lung with associated severe bronchiectasis changes in right lower lobe, pleural-parenchymal fibrosis, loss of right lung volume, and compensatory emphysema in left lung (figure 1).
- On the day of the procedure, patient weighted 24 kilograms, was afebrile with stable vital signs, and had no air entry into right lung base on physical exam.
- Prior to induction, an interdisciplinary discussion was conducted to verify the plan, optimize communication, identify challenges, and review the available resources.
- Appropriately sized double-lumen tube, bronchial blocker, or fiberoptic bronchoscope were not available at the hospital.

Figure 1: Preoperative CT scan, which showed a foreign body impacted in the inferior lobe bronchus of right lung with associated severe bronchiectasis changes in right lower lobe, pleural-parenchymal fibrosis, loss of right lung volume, and compensatory emphysema in left lung.

- Anesthesia was induced with ketamine, propofol, fentanyl, and cisatracurium.
- Under direct laryngoscopy, 5.0 cuffed single-lumen endotracheal tube (SL-ETT) was passed through the vocal cords and turned 180 degrees counterclockwise while advancing blindly to direct the ETT into the left main bronchus at a depth of 22.5 cm; auscultation of both lungs was used to confirm proper placement of the ETT.
- Patient was placed in left lateral decubitus position, and anesthesia was maintained with isoflurane for a total duration of six hours to complete the thoracotomy, right lower lobectomy, and right lung decortication.
- The cases presented challenges with alternating between OLV and conventional ventilation, suctioning secretions from right bronchi, and providing optimal conditions for surgical exposure.
- Intercostal nerve blocks were performed by surgeon for analgesia, and the patient was extubated at the end of the case with unremarkable postoperative course.
- On hospital day seven, chest radiograph (figure 2) was significantly improved and patient was discharged to home.
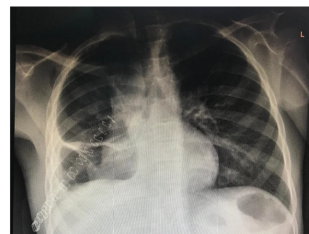
Figure 2: Chest radiograph on postoperative day seven showing post thoracotomy and right lower lobectomy changes on the right. There is persistent volume loss and elevation of the right hemidiaphragm with cicatricial atelectasis of the right mid and lower lung field due to pulmonary fibrosis. Right mediastinal shift is present due to compensatory hyperinflation of the left lung. Blunting of the right costophrenic angle is seen due to pleural scarring and likely small pleural effusion.

References:
1. Anesthesiology, 67.4, 587-589, 1987

Discussion

- Indications for OLV
  - lung isolation in setting of pulmonary hemorrhage or infection
  - surgical exposure in cardiothoracic surgery
  - controlled ventilation in patient with bronchopleural fistulas or giant bullae
- Lung isolation can be accomplished with various methods which include using a double lumen tube, uninvent tube, or bronchial blocker with or without fiberoptic guidance to confirm appropriate placement of the airway device.
- Equipment necessary for these methods may not available in many resource limited settings.
- Lung isolation options can be further limited in pediatric patients which sometimes necessitates placement of a single lumen tube into an endobronchial position with or without fiberoptic guidance.
- This patient's lung could have been isolated using an age-appropriate bronchial blocker, but due to the unavailability of a fiberoptic scope and a bronchial blocker, a SL-ETT was used.
- Although challenging, blind techniques with a SL-ETT can be performed for right lung isolation; for a blind left bronchus intubation, rotating the ETT 180 degrees while turning the patient's head to the right provides the highest success rate [1].
- Endobronchial intubation with SL-ETT limits access to the operative lung and creates challenges for operative lung bronchoscopy, suctioning, intermittent ventilation, and CPAP for supplemental oxygenation; this also limits options for addressing hypoxemia during OLV.
- OLV with SL-ETT also may not provide an adequate seal on the intubated bronchus and thus compromising lung protection and surgical exposure.
- Additionally, excellent communication among the perioperative team is essential for success. The anesthesiology and surgeon must consider all indications and limitations prior to the procedure.
- In conclusion, SL-ETT can be successfully used for left OLV in pediatric patients in resource limited settings.

Questions/Comments? Please contact:Harmandeep Singh, MD (has9053@nyp.org)

New York Academy of Medicine (NYAM)

Weill Cornell Medicine · **NewYork-Presbyterian**

The Non-Intubatable Pediatric Patient

Angelica M. Delgado, M.D., Jennifer K. Lee, M.D.
Department of Anesthesiology, New York Presbyterian Weill Cornell Medical Center
The New York Academy of Medicine Anesthesiology Residents' Night | October 3, 2019

Introduction:

Management of the pediatric airway can be challenging due to anatomical variation, post surgical changes, trauma, equipment availability, and operator experience.

Case Description:

We present the case of a 2 month old 2.31kg female with history of prematurity, encephalocele, and tracheoesophageal fistula status post repair who presented with respiratory failure on HFNC. Given that she was a known difficult airway, the patient was brought to the OR for intubation. After inhalational induction, each mode of intubation was deliberately attempted only once in conjunction with the ENT surgical team. These modes included direct laryngoscopy, direct laryngoscopy with tongue stitch and rigid scope, as well as oral and nasal fiberoptic with glidescope, all of which produced a grade 3 view. An AirQ 0.5 LMA was placed with adequate ventilation but no identifiable airway was appreciated when a fiberoptic was passed. A tracheostomy was performed while the patient was stably ventilated via the AirQ.

Airway Devices:

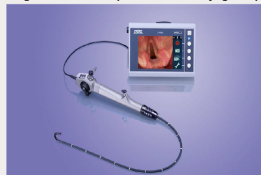**Figure A. Glide Scope for indirect laryngoscopy**

Figure B. Neonatatal Fiberoptic Scope

air-Q *Masked Laryngeal Airways*

Figure C. Pediatric Intubating Laryngeal Mask Airway

Discussion:

This case demonstrates the importance of :

- Airway management planning
- Caution with regard to causing airway trauma with multiple intubation attempts
- Limiting repeated attempts with any single mode of intubation when multiple attempts are likely
- A diverse repertoire of appropriately sized equipment for the pediatric patient
- Consultation and team based planning with other specialties such as the ENT surgical team

References:

1. AirQ LMA Image: https://cookgas.com/air-q-disposable-2/
2. Glidescope Image : https://www.pedpearls.com/videos
3. Neonatal Fiberoptic scope Image : https://www.karlstorz.com/gb/en/anesthesiology-and-emergency-medicine.htm

Poster 1

Weill Cornell Medicine · **NewYork-Presbyterian**

The Weekend Add-Ons Quality Improvement Initiative
### The New York Academy of Medicine, Anesthesiology Residents' Night

Olga Rozental, MD, PhD; Joel Ehrenfeld, MD, DPT; Margo Hoyler, MD; Michael Kim, MD; Jyun-You Liou, MD, PhD; Vanessa Ng, MD; Patricia Fogarty Mack, MD; Rohan Panchamia, MD | October 3, 2019

Introduction

Pre-operative assessments are an essential component of anesthesia care, which are mandated by the American Board of Anesthesiology and the Joint Commission. A thorough evaluation can reduce the risk of patient harm, while a last-minute evaluation may be less comprehensive and contribute to OR delays. The goal of this initiative was to promote timely evaluations for patients "added-on" for Monday morning surgery.

Current state and system

– When are Monday cases added-on?
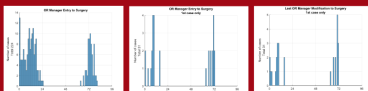
- 224 add-on cases from September – November 2018 (7 weeks); 31 cases were scheduled as first start cases (8:30 AM)
- Entered in OR manager after schedule for Monday was finalized on Friday (after 10 AM) or on Monday morning
- Weekly average first case bookings = 5

– What is the current system for adding on cases over the weekend?

– Is the current system perceived as problematic by providers?

Intervention

– The current system does not allow for generation of automated notifications to the department due to limited OR desk staffing and education regarding timely entry of add-on cases for future days.
– We implemented a novel notification system whereby on-call PACU residents identified and evaluated patients who had been added-on for Monday morning surgery on Saturday and Sunday by 4 PM.
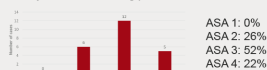
Results

– Notification rate gauged by percentage of add-on cases with completed pre-operative evaluations from May – July 2019
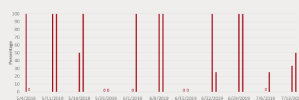
- 23 patients evaluated over 11 weekends
- Estimated completion rate: 46%
- Frequency of 100% completion rate: 31.8%
- Frequency of 0% completion rate: 31.8%

– Acuity of disease among patients from add-on cases
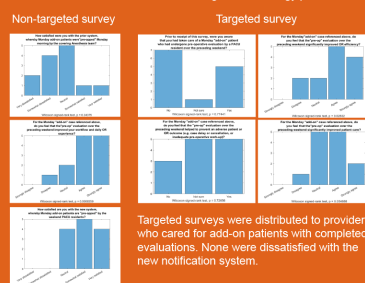

ASA 1: 0%
ASA 2: 26%
ASA 3: 52%
ASA 4: 22%

– Case volume and distribution (captured before 4 PM)
- Average number of Saturday add-ons: 2.3
- Average number of Sunday add-ons: 3
- Daily average number of weekend add-ons: 2.67 (range 1-6)
- Average time spent on pre-operative evaluations: 43 minutes (range 15-90)
- Percentage of cases that were first start: 13%
- Percentage of cases that went on Monday: 61%

Results (continued)

– Pre-operative clinical recommendations resulted from 13% of evaluations, which included cessation of ACE inhibitors and performance of EBUS in the general OR rather than the bronchoscopy suite for a patient with cardiac comorbidities.

– Post-intervention satisfaction among anesthesiology providers

Non-targeted survey   Targeted survey

Targeted surveys were distributed to providers who cared for add-on patients with completed evaluations. None were dissatisfied with the new notification system.

- 54% of providers believed that patient care improved; 69% reported better OR efficiency and 77% felt that workflow improved
- Residents were more dissatisfied with the new system than attendings or CRNAs

Conclusions

– The new notification system alerted providers of 46% of cases added-on over the weekend for Monday by 4:00 PM on Sunday.
– This system was thought to enhance patient care and OR efficiency.
– Many weekend add-on cases are not first start cases and do not happen on Monday.
– Limitations of this study include small case load, short intervention period, limited survey participation, and a lack of standardization for the evaluation process.

Poster 2

Weill Cornell Medicine · **NewYork-Presbyterian**

Improving Adherence to a PONV Prevention Protocol
New York Academy of Medicine Anesthesiology Residents' Night

Javier Sanchez MD, Jimmy Lin MD, Camille Roberts MD, Maria Quincy MD, Jolie Shosfy MD, Patricia Fogarty Mack MD, Douglas Carras MD | 10/03/2019

Why is prevention of Post-Operative Nausea and Vomiting Important?

– The general incidence of vomiting after general anesthesia is 30%
– The general incidence of nausea after general anesthesia is 50%
– In patients with risk factors, the incidence of PONV can be as high as 80%
– PONV can lead to longer PACU stays, unanticipated hospital admissions, greater cost, and lower patient satisfaction
– In high risk patients, it is roughly 100 times more expensive to treat PONV than it is to give prophylaxis for it, and treating vomiting is roughly 3 times more expensive than treating nausea.

Quality improvement in adherence to PONV prevention protocols

– A PONV prevention protocol was instituted at Weill Cornell Medicine (WCM) in 2017
– Global institutional compliance was analyzed utilizing ASPIRE (Anesthesiology Performance Improvement and Reporting Exchange) data
– Additionally, a chart review of high-risk patients undergoing breast and gynecologic surgery was performed
  » 694 cases identified between 9/1/2018 and 10/31/2018
  » In depth analysis of 70 cases performed
– A root cause analysis and various other quality improvement methods were utilized to identify barriers to successful implementation of the protocol.
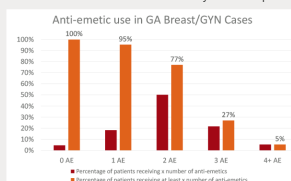
Current WCM PONV prevention protocol

Global institutional compliance

– The ASPIRE PONV prevention metric applies to adults > 18 years old receiving a general inhalational anesthetic with 3 or more risk factors for PONV
– Risk factors for PONV are based on the Apfel score and include female sex, history of PONV, history of motion sickness, non-smoking status, and administration of opioids during or after the case
– Success is measured by administration of 2 or more anti-emetics
– The average institutional compliance rate was 67% for the month of April 2019. This rate was stable dating back to June 2018.

Compliance in high PONV risk breast and gynecologic surgery

– Most patients in this category are considered high-risk (female sex, non-smokers, receiving opioids) and breast and gynecologic surgery has been shown to be emetogenic
– On average, patients in this category received 2 anti-emetics
– While 77% of these patients received 2 anti-emetics, only 27% received 3 anti-emetics as recommended by the WCM protocol

Anti-emetic use in GA Breast/GYN Cases

Barriers to compliance

– Education: lack of awareness of PONV prevention protocol
– Equipment: lack of easy access to additional pumps or propofol bottles
– Systems issues: ondansetron given pre-operatively at new ambulatory surgery center not being captured in ASPIRE

Interventions

– Quality improvement goal: to improve compliance with PONV prevention to 80% or more by January 2020
– Laminated copies of PONV prevention protocols were placed in all ambulatory surgery operating rooms
– New educational efforts implemented: grand rounds presentation and educational sessions for junior residents

Future Directions

– Technical solutions for systems issues being resolved with transition to new EMR
– Re-evaluation of current WCM PONV prevention protocol to encourage use of other anti-emetics (e.g. aprepitant) with more favorable side effect profiles that are more accessible currently
– Creation of Enhanced Recovery After Surgery (ERAS) protocol specific to ambulatory gynecologic and breast surgery

References

– Gan, Tong J, et al. Consensus Guidelines for the Management of Postoperative Nausea and Vomiting. Society for Ambulatory Anesthesiology. (2014). 118 (1): 185-113.
– Apfel CC, Läärä E, Koivuranta M, Greim CA, Roewer N. A simplified risk score for predicting postoperative nausea and vomiting: conclusions from cross-validations between two centers. Anesthesiology 1999;91:693–700
– Carroll NV, Miederhoff PA, Cox FM, Hirsch JD. Costs incurred by outpatient surgical centers in managing postoperative nausea and vomiting. J Clin Anesth 1994;6:364–9
– Frighetto L, Loewen PS, Dolman J, Marra CA. Cost effectiveness of prophylactic dolasetron or droperidol vs rescue therapy in the prevention of PONV in ambulatory gynecologic surgery. Can J Anaesth 1999;46:536–43

Enhanced Recovery After Surgery For Cesarean Delivery: Standardizing Protocols And Reducing Variability

Rohan Jotwani, MD, MBA; Ojas Mainkar, MD; Iisa Lee, MD; Justin Chung, MD; Kathy Matthews, MD; Robin Kalish, MD; Sharon Abramovitz, MD

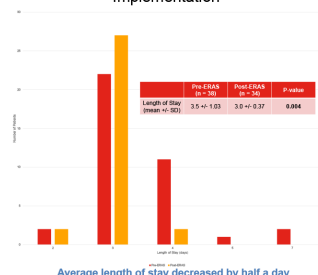**NewYork-Presbyterian**

Weill Cornell Medicine

Introduction

Enhanced recovery after surgery (ERAS) was developed as a way to standardize clinical care pathways and communicate across multidisciplinary teams to improve patient recovery. The goal of ERAS is to enhance the patient experience through active participation in recovery, while reducing hospital length of stay (LOS).

ERAS encompasses 4 main stages:
1. Planning and preparing before surgery
2. Reducing physical stress of the operation
3. Managing post-operative analgesia with a standardized regimen
4. Early feeding and ambulation

The objective of our quality improvement initiative was to implement an ERAS protocol for scheduled cesarean sections (CS) and evaluate its efficacy

LOS Data Pre- and Post-ERAS Implementation

	Pre-ERAS (n = 38)	Post-ERAS (n = 34)	P-value
Length of Stay (mean +/- SD)	3.5 +/- 1.03	3.0 +/- 0.37	0.004

Average length of stay decreased by half a day

OB Discharges – Cesarean Deliveries 2017 vs 2018

OB Discharges – All Deliveries 2018 vs 2019

Methods:

We prospectively monitored patients 3 weeks prior to and 3 weeks subsequent to implementation of an ERAS for CS protocol. Patients were provided with a detailed information sheet explaining what to expect before, during and after their CS, both in the obstetrician's office and on arrival for pre-operative laboratory testing. On the day of scheduled surgery, patients were maintained on an ERAS pathway of care, and were given a survey asking how well they were informed of items such as NPO guidelines, pain management options, and LOS.

Results

- 38 patients in the pre-ERAS group and 33 patients in the post-ERAS group.
- We were able to demonstrate a mean LOS of 3.5 +/- 1.03 for the pre-ERAS group and 3.0 days +/- 0.37 for the post-ERAS group, translating to a reduction of 0.5 days, p=0.004.
- Subgroup analysis of satisfaction scores between pre-ERAS (n=20) and post-ERAS (n=19) groups did not show a statistical difference; both groups had a median score of 5/5 [IQR 4-5], p=0.99.

Conclusions

- Decreased LOS in scheduled within the first 3 weeks of implementing ERAS, without compromising patient experience.
- A shorter LOS offers substantial cost savings for the health care system, room for more throughput, and less risk to patients.
- Future goals include sustainability of the ERAS, continued implementation in patients requiring intrapartum CS, and expansion to other hospitals within our enterprise.

References

Caughey AB, et al. Am J Obstet Gynecol. 2018.
Lucas DN, Gough KL. Int J Obstet Anesth. 2013.
Wilson RD, et al. Am J Obstet Gynecol. 2018.

New York Simulation Center for the Health Sciences (NYSIM)

Weill Cornell Medicine

NewYork-Presbyterian

Application of Mastery Learning Principles to Anesthesiology Intern Intubation Training

Liang Shen, MD, MPH, Lori Rubin, MD, Eric Brumberger, MD, Kane Pryor, MD

Background

Mastery learning is a method of **competency-based learning** emphasizing the use of **baseline testing** (pre-test), **evaluation tool creation**, **deliberate practice** with instructors, and **formative testing** (post-test) to gauge mastery. The method has been used successfully in various medical education settings including simulation teaching for procedural skills.

The anesthesiology interns in our residency program already utilize a simulation curriculum early in their training to prepare them for the operating room environment, as well as to provide overview of routine procedures such as intravenous (IV) access and endotracheal intubation. However, the curriculum does not teach procedures in a highly structured format nor does it systematically evaluate the interns on their performance. Our goal was to **enhance intern learning** of the intubation procedure using mastery learning methods as part of their simulation teaching.

Methods

We utilized mastery learning principles to construct an **objective**, **checklist evaluation tool** that reflected a typical IV anesthetic induction, followed by mask ventilation and endotracheal intubation, with each step of the procedure listed as a discrete, observable action to be performed by the trainee (Figure 1). The tool was developed by two board-certified practicing anesthesiologists and revised with input from the director of education of simulation at our institution. The tool consists of 21 steps, each step graded as "not performed (0 points)," "performed (1 point)," and "performed well (2 points)."

Six anesthesiology interns were included as trainees in the education program. On the first day of their anesthesiology rotation, each trainee was allotted 30 minutes to participate in the **pre-test**, followed by **deliberate practice and coaching** with an instructor. The same board-certified practicing anesthesiologist evaluated the trainees and provided the coaching. The session was performed in the simulation lab, which replicates the operating room (OR) environment using a Sim-Man mannequin, intubation equipment, a functioning IV line, mock anesthetic induction drugs, and an anesthesia ventilator. A **post-test** was administered to the interns **1 week later**, and evaluated by the same anesthesiologist instructor, and a short debriefing was provided. A questionnaire was emailed to the trainees after the pre-test session, and again after the post-test, to gauge reaction to the sessions.

Purpose

To apply the Mastery Learning principles of deliberate practice, coaching, and instrument creation to simulation training to improve anesthetic induction and intubation practices in anesthesiology interns

	Action (Performed and/or verbalized)	Performed Well	Performed	Not Performed
1	Checks laryngoscope light for operation			
2	Checks ETT cuff by inflation/deflation			
3	Pre-oxygenated the patient for at least 5 breaths, or achieve expired O_2 of >80%			
4	Gave appropriate dose of propofol (2-2.5 mg/kg = 120-150 mg)			
5	Gave appropriate dose of rocuronium (0.6-1.0 mg/kg = 36-60 mg)			
6	Creates adequate seal with mask • appropriate placement of hands to create seal • inspects for areas of poor seal with face • may use head straps			
7	Adjusts APL valve to mask ventilate patient			
8	Attains $ETCO_2$ >20 and <50 mmHg during mask ventilation			
9	Maintains peak airway pressure <20 cmH_2O during manual ventilation			
10	Waited for paralytic to take effect before attempting intubation by checking train-of-four			
11	Introduces laryngoscope atraumatically			
12	Places ETT into trachea atraumatically			
13	Inflates ETT cuff with <30ml air			
14	Maintains control of ETT at all times (prior to taping)			
15	Manually ventilates through ETT			
16	Verifies endotracheal intubation by observation • observes bilateral chest rise • observes ETT fog • observes appropriate $ETCO_2$ capnograph			
17	Verifies endotracheal intubation by auscultation • auscultates chest in bilateral mid-axillary lines • auscultates epigastrium • listens for audible air leak around ETT cuff at inspiratory pressure of 20-25 cmH_2O			
18	Notes ETT depth at teeth			
19	Tapes ETT			
20	Turns on appropriate dose of anesthetic gas			
21	Turns on ventilator			

Figure 1. Checklist Evaluation Tool

Outcomes

All 6 interns improved in their anesthetic induction and intubation skills (Figure 2). The pre-test average score of all interns was 13.2, with a median score of 14, while the post-test average was 24.8, with a median score of 26. The range of improvement in score was 3 to 21.

Five of 6 trainees responded to the pre-test and deliberate practice session questionnaire, and 4 of 6 responded to the post-test questionnaire. Overall, the trainees reported that **knowledge gained from both sessions were clinically-applicable**, was **likely to improve their performance in the OR**, and that they would like **more similar sessions in the future**. On the post-test questionnaire, the trainees reported **increased comfort with the simulation scenario** as compared to the pre-test questionnaire.

Conclusion

Application of mastery learning principles including the development of an objective evaluation tool, deliberate practice, and coaching, appear to **improve anesthesiology intern skills** at anesthetic induction and intubation, and yields **positive reactions from the trainees** about clinical applicability. Future plans for development of this program include expansion to the rest of the anesthesiology intern class, and consideration for addition of sessions dedicated to other procedural skills.
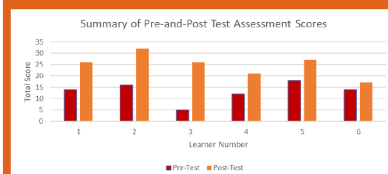
Summary of Pre-and-Post Test Assessment Scores

Figure 2. Pre and Post-test Assessment Scores

Weill Cornell Medicine
Anesthesiology

PostGraduate Assembly in Anesthesiology (PGA)

Weill Cornell Medicine
NewYork-Presbyterian

The Effect of Obstructive Sleep Apnea on Readmissions and Atrial Fibrillation after Cardiac Surgery

T. Robert Feng (MD), Robert S. White (MD), Gulce Askin (MPH), Kane Pryor (MD)
Department of Anesthesiology, New York-Presbyterian/Weill Cornell Medical Center, New York, NY

Introduction

- Obstructive sleep apnea (OSA) remains a disease with high prevalence and a wide spectrum of severity, with evidence that even mild disease can be associated with significant patient morbidity
- Effect on the cardiovascular system is particularly interesting with both clinical and animal studies demonstrating a predisposition to developing atrial fibrillation
- Several studies have demonstrated an association between OSA and post-operative morbidity in the cardiac surgery population
- However, few studies explore the effects of OSA on hospital readmissions, despite the link between OSA and atrial fibrillation
- This study seeks to understand the effect of OSA on hospital readmissions and post-operative atrial fibrillation after cardiac surgery

Methods

- Retrospective cohort study on 2007-2014 data from CA, FL, NY, MD, and KY from State Inpatient Databases, Healthcare Cost and Utilization Project
- Patients ≥18 years old for CABG or valve surgery
- Exclusions: death during index hospitalization, missing data, or insufficient follow-up
- Patients identified using ICD-9-CM codes for CABG, valve repair, and valve replacement
- Grouped into cohorts based on OSA status
- Primary outcomes were unadjusted rates and adjusted odds of 30-day readmission
- Secondary outcomes were odds of post-operative atrial fibrillation and readmission diagnoses
- Multivariable generalized estimating equations used to assess relationship between OSA status and both 30-day readmission and atrial fibrillation
- All study activities were approved by the Weill Cornell Medicine IRB

Results

- Sample size: 506,728 patients; 506,604 met inclusion/exclusion criteria
- 30-day readmission rate was 17.2% (OSA 19.6% vs. non-OSA 17.1%, p<0.001)
- OSA had higher odds of 30-day readmission vs. non-OSA (OR = 1.08, 95% CI 1.06 - 1.11)
- Patients with OSA more likely to develop post-operative atrial fibrillation vs. non-OSA (OR = 1.04, 95% CI 1.01 - 1.08)
- The most common readmission diagnoses at 30 days were atrial fibrillation (38.6%), pleural effusion (23.3%), and wound infection (13.9%)

Table 1. Demographic and clinical characteristics of patients with and without OSA following CABG and/or valve surgery.

Characteristic	Total (n = 506604)	OSA (n = 32545)	Non-OSA (n = 474059)	P-value
Age (Years)	66.2±12.1	64.5±10.5	66.3±12.2	<0.001
Gender (Female)	161037 (31.8%)	7568 (23.3%)	153469 (32.4%)	<0.001
Mortality	14467 (2.86%)	729 (2.24%)	13738 (2.90%)	<0.001
30-Day Readmission	68259 (17.2%)	4721 (19.6%)	63538 (17.1%)	<0.001
Any Complications	386108 (76.2%)	26098 (80.2%)	360010 (75.9%)	<0.001
Atrial Fibrillation	183075 (36.1%)	13159 (40.4%)	169916 (35.8%)	<0.001

Table 2. Multivariable generalized estimating equation results for 30-day readmission and atrial fibrillation after CABG and/or valve surgery.

Independent Variables	30-Day Readmission [OR (95% CI)]	Atrial Fibrillation [OR (95% CI)]
Obstructive Sleep Apnea	1.08 (1.06 - 1.11)[b]	1.04 (1.01 - 1.08)[a]
Age	1.00 (1.00 - 1.00)[b]	1.03 (1.03 - 1.03)[b]
Sex (Female)	1.14 (1.13 - 1.16)[b]	0.94 (0.92 - 0.95)[b]
Any Complications	1.07 (1.06 - 1.08)[b]	
Length of Stay	1.03 (1.02 - 1.03)[b]	

Statistical significance is denoted as: [a] p < 0.01, [b] p < 0.0001

Table 3. Diagnoses on 30-day readmission by OSA status after CABG and/or valve surgery.

Diagnosis	Total (n = 68259)	OSA (n = 4721)	Non-OSA (n = 63538)	P-value
Pneumonia	9162 (13.4%)	624 (13.2%)	8538 (13.4%)	0.685
Atrial Fibrillation	26353 (38.6%)	1967 (41.7%)	24386 (38.4%)	<0.001
Atelectasis	5048 (7.40%)	423 (8.96%)	4625 (7.28%)	<0.001
Empyema	154 (0.23%)	8 (0.17%)	146 (0.23%)	0.494
Pleural Effusions	15922 (23.3%)	1061 (22.5%)	14861 (23.4%)	0.157
Pneumothorax	190 (0.28%)	10 (0.21%)	180 (0.28%)	0.450
Deep Vein Thrombosis	3808 (5.58%)	270 (5.72%)	3538 (5.57%)	0.687
Hypoxia	1738 (2.55%)	157 (3.33%)	1581 (2.49%)	0.001
Myocardial Infarction	6884 (10.1%)	384 (8.13%)	6500 (10.2%)	<0.001
Stroke	3506 (5.14%)	218 (4.62%)	3288 (5.17%)	0.101
Urinary Tract Infection	5464 (8.00%)	337 (7.14%)	5127 (8.07%)	0.025
Wound Infection	9457 (13.9%)	903 (19.1%)	8554 (13.5%)	<0.001

Conclusions

- OSA was found to be an independent risk factor for readmission within 30 days and post-operative atrial fibrillation in patients who underwent cardiac surgery
- Both OSA and atrial fibrillation have been shown to have associations with morbidity, suggesting this population is vulnerable to readmission
- May be related to adverse cardiac remodeling and vascular changes associated with OSA
- CPAP has been shown to have benefits in reverse remodeling and decreased recurrence of atrial fibrillation
- Obesity is a well-established risk factor for OSA and many conditions linked to OSA, including adverse cardiac remodeling and post-operative atrial fibrillation
- Further research is necessary to determine the optimal method to identify and manage patients at risk for OSA undergoing cardiac surgery in the perioperative period

Limitations

- OSA status may be misdiagnosed or categorized based on varying criteria, which may contribute to the heterogeneity of the dataset and create potential for confounding
- Study is retrospective and based on an administrative dataset; accuracy of results is reliant upon accurate documentation and may lack relevant clinical information that would provide insight into a patient's OSA status or comorbidities

References

1. Nagappa M et al. Postoperative Outcomes in Obstructive Sleep Apnea Patients Undergoing Cardiac Surgery: A Systematic Review and Meta-analysis of Comparative Studies. Anesth Analg. 2017;125(6):2030-2037.
2. Kaw R et al. Incremental risk of obstructive sleep apnea on cardiac surgical outcomes. J Cardiovasc Surg (Torino). 2006;47(6):683-689.
3. Iwasaki Y-K et al. Atrial fibrillation promotion with long-term repetitive obstructive sleep apnea in a rat model. J Am Coll Cardiol. 2014;64(19):2013-2023.
4. Zhao L-P et al. Sleep apnoea and unscheduled re-admission in patients undergoing coronary artery bypass surgery. Atherosclerosis. 2015;242(1):128-134.
5. Scalzitti NJ et al. Obstructive Sleep Apnea is an Independent Risk Factor for Hospital Readmission. J Clin Sleep Med JCSM Off Publ Am Acad Sleep Med. 2018;14(5):753-758.

Perioperative Outcomes for Liver Transplant or Hepatectomy Based on Race, Insurance Status, and Socioeconomic Status

John E. Rubin, MD; Iris Chu, MD; Robert S. White, MD; Gulce Askin, MPH; Zachary A. Turnbull, MD; Christine M. Lennon, MD

Department of Anesthesiology, NewYork-Presbyterian Hospital-Weill Cornell Medicine, New York, NY; Center for Perioperative Outcomes, Weill Cornell Medicine, New York, NY

Introduction

- Hepatobiliary disease (HBD) is a leading cause of morbidity and mortality in the United States
- Liver transplant or hepatectomy may be curative for those with hepatocellular carcinoma (HCC) or cirrhosis
- In 2004, the Model for End-Stage Liver Disease (MELD) scoring system was adopted to better evaluate the severity of HBD and the utility of a liver transplant
- Pre-MELD database studies reveal disparate outcomes for patients with HCC or undergoing a liver transplant based on age, race, sex, insurance status, and socioeconomic status

Why Re-examine the Topic?

- Despite adoption of the MELD system, evidence suggests that disparities persist for surgical outcomes
- Since the last comprehensive evaluations nearly 20 years ago, there having been numerous system advancements:
  - Adoption of the MELD score to optimize patient selection
  - Improvements in surgical techniques
  - Improvements in perioperative anesthetic management
- Thus, there is a need for a contemporary reassessment of the perioperative surgical outcomes for liver transplants and hepatectomies in the post-MELD score era

Advantages and Limitations

- Most up-to-date and comprehensive analysis of healthcare outcomes for liver transplant or hepatectomy patients
- Patient chart level data
- Population cohort included in this analysis represents 32% of the US population
- Can control simultaneously for a wide range of confounders
- Difficult to draw direct conclusions from the data due to the retrospective nature of the analysis
- The HCUP database does not provide us with a MELD score for each patient or the capability to link database

Methods

- We conducted a retrospective analysis of liver transplants and hepatectomies between 2007-2014 for adults in California, Florida, New York, Kentucky, and Maryland using the State Inpatient Databases (SID), Healthcare Cost and Utilization Project (HCUP)
- Patients aged 18 and older were included
  - The primary outcome was mortality
  - Secondary outcomes were length of stay (LOS), 30-day readmission, 90-day readmission, and total charge incurred
- A multivariable generalized estimating equation was used to assess the independent effect of payer status and race on mortality, adjusting for patient demographics, comorbidities, surgical level and hospital level factors
- Statistical significance was set a priori at alpha <0.05

References

1. Peters NA, Javed AA, He J, Wolfgang CL, Weiss MJ. "Association of socioeconomics, surgical therapy, and survival of early stage hepatocellular carcinoma." J Surg Res. 2017 Apr;210:253-260. doi: 10.1016/j.jss.2016.11.042. Epub 2016 Nov 30. PubMed PMID: 28457336.
2. Nobel YR, Forde KA, Wood L, Cartiera K, Munoz-Abraham AS, Yoo PS, Abt PL, Goldberg DS. "Racial and ethnic disparities in access to and utilization of living donor liver transplants." Liver Transpl. 2015 Jul;21(7):904-13. doi: 10.1002/lt.24147. Epub 2015 Jun 9. PubMed PMID: 25866817
3. Parikh A, Washburn KW, Matsuoka L, Pandit U, Kim JE, Almeda J, Mora-Esteves C, Halff G, Genyk Y, Holland B, Wilson DJ, Sher L, Koneru B. "A multicenter study of 30 days complications after deceased donor liver transplantation in the model for end-stage liver disease score era." Liver Transpl. 2015 Sep;21(9):1160-8. PubMed PMID: 25991395
4. Buchanan P, Dzebisashvili N, Lentine KL, Axelrod DA, Schnitzler MA, Salvalaggio PR. "Liver transplantation cost in the model for end-stage liver disease era: looking beyond the transplant admission." Liver Transpl. 2009 Oct;15(10):1270-7. PubMed PMID: 19790155.
5. Nair S, Eustace J, Thuluvath PJ. "Effect of race on outcome of orthotopic liver transplantation: a cohort study." The Lancet. 2002 Jan; 358(9303):287-29. PubMed PMID: 11830194

Question/Comments? Please contact:
John E. Rubin, MD (jer9173@nyp.org)

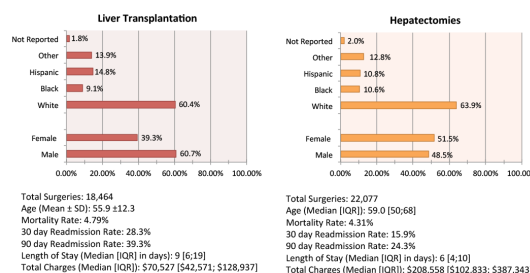## Demographics and Overall Surgical Outcomes

Liver Transplantation
- Not Reported: 1.8%
- Other: 13.9%
- Hispanic: 14.8%
- Black: 9.1%
- White: 60.4%
- Female: 39.3%
- Male: 60.7%

Total Surgeries: 18,464
Age (Mean ± SD): 55.9 ±12.3
Mortality Rate: 4.79%
30 day Readmission Rate: 28.3%
90 day Readmission Rate: 39.3%
Length of Stay (Median [IQR] in days): 9 [6;19]
Total Charges (Median [IQR]): $70,527 [$42,571; $128,937]

Hepatectomies
- Not Reported: 2.0%
- Other: 12.8%
- Hispanic: 10.8%
- Black: 10.6%
- White: 63.9%
- Female: 51.5%
- Male: 48.5%

Total Surgeries: 22,077
Age (Median [IQR]): 59.0 [50;68]
Mortality Rate: 4.31%
30 day Readmission Rate: 15.9%
90 day Readmission Rate: 24.3%
Length of Stay (Median [IQR] in days): 6 [4;10]
Total Charges (Median [IQR]): $208,558 [$102,833; $387,343]

Table 1. Risk-adjusted Odds Ratios for Liver Transplants

	Mortality	30 Day Readmission	90 Day Readmission	Length of Stay	Total Charges
Age	1.028 (1.018, 1.039)***	0.995 (0.991, 0.998)**	0.996 (0.993, 0.999)*	1.004 (1.002, 1.007)***	0.999 (0.998, 1.001)
Female Gender	0.852 (0.723, 1.004)	0.984 (0.924, 1.049)	1.039 (0.980, 1.102)	1.023 (0.983, 1.064)	0.939 (0.914, 0.965)***
Medicaid	1.186 (0.938, 1.499)	1.235 (1.110, 1.373)***	1.276 (1.132, 1.437)***	1.180 (1.103, 1.263)***	1.078 (1.043, 1.114)***
Medicare	1.295 (1.110, 1.510)***	1.196 (1.076, 1.329) ***	1.209 (1.098, 1.331)***	1.096 (1.039, 1.156)***	1.0537 (1.009, 1.101)*
Other Payer	0.977 (0.602, 1.589)	0.802 (0.566, 1.135)	0.829 (0.659, 1.045)	1.018 (0.878, 1.182)	0.953 (0.843, 1.078)
Self-pay/ no charge	2.591 (1.407, 4.770)**	0.825 (0.521, 1.306)	0.760 (0.533, 1.082)	1.035 (0.890, 1.203)	0.905 (0.836, 0.980)*
Black	1.372 (1.013, 1.859)*	1.120 (0.968, 1.298)	1.104 (0.932, 1.308)	1.005 (0.933, 1.083)	1.013 (0.967, 1.062)
Hispanic	1.052 (0.832, 1.330)	0.949 (0.872, 1.031)	0.929 (0.846, 1.019)	0.993 (0.924, 1.068)	1.017 (0.983, 1.052)
Missing	1.220 (0.753, 1.979)	0.606 (0.384, 0.956)*	0.687 (0.432, 1.093)	0.945 (0.847, 1.054)	0.979 (0.740, 1.294)
Other	1.142 (0.865, 1.508)	0.808 (0.715, 0.913)***	0.762 (0.662, 0.878)***	0.935 (0.882, 0.992)*	0.945 (0.887, 1.008)

Denotes *p<0.05, **p<0.01, ***p<0.001

Table 2. Risk-adjusted Odds Ratios for Hepatectomies

	Mortality	30 Day Readmission	90 Day Readmission	Length of Stay	Total Charges
Age	1.010 (1.004, 1.017)**	0.993 (0.990,0.997)**	0.995 (0.991, 0.998)**	0.999 (0.997, 1.001)	0.998 (0.996, 0.999)***
Female Gender	0.649 (0.553,0.762)***	0.949 (0.861, 1.045)	1.010 (0.935, 1.090)	0.884 (0.855, 0.914)***	0.896 (0.871, 0.921)***
Medicaid	1.161 (0.877, 1.538)	1.131 (0.949, 1.347)	1.192 (1.046, 1.358)**	1.300 (1.203, 1.405)***	1.097 (1.052, 1.144)***
Medicare	1.367 (1.099, 1.700)**	1.183 (1.060, 1.320)**	1.155 (1.047, 1.274)**	1.213 (1.155, 1.274)***	1.093(1.060, 1.126)***
Other Payer	1.895 (1.336, 2.687)***	0.780 (0.575, 1.057)	0.940 (0.712, 1.244)	1.066 (0.954, 1.193)	1.011 (0.943, 1.084)
Self-pay/ no charge	5.036 (3.744, 6.775)***	0.852 (0.596, 1.220)	0.865 (0.627, 1.193)	1.008 (0.838, 1.214)	0.932 (0.812, 1.071)
Black	1.022 (0.786, 1.329)	1.028 (0.863, 1.223)	1.064 (0.930, 1.216)	1.130 (1.056, 1.210)***	1.038 (0.994, 1.084)
Hispanic	0.926 (0.718, 1.915)	0.980 (0.872, 1.101)	1.016 (0.918, 1.124)	1.017 (0.952, 1.087)	1.026 (0.981, 1.075)
Missing	1.070 (0.667, 1.714)	0.771 (0.525, 1.131)	0.838 (0.609, 1.152)	1.018 (0.913, 1.135)	1.007 (0.934, 1.086)
Other	0.894 (0.682, 1.172)	0.684 (0.583, 0.802)***	0.715 (0.606, 0.843)***	0.987 (0.929, 1.049)	0.958 (0.913 1.005)

Denotes *p<0.05, **p<0.01, ***p<0.001

Results

- For Liver Transplant patients:
  - Medicare insurance status was independently associated with a higher odds of mortality compared to private payer status
  - Medicare and Medicaid were associated with increased 30- and 90- day readmission rates, length of stay, and total charges
  - African-Americans were more likely to die, but there was no increased mortality for any other racial status
- For Hepatectomy patients:
  - Medicare and self-pay insurance statuses were independently associated with a higher odds of mortality
  - Medicare and Medicaid were associated with increased 30- and 90- day readmission rates, length of stay, and total charges
  - Woman had a significantly lower risk of mortality
  - No racial disparities were observed

Conculsions

- Despite adoption of the MELD score in 2004, and other systems improvements, outcome disparities still persist for both patients undergoing liver transplantation or hepatectomy
- Insurance status has the greatest burden of disparities

Correcting arterial hypotension with a beta-blocker: a case report

Authors: Wineland, Larry MD*, Fischer, Gregory MD FASA†, Lewis, Alexis MD†

*Department of Anesthesiology, Weill Cornell Medical College, New York, NY
† Department of Anesthesiology, Memorial Sloan Kettering Cancer Center

Weill Cornell Medicine
NewYork-Presbyterian

Case: a 77 year old 102kg male presented as a late add-on case for right thoracoscopic Pleurex placement, pleural biopsy and flexible bronchoscopy.

Pre-operative details: The patient's history was notable for being a 9/11 first responder, now with recurrent right pleural effusions, most recently drained one week prior to admission, with cytology suggestive of mesothelioma. Now presenting with re-accumulation of right effusion on bedside ultrasound with near total atelectasis of right lung. Also with A Fib on apixaban, AICD placed for prior episode of VTACH, recent TTE notable for asymmetrical septal hypertrophy and moderate systolic anterior motion, with no other cardiac issues, no current PFTs available, with surgical team expressing concern for potential hemothorax component of effusion, given anti-coagulation and Hb decline to 9.6 from 10.6 one week prior.

Anesthetic Plan: pre-induction arterial line, two large bore IVs, iGEL 5 for bronchoscopy, video laryngoscopy given anterior appearing airway, 39 French left sided double lumen tube to facilitate lung isolation, magnet to disable AICD function, foley catheter, 2 units RBCS available.

Anesthetic Course: Patient was pre-oxygenated for 6 minutes, with radial arterial line placed during pre-oxygenation. HR was 102 and BP was 100/62 pre-induction. Pt was induced with 100mg propofol, 100mcg lidocaine and 100mg fentanyl. On induction pt rapidly desaturated to 62% in spite of adequate mask ventilation, decision was made to abort LMA/bronchoscopy and pt was quickly intubated using video laryngoscopy with 8.0 endotracheal tube with R bronchial blocker placed under fiberoptic guidance, with improvement in saturations to 100%, with minimal HR increase to 106 and only mild BP fluctuation, and no changes in hemodynamics or oxygenation with one lung ventilation.
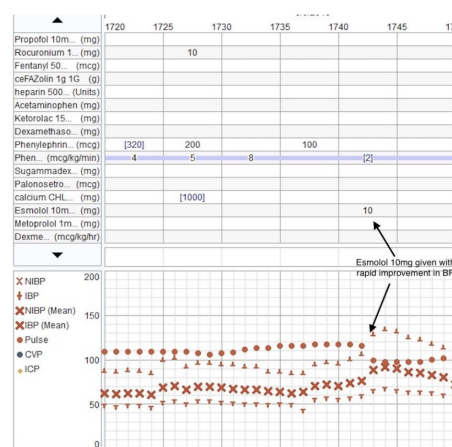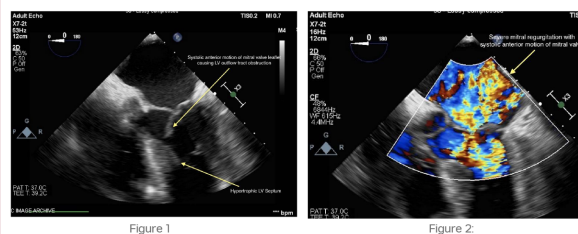

Figure 1

Figure 2:

Figure 3:

Anesthetic Course continued: After incision VATS exploration revealed large clot with hemothorax, and decision was made to convert to thoracotomy. During thoracotomy and clot evacuation, combined clot/hemothorax/EBL was approximately 5L, with HR increase to 118 and hypotension requiring phenylephrine, with extremely high doses of 8mcg/kg/min required to maintain a BP of 86/50. Given history of HOCM, urgent TEE was performed which revealed a small, hyper dynamic left ventricle with severe mitral regurgitation as a result of systolic anterior motion of the mitral valve with outflow tract obstruction (Figure 1, Figure 2 doppler). 10mg of esmolol was then given causing a reduction of HR to from 118 to 98bpm and marked improvement of BP to 140 /80 (Figure 3). A subclavian central line was placed, and after further correction of pre-load with 1700cc of normosol, 500cc of albumin and 2 units RBCs, pressors were weaned off entirely, and 2.5mg metoprolol was given to sustain stable HR. The patient was transported to PACU intubated, hemodynamically stable, and extubated the next day.

Conclusion: In this patient with HOCM who tolerated baseline tachycardia, the volume shifts and small increase in tachycardia caused by draining a hemothorax led to systolic anterior motion of the mitral valve with LV outflow obstruction, and hemodynamic instability refractory to high dose vasopressors but responsive to low dose beta blockade. HOCM patients are extremely sensitive to tachycardia and hypovolemia. Beta-blockade should be the first line treatment for hypotension alongside volume replacement.

References
Clinical Course and Management of Hypertrophic Cardiomyopathy
N Engl J Med 2018; 379:655-668
DOI: 10.1056/NEJMra1710575

Society of Cardiovascular Anesthesiologists (SCA)

Weill Cornell Medicine Anesthesiology

Anesthetic Management Of A Parturient With Repaired Anomalous Left Coronary Artery From The Pulmonary Artery After Takeuchi Procedure

NewYork-Presbyterian

Cindy Cheung, MD[1], Danielle McCullough, MD[1], Robert White, MD[1], Farida Gadalla, MD[1]

[1]Department of Anesthesiology, New York-Presbyterian Hospital Weill Cornell Medicine, New York, NY

INTRODUCTION

Anomalous left coronary artery from the pulmonary artery (ALCAPA) is a rare congenital disorder that requires early diagnosis and prompt surgical repair with good prognosis. Here we describe the anesthetic management of a parturient with ALCAPA after remote Takeuchi repair.

TAKEUCHI PROCEDURE
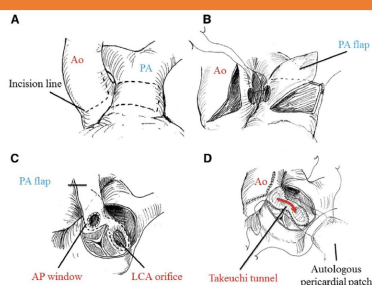
CASE DETAILS

28yoF G2P1 h/o ALCAPA s/p Takeuchi procedure during infancy and prior PVR, presented in labor at 37 wks. Antepartum TTE: mildly decreased LV systolic function and diastolic dysfunction with elevated left ventricular filling pressure (>= 20mmHg). There was supravalvular pulmonic stenosis at the ALCAPA repair with peak gradient 31 mmHg, mean gradient 18 mmHg, and elevated RVSP (53 mmHg).

ANESTHETIC CONSIDERATIONS

Peripartum concerns
Possibility of large volume blood loss from postpartum hemorrhage→ reduced preload →coronary ischemia
Valsalva during 2nd stage of labor→reduced preload (MFM w/ forceps experience available to assist labor)
Hypervolemia→worsen RV fxn

Monitoring
Continuous Telemetry during labor
Radial arterial line placed after CSE
CCU postpartum observation

Anesthetic
CSE placed early in labor with only 25mcg fentanyl as intrathecal dose and epidural infusion of bupivacaine 0.0625% +fentanyl 2mcg/mL @10ml/hr

A healthy infant was born via vaginal delivery. Postpartum TTE: incomplete recovery of LV function with mildly decreased EF (50-55%) when compared to her TTE prior to pregnancy (55-60%), in addition to moderate PI and mild RV dilation.

DISCUSSION

ALCAPA is a rare congenital anomaly (incidence 1:300,000 cases per year) that requires prompt surgical repair to reestablish coronary perfusion. Though there are few documented cases of parturients with repaired ALCAPA, it is important to understand how to care for this patient population. Patients who receive this procedure may have main pulmonary artery stenosis in the area of the intrapulmonary baffle, which could lead to PI and RV distension and failure. There is a risk for coronary ischemia in the setting of decreased flow through the intrapulmonary baffle as in the setting of large volume blood loss from PPH or systemic vasodilation from neuraxial anesthesia. Multidisciplinary meetings between anesthesia, OBGYN and cardiology is recommended. Early epidural placement would be advisable to reduce cardiac demand in the setting of pain with close hemodynamic monitoring with an arterial line. Avoidance of overt sympathectomy from a local anesthetic spinal dose would also be recommended.

REFERENCES

1. Cauldwell M, Swan L, Von klemperer K, Patel R, Steer P. Management of ALCAPA in two pregnancies. Int J Cardiol. 2015;181:353-4.
2. Ginde S, Earing MG, Bartz PJ, Cava JR, Tweddell JS. Late complications after Takeuchi repair of anomalous left coronary artery from the pulmonary artery: case series and review of literature. Pediatr Cardiol. 2012;33(7):1115-23
3. Image by Hoashi T, Kagisaki K, Okuda N, Shiraishi I, Yagihara T, Ichikawa H. Indication of Takeuchi technique for patients with anomalous origin of the left coronary artery from the pulmonary artery. Circ J. 2013;77(5):1202-7.

Anesthetic Management of Congenital Long QT Syndrome in Labor and Delivery

2019 Annual Meeting of the Society of Cardiovascular Anesthesiologists, Chicago May 18, 2019
Meghan Daly, MD, Robert White, MD, Danielle McCullough, MD
Department of Anesthesiology, New York Presbyterian Hospital Weill Cornell Medicine, New York, New York.

Introduction

Congenital long QT syndrome (LQTS) is a rare disease caused by mutations of potassium and sodium ion channels leading to abnormal myocardial repolarization. Patients with LQTS are at risk for ventricular tachycardia, torsades de pointe, and sudden cardiac death. We describe a case of uncomplicated vaginal delivery under combined spinal-epidural (CSE) analgesia in a parturient with congenital LQTS.

Case Description

A 35 year old G1P0 at 40 weeks 4 days gestational age was scheduled for induction of labor with dinoprostone. Her initial presentation of LQTS was at age 26 after syncope while running and confirmed via genetic testing at age 29. Management prior to pregnancy included ICD placement and 40mg nadolol daily.

On admission to the labor and delivery floor, initial ECG demonstrated sinus bradycardia at 50 BPM with a QTc of 430 msec. A CSE was placed early in the patient's labor course. A narcotic only spinal dose of 10 mcg of fentanyl was administered. Epidural analgesia was maintained with intermittent bolus patient-controlled epidural analgesia of 0.0625% bupivacaine and 2 mcg/cc fentanyl. Continuous telemetry monitoring was maintained throughout the hospitalization. Electrolytes were monitored daily and maintained with goals of K>4 mEq/L and Mg>2 mg/dL. QT prolonging medications were avoided; oxytocin was not used for either induction of labor or as a postpartum uterotonic. Measures were taken to minimize avoidable sympathetic stimulation, including keeping the labor room quiet. She remained hemodynamically stable throughout labor, delivery, and the postpartum period having given birth to a healthy newborn via normal vaginal delivery.
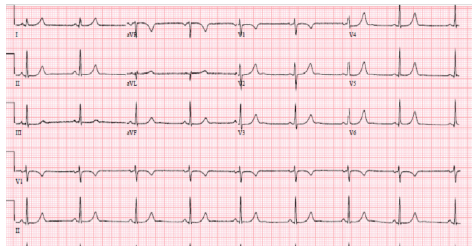

Figure 1: EKG on presentation to Labor and Delivery

Discussion

Women with LQTS are at increased risk for arrhythmias and cardiac events in the peripartum period. Beta-blockade has been associated with a reduction in cardiac event rate in this high-risk period.[1] Beta-blockers are non-teratogenic and though secreted in breast milk, have low risk of adverse effects in neonates with normal renal and hepatic function.[2]

During labor and delivery, avoidance of high sympathetic tone is important to reduce the risk of precipitating arrhythmias. This can be accomplished by minimizing environmental triggers and early initiation of labor analgesia. Epidural labor analgesia may also facilitate operative vaginal delivery and avoid the Valsalva maneuver, which can prolong the QTc in healthy non-pregnant individuals.[3]

Oxytocin is often used in the peripartum period for both induction of labor and for prophylaxis against and treatment of postpartum hemorrhage. Potential side effects of oxytocin include hypotension and prolongation of the QT interval.[2] In the management of our patient, oxytocin was avoided and she did not experience uterine atony or postpartum hemorrhage.

Conclusion

Delivery planning of parturients with congenital LQTS benefits from a multidisciplinary team of anesthesiologists, obstetricians, and cardiologists. Vaginal delivery can be safely undertaken under epidural analgesia in women with LQTS.

References

1. Ishibashi K, Aiba T, Kamiya C, et al. Arrhythmia risk and β-blocker therapy in pregnant women with long QT syndrome. Heart. 2017;103:1374-1379.
2. Drake E, Preston R, Douglas J. Brief review: Anesthetic implications of long QT syndrome in pregnancy. Can J Anesth. 2007;54:561-572.
3. Mitsutake A, Takeshita A, Kuroiwa A, Nakamura M. Usefulness of the Valsalva maneuver in the management of the long QT syndrome. Circulation 1981;63:1029-1035.

Insurance Status and Socioeconomic Markers Affect Readmission Rates after Cardiac Valve Surgery

T. Robert Feng (MD), Marguerite M. Hoyler (MD), Xiaoyue Ma (MS), Robert S. White (MD, MS)
Department of Anesthesiology, New York-Presbyterian/Weill Cornell Medical Center, New York, NY

Introduction

- Hospital readmissions are associated with inferior outcomes and increased costs
- Insurance status and other socioeconomic markers have been identified as risk factors for readmission in various other surgeries
- Despite valve surgery having high readmission rates and costs, few studies have explored the impact of insurance on valve readmissions
- Thus, we aimed to better characterize the effects of insurance and socioeconomic markers on this cohort
- We hypothesized that non-private insurance and low socioeconomic status would be associated with increased readmissions

Methods

- Retrospective cohort study on 2007-2014 data from NY, FL, CA, and MD from State Inpatient Databases, Healthcare Cost and Utilization Project
- Patients ≥18 years old for valve repair/replacement were included
- Patients identified using ICD-9-CM codes for valve repair and replacement
- Grouped into cohorts based on insurance status (Medicare, Medicaid, self-pay/no charge, other, private insurance)
- Primary outcomes were unadjusted rates and adjusted odds of 30-day and 90-day readmissions by insurance status
- Secondary outcomes were adjusted readmissions odds for other socioeconomic markers
- Multivariable generalized estimating equations used to assess relationship between variables and readmission outcomes
- All study activities were approved by the Weill Cornell Medicine IRB

Results

- Sample size: 147,752 patients
- Overall readmission rate was 19.4% at 30 days and 27.6% at 90 days
- Highest rates seen in Medicaid and Medicare, lowest rates seen in private insurance
- Medicaid and Medicare had increased odds of readmission at 30 and 90 days vs. private insurance
- Black and Hispanic race had higher odds of readmission at 30 and 90 days vs. white race
- Missing race had lower odds vs. white race
- Odds of readmission decreased with increasing median income level (quartiles based on zip code)

Table 1. Demographic and clinical characteristics with readmission rates after cardiac valve surgery

Variables	30-Day Readmission	P-value	90-Day Readmission	P-value
Sex		<0.001		<0.001
Female	12698 (21.4%)		17850 (30.0%)	
Male	16009 (18.1%)		22913 (25.9%)	
Insurance		<0.001		<0.001
Private	5593 (14.3%)		7808 (20.0%)	
Medicaid	2168 (22.9%)		3104 (32.7%)	
Medicare	19907 (21.3%)		28347 (30.3%)	
Other	487 (16.6%)		710 (24.2%)	
Self-pay/ No charge	552 (19.8%)		794 (28.6%)	
Race		<0.001		<0.001
White	20808 (18.9%)		29542 (26.8%)	
Black	2147 (25.1%)		3087 (36.1%)	
Hispanic	3049 (21.5%)		4311 (30.4%)	
Other	2321 (18.5%)		3250 (26.0%)	
Missing	382 (15.8%)		573 (23.7%)	
Median Income Level (Based on zip code)		<0.001		<0.001
1st Quartile	6551 (21.4%)		9367 (30.6%)	
2nd Quartile	7157 (19.6%)		10155 (27.8%)	
3rd Quartile	7372 (19.0%)		10407 (26.9%)	
4th Quartile	7627 (18.2%)		10834 (25.8%)	
Overall	28707 (19.4%)		40763 (27.6%)	

Table 2. Multivariable generalized estimating equation results for 30-day and 90-day readmissions after cardiac valve surgery

Variables	30-Day Readmission [OR (95% CI)]	90-Day Readmission [OR (95% CI)]
Age	1.004 (1.002 – 1.005)[c]	1.004 (1.003 – 1.006)[d]
Sex (Female)	1.143 (1.107 – 1.179)[d]	1.125 (1.093 – 1.157)[d]
Insurance (Reference = Private insurance)		
Medicaid	1.303 (1.225 – 1.385)[d]	1.355 (1.284 – 1.430)[d]
Medicare	1.266 (1.207 – 1.327)[d]	1.315 (1.261 – 1.370)[d]
Other	0.978 (0.875 – 1.093)	1.001 (0.910 – 1.102)
Self-pay/ No charge	1.066 (0.940 – 1.209)	1.077 (0.972 – 1.194)
Race (Reference = White)		
Black	1.208 (1.134 – 1.286)[d]	1.261 (1.184 – 1.343)[d]
Hispanic	1.075 (1.024 – 1.128)[b]	1.078 (1.032 – 1.127)[c]
Missing	0.782 (0.690 – 0.886)[c]	0.810 (0.713 – 0.921)[b]
Other	0.992 (0.932 – 1.057)	0.964 (0.910 – 1.022)
Median Income Level (Based on zip code, reference = 1st Quartile)		
2nd Quartile	0.954 (0.916 – 0.994)[a]	0.941 (0.907 – 0.976)[b]
3rd Quartile	0.936 (0.898 – 0.976)[b]	0.921 (0.882 – 0.961)[c]
4th Quartile	0.928 (0.889 – 0.969)[c]	0.923 (0.887 – 0.961)[d]
Elixhauser Comorbidity Score (Reference = First Tertile)		
2nd Tertile	1.070 (0.992 – 1.153)	1.080 (1.007 – 1.158)[a]
3rd Tertile	1.213 (1.175 – 1.252)[d]	1.260 (1.222 – 1.300)[d]
Length of Stay	1.359 (1.298 – 1.422)[d]	1.526 (1.457 – 1.598)[d]
Total Charges	1.264 (1.196 – 1.336)[d]	1.268 (1.120 – 1.341)[d]

Statistical significance is denoted as: a = p < 0.05, b = p < 0.01, c = p < 0.001, d = p < 0.0001

Conclusions

- Medicaid and Medicare insurance, black and Hispanic race, and low household income are risk factors for readmission following cardiac valve surgery
- Association between readmissions and socioeconomic status is likely multifactorial and difficult to elucidate
- Poor access, lower quality of care, and less preventative care are likely reasons
- More comorbidities secondary to limited access and prevention may also contribute
- Financial stressors important
- Overall, findings suggest insurance status and socioeconomic factors may be important to consider in future payment models
- Further studies are necessary to better understand causation

Strengths/Limitations

- Retrospective study – selection bias, unable to infer causation
- Administrative database – misclassification bias from miscoding/misclassification, lacks detailed clinical information
- All valve types included; although limited post hoc analyses performed on valve subgroups corroborates results
- Readmission tracking limited to occurrences within same state as index hospitalization
- Major strengths in large sample size and geographically diverse sample population

References

1. Pack QR et al. J. Am. Heart Assoc. 5:e003544, 2016
2. Iribarne A et al. Ann. Thorac. Surg. 98:1274–80, 2014
3. Feng TR et al. Int. J. Surg. 54:7–17, 2018
4. Dodson JA et al. Circ. Cardiovasc. Qual. Outcomes 5:298–307, 2012
5. Benjamin EJ et al. Circulation. 135:e146–603, 2017

Mitral Stenosis In The Parturient

2019 Annual Meeting of the Society of Cardiovascular Anesthesiologists. Chicago. May 18, 2019

Jenessa K. Job, MD, Sharon Abramovitz, MD, Robert White, MD, Nathan Liu, MD
Department of Anesthesiology, New York Presbyterian Hospital Weill Cornell Medicine, New York, New York.

Introduction

- Mitral stenosis (MS) in the pregnant patient is uncommon, but can be associated with significant maternal morbidity and mortality, especially if severe [1].
- Due to an increase in cardiac output, pregnancy may unmask undiagnosed valvulopathy, particularly obstructive lesions [2].
- Care of the parturient with MS demands meticulous attention to preoperative optimization, multidisciplinary coordination, and vigilant monitoring.

Case Description

- 35-year-old nulliparous woman with a history of severe MS secondary to rheumatic heart disease presenting at 38 weeks gestation for induction of labor (IOL) due to cholestasis.
- Patient underwent balloon valvuloplasty 14 years prior due to increasing dyspnea, now asymptomatic and maintained on low-dose aspirin.
- Transthoracic echocardiogram (TTE) during the 2nd trimester showed mitral valve (MV) area of 1.7 cm^2, mild dilation of the LA, no pulmonary hypertension, and a MV mean gradient of 7 mmHg, consistent with mild MS.
- Multiple antepartum meetings between obstetrics, anesthesiology, cardiology, nursing, and the cardiac intensive care unit took place to coordinate peripartum care.
- Patient was admitted to the labor and delivery unit, placed on continuous telemetry monitoring, and received labor epidural. Invasive hemodynamic monitoring considered but deferred.
- Cesarean section required for failed IOL. Patient and infant tolerated the procedure well with no complications.
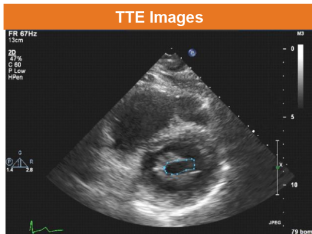
TTE Images

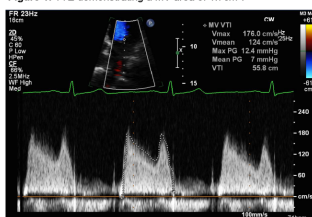**Figure 1:** TTE demonstrating a MV area of 1.7cm^2.

Figure 2: TTE showing a mean peak gradient of 7 mmHg.

Discussion

Disease Severity and Outcome
- Symptomatic MS in the parturient occurs when the MV area is less than 2.5 cm^2, with increasing morbidity as stenosis worsens [2].
- Larger LA diameter, smaller MV area, and pulmonary hypertension are associated with poorer outcomes[1], with pulmonary edema posing the greatest threat to the mother soon after delivery due to increased cardiac output from the autotransfusion of blood following uterine contraction [3].

Pre-pregnancy and Antepartum Management
- In patients with moderate to severe MS who are planning to become pregnant, corrective treatment is advised before pregnancy. If MS is first diagnosed during pregnancy, treatment with percutaneous transluminal commissurotomy or surgical repair may be necessary in severe cases or if medical management fails. [1]
- The mainstays of antepartum optimization in parturients with severe MS are heart rate reduction with beta-blockers, controlling LA pressure with dietary salt restriction and diuretics, and preservation of sinus rhythm with medications or cardioversion if necessary [2].
- Patients may require anticoagulation, particularly in the setting of chronic atrial fibrillation [1].

Intrapartum Management
- During delivery, an anesthetic technique that allows for gradual titration of analgesia to avoid sudden sympathectomy, hypotension, and reflex tachycardia is ideal [2].
- Thus, epidural anesthesia is a suitable choice, however general anesthesia may be necessary in some patients [2].
- Appropriate monitoring includes telemetry and continuous pulse oximetry [2]. Invasive monitoring of arterial blood pressure should be considered [3].

Conclusions

- Interdisciplinary coordination and planning during the antepartum period is paramount.
- For this patient, preoperative consultations with cardiology and anesthesiology as well as communication with the obstetricians and nursing staff led to adequate preparation, appropriate peripartum monitoring, and a favorable outcome for the patient and her infant.
- Although this patient's disease was mild, this approach to managing MS and coordinating care would also allow for appropriate care of patients with more severe MS.

References

1. Demir S, Bozkurt A, Akpinar O, Buyukkurt S, Akkus O, Demir A, Avsar MK, Seydaoglu G, and Acarturk E. The Effect of Mitral Stenosis on Maternal and Fetal Outcome in Pregnancy. Journal of Clinical & Experimental Cardiology. 2013; 4(3): 1-5.
2. Hess PE. Comorbidities in Obstetric Anesthesia. International Anesthesiology Clinics. 2014; 52(3): 110-131.
3. Burt CC and Durbridge J. Management of cardiac disease in pregnancy. Continuing Education in Anaesthesia, Critical Care & Pain. 2009; 9: 44-47.

Reporting the First Transcatheter Tricuspid Valve in Valve for Severe Bioprosthetic Tricuspid Stenosis in a Pregnant Woman

Mudit Kaushal MD, Shanna Hill MD

Department of Anesthesiology, Weill Cornell Medicine, New York, NY

Introduction:

1. 36y pregnant woman with severe bioprosthetic tricuspid stenosis (TS), worsening right heart failure (RHF), and depressed cardiac output in second trimester.
2. The proposed procedure was a Transcatheter Tricuspid Valve in Valve (VinV) Replacement at 23 weeks, 3 days

Case Presentation:

Preoperative:
- NYHA class II-III symptoms requiring O_2 with exertion. Physical exam: JVD, hepatomegaly, and peripheral edema. Fetal scan at 18 weeks: estimated fetal weight in 34th percentile, CI 2.2L/min/m2 (by TEE).
- Previous bioprosthetic tricuspid valve replacement in 2005 now with severe TS (MG 14 mmHg), moderate TR, normal RV size and function, and normal LV size and function.

Intraoperative :
- Goals: Maintain preload, support RV systolic and diastolic function.
- Plan for pre-induction A-line, RSI, GETA, CVC, phenylephrine and milrinone infusions. LV pacing wire, 29mm Edwards Sapien 3 valve placed via left femoral vein.

Postoperative:
- Weaned off milrinone and extubated POD 1.
- Improved exercise tolerance and weaned off oxygen. TTE showed CI 2.8 L/min/m2, VinV gradient 4mmHg.
- Induced at 37 weeks and delivered by NSVD. APGARs 8 and 9.

Pre-Valve Deployment

Table 15 Doppler parameters of prosthetic tricuspid valve function

	Consider valve stenosis*
Peak velocity†	>1.7 m/s
Mean gradient†	≥6 mm Hg
Pressure half-time	≥230 ms
EOA and VTI$_{PrTV}$/VTI$_{LVO}$	No data yet available for tricuspid prostheses

PrTV, Prosthetic tricuspid valve.
*Because of respiratory variation, average ≥5 cycles.
†May be increased also with valvular regurgitation.

Figure 1: ASE Criteria for Bioprosthetic TV Stenosis

Figure 2: Continuous wave doppler measurement through Tricuspid Valve in modified ME Bicaval view consistent with bioprosthetic Tricuspid Stenosis
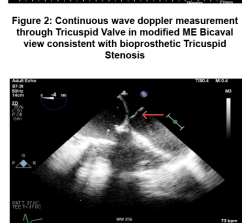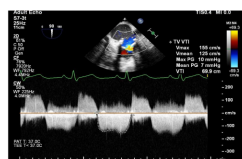
Figure 3: ME 4-chamber view showing the interatrial septum bowing into the left atrium

Post-Valve Deployment
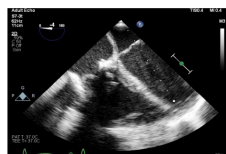
Figure 4: ME 4-chamber view showing RV dilation after the Tricuspid Valve in Valve

Figure 5: Continuous wave doppler measurement through the Tricuspid Valve in the modified ME Bicaval view showing an acceptable transvalvular inflow gradient
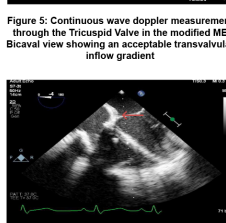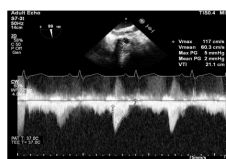
Figure 6: ME 4-chamber view showing the interatrial septum between the atria

Discussion:

- ACC/AHA Class I recommendation for a stenotic bioprosthetic TV is reoperative TVR.

- Tricuspid VinV procedure currently carries a class IIb recommendation. Given concerns for the fetus, minimally invasive Tricuspid VinV was deemed the best option.

- There is no defined acceptable TVinV gradient per ASE.

- In a recent JASE case series of tricuspid ViV procedures, the mean baseline bioprosthetic TV gradient was 9.2 ± 4.5, vs. 3.9 ± 2.0 mmHg for early post TVinV (p < 0.01).

- Per the largest case series of 149 tricuspid ViV patients, at 13 months: 22 patients died (14%), 10 (6%) required reintervention, and 77% were in NYHA class I or II status.

- Given expected increase in plasma volume throughout pregnancy, we were concerned that our patient's RHF would worsen and limit left-sided function, further decreasing uteroplacental perfusion. Allowing increased right-sided forward flow through the valve-in-valve improved cardiac output and her overall clinical picture.

References
- J Am Soc Echocardiogr. 2009 Sep;22(9):975-1014
- J Am Soc Echocardiogr. 2019 Feb 14. pii: S0894-7317(18)30737-5
- J Am Coll Cardiol. 2017 Jul 11;70(2):252-289

Pulsus Bisferiens in a Patient with a Contained Rupture of a Thoracoabdominal Aortic Aneurysm

Christina Lee, MD; John E. Rubin, MD; June M. Chan, MB BS, FANZCA; Adam D. Lichtman, MD, FASE
Department of Anesthesiology, Weill Cornell Medical College, New York, NY

Weill Cornell Medicine
NewYork-Presbyterian

Introduction

- Pulsus bisferiens is a rare biphasic systolic arterial waveform[1]
- Multiple etiologies have been associated with pulsus bisferiens including[1,2,3]:
  - Aortic insufficiency
  - Subaortic stenosis
  - Hypertrophic cardiomyopathy (HOCM)
  - Aortic dissection
- One proposed cause is a Venturi effect on the ascending aorta or a dissection flap following high-velocity ventricular ejection[2,3]
- This is a case of pulsus bisferiens caused by a contained rupture of a thoracoabdominal aortic aneurysm (TAAA) in which the bisferiens pulse was abolished after the aneurysm was excluded.

Case Report

- 83-year-old man with a contained rupture of a TAAA and a Type I endoleak of a prior endovascular thoracic aortic aneurysm repair.
- History significant for:
  - Dual-chamber pacemaker dependence
  - Bioprosthetic aortic valve replacement
  - Ascending aortic aneurysm repair
  - Endovascular repairs of thoracic and abdominal aortic aneurysms
- Preoperative CT angiography demonstrated native thoracic aortic aneurysm measuring up to 20cm x 12.3cm [Fig 3, 4].
- TTE revealed mild dynamic compression of the posterior left ventricle by the aortic aneurysm, an ejection fraction of 51%, and an intact bioprosthetic aortic valve with no aortic stenosis or regurgitation [Fig 2A, B].
- The patient was intubated prior to transfer to the operating room, with arterial and central venous catheters in situ.
- The patient's arterial line waveform was notable for pulsus bisferiens with a double systolic peak followed by a dicrotic notch and a single diastolic waveform [Fig 1A].
- There was no change in the waveform with heart rate, fluid challenge or blood pressure alterations.
- After deployment of the aortic stent graft, the pulsus bisferiens waveform was immediately abolished [Fig 1B], and the arterial line tracing normalized.

Before Exclusion
After Exclusion

Figure 1. Electrocardiogram and arterial waveform before and after exclusion of the thoracoabdominal aortic aneurysm. Prior to exclusion (A), the pulsus bisferiens waveform can clearly be seen. Direct comparison of the arterial waveforms demonstrates prolonged systolic phase before aneurysm exclusion, delayed dicrotic notch, and shortened diastolic phase compared to after the aneurysm was excluded (B).
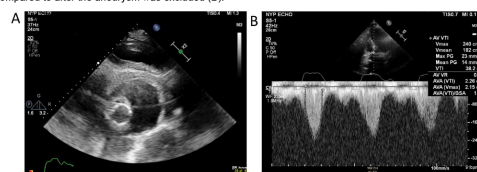

Figure 2. A) Preoperative transthoracic echocardiography demonstrating compression of the left ventricle by the thoracoabdominal aortic aneurysm. B) Preoperative pulsed-wave doppler measurements using transthoracic echocardiography demonstrating a normally functioning bioprosthetic aortic valve.
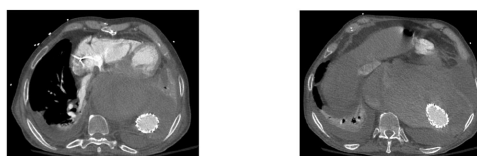

Figure 3: Preoperative computed tomographic angiography demonstrating compression of the left atrium and partial left ventricular compression by the aneurysm.

Figure 4: At its maximum size, the thoracoabdominal aortic aneurysm measured 12.3cm x 20 cm just below the level of the diaphragm. An aortic graft from prior surgery can be visualized within the aneurysm with contrast dye.

Discussion

- Pulsus bisferiens has been associated with subaortic stenosis, severe aortic regurgitation, or hypertrophic cardiomyopathy[1,2,3]
- These pathologies were excluded in this patient on preoperative imaging.
- One case report noted pulsus bisferiens associated with an aortic dissection[3]
- Loss of the bisferiens waveform with graft deployment strongly suggests that it was directly related to the aneurysm or endoleak.
- Two mechanisms are postulated for the bisferiens pulse in this case:
  - Dynamic compliance of the aneurysm or the endoleak acted as a "pop-off" and caused a biphasic systolic pulse; once the aneurysm was excluded, the reduced aortic compliance eliminated the artifact
  - Alternatively, as the aneurysm enlarged during ventricular systole, dynamic compression of the left ventricle during mid-systole occurred, causing a pause in systolic ejection flow; once ventricular systolic pressure exceeded extrinsic pressure on the left ventricle from the aneurysm, ejection flow resumed. Once the aneurysm was excluded from circulation, this effect was eliminated.

Conclusion

- This case demonstrates a novel cause of pulsus bisferiens due to a ruptured thoracoabdominal aortic aneurysm.
- Identification of a pulsus bisferiens waveform on a patient with concern for an aortic aneurysm should warrant additional investigation, including transthoracic echocardiography and imaging of the aorta, since the underlying cause will likely change the intraoperative and postoperative hemodynamic management

References
1. Fleming, P. "The mechanism of the pulsus bisferiens." Br Heart J. 1957. 19(4): 519-524.
2. Barison A. et al. "Haemodynamic findings in obstructive hypertrophic cardiomyopathy: pulsus bisferiens and Brockenbrough-Braunwald-Morrow sign." J Cardiovasc Med. 2016. 17 (suppl 2): e154-155).
3. Riojas, CM et al. "Aortic Dissection as a Cause of Pulsus Bisferiens: A Case Report and Review." Ann Vasc Surg. 2016. 30: 305.e1-305.e5.

High-Grade Intracardiac Sarcoma Causing Right Ventricular Outflow Tract Obstruction

Christina Lee MD, Sankalp Sehgal MD
Department of Anesthesiology, New York Presbyterian Hospital-Weill Cornell Medicine, New York, NY

SOCIETY OF CARDIOVASCULAR ANESTHESIOLOGISTS
Knowledge • Care • Investigation

Weill Cornell Medicine
NewYork-Presbyterian

INTRODUCTION

- Primary tumors of the heart are rare, occurring at a frequency of 0.02%.
- Metastatic tumors to the heart occur more frequently than primary malignant cardiac tumor, of which sarcomas are a rare source.[1,2]
- Most of these are diagnosed post-mortem by autopsy.
- The presence or absence of symptoms is dependent on the site of metastasis within the cardiovascular system, and there are no definitive guidelines for treatment.[2]
- This is a rare case of an aggressive metastatic cardiac sarcoma causing obstruction of the right ventricular outflow tract (RVOT) and proximal pulmonary arteries (PAs) that mimicked intracardiac thrombus.

CASE DESCRIPTION

- A 48-year-old female with a history of high-grade sarcoma of right hip s/p aggressive chemotherapy and hip reconstruction 5 years ago presented with increasing shortness of breath.
- Transthoracic echocardiogram showed a large mass in the right ventricle (RV) outflow tract obstructing pulmonic valve with severe pulmonic stenosis, normal RV function.
- Cardiac magnetic resonance imaging (CMR) revealed a large mass in the RVOT and bilateral PAs equivocal for thrombus versus tumor.
- Due to the aggressive nature of the mass, decision was made to perform surgical resection with possible valve replacement.
- Intraoperative transesophageal echo (TEE) confirmed the mass involving both leaflets of the pulmonic valve, extensive invasion into the RV, main PA and left PA with severely elevated PA pressures(Figure 2).
- The patient underwent extensive surgical debulking of the mass, however complete resection was challenging due to extensive invasion into the myocardial tissue.
- After surgery, patient was referred for adjuvant chemotherapy.
- Tumor pathology revealed a high-grade sarcoma consistent with pathology from previous hip sarcoma, thus confirming metastatic nature of the mass.
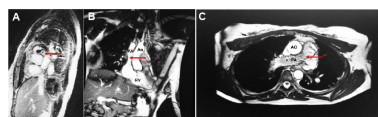
Figure 1: Cardiac MRI revealing mass within right ventricle outflow tract demonstrated by filling defect marked by red arrow; (1A) sagittal view; (1B) coronal view with RVOT and main PA defect; (1C) axial view of mass extending into pulmonary arteries (1C) [Ao = Aorta; PA = Pulmonary artery; RV = Right ventricle]
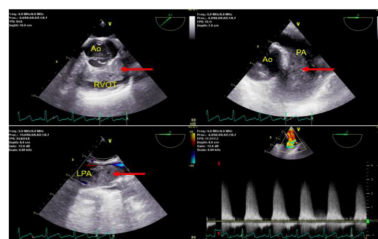
Figure 2: Intraoperative Transesophageal echo (TEE) demonstrating mass (red arrow) in the RV cavity and RVOT involving the pulmonic valve with pulmonic stenosis. There is extensive invasion into the RV, main PA and left PA with diminished blood flow. [Ao = Aorta; PA = Pulmonary artery; RVOT = Right ventricle outflow tract; LPA = Left pulmonary artery]

DISCUSSION

Signs and Symptoms of Cardiac Sarcoma
- Metastatic sarcoma is more common than primary cardiac sarcoma.
- The site of cardiac metastasis often determines the symptoms experienced.[1,2]
- Replacement of normal myocardium by tumor can lead to reduced cardiac output while intracavitary tumors can result in symptoms similar to constrictive disease.[1]
- Other clinical presentations may include arrhythmias, pericardial effusion, or restrictive disease.

Imaging as an Important Diagnostic Tool
- Because symptoms are often nonspecific, imaging is essential in reaching a diagnosis.
- Echocardiography is key to assess the location, size and tumor extent as well as to help distinguish primary from metastatic cardiac tumors.
- Initial imaging was equivocal for thrombus, but characteristics of the mass were more consistent with tumor on TEE.
- Metastatic tumors tend to be irregularly shaped with direct invasion of the heart.[3]
- CMR can be more sensitive than echocardiography in detecting intracardiac masses, particularly in assessing for extra-cardiac disease and metastasis.

Treatment and Prognosis
- Surgery and Chemotherapy are the mainstay therapies.
- Complete resection is often not possible due to anatomic location of tumor or infiltrative growth.[2]
- Overall, prognosis remains poor for metastatic cardiac sarcomas (median survival < 24 mo)

CONCLUSION

This patient presented with a metastatic intracardiac carcinoma. Our case reflects the importance of differentiating it from other entities such as thrombus and primary cardiac sarcoma. Echocardiography and CMR are key imaging modalities that can help determine anatomy and etiology. A complete resection can be challenging due to extensive invasion into the myocardium. Surgical debulking can be performed as a palliative measure.

REFERENCES

1. Bussani, R et al. Cardiac Metastases. J Clin Pathol. 2007; 60:27-34
2. Yanagawa, B et al. Surgery for Tumors of the Heart. Semin Thoracic Surg. 2018; 00:1-13.
3. Nomoto, N et al. Primary and metastatic cardiac tumors: echocardiographic diagnosis, treatment and prognosis in a 15-years single center study. J Cardiothor Surg. 2017; 12:103-111.

Peripartum Management of a Patient with Repaired Transposition of the Great Arteries

Abdullah Rasheed, Robert White, Danielle McCullough
NewYork-Presbyterian Hospital – Weill Cornell Medical Center

Weill Cornell Medicine
NewYork-Presbyterian

Introduction

D-transposition of the great arteries (TGA) is a congenital heart defect (CHD) in which the aorta and the pulmonary trunk are anomalously connected to the right and left ventricles, respectively. TGA is routinely corrected with the arterial switch operation, however the Rastelli procedure may be required for complex cases. Surgical repairs have good outcomes, but long term follow-up is limited.[1, 2]

Case Presentation

A female teenager G1P0 with morbid obesity, OSA, chronic DVTs on prophylactic enoxaparin, and repaired TGA presents for peripartum evaluation and delivery planning. She was born with TGA, VSD, ASD, infundibular pulmonary stenosis, and PA stenosis status post central shunt procedure in infancy followed by a left pulmonary artery (LPA) angioplasty and Rastelli procedure, consisting of an intracardiac baffle/VSD closure and Right Ventricle-Pulmonary Artery (RV-PA) conduit, as a toddler. 3 years later, she underwent LPA stenting for LPA stenosis. Her course was complicated by RV-PA conduit stenosis and LVOT obstruction status post RV-PA conduit replacement and resection of sub-aortic stenosis 3 years after her prior operation. Her history was further complicated by severe RV-PA conduit calcification and obstruction, supra-systemic RV pressure, and severe RV dysfunction status-post RV-PA conduit exchange and central PA angioplasty as a teenager. MRI 5 months prior to delivery revealed a diffusely small conduit with severe stenosis, mild hypoplasia of the branch PAs, severe RV dilation with severely diminished RV systolic function, and severe RV hypertrophy.

Rastelli Procedure
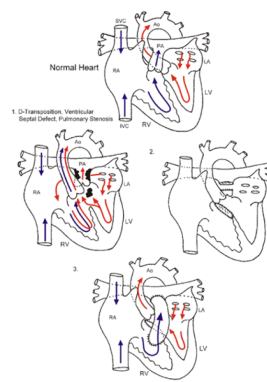
Rastelli GC, Wallace RB, Ongley PA: Complete repair of transposition of the great arteries with pulmonary stenosis. A review and report of a case corrected by using a new surgical technique. Circulation. 39(1):83-95, 1969.

Management

Multidisciplinary peripartum planning was conducted in consultation with pediatric cardiology, pediatric cardiothoracic anesthesiology, obstetrics, maternal-fetal-medicine, obstetric anesthesiology, and nursing. The multi-disciplinary team evaluated multiple treatment strategies and ultimately agreed upon a comprehensive care plan including induction of labor at term, peripartum telemetry monitoring with assistance of a cardiac RN, direct transfer to CCU after post-partum stabilization, and holding enoxaparin 24 hours prior to induction.

Outcome

The patient arrived at 37 weeks, 2 days for induction of labor. She had an uncomplicated normal spontaneous vaginal delivery of a healthy male under combined spinal-epidural. Mother and baby were discharged home on post-delivery day 2 with outpatient cardiology follow up.

Discussion

Substantially improved surgical and medical management of children with CHD has introduced an expanding cohort of adults with congenital heart disease (ACHD).[1] These patients present anesthesiologists with unique perioperative and peripartum challenges. The normal hemodynamic changes of pregnancy pose additional risk to ACHD patients,[2, 3] as in our patient with severe RV dilation, RV hypertrophy and reduced RV function at baseline. This increased risk emphasizes the importance of comprehensive multidisciplinary peripartum planning. Appropriate team-based care in patients with repaired TGA has thus far demonstrated reassuring maternal and fetal outcomes.[2] Given the paucity of literature regarding ACHD patients in the peripartum period,[2, 3] further research into peripartum and perioperative management of this expanding sub-population is warranted.

References

1. Khan A, Gurvitz M: Epidemiology of ACHD: What Has Changed and What is Changing? Progress in cardiovascular diseases. 61:275-281, 2018.
2. Stoll VM, Drury NE, Thorne S, et al.: Pregnancy Outcomes in Women With Transposition of the Great Arteries After an Arterial Switch Operation. JAMA cardiology. 3:1119-1122, 2018.
3. Moe TG, Bardo DME: Long-term Outcomes of the Arterial Switch Operation for d-Transposition of the Great Arteries. Progress in cardiovascular diseases. 61:360-364, 2018.

Evaluation of Right Ventricular Systolic Function acutely after Elective Cardiac Surgery: A 3D echocardiography feasibility study

Weill Cornell Medicine
NewYork-Presbyterian

Lisa Q. Rong MD[1], Robert Sickeler MD[1], Maria Chiara Palumbo MS[2], Jiwon Kim MD[2], Jonathan W. Weinsaft MD[2]
1 Department of Anesthesiology, Weill Cornell Medicine, NY NY
2 Greenberg Division Department of Cardiology, Weill Cornell Medicine, NY NY

Introduction

- Mechanistic causality of right ventricular (RV) dysfunction after cardiopulmonary bypass (CPB) surgery is poorly understood. (1-2)
- Three dimensional (3D) and strain echocardiography enable new insights into cardiac performance, but have not been used to test impact of CPB on RV performance. (3)
- Echo-quantified volumetric and strain analyses will provide improved understanding of RV functional changes induced by CPB.

Methods

- Transesophageal echo (TEE) was performed while pre-CPB (before sternotomy) and post CPB (after chest closure) as part of a prospective protocol.
- RV volumes and strain were respectively measured on 3D and 2D TEE, including curvature (septal mean value, free wall mean value) quantified via custom software on the 3D model.
- Results were compared to conventional RV analyses, including TAPSE, S', and FAC. 3D and curvature measurements were performed blinded to 2D indices.

Contact: Lisa Q. Rong, lir9065@med.cornell.edu

2D RV Strain

EDA	21.99 cm²
ESA	14.94 cm²
FAC	32.05 %
GLS	-18.21 %
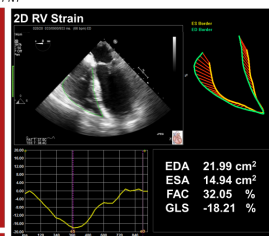
Figure 1: Example of 2D RV strain and fractional area of change calculations on healthy patient

3D RV Volume

EDV	139.1 ml
ESV	62.6 ml
SV	76.5 ml
EF	55.0 %
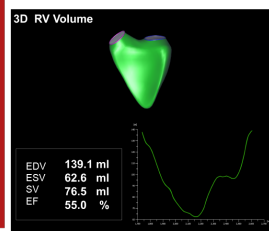
Figure 2: Example of 3D RV volume measurement and ejection fraction calculations on healthy patient

Curvature > 0   Convex Surface
Curvature = 0   Flat Surface
Curvature < 0   Concave Surface
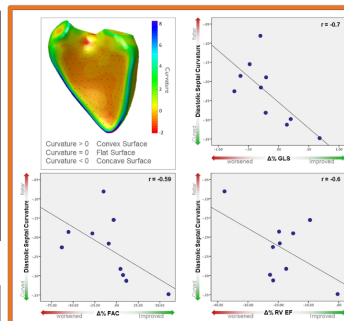
Figure 3: Septal curvature compared to established RV metrics

Table 1: Measured data	Pre CPB	Post CPB	p-value
2D Echocardiography and Strain Analysis			
TAPSE	1.5 ± 0.3	1.1 ± 0.4	0.006
S'	7.6 ± 1.8	6.0 ± 2.9	0.126
FAC	37.8 ± 11.7	31.1 ± 7.5	0.164
Septal Strain	20.4 ± 7.3	13.3 ± 6.9	0.035
Free Wall Strain	22.0 ± 6.7	17.3 ± 6.8	0.122
GLS	21.2 ± 7.7	14.8 ± 5.4	0.05
3D Volume Analysis and Curvature			
RV EF	53.2 ± 7.1	42.9 ± 4.8	<0.001
Septal curvature (diastole)	-0.23 ± 0.08	-0.15 ± 0.06	0.002
Free Wall Curvature (diastole)	0.71 ± 0.05	0.77 ± 0.04	<0.001

Results

- The population comprised 10 patients undergoing elective cardiac surgery (1 AVR, 3 AVR/CABG, 3 CABG, 3 Aortic graft).
- Among conventional RV indices, only TAPSE decreased significantly post-CPB (1.5 ±0.3 vs. 1.1±0.4 p=0.006) whereas S' and FAC did not (p=NS).
- Regarding novel indices, 3D RVEF (53.2± 7.1 vs. 42.9±4.8, p<0.001), GLS (21.2±7.7 vs. 14.8 ± 5.4, p=0.05), septal strain (20.4±7.3 vs. 13.3±6.9 p=0.03) and septal curvature (systole: -0.27±0.04 vs. -0.18±0.05 p=0; diastole: -0.23±0.08 vs. -0.15±0.06 p=0.002) all significantly decreased **(Table 1)**.
- Baseline diastolic septal curvature was associated with percent decrease in RV function: Δ%RVEF (r=-0.6, p=0.07), Δ%FAC (r=-0.59, p=0.07), Δ%septal strain (r=-0.67, p=0.03) and Δ%GLS (r=-0.7, p=0.02) (Figure 3).

Conclusions

- Geometric 3D TEE analysis in the perioperative period in cardiac surgery is a promising tool to use for stratification of RV function after CPB. Specifically, the improved baseline septal curvature (higher absolute value) seems to predict improved post-CPB RV function.

References

1. Bootsma IT, de Lange F, Koopmans M et al. Right Ventricular Function After Cardiac Surgery Is a Strong Independent Predictor for Long-Term Mortality. J Cardiothorac Vasc Anesth 2017;31:1656-1662.
2. Maslow AD, Regan MM, Panzica P et al. Precardiopulmonary bypass right ventricular function is associated with poor outcome after coronary artery bypass grafting in patients with severe left ventricular systolic dysfunction. Anesth Analg 2002;95:1507-18.
3. Grønlykke L, Korshin A, Holmgaard F et al. Severe loss of right ventricular longitudinal contraction occurs after cardiopulmonary bypass in patients with preserved right ventricular output. Int J Cardiovasc Imaging 2019.

Echocardiographic Predictors of Intraoperative Right Ventricular Dysfunction: A 2D and Speckle Tracking Echocardiography Study

Lisa Q. Rong MD[1], Ibrahim Warsame MD[1], Brian Yum MD[2], Christiane Abouzeid MD[2], Maria Chiara Palumbo MS[2], Jonathan W. Weinsaft MD[2], Jiwon Kim MD[2]

[1] Department of Anesthesiology, Weill Cornell Medical College, New York City, NY
[2] Greenberg Division Department of Cardiology, Weill Cornell Medicine, NY, NY

Weill Cornell Medicine
NewYork-Presbyterian

Introduction

- Intraoperative or post-cardiopulmonary bypass (CPB) right ventricular (RV) dysfunction confers a poor prognosis in the post-operative period.
- Conventional predictors for RV function are limited due the effect of cardiac surgery on traditional RV indices.
- Novel echocardiographic techniques hold the promise to improve RV functional stratification.

Methods

- Comprehensive echocardiographic data were collected prospectively during elective cardiac surgery.
- Tricuspid annular plane systolic excursion (TAPSE), peak RV systolic velocity (S'), and RV fractional area change (FAC) were quantified on transesophageal echo (TEE).
- RV global and regional (septal and free wall) longitudinal strain was quantified using speckle-tracking echo in RV-focused views.
- Two intraoperative time points were used for comparison: pre-sternotomy (baseline) and post-chest closure.

Contact: Lisa Q. Rong, lir9065@med.cornell.edu

Table 1. Clinical Characteristics

	Overall (n=53)	RV Dysfunction Present (n=37)	RV Dysfunction Absent (n=16)	p
Age (years)	63 ± 11	61±11	67±10	0.09
Male gender	69.8% (37)	75.7% (28)	54.3% (9)	0.20
BMI	27.8 ± 4.6	28.2±4.7	27.2± 4.3	0.60
CV Risk Factors	78.8% (41)	75.0% (27)	87.5% (14)	0.47
Hypertension	60.4% (32)	51.4% (19)	40.6% (13)	0.07
Hyperlipidemia	11.3% (6)	13.5% (5)	6.3% (1)	0.66
Diabetes	9.4% (5)	13.5% (5)	0.0% (0)	0.31
Prior MI				
Operation				
CABG	39.6% (21)	37.8% (14)	43.8% (7)	0.69
Valve Surgery	64.2% (34)	67.6% (25)	56.3% (9)	0.43
Aortic Surgery	43.4% (23)	43.2% (16)	43.8% (7)	0.97
Other	18.9% (10)	10.8% (4)	37.5% (6)	0.05
NYHA Class (I/II/III/IV)	72% (36)/ 18% (9)/ 10% (5)/ 0% (0)	66% (23)/ 23% (8)/ 11% (4)/ 0% (0)	86% (13)/ 7% (1)/ 7% (1)/ 0% (0)	0.15

Table 2. Echocardiographic Parameters

	Overall (n=53)	Post RV Dysfunction + (n=37)	Post RV Dysfunction - (n=16)	p
Baseline				
LVEF	56.8 ± 13.0	55.9 ± 14.0	59.2 ± 10.0	0.45
TAPSE	1.5±0.3	1.4±0.3	1.6±0.4	0.14
S'	8.0±2.1	7.9±2.4	8.5±2.4	0.48
GLS	-19.0±6.5	-17.7±6.5	-21.8±5.4	0.03
Septal Strain	-17.9±5.9	-16.9±5.5	-20.3±6.4	0.08
Free Wall Strain	-21.5±6.4	-20.3±6.4	-24.2±5.8	0.04
FAC	36.8±9.3	34.7±9.1	41.6±8.1	0.01
Post Chest Closure				
LVEF	55.8±12.9	54.1±13.0	60.0±12.2	0.17
TAPSE	1.1±0.3	1.1±0.3	1.1±0.4	0.94
S'	6.2±2.5	6.0±2.3	6.7±2.9	0.41
GLS	-13.5±6.9	-10.1±4.3	-21.2±5.3	<0.001
Septal Strain	-12.4±6.6	-9.9±5.2	-18.2±5.9	<0.001
Free Wall Strain	-15.5±7.8	-12.4±5.6	-22.8±7.6	<0.001
FAC	29.3±10.6	24.0±6.9	41.7±6.6	<0.001
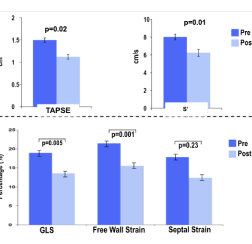
Figure 1: RV parameters including linear and deformational indices decline intraoperatively.

Figure 3: Pre-sternotomy TEE-derived RV strain analysis acquired in a patient undergoing cardiac surgery.
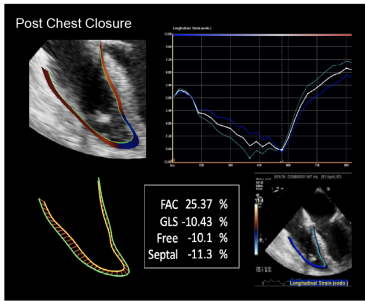
Figure 4: Post chest closure TEE analysis as acquired in the same patient

Results

- 53 patients undergoing cardiac surgery from 11/2017 to 11/2018.
- 38% had impaired RV function at baseline defined as RV FAC <35%.
- All conventional RV functional indices including TAPSE, S' and FAC declined immediately following chest closure when compared to baseline.
- Speckle tracking echocardiographic data demonstrated a significant decline in RV global longitudinal strain (GLS).
- Pre-sternotomy FAC, GLS and free wall strain predicted RV dysfunction at chest closure, whereas traditional linear RV indices such as TAPSE and RV S' at baseline had no impact on intraoperative RV dysfunction.
- Left ventricular (LV) and RV hemodynamic parameters remained unchanged.

Conclusions

- Global and regional RV function acutely decline intraoperatively.
- Impaired RV strain is associated with intraoperative RV functional decline.
- RV strain provides incremental value to traditional RV indices in predicting those who will develop RV dysfunction.

Three-dimensional echocardiography for transcatheter aortic valve replacement – A systematic review and meta-analysis

Lisa Q. Rong MD[a], Irbaz Hameed MD[b], Arash Salemi MD[b], Mohamed Rahouma MD[b], Faiza M. Khan MD[b], Linda Shore-Lesserson MD[c], Mario Gaudino MD[b]

[a] Department of Anesthesiology, Weill Cornell Medicine, New York, NY, USA.
[b] Department of Cardiothoracic Surgery, Weill Cornell Medicine, New York, NY, USA.
[c] Department of Anesthesiology, North Shore University Hospital, Manhasset, NY, USA.

Weill Cornell Medicine
NewYork-Presbyterian

Background

- TAVR is standard of care for many patients with severe symptomatic aortic stenosis and relies on accurate sizing of the aortic annulus.
- It has been suggested that 3-dimensional transesophageal echocardiography (3DTEE) 3D TEE may be used instead of multidetector computed tomography (MDCT) for pre-transcatheter aortic valve replacement (TAVR) planning.

Objectives

- This systematic review and meta-analysis compared 3D TEE and MDCT for pre-TAVR measurements.

Methods

- A systematic literature search was performed (Figure 1).
- The primary outcome was the correlation coefficient between 3DTEE and MDCT measured annular area.
- Secondary outcomes included
  - correlation coefficients for mean annular diameter, annular perimeter, and left ventricular outflow tract area (LVOT-A).
  - inter- and intra-observer agreements; mean differences between 3D TEE and MDCT measurements.
  - pooled sensitivities, specificities, and receiver operating characteristic area under curve values of 3D TEE and MDCT for discriminating post-TAVR paravalvular aortic regurgitation (PVAR).

Figure 1: Preferred Reporting Items for Systematic Reviews and Meta-Analyses (PRISMA)
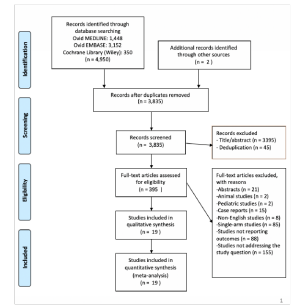
Figure 2. Correlation between 3D TEE and MDCT in measuring annular area
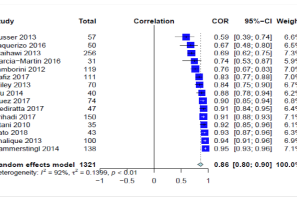
Table 1: Summary of Included Studies

Table 2. Meta-regression of patient and imaging variables on the primary outcome of correlation between 3D TEE and MDCT annular area measurement.

Variable	Number of studies	Beta ± SD, P-value
Age	13	0.0009±0.0223, P=0.98
Male gender	13	-0.0075±.0065, P=0.24
Body mass index (BMI)	4	-2.7758±0.8160, P<0.001
Body surface area (BSA)	3	-2.5466±0.6751, P<0.001
Left ventricular ejection fraction	3	-0.0401±0.0288, P=0.16
Trans-aortic gradient	10	-0.0362±0.0139, P=0.01
Aortic valve area	10	0.605±60.9431, P=0.52

Figure 3 Pooled receiver operating characteristic curves of (A) 3D TEE and (B) MDCT annular perimeter covering index for predicting paravalvular aortic regurgitation (PVAR).
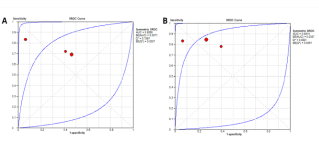
Methods

- A random effects model was used. Meta-regression and leave–one-out analysis for the primary outcome were performed (Table 2).

Results

- 19 studies with a total of 1599 patients were included (Table 1).
- Correlations between 3D TEE and MDCT annular area, annular perimeter, annular diameter, and LVOT-A measurements were strong (0.86 [95% Confidence Interval (CI) 0.80-0.90]; 0.89 [CI 0.82-0.93]; 0.80[CI 0.70-0.87]; and 0.78 [CI 0.61-0.88] respectively). (Figure 2)
- Mean differences between 3D TEE and MDCT between annular area, annular perimeter and mean annular diameter measurements were small and not statistically different.
- Inter-and intra-observer agreement and discriminatory abilities for PVAR were good for both 3D TEE and MDCT. (Figure 3)

Conclusion

- 3D TEE is comparable to MDCT for pre-TAVR planning.
- 3D TEE may be potentially advantageous for TAVR measurements in patients with renal dysfunction due to the lack of contrast exposure.

References:

- Liberati A., Altman DG., Tetzlaff J., et al. The PRISMA statement for reporting systematic reviews and meta-analyses of studies that evaluate healthcare interventions: explanation and elaboration. BMJ 2009;339:b2700

Contact lir9065@med.cornell.edu

Society for Obstetric Anesthesia and Perinatology (SOAP)

Postpartum Readmission Rates and Inpatient Mortality In Pregnancies Complicated By Sickle Cell Disease: A Multistate Analysis 2007-2014

Evelyn E. Bae M.D.[1], Virginia Tangel M.A.[2], Robert S. White M.D.[1], Anna S. Nachamie B.S.[2], Sharon E. Abramovitz M.D.[1], Nathan A. Liu M.D.[1]
[1]NewYork-Presbyterian Hospital/Weill Cornell Medicine; Department of Anesthesiology [2]Weill Cornell Medicine Center for Perioperative Outcomes; Department of Anesthesiology

NewYork-Presbyterian
Weill Cornell Medicine

Introduction

Sickle cell disease (SCD) in pregnancy is associated with increased risk of maternal complications, including more frequent sickle cell and pain crises and increased maternal mortality and morbidity.[1]

Previous studies have reported increased hospital admissions and greater length of stay (LOS) in sickle cell populations throughout pregnancy.[2]

However readmission rates up to 90 days postpartum as well as cost differences in hospital charges between sickle cell and non-sickle cell pregnancies have not previously been studied.

The primary aim of this study was to compare 30- and 90-day hospital readmission rates in pregnant patients with SCD, sickle cell trait alone, and those without SCD.

As secondary outcomes we analyzed in-hospital mortality, LOS, total hospital charges, and sickle-cell associated minor complications (blood transfusion, deep venous thrombosis, urinary traction infection, sepsis/shock) and major complications (supraventricular arrhythmias, cardiac arrest, myocardial infarction, stroke, pulmonary embolism, pneumonia, acute renal failure).

Figure 1. Demographics of pregnant patients admitted to delivery by sickle cell disease status for important confounders of age, race, insurance type, and obstetric comorbidities
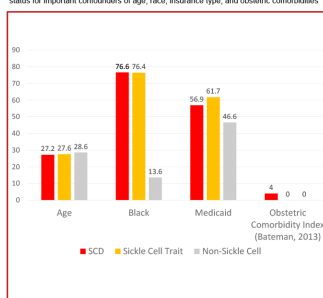
Figure 2. Multivariate outcome measures (adjusted odds ratios) for pregnant patients admitted for delivery by sickle cell disease status

Outcome	Sickle Cell Disease	Sickle Cell Trait	Non-Sickle Cell
30-day readmission	1.26 (1.12,1.42)**	1.12 (1.04,1.21)*	1.0
90-day readmission	1.90 (1.73,2.08)**	1.09 (1.03,1.17)*	1.0
In-hospital mortality	4.92 (2.65,9.15)**	1.15 (0.51,2.60)	1.0
Minor sickle cell complication	2.32 (1.89,2.85)**	1.1 (0.95,1.29)	1.0
Major sickle cell complication	3.44 (2.88,4.11)**	1.34 (1.15,1.57)**	1.0
Length of stay	1.11 (1.07,1.14)***	1.03 (1.01,1.04)**	1.0
Total charges in 2016 dollars	1.16 (1.13,1.20)**	1.04 (1.03,1.05)**	1.0

* p < 0.05, ** p < 0.01, *** p < 0.001

Results

Primary outcome:
- SCD patients were 26% more likely to be readmitted up to 30 days post-delivery and 90% more likely to be readmitted up to 90 days post-delivery.

Secondary outcomes:
SCD patients:
- Were nearly five times more likely to die in-hospital than non-SCD patients
- Had a longer median LOS (3 days, IQR: 2-5) in the SCD group vs. 2 days (IQR: 2-3) in the non-SCD group.
- Had greater median total charges for their hospital stay: $17,808 (IQR: $10,490-$30,125) in the SCD group vs. $13,365 (IQR: $8,526-$20,798) in the non-SCD group.
- Were more than two times as likely to experience minor complications and three times as likely to experience major complications than non-SCD patients.

Sickle cell trait patients did not have increased rates of in-hospital mortality as compared to non-SCD women but were 12% more likely to be readmitted at both 30 and 90 days postpartum and experience a major complication.

Conclusions

- SCD in pregnancy is associated with increased readmissions, inpatient mortality, LOS, hospital charges, and postpartum complications.
- The presence of sickle cell trait was associated with a significant but smaller likelihood of morbidity.
- Our findings confirm disparate outcomes in sickle cell pregnancies and provider further insight into the impact of SCD on patterns of health care utilization.

Methods

- We conducted a retrospective analysis of discharge data for 6,911,916 inpatient deliveries in the states of California, Florida, New York, Maryland, and Kentucky from 2007 to 2014 using data from the State Inpatient Databases Healthcare Cost and Utilization Project.
- We compared unadjusted rates and adjusted odds of 30- and 90-day readmission rates, in-hospital mortality, LOS, and total hospital charges (in 2016 dollars) in SCD, sickle cell trait, and non-sickle cell patients.
- Covariates included: age, sex, primary insurance payer, state, year of delivery, median household income by quartile, hospital delivery volume by quartile, delivery type (vaginal, operative vaginal, Cesarean), and present-on-admission indicators using the obstetric comorbidity index as defined by Bateman et al. (2013).[3]

References

1. Villers MS, Jamison MG, De Castro LM, James AH. Morbidity associated with sickle cell disease in pregnancy. Am J Obstet Gynecol. 2008;199(2).
2. Oteng-Ntim E, Meeks D, Seed PT, et al. Adverse maternal and perinatal outcomes in pregnant women with sickle cell disease. Systematic review and meta-analysis. Blood. 2015;125(21):3316-3325.
3. Bateman BT, Mhyre JM, Hernandez-Diaz S, et al. Development of a comorbidity index for use in obstetric patients. Obstet Gynecol. 2013;122(05):957–965

Question/Comments? Please contact: Evelyn E. Bae (evb9029@nyp.org) or via Twitter *@SAbramovitzMD @VirginiaTangel @RobertWhiteMD*

Opioid Use Disorder and Maternal Outcomes Following Cesarean Section, A Multistate Analysis 2007 - 2014

Maria M. Quincy MD, Roniel Weinberg MD, Virginia Tangel MA, Sharon Abramovitz MD, Jaime Aaronson MD, Robert S. White MD MS

NewYork-Presbyterian
Weill Cornell Medicine

Introduction

Opioid use disorder is a public health crisis in the United States, with an overdose mortality rate of more than 63,000 in 2016. Opioid abuse poses significant maternal and fetal risks, including intrauterine growth restriction, placental abruption, preterm delivery and neonatal abstinence syndrome. Recent research examining the association of maternal opioid use with maternal mortality and morbidity, as well as fetal outcomes, showed an increase in maternal death during hospitalization, cardiac arrest, and obstetric complications.

There are no current studies that investigate maternal complications in a national cohort of patients with opioid use disorder who undergo cesarean delivery. Using data from the State Inpatient Database (SID), we examined the rates of maternal mortality and other post-delivery outcomes associated with opioid abuse among women undergoing cesarean delivery.

As secondary outcomes we analyzed hospital length of stay, 30- and 90-day readmissions and hospital charges.

Figure 1. Demographics of pregnant patients admitted for cesarean delivery. Age in years, race, Medicaid insurance, and obstetric comorbidity index per Bateman in percentiles

Figure 2. Multivariate outcome measures (adjusted odds ratios, CI 95%, IRR) for women admitted for cesarean delivery

Outcome	Opioid use disorder vs. absence of opioid use disorder
30 day readmission	1.46 (1.30, 1.65)
90 day readmission	1.70 (1.55, 1.88)
In hospital mortality	2.48 (1.20, 5.10)
Length of stay	1.02 (1.00, 1.04)
Total charges in 2016 dollars	1.05 (1.03-1.07)

Results

Unadjusted rates:
Opioid use disorder patients (compared to non-opioid):
- 30 day readmission rates: 4.2% vs. 1.2%
- 90 day readmission rates 6.7% vs. 2.65
- Median total charges: $19,804 vs. $17,447
- Any complication: 2% vs. 0.8%

Adjusted odds ratios:
Opioid use disorder patients (compared to non-opioid):
- Inpatient mortality (2.48; 95% CI 1.20-1.50)
- 30 day readmission (1.46; 95% CI 1.30-1.65)
- 90 day readmission (1.70; 95% CI 1.55-1.88)
- Length of stay (1.02; 95% CI 1.00-1.04)
- Increased total charges (1.05; 95% CI 1.03-1.07)

Conclusions

Women with opioid use disorder experienced increased inpatient mortality, length of stay, readmissions, and total hospital charges. With the increasing number of reproductive-age and pregnant women affected by opioid use disorder, it is essential to further understand its implications during pregnancy, as well as the postpartum period. Although our findings are retrospective and observational, they highlight the need for further research to show the implications of opioid use disorder on maternal and fetal outcomes.

Methods

- We conducted a retrospective analysis of discharge data for 2,425,527 inpatient cesarean deliveries in the states of California, Florida, New York, Maryland, and Kentucky from 2007 to 2014 using data from the State Inpatient Databases Healthcare Cost and Utilization Project. Of these, 10,703 were identified as having opioid use disorder.
- We compared unadjusted rates and adjusted odds of 30- and 90-day readmission rates, in-hospital mortality, LOS, and total hospital charges (in 2016 dollars) in patients identified with opioid use disorder compared with those without.
- Covariates included: age, sex, race, primary insurance payer, state, year of delivery, median household income by quartile, hospital delivery volume by quartile, and present-on-admission indicators using the obstetric comorbidity index as defined by Bateman et al.[3]
- We conducted our data analysis using SAS 9.4 and Stata SE 15.

References

1. CDC Drug Surveillance Report 2018 pg.8
2. Opioid use disorder documented at delivery hospitalization – United States 1999 -2014 in Morbidity and Mortality Report weekly 2018; 67(31); 845-849
3. Maeda A., Bateman BT, et al. Opioid Abuse and Dependence during Pregnancy: Temporal Trends and Obstetrical Outcomes. Anesthesiology 2014; 121(6): 1158-1165.
4. Bateman BT, Mhyre JM, Hernandez-Diaz S, et al. Development of a comorbidity index for use in obstetric patients. Obstet Gynecol. 2013;122(05):957–965

@SAbramovitzMD • @JamieAaronson • @VirginiaTangel • @RobertWhiteMD

Question/Comments? Please contact: Maria M. Quincy (maq9021@nyp.org)

Racial and ethnic disparities in obstetric complications:
A retrospective analysis, 2007-2014

STUDY POPULATION

6,911,916

deliveries from the State Inpatient Databases for:

CA FL KY MD NY

We analyzed the incidence of **obstetric complications** by race/ethnicity.

↓

Additionally, we analyzed **individual complications** if they had a prevalence > 1% in the entire dataset.

RESULTS
Black women are more likely to experience obstetric complications than white women. They are:

16%	more likely to experience *any* obstetric complication
85%	more likely to have a stillborn baby
79%	more likely to receive a blood transfusion
71%	more likely to have a length of stay of +7 days
34%	more likely to develop oligohydramnios
26%	more likely to have a placental abruption
10%	more likely to have membranes rupture prematurely
9%	more likely to experience postpartum hemorrhage

SOLUTIONS
How can we reduce racial disparities?

For providers:

- education on the history of health disparities
- training to improve communication with patients
- information to reduce implicit bias

For hospitals:

- broader use of **Enhanced Recovery After Surgery (ERAS)** programs that deliver evidence-based perioperative care to all patients through a systematic approach

- utilization of clinical informatics tools that support cultural competency, medical decision-making, and patient-centered care

Tangel V, Budnick A, Abramovitz S, White RS.   @SAbramovitzMD • @VirginiaTangel • @RobertWhiteMD

Weill Cornell Medicine Anesthesiology

World Airway Management Meeting (WAMM)

Close the bag: a project to methodically improve the quality of the emergency airway bag.

Weill Cornell Medicine
NewYork-Presbyterian

J.D. Samuels[1], B. Like[1], P. Mack[1], V. Malhotra[1], M. Spiegel[1]

[1] NewYork-Presbyterian/Weill Cornell Medical Center, New York, NY, United States

BACKGROUND

- Emergency anesthesia airway bags (EAABs) are ubiquitous in tertiary medical centers yet there is little in the literature that discusses them.[1,2]
- Our institution's EAAB was often overfilled, yet inconsistently equipped, without clear guidelines as to how it should be stocked.
- We developed a new standardized checklist of contents in order to consistently maintain adequate par levels of medications and essential airway supplies.
- Additionally, we researched various styles of EAABs to maximize functionality and ease of transport.

METHODS

- Weill Cornell Medical College/NewYork-Presbyterian Hospital, New York, NY, USA. From September – November 2018, we surveyed the drugs and airway equipment used during emergency intubations, equipment preferences of anesthesiology attendings and residents, and conducted random checks of our EAAB.
- Data was collected regarding supplies available in code carts and intubation boxes available throughout the hospital. Each day the PACU code EAAB was weighed, to determine the pre-intervention variance.
- Mathematical models and discussions with senior faculty and pharmacists were then used to determine a supplies checklist for our EAAB.
- A ___ question pre- and post intervention survey, SurveyMonkey (*San Mateo, CA),* was conducted on anesthesiology residents and faculty. Only faculty that take surgical call were included. Questions included: ___.
- Post intervention spot checks were conducted to determine continued compliance and uniformity.
- All ethical guidelines of our institution were followed.
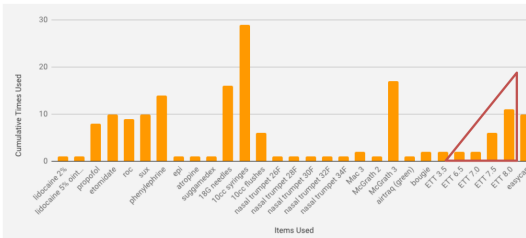
Figure 1

Emergency Anesthesia Airway Bag Checklist

Airway	Count		Count	Drugs	Count		Count
Green Oral Airway	1	Bougie	1	Propofol (200mg/20cc)	2	10cc Syringe	8
Yellow Oral Airway	1	I-Gel 3	1	Etomidate (20mg/10cc)	2	18G Blunt Tip Needle	8
Purple Oral Airway	1	I-Gel 4	1	Rocuronium (50mg/5cc)	4	Blank Drug Sticker	1
6.0 ETT	1	I-Gel 5	1	Succinylcholine (200mg/10cc)	2	NS Flushes (10cc)	2
6.5 ETT	1	EZ Capnography	1	Ephedrine (25mg/5cc)	2		
7.0 ETT	1	Airtraq (green)	1	Phenylephrine (400mcg/10cc)	2		
7.5 ETT	1	Needle Cricothyrotomy Kit	1	Epinephrine (1mg/10cc)	1		
8.0 ETT	2	Nasal Trumpet 26	1	Epinephrine (100mcg/10cc)	1		
McGrath Blade Size 3	2	Nasal Trumpet 28	1	Atropine (1mg/10cc)	1		
McGrath Blade Size 4	1	Nasal Trumpet 30	1	Glycopyrrolate (1mg/5cc)	1		
MAC 3 Blade w/ Handle	1	Nasal Trumpet 32	1	Sugammadex (200mg/2cc)	8		
MAC 4 Blade w/ Handle	1	Nasal Trumpet 34	1	Esmolol (100mg/10cc)	1		
				Labetalol	1		

Figure 2

Figure 3

RESULTS

- Random checks of equipment in our EAAB demonstrated inconsistently stocked airway supplies and medications, which translated to significant variability in the weight of the bag (2.5-3.4kg).
- During emergent intubations, McGrath 3's were the favored laryngoscopes (>85%) along with size #8.0 endotracheal tubes (>50%), while rocuronium, succinylcholine, etomidate, propofol and phenylephrine were the most frequently used drugs (Figure 1).
- Successive airway emergencies occurred frequently, which at times led to a lack of necessary supplies and/or medications.

CONCLUSIONS

- Our institution's new EAAB checklist (Figure 2) standardizes the par levels of airway equipment and medications to be stocked in the EAAB.
- This final list was guided by physician survey responses and the data documenting supplies and medications utilized during intubations.
- In addition, this new EAAB supply checklist includes sufficient supplies/medications for successive airway emergencies.
- New ergonomic EAAB purchased along with pharmacy guided drug organization cartons (Figure 3)
- Post-implementation data and physician surveys will be obtained to assess physician satisfaction and document improvement in the availability of appropriate supplies and medications.

REFERENCES

1. Apfelbaum JL, Hagberg CA, Caplan RA, et al. *Anesthesiology* 2013; **118**:251–70.
2. Frerk C, Mitchell VS, McNarry AF, et al. *BJA* 2015; **115**:827–48.
3. Cook TM, Woodall N, Frerk C, *et al. BJA*, 2011; **106**(5):617–631.
4. Hagberg CA, Gabel JC, Connis RT, *et al. BJA*, 2015; **115**(6):812–814.

Weill Cornell Medicine **NewYork-Presbyterian**

Emergent Airway Management in a Patient with *in situ* Tracheobronchial Stents

Samuels JD, Rubin JE, Lee C, Adams EM, Panchamia RK
Department of Anesthesiology, NewYork Presbyterian Hospital-Weill Cornell Medicine, New York, NY

Introduction

Placement of airways stents have become common procedures for both treatment and palliation of tracheobronchial malacia or occlusion.[1] The presence of a stent, particularly a tracheal stent, may pose unique challenges to the anesthesiologist. Herein, we report the management of an emergent airway following tracheobronchial stent placement.

Case Presentation

• A 63 year-old man with a history of colon cancer with metastases to the lungs, who developed rapid onset pneumonitis after radiation therapy.
• Presented to our institution with dyspnea and a productive cough
• Bronchoscopy revealed a necrotic endobronchial mass obstructing the right upper lobe as well as friable tracheal walls.
• A week later, he went to the operating room for rigid bronchoscopy, which revealed a worsening status, including partial to complete dehiscence of the tracheal walls and right mainstem bronchus.
• Because the patient was not a candidate for definitive surgery, a long silicone tracheal Y stent (15x12x12 mm) was placed in the tracheobronchial tree, in addition to a self-expanding metallic stent (12x40mm) in the right mainstem bronchus.
• The procedure was uneventful.
• Vital signs stable. Transferred to the post-anesthesia care unit on nasal cannula.

Initial Presentation to Airway Team:

• Although initially stable from a respiratory standpoint, the patient quickly developed acute hypoxemic respiratory failure over the course of one hour in PACU
• He was placed on a facemask with 100% FiO2 to maintain oxygen saturation above 92%.
• Thoracic surgery was consulted; there was a high suspicion for stent migration or mucus plugging.
• Given the severity of the patient's respiratory status, we decided to proceed with fiberoptic-assisted intubation followed by bronchoscopy to assess the problem.

Intraoperative Course:

• We performed indirect video-assisted laryngoscopy with a McGrath® (*Medtronic, Minneapolis, MN, USA*) MAC #3 blade, revealing a Cormack–Lehane grade 1 view.
• After passing a Rusch #7.0 (*Teleflex, Morrisville, NC, USA*) #9.3 mm outer diameter endotracheal tube (ETT) through the vocal cords, we physically held the tube in place.
• A large adult Olympus® (*Shinjuku, Tokyo, Japan*) bronchoscope was advanced through the lumen of the ETT, revealing nearly complete occlusion of the tracheal stent by mucus plugs, which would not be adequately aspirated from the bronchoscope's position.
• We attempted to advance the bronchoscope into the tracheal stent to better remove the mucus plugs, but the stent's anterior position made maneuvering of the ETT into the stent lumen difficult.
• We removed the bronchoscope from the ETT and placed it through the glottic opening parallel to the endotracheal tube.
• Under direct visualization via transoral bronchoscopic guidance, we were able to insert a SunMed® (*Grand Rapids, MI, USA*) adult bougie into the stent, then advance the ETT by Seldinger technique, effectively creating a stent-in-stent effect.
• The thoracic surgeons then aspirated purulent secretions and confirmed proper stent position.

Fig 1. An *in situ* Silicone Tracheal Stent

Fig 1. An *in situ* silicone tracheal stent. Notably, the stent does not completely appose the tracheal walls and is positioned relatively anterior within the tracheal lumen. This image was acquired in the operating room prior to admission to PACU.

Postoperative Course

• The patient was transferred to the Medical Intensive Care Unit for further care. He remained intubated, sedated and paralyzed for concerns about airway management.
• On POD#1 the patient returned to the OR for placement of a T tube to facilitate removal of secretions.
• A large air leak was present with the T tube on positive pressure ventilation, but resolved with spontaneous ventilation.
• In the MICU, the patient developed worsening hypoxemia and hypotension, requiring increasing use of vasopressors.
• He died on post-operative day two after the family withdrew care.

Conclusions

• Negotiating an endotracheal tube through an airway stent may be challenging for the anesthesiologist.
• Care must be taken to avoid dislodging and migrating and in situ stent.
• We have shown that a fiberoptic bronchoscopy coupled with an bougie introducer can be a safe and effective method by which to perform a stent-in-stent technique to secure and airway
• The patients' family has approved publication of this case report.

References

1. David N, Madden BP, Sheth A, et al. Br J Anes. 2006; 96 (1): 132-5.

Jon Samuels (jos2001@med.cornell.edu

Departmental Posters

Weill Cornell Medicine **NewYork-Presbyterian**

Protective intraoperative ventilation with higher versus lower levels of positive end-expiratory pressure in obese patients (PROBESE)

Lead author: Thomas Bluth, M.D.,[1] for the PROBESE Writing Committee
WCM co-authors: Peter A. Goldstein, M.D.,[2] Zachary A.Turnbull, M.D.,[2]
WCM co-investigators: Jon D. Samuels, M.D.,[2] Farida Gadalla, M.D.,[2] Matthew T. Murrell, M.D., Ph.D.,[2] Farrell E. Cooke, B.S.,[2] Michele L. Steinkamp, R.N.[2] Cheguevara Afaneh, M.D.,[3] Gregory F. Dakin, M.D.[3] Kelly A. Garrett, M.D.,[3] Alfons Pomp, M.D.,[3] Douglas S. Scherr, M.D.[4]
[1]Pulmonary Engineering Group, Department of Anesthesiology and Intensive Care Medicine, University Hospital Carl Gustav Carus, Dresden, Germany
[2]Department of Anesthesiology, WCM, New York, NY [3]Department of Surgery, WCM, New York, NY and [4]Department of Urology, WCM, New York, NY

Introduction

– Postoperative pulmonary complications (PPCs) increase the morbidity and mortality associated with surgery in obese patients
– High levels of positive end-expiratory pressure (PEEP) with lung recruitment maneuvers (RMs) may improve intraoperative respiratory function, but they can also compromise hemodynamics, and the effects on PPCs are uncertain

Objective

– To determine whether a higher level of PEEP with alveolar recruitment maneuvers decreases postoperative pulmonary complications in obese patients undergoing surgery compared with a lower level of PEEP

Methods

– Prospective randomized trial conducted at 77 sites in 23 countries
– Eligibility criteria:
  » BMI ≥35 kg/m^{2}
  » Scheduled for non-cardiac, non-neurological surgery under general anesthesia
  » Expected duration of surgery >2 hours
  » Assess Respiratory Risk in Surgical Patients in Catalonia (ARISCAT) score ≥26
– Patients were randomized to a high PEEP group, consisting of a PEEP level of 12 cm H_2O with alveolar recruitment maneuvers (a stepwise increase of tidal volume and eventually PEEP) or to a low PEEP group, consisting of a PEEP level of 4 cm H_2O. All patients received volume-controlled ventilation with a tidal volume of 7 mL/kg of predicted body weight.
– Primary outcome: the collapsed composite of all PPCs developing within the first 5 postoperative days, with each complication weighted equally. Patients who developed at least one complication were considered as meeting the primary endpoint.
– Secondary outcomes:
  » Collapsed severe PPC composite, excluding mild respiratory failure
  » Intraoperative adverse events (AEs) such as hypoxemia, hypotension, and bradycardia
  » Unexpected need for intensive care unit (ICU) admission or ICU readmission
  » Hospital-free days at follow-up day 90
  » Postoperative wound healing
  » Postoperative extrapulmonary complications (PEPCs)

Primary and Secondary Outcomes

	High Level of PEEP (n = 989)	Low Level of PEEP (n = 987)	P value
Primary outcome			
Postoperative pulmonary complications	211 (21.3%)	233 (23.6%)	0.23
Components of the Primary Outcome			
Mild respiratory failure	135 (13.7%)	154 (15.6%)	0.22
Moderate respiratory failure	42 (4.2%)	58 (5.9%)	0.10
Severe respiratory failure	30 (3.0%)	36 (3.6%)	0.45
Atelectasis	44 (4.4%)	55 (5.6%)	0.25
Pleural effusion	43 (4.3%)	21 (2.1%)	0.005
New pulmonary infiltrates	14 (1.4%)	18 (1.8%)	0.47
Cardiopulmonary edema	17 (1.7%)	9 (0.9%)	0.12
Bronchospasm	12 (1.2%)	10 (0.1%)	0.67
Pulmonary infection	10 (1.0%)	10 (1.0%)	>0.99
Aspiration pneumonitis	2 (0.2%)	1 (0.1%)	>0.99
Acute respiratory distress syndrome	3 (0.3%)	1 (0.1%)	0.62
Pneumonothorax	1 (0.1%)	3 (0.3%)	0.37
Secondary outcomes			
Severe postoperative pulmonary complications	116 (11.7%)	134 (13.6%)	0.22
Postoperative extrapulmonary complications	167 (16.9%)	150 (15.2%)	0.31
Systemic inflammatory response syndrome	93 (9.4%)	83 (8.4%)	0.44
Sepsis	18 (1.8%)	15 (1.5%)	0.60
Severe sepsis	7 (0.7%)	10 (1.0%)	0.46
Septic shock	7 (0.7%)	8 (0.8%)	0.79
Gastrointestinal failure	65 (6.6)	56 (5.7%)	0.40
Acute kidney failure	31 (3.1%)	32 (3.2)	0.89
Extrapulmonary infection	29 (2.9%)	23 (2.3%)	0.40
Hepatic failure	9 (0.9%)	9 (0.9%)	>0.99
Coma	2 (0.2%)	2 (0.2%)	>0.99
Disseminated intravascular coagulation	1 (0.1%)	0	>0.99
Acute myocardial infarction	0	0	
Impaired postoperative wound healing	22 (2.2)	26 (2.6%)	0.55
Unexpected need for ICU admission/readmission	41 (4.1%)	32 (3.2%)	0.29
Intraoperative adverse events			
Hypoxemia	49 (5.0%)	134 (13.6%)	<0.001
Hypotension	313 (31.6%)	170 (17.2%)	<0.001
Bradycardia	98 (9.9%)	59 (6.0%)	0.001
Mortality during hospital stay	12 (1.2%)	5 (0.5%)	0.09

Results

– Patient population
  » N = 989 in high PEEP group
  » N = 987 in low PEEP group
  » High PEEP group achieved an average PEEP of 11.5 cm H_2O after intubation and 98.3% received alveolar recruitment maneuvers
  » Low PEEP group achieved an average PEEP of 4.0 cm H_2O after intubation and 1.1% received alveolar recruitment maneuvers
– Primary outcome
  » 21.3% of participants in the high PEEP group had postoperative pulmonary complications, compared to 23.6% in the low PEEP group (p = 0.23)
– Secondary outcomes
  » Severe postoperative pulmonary complications: 11.7% in the high PEEP group vs. 13.6% in the low PEEP group (p = 0.22)
  » Postoperative extrapulmonary complications: 16.9% in the high PEEP group vs. 15.2% in the low PEEP group (p = 0.31)
  » Intraoperative hypoxemia: 5.0% in the high level PEEP group vs. 13.6% in the low PEEP group (p = <0.001)
  » Intraoperative hypotension: 31.6% in the high PEEP group vs. 17.2% in the low PEEP group (p = <0.001)
  » Intraoperative bradycardia: 9.9% in the high PEEP group vs. 6.0% in the low PEEP group (p = 0.001)

Conclusion

– Among obese patients undergoing surgery under general anesthesia, an intraoperative mechanical ventilation strategy with a higher level of PEEP and alveolar recruitment maneuvers, compared with a strategy with a lower level of PEEP, did not reduce postoperative pulmonary complications
– During the intraoperative period, hypotension was more frequent in patients randomized to the high PEEP group, whereas hypoxemia was more common in patients randomized to the low PEEP group

Enhanced Recovery after Ambulatory Orthopedic Surgery

Weill Cornell Medicine
NewYork-Presbyterian

Elizabeth Fouts-Palmer[1], Nathan Painter[1], Sarah Wu[1], Sabrina Petrillo[2] and Roniel Weinberg[1]

Department of Anesthesiology[1], Weill Cornell Medical College and NewYork-Presbyterian/Lower Manhattan Hospital[2], New York, NY

Introduction

Enhanced recovery after surgery (ERAS®) programs have been widely adopted in efforts to decrease patient length of stay and encourage early ambulation and return of function after a variety of procedures, including major orthopedic procedures[1]. Here we present our experience implementing an enhanced recovery pathway for patients having ambulatory orthopedic procedures at our institutions, with a focus on promoting consistent use of preemptive multimodal analgesia and anti-nausea measures.

We conducted a retrospective review of the electronic medical record to evaluate the effectiveness of an enhanced recovery pathway (ERP) for patients having ambulatory orthopedic procedures at a community hospital (Hosp) and ambulatory surgery center (ASC).

Locations and procedure types

Hospital
- 180 bed community hospital
- 645 cases before ERP
- 791 cases after ERP
- Mean age 47 years

ASC
- Opened April 2018
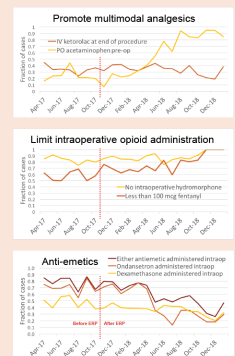- 302 cases identified
- Mean age 46 years
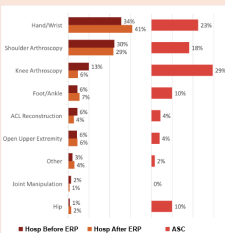
Change in percentage of patients receiving IV, PO or any opioid in the PACU after all ambulatory orthopedic procedures
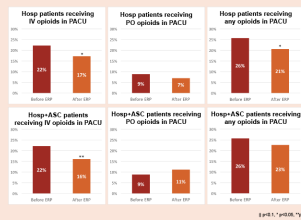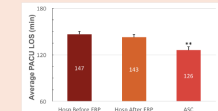

Change in percentage of patients receiving any opioid in PACU after selected procedures
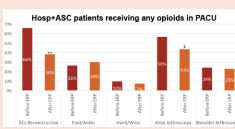
Adherence to major components of ERP

ASA physical status variation between groups

Change in PACU length of stay:

NB: Cases occurring after October 2018 lacked anesthesia end time, a total of 142 Hospital cases and 140 ASC cases are excluded from this analysis.

Conclusions

- We observed significant reductions in the percentage of patients receiving opioids in the PACU, particularly after ACL repair.
- There was no significant change in PACU length of stay, although it is unclear to what extent less acute cases have shifted to the ASC.
- An increased use of non-opioid analgesics was observed, corresponding with a decrease in perioperative opioid administration.

Future Work

- Data-driven feedback to anesthesia providers regarding effectiveness of ERP to encourage ongoing improvements
- Expansion to other surgical services
- Reintroduction of gabapentinoids for selected patients (pregabalin removed from pathway due to concerns about over-sedation.)

Literature cited
1. E. Soflin, J. Y. (2016). Enhanced recovery after surgery for primary hip and knee arthroplasty: A review of the evidence. *British Journal of Anaesthesia*, 117, iii62-iii72

For further information contact Dr. Fouts-Palmer: eaf2004@med.cornell.edu

Disclosures: None of the authors have any conflicts of interest to disclose.

Weill Cornell Medicine

NewYork-Presbyterian

Characteristics and Anatomic Distribution of Early vs. Late Stroke After Cardiac Surgery

Natalia S. Ivascu MD[1], Faiza M. Khan MD[2], Mohammed Rahouma MD[2], Irbaz Hameed MD[2], Ahmed Abouarab MD[2], Alan Z. Segal MD[3], Mario F. L. Gaudino[2], Leonard N. Girardi MD[2]

INTRODUCTION

- Acute cerebral injury after cardiac surgery occurs in a small percentage of patients, but can be life altering and life threatening
- Early work suggested most perioperative strokes were delayed[1,4]
- Perioperative stroke remains a significant predictor of major perioperative complications like sepsis, acute respiratory failure, renal failure, and reoperations regardless of how a heart operation is conducted
- This study sought to determine the incidence of perioperative stroke in a tertiary cardiovascular surgery center over a range of operations, as well as better understand the timing and location of these events and evaluate their correlation with short term outcomes

OBJECTIVES

- Primary Objective: Identify the specific predictors of early and late stroke in patients after open heart surgery
- Secondary Objectives: Risk factors for perioperative stroke, anatomic location of stroke according to time of presentation, and impact of stroke on operative mortality

METHODS

- Retrospective review of adult patients undergoing open cardiac surgery with cardiopulmonary bypass from 2006 to 2016 at New York Presbyterian Hospital/Weill Cornell Medicine
  - 7957 patients analyzed
- Patients' demographic, clinical, and perioperative data were retrieved from the medical record
- Type of stroke, affected cerebral vessel, and laterality were identified
- Regression analysis was used to identify predictors in 3 groups: no stroke, early stroke, and late stroke
  - "Early" stroke = symptoms within the first 24 hrs after surgery
  - "Late" stroke = neurologic deficit after first 24 hrs after surgery

RESULTS

- 117 patients were included in the stroke cohort from the 7957 operations analyzed
  - Early stroke occurred in 84 (71.8%) patients
  - Late stroke occurred in 33 (28.3%) patients
- Primary Objective:
  - Early Stroke Predictors: age, prior CVD, PVD, CHF, calcified aorta and emergent procedures
  - Late Stroke Predictors: age
- Secondary Objectives:
  - Stroke was the strongest predictor of operative mortality, regardless of timing (P<0.001)
    - Other predictors: age, female gender, previous surgery, preoperative CHF, calcified aorta, endocarditis, aortic surgery, urgent or emergency cases
  - Early Strokes were commonly:
    - Right sided (45.5%, P<0.001) OR bilateral (43.9%)
    - Included multivessel involvement (45.5%, P=.002)
    - Anterior (57.6%, P<0.001) or both anterior AND posterior (42.2%, P=0.002)
  - Late Strokes were commonly:
    - Left sided (57.1%, P<0.001) NOT bilateral (7.1%)
    - Rare to include multivessel involvement (7.1%, P=.002)
    - Evenly distributed between anterior and posterior, but rare to include anterior and posterior (3.6%, P<.001)
  - Predictors for perioperative stroke: age, CHF, calcified aorta, emergent procedures

Table: Details of radiologically identified strokes (n = 94)

Variables	Early Stroke (n=66)	Late Stroke (n=28)	P Value
Vessel, n (%)			
ACA	2 (3.0)	2 (7.1)	0.002
MCA	27 (40.9)	12 (42.9)	
PCA	6 (9.1)	10 (35.7)	
Isocerebellar	2 (3.0)	1 (3.6)	
Multiple	28 (42.4)	2 (7.1)	
Type of Stroke, n (%)			
Embolic	64 (97.0)	27 (96.4)	0.66
Watershed	1 (1.5)	0 (0.0)	
Lacunar	1 (1.5)	1 (3.6)	
Site, n (%)			
Left	7 (10.6)	16 (57.1)	<0.001
Right	30 (45.5)	10 (35.7)	
Bilateral	29 (43.9)	2 (7.1)	
Location, n (%)			
Anterior	38 (57.6)	15 (53.6)	0.001
Posterior	9 (13.6)	12 (42.9)	
Both	19 (28.8)	1 (3.6)	

CONCLUSION

- Early and late strokes are correlated with different risk factors and exhibit unique anatomic patterns
  - Late stroke, mostly due to age, may not be improvable
  - Early stroke has preoperative risk factors that may influence patient selection and attention to modifiable conditions
- Early and late strokes predict high incidence of operative mortality
- Results show a different anatomic stroke pattern than previous reports
  - Virtually no watershed strokes in the population
  - High percentage of strokes in multiple distributions in early stroke patients → supports the theory that intraoperative events represent a unique mechanism of stroke related to surgical conditions

REFERENCES
1. Hogue CW, Murphy SF, Schechtman KB, Dávila-Román VG. Risk factors for early or delayed stroke after cardiac surgery. Circulation. 1999;100:642-647.
2. Filsoufi F, Rahmanian PW, Castillo JG, Bronster D, Adams DH. Incidence, topography, predictors and long-term survival after stroke in patients undergoing coronary artery bypass grafting. Ann Thorac Surg. 2008;85:862-871.
3. Wolman RL, Nussmeier NA, Aggarwal A, et al. Cerebral injury after cardiac surgery: identification of a group at extraordinary risk. Multicenter Study of Perioperative Ischemia Research Group (McSPI) and the Ischemia Research and Education Foundation (IREF) Investigators. Stroke. 1999;30(3):514-522.
4. Boivie P, Edström C, Engström KG. Side differences in cerebrovascular accidents after cardiac surgery: a statistical analysis of neurologic symptoms and possible implications for anatomic mechanisms of aortic particle embolization. J Thorac Cardiovasc Surg. 2005;129:591-598.
5. Weinstein GS. Left hemispheric strokes in coronary surgery: implications for end-hole aortic cannulas. Ann Thorac Surg. 2001;71: 128-132.
6. Zingone B, Rauber E, Gatti G, et al. The impact of epiaortic ultrasonographic scanning on the risk of perioperative stroke. Euro J Cardiothorac Surg. 2006;29:720-728.
7. Schachner T, Zimmer A, Nagele G, Laufer G, Bonatti J. Risk factors for late stroke after coronary artery bypass grafting. J Thorac Cardiovasc Surg. 2005;130:485-490.
8. Mack MJ, Leon MB, Smith CR, et al. PARTNER 1 trial investigators. 5-year outcomes of transcatheter aortic valve replacement or surgical aortic valve replacement for high surgical risk patients with aortic stenosis (PARTNER 1): a randomised controlled trial. Lancet. 2015;385:2477-2484.
9. Selnes FW, DiMaio JM, Caplan LR, et al. Comparing on-pump and off-pump coronary artery bypass grafting: numerous studies but few conclusions: a scientific statement from the American Heart Association Council on Cardiovascular Surgery and Anesthesia in collaboration with the Interdisciplinary Working Group on Quality of Care and Outcomes Research. Circulation. 2005;111:2858-2864.
10. Puskas JD, Williams WH, Mahoney EM, et al. Off-pump vs conventional coronary artery bypass grafting: early and 1-year graft patency, cost, and quality-of-life outcomes: a randomized trial. JAMA. 2004;291:1841-1849.
11. Hedberg M, Engström KG. Stroke after cardiac surgery—hemispheric distribution and survival. Scand Cardiovasc J. 2013;47:136-144.
12. Tournpoulis H, Anagnostopoulos CE, Chamogeorgakis TP, et al. Impact of early and delayed stroke on in-hospital and long-term mortality after isolated coronary artery bypass grafting. Am J Cardiol. 2008;102:411-417.
13. Salazar JD, Wityk RJ, Grega MA, Borowicz LM, Doty JR, Petrofski JA. Stroke after cardiac surgery: short- and long-term outcomes. Ann Thorac Surg. 2001;72:1195-1202.
14. Gold JP, Charlson ME, Williams-Russo P, et al. Improvement of outcomes after coronary artery bypass. A randomized trial comparing intraoperative high versus low mean arterial pressure. J Thorac Cardiovasc Surg. 1995;110(5):1302-1314.
15. Sun LY, Chung AM, Farkouh ME, et al. Defining an intraoperative hypotension threshold in association with stroke in cardiac surgery. Anesthesiology. 2018;129:440-447.

[1]Department of Anesthesiology, Weill Cornell Medicine, New York, New York
[2]Department of Cardiothoracic Surgery, Weill Cornell Medicine, New York, New York
[3]Department of Neurology, Weill Cornell Medicine, New York, New York

Published in Journal of Cardiac Surgery Vol. 34 in May 2019

Chronic Pain in Refugee Torture Survivors

Gunisha Kaur, MD, MA, Roniel Weinberg, MD, Andrew Milewski, PhD,
Samantha Huynh, BS, Elizabeth Mauer, MS,
Hugh Hemmings, MD PhD, Kane Pryor, MD

Weill Cornell Medicine
Clinical & Translational Science Center

Background

- Chronic pain is the leading cause of disability after torture, affecting 85% of survivors (27 million people) globally[1,2]. Pain is most often diagnosed as psychosomatic or nociceptive[3].
- While a vast majority of torture survivors experience chronic somatic pain, evaluators fail to accurately diagnose pain in patients due to confounding psychiatric illness and a lack of diagnostic tools[4,5].
- Objective: To determine the sensitivity of the global standard assessment (United Nations Istanbul Protocol, UNIP) for somatic pain in torture survivors versus a validated pain screen (Brief Pain Inventory Short Form, BPISF), as compared to the reference standard (a pain specialist physician).

Methods

- We enrolled 25 subjects in the first-ever, adequately powered clinical study of pain diagnosis in refugee torture survivors worldwide.
- 20 subjects were identified as torture survivors by the World Medical Association (WMA) definition. 5 subjects were excluded after UNIP analysis as they did not meet WMA criteria.
- Subjects received the BPISF, followed by a non-invasive examination by a pain specialist physician.

Brief Pain Inventory – Short Form

Table 1: Subject Data

Subject #	Persecution Type	Type of Torture	UNIP Δ	BPISF ◊	Pain ♦ Specialist	UNIP Evaluator
1	Political	Psych, shot, rifle assault	No	None	None	FM
2	Gang	Psych, beatings, cigarette burns	No▲	N/A	Mod-Severe	IMP
3*	Political	Psych, beating, assault with object, stabbing, starvation	No/No	Mild	Moderate	Psych MD/IM
5	Race	Psych, assault with object, rape	No	N/A	None	Psych MD
6*	Political	Psych, stabbed, beating, assault with object	No/No	Mild	Mild	Psych MD/IM
7*	Political	Psych, assault with object, FGM, rape, burned	Yes/Yes	Mild	Moderate	Psych PhD/IMP
8	LGBTQI	Psych, assault with object, beatings, near drowning, electrical wire	No	N/A	Severe	Psych PhD
9*	FGM, DV	Psych, beating	No▲/ Yes▲	N/A	Moderate	Psych PhD/Gyn
11	Gang	Psych, beating, choking, rape	No	Severe	Severe	Psych MD
14	FGM, DV	Psych, beating, assault with object, FGM, burned with iron, rape	No▲	N/A	Mod-Severe	FM
15	Gang	Psych, beating, choking	No	Mild	Severe	Psych MD
16	LGBTQI	Psych, beating, assault with object	No	Mild	Mild	Psych PhD
18	LGBTQI	Psych, assault with object, bitten, broken arm, cut with knife	No	Mild	Mild	IM
19	Political	Psych, beating, assault with object	Yes	Mod.	Mild-Mod.	FM
20	FGM	FGM	Yes	Mild	Severe	Gyn
21*	Gang	Psych, shooting	No/ Yes▲	Mild	Mod.-Severe	Psych MD/IM
22	Political	Psych, sexual assault, rape, beating	No	Mild	Moderate	Psych PhD
23	FGM, DV	Psych, FGM, assault with object, knifing, rape	Yes	Mod.	Mild-Mod.	Gyn
24	Gang	Rape, beating	No	Sev.	Severe	Psych PhD
25	Political	Psych, beating, assault with object, waterboarding, near drowning	No	Sev.	Mild-Mod.	Psych PhD

Abbreviations: Brief Pain Inventory Short Form (BPISF); The United Nations Istanbul Protocol (UNIP); domestic violence (DV); female genital mutilation (FGM); lesbian, gay, bisexual, transgender, questioning, intersex (LGBTQI); psychological (psych); not applicable (N/A); moderate (mod); severe (sev); Internal Medicine (IM); Internal Medicine and Pediatrics (IMP); Family Medicine (FM); Gynecologist (Gyn); Psychiatrist (Psych MD); Psychologist (Psych PhD)
Δ. Whether the UNIP evaluation identified chronic pain or pain syndromes.
◊. Severity of the pain identified by the BPISF.
♦. Severity of the pain identified by the pain specialist.
*. These subjects had two UNIP evaluations: two entries are shown for the UNIP and the UNIP evaluator columns.
▲. Chronic pain or a pain syndrome was identified in the narrative portion of the UNIP evaluation, but not in the conclusion section.

Figure 1: Evaluator's ability to diagnose and treat somatic pain using the Index Test versus the Reference Standard

- Index Test (United Nations Istanbul Protocol)
- Reference Standard (Pain Specialist Physician)

Figure 2: Sensitivity of Index Test vs. Brief Pain Inventory – Short Form

- Index Test (United Nations Istanbul Protocol)
- BPISF (Validated Pain Screen)

Results

- We found that providers using only the standard UNIP (index test) detected and treated pain in a **maximum of 16% of patients as compared to 85% of patients who were diagnosed with chronic pain by the reference standard**.
- When employed, the validated BPISF screen had a sensitivity of 100% and a negative predictive value of 100%, as compared to a sensitivity of 24% and negative predictive value of 19% by the UNIP.

Discussion

- Our data provide an impetus and mechanism to advance the standard of care of torture survivors by supplementing the standard global assessment protocol, the UNIP, with a screen for chronic pain.
- The significant sensitivity and negative predictive value differences between the UNIP and the BPISF suggest that integrating a validated pain screen into the UNIP will decrease the failure of pain diagnoses by general evaluators.
- Accurate diagnosis of pain is a critical part of treatment and rehabilitation. Physical and psychological sequelae of torture independently modulate each other, wich suggests that without addressing both physical and psychological trauma in torture survivors, rehabilitation will be limited.

This investigation was funded by NIH grant KL2TR002385 of the Clinical and Translational Science Center at Weill Cornell Medicine.

References
1. Global Trends: Forced Displacement in 2018. United Nations High Commissioner for Refugees.
2. Steel Z, Chey T, Silove D, Marnane C, Bryant RA, van Ommeren M. Association of torture and other potentially traumatic events with mental health outcomes among populations exposed to mass conflict and displacement: a systematic review and meta-analysis. JAMA. 2009;302: 537-549
3. Olsen DR, Montgomery E, Bøjholm S, Foldspang A. Prevalent musculoskeletal pain as a correlate of previous exposure to torture. Scand J Public Health. 2006;34: 496-503
4. Nice OS, Garland CF, Hilton SM, Baggett JC, Mitchell RE. Long-term health outcomes and medical effects of torture among US Navy prisoners of war in Vietnam. JAMA. 1996;276: 375-381.
5. Crosby SS. Primary care management of non-English speaking refugees who have experienced trauma: a clinical review. JAMA. 2013;310: 519-528. doi: 10.1001/jama.2013.8788.

Female genital mutilation/cutting: a systematic review and meta-analysis of somatic pain and obstetric sequelae

Jacob Lurie, M.P.H., Alessandra Weidman, M.P.H., Samantha Huynh, B.S., Diana Delgado, M.L.S., Imaani Easthausen, M.S., Gunisha Kaur, M.D., M.A.

Department of Anesthesiology, Weill Cornell Medical College, New York, NY

Introduction

- Between 100 million and 200 million women have been affected by female genital mutilation/cutting (FGM/C), and more than 30 million girls under the age of 15 are at risk of FGM/C in the next decade.
- As forcibly displaced individuals increasingly cross transnational boundaries, healthcare providers globally must familiarize themselves with the complicated clinical presentation and management of women and girls who have been subjected to FGM/C.
- Health professionals often do not clinically recognize FGM/C or do not understand the negative health consequences associated with the practice; physicians in developed countries are unfamiliar and uncomfortable treating patients with FGM/C.
- There is a substantial need for research on the acute and chronic complications of FGM/C, their prevalence and manifestation, and guidance on treatment and management

Objectives

- The goal of this study was to analyze available data regarding pain outcomes and obstetric complications in the setting of FGM/C.
- We also aimed to estimate the odds of painful sequelae among women with FGM/C compared to women without FGM/C using data pooled from multiple different studies and sources.

Methods

- We performed this systematic review and meta-analysis according to the Preferred Reporting Items for Systematic Reviews and Meta-Analyses (PRISMA) guidelines.
- A comprehensive literature search from inception through October, 2018 of Ovid Medline, Ovid EMBASE, The Cochrane Library (Wiley), and POPLINE for studies reporting the prevalence of painful sequelae and obstetric complications resulting from female genital mutilation/cutting was completed.
- Two reviewers independently screened 6,260 abstracts, and of 551 full-text studies assessed for eligibility, 110 met eligibility criteria.
- These reviewers also extracted data and assessed publication quality. Pooled odds ratios were estimated for each outcome of interest.

Different types of FGM

= Parts removed   = Stitches

No FGM   Type 1   Type 2   Type 3

Figure 1. The World Health Organization Classification of FGM/C. The World Health Organization (WHO) has categorized FGM/C severity into four types: Type I, or clitoridectomy, which consists of partial or total removal of the clitoris and its prepuce, Type II, or excision, which consists of the removal of the clitoris and labia minora, Type III, the most severe form, which is known as infibulation and consists of narrowing the vaginal orifice, and Type IV (not depicted), which consists of any other form of genital mutilation/cutting

Figure 2. Forest plots depicting meta-analyses of episiotomy and perineal tears in the setting of female genital mutilation/cutting.

Figure 3. Forest plots depicting meta-analyses of dysmenorrhea, dyspareunia, dysuria, and urinary tract infection in the setting of female genital mutilation/cutting.

Analysis

- Women with FGM/C were observed to have a three-fold increase in odds of experiencing dyspareunia compared to women without FGM/C (pooled OR: 2.97; 95% CI: 1.63-5.41; I^2: 89%; p-value: 0.003).
- Significant associations were also observed between FGM/C and perineal tears during childbirth (pooled odds ratio: 2.20; 95% CI: 1.25-3.87; I^2: 70%; p-value: 0.01), dysmenorrhea (pooled odds ratio: 1.89; 95% CI: 1.13-3.16; I^2: 90%; p-value: 0.02), episiotomy (pooled odds ratio: 1.87; 95% CI: 1.25-2.81; I^2: 96%; p-value: 0.004), and dysuria (pooled odds ratio: 1.43; 95% CI: 1.17-1.75; I^2: 0%; p-value: 0.01).
- There was insufficient evidence to make conclusions about associations between FGM/C and prolonged labor (pooled odds ratio: 1.43; 95% CI: 0.54-3.79; I^2: 99%; p-value: 0.43), urinary tract infection (pooled odds ratio: 2.10; 95% CI: 0.80-5.54; I^2: 90%; p-value: 0.10), cesarean delivery (pooled odds ratio: 1.33; 95% CI: 0.89-1.98; I^2: 97%; p-value: 0.15), and instrumental delivery (pooled odds ratio: 1.06; 95% CI: 0.66-1.71; I^2: 54%; p-value: 0.783).

Discussion

- This investigation determined that several pain and obstetric complications are significantly associated with FGM/C, including dyspareunia, dysuria, dysmenorrhea, perineal tears, and episiotomy.
- Long-term pain outcomes of FGM/C describes in this study are relevant to practitioners globally who are increasingly likely to encounter patients with FGM/C due to amplified migration.

Conclusion

- Our systematic review and meta-analysis were conducted according to PRISMA guidelines, followed a registered protocol (CRD42018115848), and utilized validated tools to assess risk of bias and study quality.
- This meta-analysis provides evidence that specific painful outcomes and obstetric complications are significantly more common in patients with female genital mutilation/cutting.
- Data from this study indicate that providers globally must familiarize themselves with the unique health consequences of FGM/C, including accurate diagnosis, pain management, and obstetric planning.

Medical Mission Location as Compared to Country Need: A Systematic Review

Keerteshwrya Mishra[1], Sonal Jessel[2], Jacob Lurie[3], Kane O. Pryor[4] and Gunisha Kaur[4]

Wayne State University School of Medicine[1], Columbia University[2],
Icahn School of Medicine at Mount Sinai[3], Weill Cornell Medicine[4]

Background

- Academic institutions in developed countries are increasingly participating in medical missions due to the growing interest in understanding the global burden and epidemiology of diseases, global healthcare disparities, and biopsychosocial influences on health[1,2].
- Medical anthropologists have hypothesized that in addition to the potential unintended consequences of medical missions, academic institutions do not actually participate where need is the greatest but rather in more well-developed regions.
- **Objective:** To investigate whether or not a gap in medical missions exists between academic medical mission location and countries in greatest need.

Methods

Part 1:
- Medline and Embase were queried from 2013 to 2017 to identify articles published by academic physicians participating in medical missions, as a surrogate indicator of where missions occur.
- Key data such as country visited, country of origin, type of service, funding, and clinical specialty of physicians, were extracted and characterized based on country visited.

Part 2:
- Maternal Mortality Ratio, Life Expectancy, and Human Development Index data (2015 – 2017) from the World Bank, United Nations, and World Health Organization was collected[3]. The top 25 countries ranking worst globally in each category were delineated. From these data, a composite list of the top most disadvantaged countries was generated.
- This final list of countries most in need was overlayed on and compared to the list of countries visited most frequently by medical missions.

Figure 1: PRISMA Style Flow Diagram of Systematic Review.
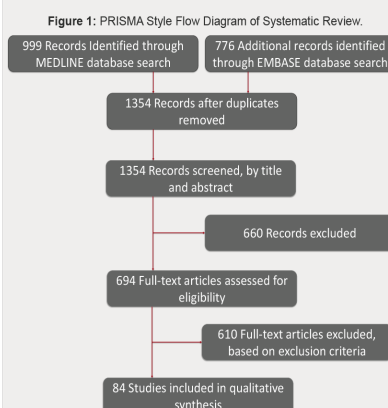
Figure 2: Countries visited as compared to countries in greatest need by poverty, health, or human development indicator data.
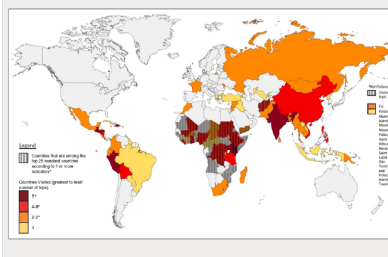
Results

- 107 academic medical missions were reported over the five-year period reviewed.
- Of these interventions, **only 29% (n = 31) occurred in a country ranking in greatest need.**
- An additional 6% (n = 6) of interventions took place in these countries during emergency situations such as the 2015 Ebola pandemic in West Africa.
- 32% (n = 34) of all academic missions occurred in low-income countries, 51% (n = 55) in lower-middle income countries, 15% (n = 16) in upper-middle income countries, and 2% (n = 2) in high-income countries.

Discussion

- The data indicate that **only a fraction of academic medical missions occur in the world's most disadvantaged countries,** where need and benefit of intervention are the greatest.
- Reasons for this might include the safety profile of a region, longstanding partnerships with local institutions, and ease of travel, and should be investigated further.
- The investigation was limited by the use of publications in academic journals as a surrogate for interventions by academic medical missions.

References
1. Merson MH. University engagement in global health. N Engl J Med. 2014; 370(18): 1676.
2. Drain PK, Holmes KK, Skeff KM, Hall TL and Gardner P. Global health training and international clinical rotations during residency: Current status, needs, and opportunities. Acad Med. 2009; 84(3): 320–5.
3. The World Bank. Maternal Mortality Ratio (modeled estimate, per 100,000 live births).

Anaesthetic depth and complications after major surgery: an international, randomised controlled trial

Timothy Short, M.D.,[1] Douglas Campbell, B.M.,[1] Christopher Frampton, Ph.D.,[2] et al.
WCM Investigators: Kane Pryor, M.D.,[3] Michele Steinkamp, R.N.,[3] Farrell Cooke, B.S.,[3] Rachel Friedlander, B.S.,[3] Jaideep Malhotra, M.D.,[3] Lori A. Rubin, M.D.[3]

[1]Department of Anesthesia, Auckland City Hospital, Grafton, Auckland, New Zealand
[2]Department of Psychological Medicine, University of Otago, Christchurch, New Zealand
[3]Department of Anesthesiology, Weill Cornell Medical College, New York, NY

INTRODUCTION

- The development of processed electroencephalographic monitors such as the bispectral index (BIS) now allows for anesthesia depth to be individualized[1], allowing patients that are sensitive to anesthetics to receive less drug
- A meta-analysis of studies examining an association between increasing anesthetic depth and mortality revealed a 21% increase in mortality associated with deep anesthesia[2]
  - Most of the studies did not report blood pressure, and those that did showed a stronger relationship between deep anesthesia and complications when blood pressure was also low
- Several small, randomized studies did not find this association between anesthetic depth and mortality[3-4]

OBJECTIVE

- To compare all-cause 1-year mortality in older patients having major surgery and randomly assigned to light or deep general anesthesia

METHODS

- 73 centers across 7 countries participated in this study
- Eligible patients were older with significant comorbidity defined as:
  - Operation duration ≥ 2 hours
  - Expected hospital stay ≥ 2 days
  - Age ≥ 60 years
  - ASA status of 3 or 4
- Patients received volatile anesthetic-based general anesthesia with or without major regional anesthesia
- 6668 patients were randomized to have a BIS of 50 or a BIS of 35 during surgery
- <u>Primary outcome</u>: 1-year all-cause mortality
- <u>Secondary outcomes</u>:
  - Incidences of myocardial infarction, cardiac arrest, pulmonary embolism, stroke, and a composite of these four cardiovascular outcomes
  - Sepsis, surgical site infection, and a composite of these two septic outcomes
  - Total intensive care unit stay, awareness during anesthesia, WHODAS 2.0 score at 30 days and 1 year, disability-free survival (defined as alive and less than a 4-point decline in WHODAS 2.0 score at 1 year), persistent pain, and cancer recurrence

Primary, secondary, exploratory, and other outcomes

	BIS 50 (n=3316)	BIS 35 (n=3328)	Ratio (95%CI)* or p value
Primary outcome			
All-cause mortality	212 (6%)	238 (7%)	0.88 (0.73-1.07)
Secondary outcomes			
Myocardial infarction	77 (2%)	77 (2%)	1.00 (0.73-1.38)
Cardiac arrest	23 (1%)	12 (<1%)	1.9 (0.96-3.9)
Pulmonary embolism	33 (1%)	43 (1%)	0.77 (0.49-1.22)
Stroke	43 (1%)	33 (1%)	1.31 (0.83-2.1)
Sepsis	204 (6%)	219 (7%)	0.93 (0.76-1.13)
Surgical site infection	240 (7%)	212 (6%)	1.15 (0.95-1.39)
Unplanned ICU admission	170 (5%)	190 (6%)	0.89 (0.72-1.10)
Awareness during anesthesia	1	0	..
WHODAS 2.0 score			
30 days post surgery	18 (14-25)	18 (13-25)	0.78
1 year post surgery	16 (13-23)	16 (13-23)	0.19
Disability-free survival at 1 year	2035 (68%)	2021 (68%)	1.05 (0.94-1.17)
Persistent pain			
Day 30	729 (22%)	745 (22%)	0.98 (0.87-1.10)
Day 30 score	230 (90-440)	205 (80-405)	0.14
1 year	250 (8%)	224 (7%)	1.13 (0.93-1.36)
1 year score	213 (60-460)	224 (76-524)	0.32
Neuropathic pain			
1 year	237 (7%)	211 (6%)	1.13 (0.93-1.38)
1 year score	140 (60-300)	180 (70-355)	0.038
Recurrence of cancer at 1 year	216 (14%)	211 (13%)	1.02 (0.85-1.25)
Exploratory outcomes			
Composite of mortality, myocardial infarction, cardiac arrest, pulmonary embolism, and stroke	333 (10%)	360 (11%)	0.92 (0.79-1.08)
Composite of sepsis and surgical site infection	372 (11%)	359 (11%)	1.05 (0.90-1.22)
Other outcomes			
Quality of recovery score			
Day 1	101 (86-144)	101 (86-116)	0.66
Day 2	109 (93-124)	108 (92-123)	0.53
Day 3	104 (89-118)	104 (88-118)	0.64
Day 30	132 (118-142)	132 (118-142)	0.89
Duration of postoperative hospital stay, days	6 (4-10)	6 (3-9)	0.54

Data are n (%), n, or median (IQR), unless otherwise stated. Quality of recovery score was the 15-item score; its range is 0 to 150, with 150 being excellent in all domains. WHODAS 2.0 - WHO Disability Assessment Schedule, which estimates the amount of disability; scores of 24 or more indicate at least moderate disability. *Hazard ratio for BIS 50 compared with BIS 35 for primary outcomes; odds ratio for BIS 50 compared with BIS 35 for other outcomes. Adapted from Table 3.

RESULTS

- **Patient population**
  - 3326 BIS 50 participants
  - 3342 BIS 35 participants
  - The average BIS was 47.2 for the BIS 50 group and 38.8 for the BIS 35 group
- **Primary outcome**
  - All-cause mortality was 6% for the BIS 50 group and 7% for the BIS 35 group ($p = 0.88$)
- **Secondary outcomes**
  - Myocardial infarction
    - 2% for BIS 50 and 2% for BIS 35 (p = 1.00)
  - Sepsis
    - 6% for BIS 50 and 7% for BIS 35 (p = 0.93)
  - Surgical site infection
    - 7% for BIS 50 and 6% for BIS 35 (p = 1.15)
  - Disability-free survival at one year
    - 68% for BIS 50 and 68% for BIS 35 (p = 1.05)
  - Recurrence of cancer at 1 year
    - 14% for BIS 50 and 13% for BIS 35 (p = 1.02)

CONCLUSION

- Among patients at increased risk of complications after major surgery, light general anesthesia was not associated with lower 1-year mortality than deep general anesthesia
- This trial defines a broad range of anesthetic depth over which anesthesia may be safely delivered when titrating volatile anesthetic conditions using a processed electroencephalographic monitor
- The low incidence of awareness supports the safety of targeting a bispectral index of 50 using relatively low doses of volatile anesthetics in older patients

REFERENCES
1. Punjasawadwong Y, Phongchiewboon A, Bunchungmongkol N. Bispectral index for improving anaesthetic delivery and postoperative recovery. Cochrane Database Syst Rev 2014; 6: CD003843.
2. Zorrilla-Vaca A, Healy RJ, Wu CL, Grant MC. Relation between bispectral index measurements of anesthetic depth and postoperative mortality: a meta-analysis of observational studies. Can J Anesth 2017; 64: 597–607.
3. Chan M, Cheng B, Lee T, Gin T, CODA Trial Group. BIS-guided anesthesia decreases postoperative delirium and cognitive decline. J Neurosurg Anesthesiol 2013; 25: 33–42.
4. Short T, Leslie K, Campbell D, et al. A pilot study for a prospective, randomized, double-blind trial of the influence of anesthetic depth on long term outcome. Anesth Analg 2014; 118: 981–86.

Published in The Lancet on October 20, 2019

Structural basis of lipid and ion transport by TMEM16 scramblases

Maria Falzone[1], George Khelashvili[2], Xiaolu Cheng[2], Byoung-Cheol Lee[3], Jan Rheinberger[4], Ashleigh Raczkowski[5],
Edward Eng[5], Crina Nimigean[2,4,6], Harel Weinstein[2], Alessio Accardi[2,4,6]

[1]Graduate School, [2]Physiology and Biophysics, Weill Cornell Medical College, New York, NY, USA, [3]Department of Structure and Function on Neural Network, KBRI, Deagu, Republic of Korea, [4]Anesthesiology, Weill Cornell Medical College, New York, NY, USA, [5]Simons Electron Microscopy Center, New York Structural Biology Center, New York, USA,, [6]Biochemistry Weill Cornell Medical College, New York, NY, USA.

Backbone amides are conserved determinants of inter-anion selectivity in CLCs

Eva Fortea[1], Lilia Leisle[1], Kin Lam[3], Tao Jiang[3], Alessandra Picollo[2], Jason D. Galpin[2], Emad Tajkhorshid[3], Christopher A. Ahern[2] & Alessio Accardi[1]
[1]Department of Anesthesiology, Department of Biophysics and Physiology, Department of Biochemistry, Weill Cornell Medical College, New York, NY, USA
[2]Department of Molecular Physiology and Biophysics, University of Iowa, Carver College of Medicine, Iowa City, IA, USA
[3]Department of Physics, Department of Biochemistry, Center for Biophysics and Quantitative Biology, NIH Center for Macromolecular Modeling and Bioinformatics,
Beckman Institute for Advanced Science and Technology, University of Illinois at Urbana-Champaign, Urbana, Illinois 61801, United States

Weill Cornell Medicine

ABSTRACT

Most known Cl^- channels are more permeable to anions such as I^- or NO_3^- than to their namesake Cl^- ion. Anion permeability in these channels is determined by the dehydration energy of the permeating ion, and follows the Hofmeister sequence $I^->Br^->NO_3^->Cl^-$. CLC channels, in contrast, are more permeable to Cl^- and have a unique selectivity sequence of $Cl^->Br^->NO_3^->I^-$. It has been proposed that CLC selectivity is primarily determined by interactions of pore-lining side chains with the permeating anions. Specifically, a serine residue (Ser_{cen}) which participates in the central ion binding site was shown to control the Cl^- vs. NO_3^- selectivity of various CLC channels and transporters. Surprisingly, in the recent structure of a CIC-K channel, Ser_{cen} points away from the pore. Here, we show that mutations at Ser_{cen} do not alter the selectivity sequence of CLC-K and CLC-1 channels, suggesting that this position is not the conserved determinant of CLC selectivity. Since the CLC pore is also lined by backbone amides that are structurally conserved that coordinate the permeating ions, we hypothesized that these moieties might be conserved determinants of anion selectivity in the CLC family. Here, we test this hypothesis using atomic-scale mutagenesis to selectively replace the amides of pore lining amino-acids with their respective alfa-hydroxy acid counterparts. This approach, enables us to replace the hydrogen-bonding amide groups with esters, without altering the side-chains of the respective residues. Site-specific incorporation of α-hydroxy acids in CLC-0 and CLC-K yielded robust currents with degraded inter-anion discrimination for both channels. Interestingly, in CLC-0 the central binding site appears to play the major role in anion recognition, while in CLC-K this function is taken over mostly by the external binding site. This observation may be ascribed to the presence of the gating Glu in CLC-0 and its absence in CLC-K. Taken together, our data suggests that the pore-lining backbone amides are likely to be the conserved determinants of inter-anion selectivity in CLCs and that side chains contribute to selectivity only in a subset of CLCs.

INTRODUCTION

- CLC ion translocation pathway is well conserved between channels and transporters[1,2,3,4] and all CLCs share a common selectivity sequence of $Cl^->Br^->NO_3^->I^-$. The permeant ions in the pathway are coordinated by:
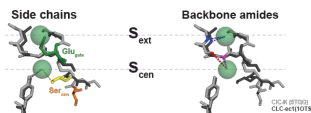
- Mutating Ser_{cen} to Pro switches the selectivity from Cl^- to NO_3^- in channels (CLC-0) and transporters (CLC-ec1, CLC-5) and *vice versa*. **Thus Ser_{cen} was proposed to be the key determinant for inter-anion specificity**[5,6,7,8].
- However, Ser_{cen} points away from the pore in the CIC-K channel structure. **This raises the question of how a non-structurally conserved residue can underlie a conserved selectivity.**

Hypothesis:
Backbone amides coordinating permeating ions are the conserved determinants of selectivity amont the CLCs.

APPROACH AND CONTROLS
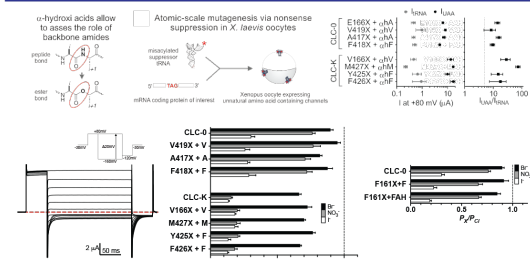
- Site-specific incorporation of α-hydroxi acids along the pore of CLC channels is efficient and yields robust currents.
- Site-specific incorporation of α-amino acids through nonsense supression yiels wt-like currents.
- Substitution of a backbone amide outside of the CLC-0 pore has no effects on inter-anion selectivity

ACKNOWLEDGEMENTS AND CITATIONS

1. Dutzler et al., Nature, 2002; 2. Dutzler et al., Science, 2003; 3. Feng et al., Science, 2010; 4. Park et al., Nature, 2017; 5. Zifarelli & Pusch, EMBO J, 2009; 6. Bergsdorf et al., J Biol Chem, 2009; 7. Picollo et al., Nat Struct Mol Biol, 2009; 8.Wege et al., Plant J, 2010

RESULTS

1. Ser_{cen} is not the conserved determinant of inter-anion selectivity in the CLCs.

- S107P mutation switches selectivity of CIC-ec1 from chloride to nitrate as in CLC-0.
- The C-D loop in S107P adopts a different conformation where P107 and G108 clash with the ion binding sites.
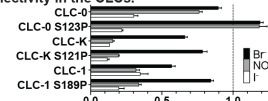
2. S_{cen} and S_{ext} play different roles in selectivity in CLC-0 and CLC-k
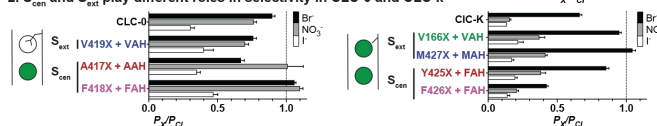
- CLC-0 and CLC-K show strongly degraded inter-anion selectivity upon substitution of backbone amides along the ion pore.
- In CLC-0 S_{cen} is the major site for anion recognition. In contrast, in CLC-K S_{ext} and S_{cen} are both main determinants.

3. The presence of Glu_{ex} modulates the the energetic contribution of backbone amides in S_{ext} to inter-anion recognition.
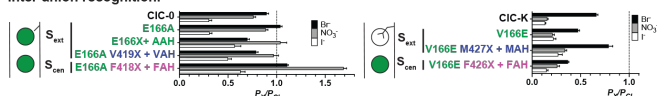
4. MD simulations with CLC-K show that the backbone amide to ester replacement at M427 shifts the binding mode to S_{cen} while its replacement at Y425 shifts ion occupancy towards S_{ext}

- The upper right panel shows spontaneous binding of chloride to S_{ext}. When the backbone in M427 is mutated the Cl^- binding mode shifts to S_{cen}.

- The lower rigth panel shows a spontaneous binding of chloride to S_{cen}. When the backbone in Y425 is mutated the Cl^- binding mode shits to S_{ext}.

- MD simulations with CLC-K are in agreement with the experimental data. Incorporation of α-hydroxi acids in position M427 and Y425 shifts the Cl^- binding away from the mutated binding site.

CONCLUSIONS

1) The residue at the Ser_{cen} position plays a role in some but not all CLCs, and therefore cannot be the common determinant of anion selectivity in the CLCs, as they share the selectivity sequence.
2) Using site-specific incorporation of α-hydroxi acids in CLC channels we show that the hydrogen bonds between pore-lining backbone amides and the permeating anion are key energetic determinants of inter-anion selectivity in the CLCs.
3) In CLC-0 S_{cen} is the major determinant of anion selectivity. However, in CLC-K both S_{ext} and S_{cen} play important roles in determining anion selectivity.
4) The differential role of S_{ext} in CLC-0 and CLC-K is due to the presence of the gating glutamate. Both sites become important in CLC-0 selectivity when the gating glutamate side chain is removed. Conversely, S_{cen} becomes more important in CLC-K when the neutral Val is replaced with negatively charged glutamic acid side chain.
5) MD simulations show that replacement of a pore-lining amide with an ester group at S_{ext} favours occupancy of S_{cen}, and vice versa. These results are in agreement with our electrophysiological measurements.
6) We propose that anionic selectivity in the CLCs is primarily determined by the hydrogen bonds of the pore-lining backbone amides, and that side chains such as the gating glutamate and Ser_{cen} play secondary modulatory roles.

Cortical features predict movement dynamics during emergence from anesthesia

Sijia Gao[1,2] Vikram Krishnamurthy[2] and Diany Paola Calderon[1*]

[1]Dept. of Anesthesiology Weill Cornell Medical College, New York; [2]Dept of Electrical and Computer Engineering. Cornell University

INTRODUCTION:

Recovery of a conscious state during emergence from anesthesia is usually identified by the presence of full cortical desynchronization, initiation of movement and behavioral reactivity to sensory stimuli(1). However, the variety of cortical patterns in the electroencephalogram (EEG) associated with the type of anesthetic and the poor description of motor behavior during emergence have made EEG and behavior difficult to implement as precise tracking methods for emergence from anesthesia. Here, we propose a novel approach to improve tracking of arousal by using the combination of cortical activity and behavior when assessing awakening.

To test this hypothesis, we ramped down anesthetic concentration while simultaneously recorded local field potentials (LFPs) and movement in mice using video and a vibration sensor . The application of a smoothed-Z score algorithm and k-means to spectrograms derived five cortical periods while rodents restored motor behavior during emergence from isoflurane. These periods composed by several states correlated with specific motor behaviors such as trunk movement, abduction and adduction of hindlimbs, and organized movements. These cortical states served as predictors of motor behavior in sevoflurane and our arousal-rodent model(2). The analysis was unable to predict righting reflex, a behavior often used to detect awakening(3-4) suggesting that cortical involvement is absent in this behavior.

Restoring motor behavior is a dynamic process that begins tens of minutes earlier than the righting reflex. Defined cortical states served as predictors of intervals in which particular motor behaviors were detected in two mechanistically different anesthetics and a pharmacologically induced-arousal model.

METHODS:

Mice with implanted head holders were induced at a concentration of isoflurane 3% and then transferred to the stereotaxic frame for recordings. Anesthetic was delivered through a nose cone at a concentration of 1.25% isoflurane. In the natural emergence model, anesthetic was lightened step wise until the volatile gas was turned off.

In pharmacologically induced-arousal model, GABA antagonist bicuculline (10mM) was unilaterally injected to NGC using a microinjection pump while anesthetic was maintained as isoflurane 1.25%.

We simultaneously recorded LFPs from motor cortex bilaterally. We detected the strength of the movement using a vibration sensor placed under the mouse abdomen.

Spectral analysis LFPs were first down sampled to 1000Hz offline. We then used the function *mtspecgramc in Chronux* toolbox in MATLAB to compute spectrogram with the following parameters: frequency band = [2, 150] Hz, tapers = [3, 5], movingwin = [5, 2.5] seconds. Power at each frequency was normalized by the total power at the same time instant, transformed to dB.

Detection and classification of dominant frequency For every time instant, we first calculated power of frequency intervals between 2 and 150Hz. Then, we implemented a smoothed Z-score thresholding algorithm to identify the dominant frequency. We clusterized dominant frequencies using Kmeans.

Motor behavior examined from the video Motor behavior was visually inspected from the video and classified as follows: (i) trunk movement (ii) hindlimb movement including abduction, adduction, alternation and body wobbly (iii) and organized movements.

RESULTS:

1. Specific cortical features precede motor arousal during emergence from isoflurane
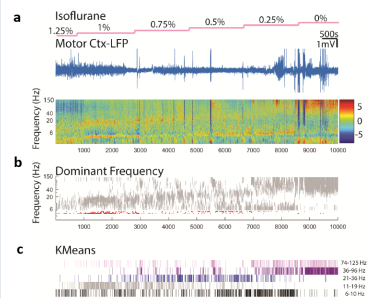
a. Representative trace of LFP recorded in motor cortex as well as its spectrogram. b. Dominant frequencies as a function of time c. KMeans clustering of the dominant frequencies

2. Restoring motor behavior is a dynamic process during emergence from anesthesia
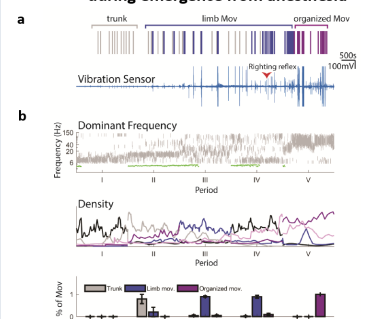
a. Motor behavior examined from the video and the vibration sensor. b. Averaged dominant frequencies, density of the clustered dominant frequencies and motor behavior distribution per period.

3. Emergence from sevoflurane undergo equivalent cortical and motor arousal features as isoflurane
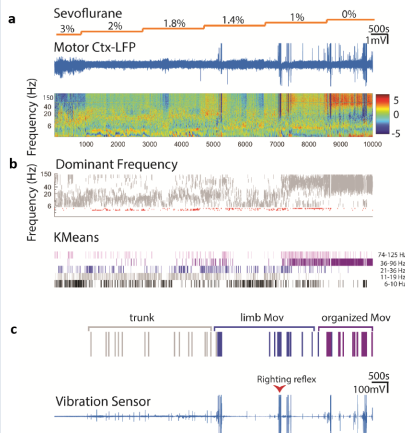
a. Representative trace of LFP recorded from motor cortex as well as its spectrogram during emergence from sevoflurane anesthesia. b. Dominant frequencies and Kmeans classification results. c. Motor behavior observed from the video and detected by the vibration sensor.
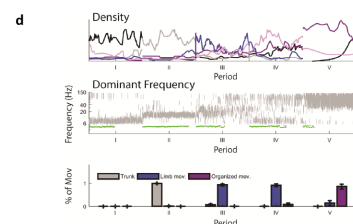
d. Averaged density of the classified dominant frequencies and motor behavior distribution per cortical period.

4. Cortical and motor arousal features may assess awakening in other conditions
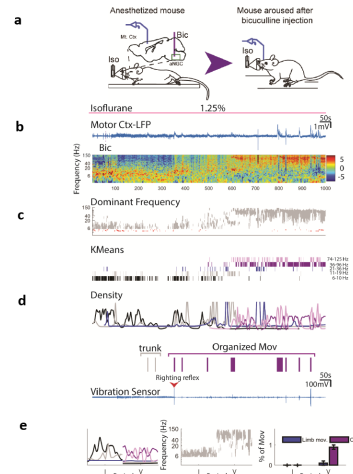
a. Experimental schematic of pharmacologically-induced arousal model. b. Example trace of LFP recorded in motor cortex as well as its spectrogram before and after bic injection. c. Dominant frequencies and Kmeans classification results. d. Density of the classified dominant frequency, motor behavior observed from the video and voltage of the vibration sensor. e. Averaged density of the classified dominant frequencies and motor behavior distribution per period.

CONCLUSIONS:

- Cortical states served as predictors of intervals in which particular motor behavior were detected in two mechanistically different anesthetics.
- Restoring motor behavior is a dynamic process that begins tens of minutes earlier than the righting reflex.
- The righting reflex is an unreliable test to assess recovery of wakefulness.
- Understanding the cortical features associated with the dynamics of motor behavior will reveal novel biomarkers to accurately track emergence from general anesthesia.

REFERENCES:

1. Reshef ER, Schiff ND, Brown EN. A Neurologic Examination for Anesthesiologists: Assessing Arousal Level during Induction, Maintenance, and Emergence. Anesthesiology. 2019;130(3):462-71
2. Gao, S., et al. "Activating an anterior nucleus gigantocellularis subpopulation triggers emergence from pharmacologically-induced coma in rodents." *Nature communications* 10.1 (2019): 2897.
3. Alkire MT, McReynolds JR, Hahn EL, Trivedi AN. Thalamic microinjection of nicotine reverses sevoflurane-induced loss of righting reflex in the rat. Anesthesiology. 2007;107(2):264-72.
4.Taylor NE, Van Dort CJ, Kenny JD, Pei J, Guidera JA, Vlasov KY, Lee JT, Boyden ES, Brown EN, Solt K. Optogenetic activation of dopamine neurons in the ventral tegmental area induces reanimation from general anesthesia. Proc Natl Acad Sci U S A. 2016.

Reduced brain-derived neurotrophic factor signaling exacerbates synaptic dysfunction following isoflurane exposure

Weill Cornell Medicine

KW Johnson[1], RA Williams[1], FS Lee[2,3], HC Hemmings Jr.[1,4] and J Platholi[1,2]

Departments of Anesthesiology[1], Neuroscience[2], Psychiatry[3], and Pharmacology[4], Weill Cornell Medicine, New York, NY

Introduction:
The synapse is a major site of general anesthetic action, but whether long-term structural and/or functional synaptic changes persist beyond the acute mechanisms of anesthetic action are unclear. Recent evidence of dendritic spines as a subcellular substrate for anesthetic action suggests a role for spine plasticity in the deleterious neurocognitive effects of anesthetics, but whether and how anesthetics induce enduring structural spine changes, particularly in vulnerable populations, remains unknown.
Brain-derived neurotrophic factor (BDNF) is a key modulator of synaptic plasticity that regulates both pre- and post-synaptic mechanisms including neurotransmitter release and spine dynamics, respectively. This project addresses the hypothesis that reduced BDNF signaling resulting from the Val66Met allele alters synaptic transmission and dendritic spine structure leading to greater synaptic dysfunction following anesthesia.

• Isoflurane reversibly reduces synaptic vesicle (SV) exocytosis and spine number
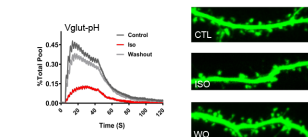
• BDNF modulates SV exocytosis
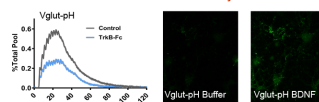
• BDNF release is reduced by isoflurane

• TrkB activation is reduced by isoflurane

• BDNF Val66Met neurons have fewer spines and PSD-95 clusters compared to wt

• Isoflurane-induced spine loss is exacerbated in BDNF Val66Met neurons compared to wt

• Isoflurane-induced reduction in SV exocytosis is irreversible in Val66Met neuron

• Isoflurane-induced spine loss and reduction are irreversible in Met66Met neuron

Results:
• Isoflurane decreases BDNF release and phosphorylation of TrkB.

• BDNF Val66Met neurons have fewer spines and PSD-95.

• Attenuation of endogenous BDNF leads to sustained reduction in SV exocytosis by isoflurane.

• Attenuation of endogenous BDNF leads to sustained dendritic spine loss by isoflurane.

Conclusions:
• Our results identify attenuation of BDNF release as a new molecular signaling pathway contributing to sustained reduction of SV exocytosis and dendritic spine density by isoflurane.

References:
Rochefort and Konnerth (2012). EMBO rep. Aug;13(8):699-708.
Blanpied and Ehlers (2004). Biol. Psychiatry Jun;55(12):1121-1127.
Jevtovic-Todorovic et al. (2003). J Neurosci. Feb;23(3):876-882.
Paule et al. (2011). Neurotoxicol Teratol. Mar-Apr;33(2):220-230.
Raper et al. (2015). Anesthesiology. 123(5):1084-1092.
Poo (2001). Nat. Rev. Neurosci. Jan;2(1):24-32.
Chapleau et al. (2009). J. Neurodev. Disord. Sep;1(3):185-196.

Methods:
Primary hippocampal cultures
Hippocampal neurons from wild-type (Val66Val) and loss-of-function BDNF Val66Met knock-in mice with reduced BDNF secretion (Val66Met, Met66Met) were used to assess the 'dose-dependent' role of BDNF signaling in disruption of spine changes. Neurons were cultured for 21 days in vitro and transfected with a cell filler (eGFP or mCherry) and/or optogenetic biosensors to allow visualization by fluorescence microscopy or fixed in culture for immuno-fluorescence.

Presynaptic function
Isoflurane-induced changes in BDNF or SV release were measured using the genetically encoded biosensors BDNF-pHluorin and Vglut-pHluorin, respectively.

Postsynaptic structure
Time-lapse microscopy was used to visualize isoflurane-induced effects on dendritic spine density and morphology using a CSU-X1 spinning disk confocal.

The Effect of Isoflurane on Axonal Endoplasmic Reticulum Ca²⁺ Dynamics in Hippocampal Neurons

Weill Cornell Medicine

Vanessa Osman[1] and Hugh C. Hemmings Jr., MD., PhD.[1,2]
Department of Pharmacology[1], Department of Anesthesiology[2], Weill Cornell Medicine, New York, NY

Introduction:

Volatile anesthetics
Volatile anesthetics are a staple of modern medicine, but despite their widespread clinical use, their precise cellular and molecular mechanisms of action remain unclear. Pre-synaptically, volatile anesthetics depress synaptic transmission by depressing activity dependent Ca^{2+} influx thereby decreasing neurotransmitter release via synaptic vesicle (SV) exocytosis [1]. The mechanisms upstream are unknown.

Endoplasmic Reticulum (ER)
The ER is the largest store of releasable Ca^{2+} [2]. Axonal ER Ca^{2+} controls presynaptic Ca^{2+} and SV exocytosis through sequestration [3].

ER Ca²⁺ Pathways
ER Ca²⁺ efflux: Ryanodine receptors (RyR) and inositol 1,4,5-triphosphate receptors (IP₃R) (Figure 1A)
ER Ca²⁺ influx: Sarcoplasmic/endoplasmic reticulum Ca2+ ATPase (SERCA) pump (Figure 1A)

Malignant Hyperthermia (MH)
MH is a pharmacogenetic disorder resulting from a mutation in RyR1 leading to exaggerated SR Ca^{2+} release. It is characterized by a hypermetabolic reaction to volatile anesthetics resulting in hyperthermia, acidosis, and muscle rigidity [4].

Dantrolene, a known RyR1 antagonist, is the only approved drug for treating MH [5].

We hypothesize that isoflurane, a commonly used volatile anesthetic, depresses presynaptic Ca^{2+} entry and synaptic vesicle (SV) exocytosis through ER Ca^{2+} dynamics, and this is affected by RyR1 mutations.

Methods

Primary culture of postnatal P1 rat hippocampal neurons
Transfection (Ca^{2+} phosphate-mediated gene transfer) with ER-GCaMP6-150 (7 DIV)
Experiment/Imaging at 15-21 DIV
Analysis with ImageJ to determine changes in ER Ca^{2+}

Measuring [Ca²⁺]ER using ER-GCaMP6-150

Figure 1: A) Fluorescent ER-GCaMP6-150. Presynaptic pathways relevant to ER Ca^{2+} dynamics. B) targeting scheme for ER-GCaMP6-150 [3]

Figure 2: Fluorescent images of a hippocampal neuron co-transfected with ER-GCaMP6-150 (green) and VAMP mCherry (red). Co-localization of both is used to isolate presynaptic ER during analysis. Live-cell imaging measuring [Ca^{2+}] before (A) and during (B) electrical stimulation. C) Snapshot of presynaptic marker VAMP mCherry used to identify presynaptic ER.

ER Ca²⁺ concentration reduced by Isoflurane both at baseline and during electrical stimulation

Figure 3: A) Fractional change in ER Ca^{2+} from each ER-GCaMP6-150 transfected cell comparing after isoflurane/control perfusion to baseline before isoflurane perfusion. B) Representative traces of ER-GCaMP6-150 fluorescence changes while undergoing 20 AP at 20 Hz stimulations under 3 stimulations while perfused with control solution (n=1, 50 boutons, DIV 16). C) Representative traces of ER-GCaMP6-150 fluorescence changes while undergoing 20 AP at 20 Hz stimulations under 3 stimulations perfused with control, isoflurane, and washout (n=1, 50 boutons, DIV 16). D) Stimulation peaks of ER-GCaMP6-150 fluorescence over 3 stimulations at 20 AP at 20 Hz where a white circle represents perfusion with control solution and a blue circle represents perfusion with a clinically relevant concentration of isoflurane

Next Steps: Dissecting ER Ca²⁺ Influx vs Efflux

Does isoflurane decrease ER Ca^{2+} concentration through action on influx pumps (SERCA) or action on efflux receptors (RyR/IP₃R)?

Pharmacological modulation of ER Ca²⁺ concentration is an important tool

Figure 4: Representative traces of ER-GCaMP6-150 fluorescence changes while undergoing 20 AP at 20 Hz stimulations for : A) control, ryanodine, and washout (n=1, 50 boutons, DIV 16) and B) control and CPA. CPA completely blocks stimulation-evoked increase in ER Ca^{2+}.

Conclusions

- Baseline ER Ca^{2+} concentration are reduced by isoflurane
- Electrical stimulation-induced increases in ER Ca^{2+} concentration are reduced by isoflurane
- These data suggests that isoflurane's effect on ER Ca^{2+} may play a role in isoflurane's neuronal mechanisms of action

References

1. Baumgart, J.P., Z.-Y.Z., Hara, M., Cook, D.C., Hoppa, M.B., Ryan, T.A., and Hemmings, H.C. *Isoflurane inhibits synaptic vesicle exocytosis through reduced Ca²⁺ influx, not Ca²⁺-exocytosis coupling.* PNAS, 2015. **112**(38): p. 11959-11964.
2. Ashby MC, T.A., *ER calcium and the functions of intracellular organelles.* Semin Cell Dev. Biol, 2001. **12**(1): p. 11-7.
3. de Juan-Sanz, J, G.T.H., Eric R. Schreiter, Fernando de Juan, Douglas S. Kim, and Timothy A. Ryan, *Axonal Endoplasmic Reticulum Ca2+ Content Controls Release Probability in CNS Nerve Terminals.* Neuron, 2017. **93**: p. 867-881.
4. Henry Rosenberg, N.P., Anja Schiemann, Terasa Bulger, and Kathryn Stowell, *Malignant hyperthermia: a review.* Orphanet Journal of Rare Diseases, 2015. **10**(93).
5. Cannon, S.C. *Mind the magnesium in dantrolene suppression of malignant hyperthermia.* PNAS, 2017. **114**(18): p. 4576-4578.

Optical measurements of anesthetic action on GABA exocytosis

Weill Cornell Medicine

*I.A. SPEIGEL[1], H.C. HEMMINGS JR.[1,2]
Departments of Anesthesiology[1] and Pharmacology[2], Weill Cornell Medicine, New York, NY, USA

647.28/ F23

Introduction:

Volatile anesthetics such as isoflurane disrupt synaptic transmission and inhibit vesicular neurotransmitter release. GABA release from interneurons is significantly less sensitive than glutamate release. The molecular basis for this difference remains unknown (**A**).

A direct comparison of anesthetic actions on glutamatergic versus GABAergic release mechanisms is limited because interneuron subtypes vary in cellular and synaptic physiologies (**B**).

Hypothesis: Individual interneurons neurons vary in sensitivity to isoflurane's effect on neurotransmitter release

Rhagati et al, 2010

Methods:

Select imaging of GABAergic versus Glutamatergic release was performed using live-cell imaging of action potential (AP) triggered exocytosis using the optical biosensor **synaptophysin-pHluorin** expressed in transgenic primary hippocampal neuron cultures.

GAD2-IRES-Cre⁺/⁺ was bred with Ai14(R26-STOP⁴-tdTomato) ⁺/⁺ to drive fluorescent marker tdTomato expression in GABAergic interneurons based on endogenous GAD65 expression (Jackson laboratory strains #010802 and #007908).

Hippocampal primary neurons were harvested from P0-2 offspring, transfected on DIV 6-8, and imaged on DIV 17-20 with a widefield system (Zeiss, LED-illuminated).

Left | GAD2Cre::Ai14 *in vitro* expression.
tdTomato is sparsely expressed in culture.

Brightfield/tdTomato

Control	0.7 mM Isoflurane	Wash	NH₄Cl
[5 min rest]	[5 min rest]	[5 min rest]	[5 min rest]

↑100AP ↑100AP ↑100AP ↑100AP

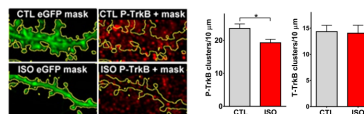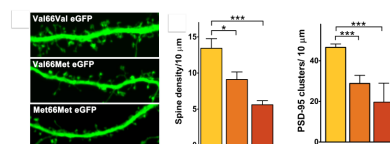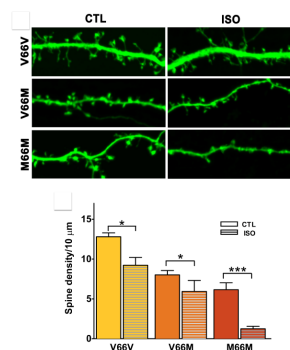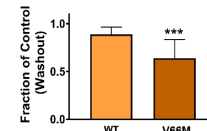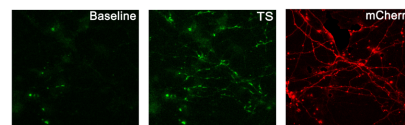**Live-cell imaging protocol for exocytosis measurements**
Control/wash solution (Tyrode's Buffer pH 7.4, 10μm CNQX, 50μm APV) with 0.7mM isoflurane (2 rat MAC) was perfused at ~1ml/min. For sham conditions, isoflurane was omitted. Neurons in which the average Exocytosis was driven by electrical stimulation (100 AP/10Hz , 30mA/ms, 10V/cm² field). Images were acquired at 10Hz (Zeiss Zen software) and analyzed in ImageJ with the TimeSeries Analyzer plugin.

Glutamatergic and GABAergic neuron exocytosis distinguished *in vitro*

Transfection of GAD2Cre::Ai14 neurons with syn-pH allows axonal arbors to be identified as Glutamatergic or GABAergic based on tdTomato colocalization. Syn-pH⁺ axons and terminals are visible due to high resting levels on the axonal plasma membrane generating a "string of pearls" profile.

synaptophysin-pHluorin (syn-pH) fluorescence reflects vesicle alkalization during exocytosis and re-acidification during endocytosis (top). Fluorescence was analyzed in 2μm diameter ROIs targeting synaptic boutons, and ROIs averaged within each cell during treatments (right).

Isoflurane effect on exocytosis (100AP)

Isoflurane effect on GABA vs Glutamate exocytosis. Peak $F\Delta/F_{baseline}$ values were analyzed from cells with washout >70% control. **Left**: Exocytosis measurements taken from individual neurons. **Right**: Cell-type average isoflurane effect on exocytosis (Bars represented as Mean +/- SD). Cellular genotype (GABA vs Glutamate) was a significant source of variance (p=0.0025, RM 2-Way ANOVA) Note: one GABA cell is cropped from view.

Sham/control effect on exocytosis (100AP)

Sham conditions have no effect on GABA/ Glutamate exocytosis. The sham condition, which controls for the effect repeated electrical stimulation in absence of isoflurane, has no effect on either neuron type.

Results:

- The GAD2-Cre driver mouse targets fluorescent reporter expression to a subset of hippocampal neurons *in vitro*.
- Analysis with Repeated Measures Two-Way ANOVA shows an interaction effect between treatment (control/isoflurane) and cellular genotype (p=0.0001).
- Cellular genotype (GABA vs Glutamate) was a significant source of variance (p=0.0025)
- In glutamate but not GABA cells, isoflurane had a significant effect on exocytosis (p=0.0433 and p=0.8522, Tukey's post-hoc analysis)
- Both datasets passed the Shapiro-Wilcox Normality test (Glutamate p=0.5317, GABA p=0.197).

Conclusions:

- pHluorin-based exocytosis sensors in transgenic systems enable presynaptic effects to be measured at the level of the individual genetically identified neuron
- Genotype (GABA vs. Glutamatergic) determines the effect of isoflurane effect on exocytosis
- However the GABA response to isoflurane varies markedly, suggesting heterogeneity in isoflurane-sensitive cellular and synaptic properties.

Significance:

Many cortical/hippocampal cardinal interneuron species can now be targeted by transgenic expression systems, so anesthetic actions on GABA release can be dissected into more specific interneuron cellular identities.

This information is critical to further the understanding of the cellular and behavioral effects of anesthetics, as interneurons modulate nearly every aspect of neuronal excitability and network function, with specialized subpopulations serving distinct roles in circuit function.

References

Baumgart JP, Zhou ZY, Hara M, Cook DC, Hoppa MB, Ryan TA, Hemmings HC Jr. *Isoflurane inhibits synaptic vesicle exocytosis through reduced Ca2+ influx, not Ca2+-exocytosis coupling.* Proc Natl Acad Sci U S A. 2015

Raghanti MA, Spocter MA, Butti C, Hof PR, Sherwood CC. *A comparative perspective on minicolumns and inhibitory GABAergic interneurons in the neocortex.* Front Neuroanat. 2010 Feb

Westphalen RI, Desai KM, Hemmings HC Jr. *Presynaptic inhibition of the release of multiple major central nervous system neurotransmitter types by the inhaled anaesthetic isoflurane.* Br J Anaesth. 2013

Native-state prolyl isomerization regulates activation kinetics of a CNG channel

Philipp A.M. Schmidpeter and Crina M. Nimigean

Department of Anesthesiology, Weill Cornell Medicine, New York, NY, USA
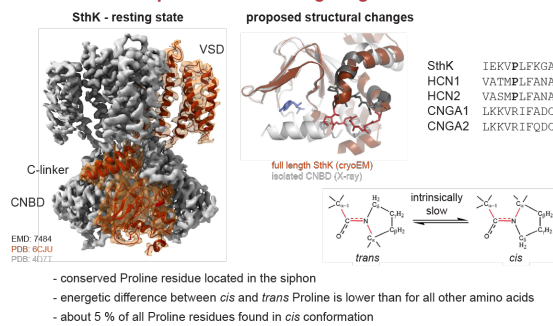
Abstract

The cyclic nucleotide-gated channel SthK activates biphasically upon cAMP application, with the slow phase reminiscent of the cAMP-induced modulation of eukaryotic HCN channels. The mechanistic underpinning for this effect is elusive.

Here we show that SthK employs regulatory prolyl cis/trans isomerization in the cyclic-nucleotide binding domain to slow down cAMP-induced activation kinetics and fine-tune activity. Substitution of a single Proline in SthK by Alanine abolishes the slow activation phase and increases the apparent affinity of SthK for cAMP four-fold, as measured in stopped-flow assays. The same effects are observed for WT SthK in the presence of prolyl isomerases (PPIases), in a PPIase concentration-dependent way. Neither the Pro→Ala mutation nor application of PPIases affect the steady-state single-channel characteristics in planar lipid-bilayer recordings.
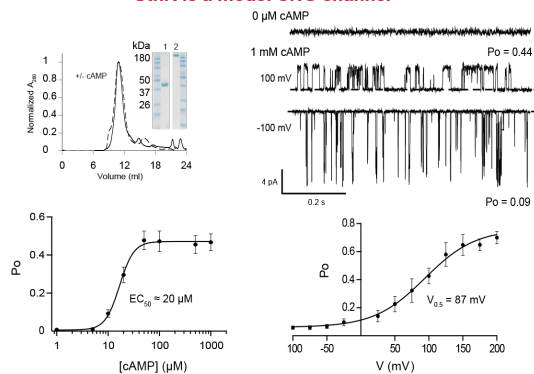
This suggests a mechanism where two channel conformations differentiated by a Proline residue in cis or trans configuration exist in equilibrium: while cis Proline is favored in the apo-state, addition of cAMP shifts the equilibrium towards trans Proline in the open state. Activation of these two SthK conformations with different rates can explain the biphasic activation kinetics. Removal of the cis species in SthK P300A or addition of PPIases that help to rapidly shift the equilibrium towards trans Proline in WT, will both lead to the disappearance of the slow phase.

The cryoEM structure of SthK P300A revealed subtle differences from the WT structure, suggesting that the mutant indeed adopts a pre-active conformation. We propose that prolyl isomerization functions as molecular pacemaker for SthK that can be modulated by PPIases.

The siphon is central to gating of CNG channels

SthK - resting state

EMD: 7484
PDB: 6CJU
PDB: 4D7T

proposed structural changes

SthK	IEKV**P**LFKGAGE
HCN1	VATM**P**LFANADP
HCN2	VASM**P**LFANADP
CNGA1	LKKV**R**IFADCEA
CNGA2	LKKV**R**IFQDCEA

full length SthK (cryoEM)
isolated CNBD (X-ray)

intrinsically slow

trans ⇌ cis

- conserved Proline residue located in the siphon
- energetic difference between cis and trans Proline is lower than for all other amino acids
- about 5 % of all Proline residues found in cis conformation

SthK is a model CNG channel

0 μM cAMP

1 mM cAMP   Po = 0.44

Po = 0.09

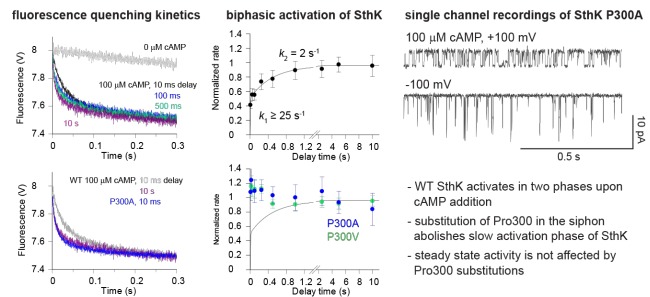$EC_{50} \approx 20$ μM

$V_{0.5} = 87$ mV

- SthK can be purified in the absence and presence of cAMP
- single channel recordings reveal that cAMP is necessary to activate SthK
- activity of SthK is further modulated by voltage

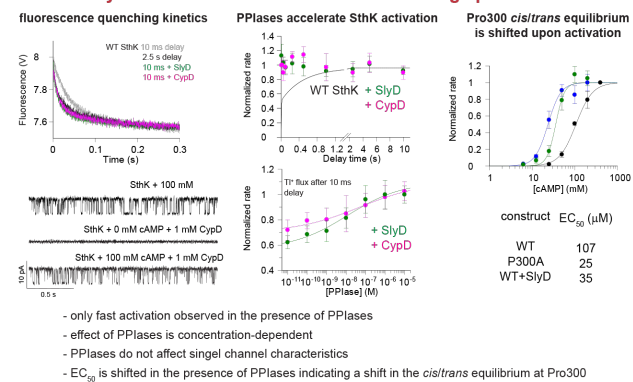## Stopped-flow flux assay to determine the activation kinetics of SthK
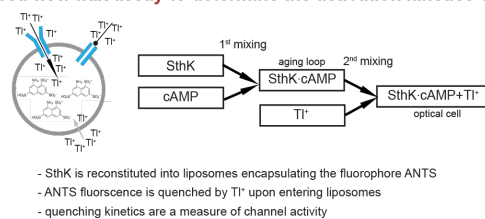
- SthK is reconstituted into liposomes encapsulating the fluorophore ANTS
- ANTS fluorscence is quenched by Tl⁺ upon entering liposomes
- quenching kinetics are a measure of channel activity

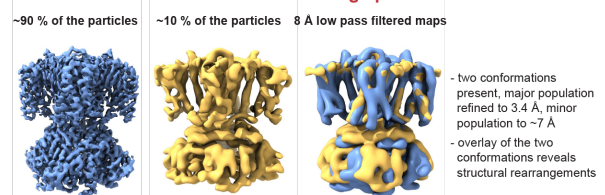## A single Proline residue determines activation kinetics of SthK

fluorescence quenching kinetics

0 μM cAMP
100 μM cAMP, 10 ms delay
100 ms
500 ms
10 s

biphasic activation of SthK

$k_2 = 2$ s⁻¹
$k_1 \geq 25$ s⁻¹

WT 100 μM cAMP, 10 ms delay
10 s
P300A, 10 ms

P300A
P300V

single channel recordings of SthK P300A

100 μM cAMP, +100 mV
-100 mV

- WT SthK activates in two phases upon cAMP addition
- substitution of Pro300 in the siphon abolishes slow activation phase of SthK
- steady state activity is not affected by Pro300 substitutions

Prolylisomerases abolish the slow-activating species of SthK

fluorescence quenching kinetics

WT SthK 10 ms delay
2.5 s delay
10 ms + SlyD
10 ms + CypD

PPIases accelerate SthK activation

WT SthK + SlyD + CypD

Tl⁺ flux after 10 ms delay

+ SlyD
+ CypD

SthK + 100 mM

SthK + 0 mM cAMP + 1 mM CypD

SthK + 100 mM cAMP + 1 mM CypD

Pro300 cis/trans equilibrium is shifted upon activation

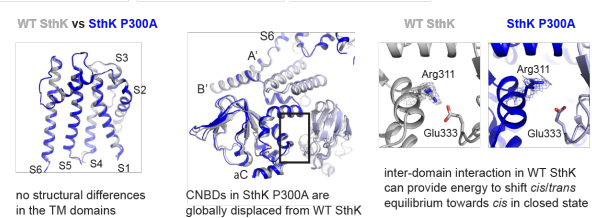| construct	EC_{50} (μM)
WT	107
P300A	25
WT+SlyD	35

- only fast activation observed in the presence of PPIases
- effect of PPIases is concentration-dependent
- PPIases do not affect singel channel characteristics
- EC_{50} is shifted in the presence of PPIases indicating a shift in the cis/trans equilibrium at Pro300
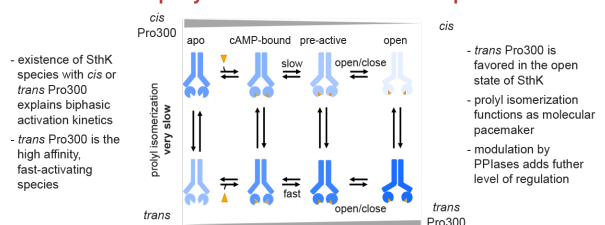
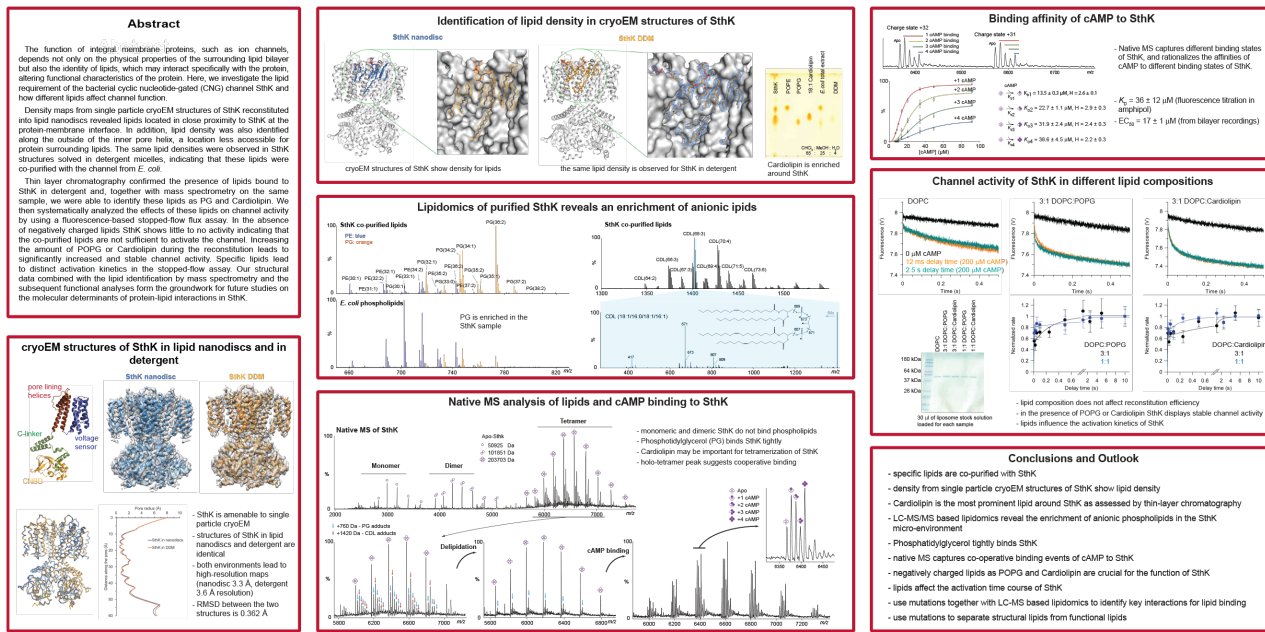## Structure of the fast-activating species of SthK

~90 % of the particles   ~10 % of the particles   8 Å low pass filtered maps

- two conformations present, major population refined to 3.4 Å, minor population to ~7 Å
- overlay of the two conformations reveals structural rearrangements

Structural differences between WT SthK and SthK P300A

WT SthK vs SthK P300A

S3, S2, S1, S4, S5, S6

S6, A', B', aC

WT SthK   SthK P300A
Arg311   Arg311
Glu333   Glu333

no structural differences in the TM domains

CNBDs in SthK P300A are globally displaced from WT SthK

inter-domain interaction in WT SthK can provide energy to shift cis/trans equilibrium towards cis in closed state

Native-state prolyl isomerization as molecular pacemaker

cis Pro300

apo   cAMP-bound   pre-active   open
slow   open/close

prolyl isomerization very slow

fast   open/close

trans Pro300

cis Pro300

- existence of SthK species with cis or trans Pro300 explains biphasic activation kinetics
- trans Pro300 is the high affinity, fast-activating species

- trans Pro300 is favored in the open state of SthK
- prolyl isomerization functions as molecular pacemaker
- modulation by PPIases adds further level of regulation

trans Pro300

Schmidpeter PA, Gao X, Uphadyay V, Rheinberger J, Nimigean CM. J Gen Physiol. 2018 Jun 4;150(6):821-834.   Rheinberger J, Gao X, Schmidpeter PA, Nimigean CM. Elife. 2018 Jul 20;7. pii: e39775.

Lipid-modulation of SthK, a cyclic nucleotide-gated channel

Philipp A.M. Schmidpeter[1], Di Wu[2], Jan Rheinberger[1], Haiping Tang[2], Carol V. Robinson[2] and Crina M. Nimigean[1]

[1] Department of Anesthesiology, Weill Cornell Medicine, New York, NY, USA, [2] Department of Chemistry, University of Oxford, Oxford, UK

Weill Cornell Medicine

UNIVERSITY OF OXFORD

Abstract

The function of integral membrane proteins, such as ion channels, depends not only on the physical properties of the surrounding lipid bilayer but also the identity of lipids, which may interact specifically with the protein, altering functional characteristics of the protein. Here, we investigate the lipid requirement of the bacterial cyclic nucleotide-gated (CNG) channel SthK and how different lipids affect channel function.

Density maps from single particle cryoEM structures of SthK reconstituted into lipid nanodiscs revealed lipids located in close proximity to SthK at the protein-membrane interface. In addition, lipid density was also identified along the outside of the inner pore helix, a location less accessible for protein surrounding lipids. These same lipid densities were observed in SthK structures solved in detergent micelles, indicating that these lipids were co-purified with the channel from E. coli.

Thin layer chromatography confirmed the presence of lipids bound to SthK in detergent and, together with mass spectrometry on the same sample, we were able to identify these lipids as PG and Cardiolipin. We then systematically analyzed the effects of these lipids on channel activity by using a fluorescence-based stopped-flow assay. In the absence of negatively charged lipids SthK shows little to no activity indicating that the co-purified lipids are not sufficient to activate the channel. Increasing the amount of POPG or Cardiolipin during the reconstitution leads to significantly increased and stable channel activity. Specific lipids lead to distinct activation kinetics in the stopped-flow assay. Our structural data combined with the lipid identification by mass spectrometry and the subsequent functional analyses form the groundwork for future studies on the molecular determinants of protein-lipid interactions in SthK.

Identification of lipid density in cryoEM structures of SthK

cryoEM structures of SthK show density for lipids · the same lipid density is observed for SthK in detergent · Cardiolipin is enriched around SthK

cryoEM structures of SthK in lipid nanodiscs and in detergent

- SthK is amenable to single particle cryoEM
- structures of SthK in lipid nanodiscs and detergent are identical
- both environments lead to high-resolution maps (nanodisc 3.3 Å, detergent 3.6 Å resolution)
- RMSD between the two structures is 0.362 Å

Lipidomics of purified SthK reveals an enrichment of anionic lipids

PG is enriched in the SthK sample

Native MS analysis of lipids and cAMP binding to SthK

- monomeric and dimeric SthK do not bind phospholipids
- Phosphatidylglycerol (PG) binds SthK tightly
- Cardiolipin may be important for tetramerization of SthK
- holo-tetramer peak suggests cooperative binding

Binding affinity of cAMP to SthK

- Native MS captures different binding states of SthK, and rationalizes the affinities of cAMP to different binding states of SthK

- $K_D = 36 \pm 12$ μM (fluorescence titration in amphipol)
- $EC_{50} = 17 \pm 1$ μM (from bilayer recordings)

Channel activity of SthK in different lipid compositions

- lipid composition does not affect reconstitution efficiency
- in the presence of POPG or Cardiolipin SthK displays stable channel activity
- lipids influence the activation kinetics of SthK

Conclusions and Outlook

- specific lipids are co-purified with SthK
- density from single particle cryoEM structures of SthK show lipid density
- Cardiolipin is the most prominent lipid around SthK as assessed by thin-layer chromatography
- LC-MS/MS based lipidomics reveal the enrichment of anionic phospholipids in the SthK micro-environment
- Phosphatidylglycerol tightly binds SthK
- native MS captures co-operative binding events of cAMP to SthK
- negatively charged lipids as POPG and Cardiolipin are crucial for the function of SthK
- lipids affect the activation time course of SthK
- use mutations together with LC-MS based lipidomics to identify key interactions for lipid binding
- use mutations to separate structural lipids from functional lipids

Schmidpeter PA, Gao X, Uphadyay V, Rheinberger J, Nimigean CM. J Gen Physiol. 2018 Jun 4;150(6):821-834.   Rheinberger J, Gao X, Schmidpeter PA, Nimigean CM. Elife. 2018 Jul 20;7. pii: e39775.   Gupta K, Li J, Liko I, Gault J, Bechara C, Wu D, Hopper JTS, Giles K, Benesch JLP, Robinson CV. Nat Protoc. 2018 May;13(5):1106-1120.

Anesthetics-induced burst suppression uncovers rapid widespread alterations in network excitability caused by an acute seizure focus

Jyun-You Liou[1,2,4,*], Eliza Baird-Daniel[3,*], Mingrui Zhao[3], Andy Daniel[3], Catherine A Schevon[4], Hongtao Ma[3], Theodore H Schwartz[3]

1. Department of Anesthesiology, Weill Cornell Medicine, New York-Presbyterian Hospital, New York, NY 10065, USA
2. Department of Physiology and Cellular Biophysics, Columbia University, New York, NY 10032, USA
3. Department of Neurological Surgery, Weill Cornell Medicine, New York-Presbyterian Hospital, New York, NY 10065, USA
4. Department of Neurology, Columbia University Medical Center, New York, New York 10032

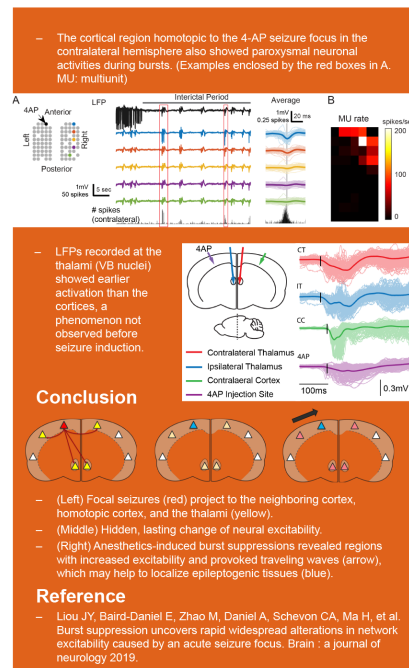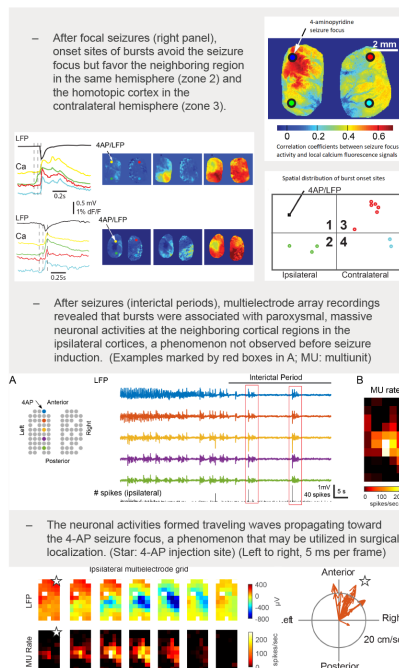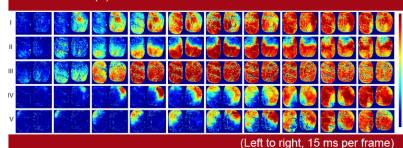**Weill Cornell Medicine**   **NewYork-Presbyterian**

Introduction

- Burst suppression is an EEG pattern characterized by alternating high amplitude discharges and electrical silence.
- High dose anesthetics induced globally synchronous burst suppression in healthy brains.
- Local asynchrony, however, can be observed in patients with focal epilepsies.
- What does this local asynchrony reveal?
- Do the distributions of local asynchrony provide information that may be used to localize seizure foci during epilepsy surgery?

Material and Methods

- Adult male Spague-Dawley rats anesthetized under 1-2% isoflurane
- Craniotomy and LFP confirmation of achieving burst suppression
- Widefield calcium imaging
  » Calcium indicator: Oregon Green 488 BAPTA-AM
  » Recording: CCD camera (Dalsa camera in Imager 3001, Optical Imaging, Rehovot, Israel) with 55-66 Hz frame rate
- Multielectrode array electrophysiology
  » Two 5x10 Utah array grids with each covering each hemisphere, sampling rate 30kHz (Blackrock Microsystems Inc, SLC, UT).
- Acute seizure focus created by local 4-aminopyridine injection at the neocortex (500 nL, 15 mM)
- Compare burst dynamics before versus after seizures

Results

- Calcium imaging showed that bursts were focal-onset events. However, the distribution of onset sites were not spatially localized
- (I) Right upper (II) Posterior left (III) Posterior bilateral (IV) Right anterior (V) Left anterior


(Left to right, 15 ms per frame)

- After focal seizures (right panel), onset sites of bursts avoid the seizure focus but favor the neighboring region in the same hemisphere (zone 2) and the homotopic cortex in the contralateral hemisphere (zone 3).

- After seizures (interictal periods), multielectrode array recordings revealed that bursts were associated with paroxysmal, massive neuronal activities at the neighboring cortical regions in the ipsilateral cortices, a phenomenon not observed before seizure induction. (Examples marked by red boxes in A; MU: multiunit)

- The neuronal activities formed traveling waves propagating toward the 4-AP seizure focus, a phenomenon that may be utilized in surgical localization. (Star: 4-AP injection site) (Left to right, 5 ms per frame)

- The cortical region homotopic to the 4-AP seizure focus in the contralateral hemisphere also showed paroxysmal neuronal activities during bursts. (Examples enclosed by the red boxes in A. MU: multiunit)

- LFPs recorded at the thalami (VB nuclei) showed earlier activation than the cortices, a phenomenon not observed before seizure induction.

Conclusion

- (Left) Focal seizures (red) project to the neighboring cortex, homotopic cortex, and the thalami (yellow).
- (Middle) Hidden, lasting change of neural excitability.
- (Right) Anesthetics-induced burst suppressions revealed regions with increased excitability and provoked traveling waves (arrow), which may help to localize epileptogenic tissues (blue).

Reference

- Liou JY, Baird-Daniel E, Zhao M, Daniel A, Schevon CA, Ma H, et al. Burst suppression uncovers rapid widespread alterations in network excitability caused by an acute seizure focus. Brain : a journal of neurology 2019.

ESCRT-III ASSEMBLES SIMULTANEOUSLY AND WITHOUT PREFERENCE ON SUPPORTED LIPID BILAYERS OF VARYING CURVATURES

Nebojsa Jukic[1,2], Alma P. Perrino[1,2], Simon Scheuring[1,2]

INTRODUCTION

Endosomal Sorting Complex Required for Transport III proteins (ESCRT-III) are downstream effective components of an evolutionarily conserved system of proteins that is involved in crucial processes in eukaryotic cells resulting in membrane deformation and scission. Snf7, the major component of this system, must polymerize efficiently on lipid bilayers displaying a variety of curvatures to account for differences in function and intracellular localization. High-speed atomic force microscopy (HS-AFM) has provided insights into the assembly, structural arrangement and turnover of Snf7 assemblies on planar supported lipid bilayers. We now established novel non-planar supports, and demonstrate that Snf7 assembles concurrently and without preference on supported lipid bilayer patches of different curvatures, saturating the sample surface in minutes. By analyzing the dimensions and topographical properties of the spirals, we find that the non-planar substrate introduces constraints into the size distribution of Snf7 assemblies, and that assembly topology is an emergent property of the ensemble (the spiral). Furthermore, we show that there is no significant difference in Snf7 assembly stability in relation to surface curvature. This implies that Snf7 assembly into three-dimensional spirals on curved lipid bilayer patches does not constitute an unfavorable conformation, and that Snf7 assemblies are able to form rapidly on lipid bilayers regardless of their shape – a requirement that is crucial for efficient Snf7 recruitment to budding sites in various physiological conditions and functions.

METHODS
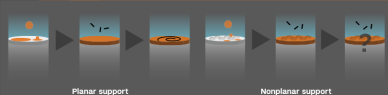
Liposomes consisting of DOPC and DOPS are deposited on a planar support (mica) or on a nanopatterned support. Snf7 is then added into the fluid chamber of the HS-AFM and subsequently imaged by intermittently probing the surface of the sample with a nanoscopically small tip mounted on a cantilever.

RESULTS
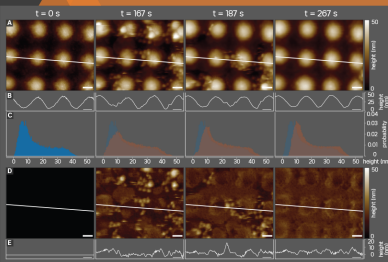
HS-AFM topographs representing efficient coverage of nanopatterned substrate with DOPC:DOPS lipid bilayer over time. A: Small unilamelar vesicles are added to the imaging solution and deposit on the surface of the substrate. Then, vesicles start to rupture and form supported lipid bilayer patches. The patches grow in size and merge, until the surface is completely covered with lipid bilayer after several minutes of imaging. B: line profiles of the corresponding HS-AFM topographs as desribed in A. The height of the protrusions of the support is about 25 nm, as measured from the bottom of the substrate to the top of the protrusion. C: the histogram of the individual frames shifts over time, steadily populating higher values until all of the values have shifted by about 4 nm, corresponding to the thickness of a lipid bilayer. The histogram of the reference frame (t = 0 s) is displayed in blue; the histograms of the subsequent frames are in orange. D: Higher-contrast representation of the same HS-AFM topographs as shown in A, with the height of the protrusions subtracted using the first frame (t = 0 s) as a reference. E: line profiles of the subtracted frames as shown in D. Scale bars: 50 nm.
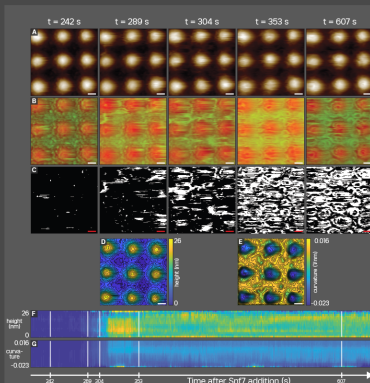
Snf7 polymerization on a nanopatterned substrate covered with a DOPC:DOPS lipid bilayer. A: HS-AFM topographs of Snf7 polymerization. First Snf7 filaments are visible 4 min after addition of the protein to the imaging solution. Subsequent frames show Snf7 increasingly covering the surface, with nascent Snf7 spirals clearly discernible 6 min after addition of protein. The polymerization process is largely complete 10 min after protein addition, with the whole surface of the lipid bilayer covered with protein. Snf7 assemblies are relatively stable thereafter and reorganization of individual assemblies occurs very rarely in absence of perturbations to the system. B: Result of a locally adaptive thresholding protocol being applied to the HS-AFM topographs in A. Intensity of substrate displayed in red, intensity of the protein layer displayed in green. C: Binarization of the thresholded images. White pixels correspond to pixels recognized as "occupied" by protein, black pixels "unoccupied". D: Contour plot of the height values of the HS-AFM topograph at t = 242 s (A, far left). All height values are separated into bins 2 nm wide. E: Contour plot of the calculated curvature for each pixel in reference frame (A, left). Curvature values are separated into 20 bins. F: occupancy plot of binned pixels as a function of time and height. Rows correspond to bins in D, containing pixels in a 2 nm height range of the underlying substrate; columns correspond to frames of the HS-AFM video (1 frame = 1 s). Occupancy is calculated as percentage of pixels corresponding to one bin that are occupied by protein. G: occupancy plot of binned pixels as a function of time and curvature. Scale bars: 50 nm.
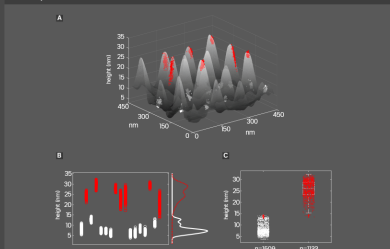
Separation of spiral centers after polymerization: two spiral populations emerge. A: Surface plot of nanopatterned substrate with spiral centers represented by dots. Spirals with centers positioned near the top of the protrusions are labeled with red dots; spirals with centers positioned in the bottom of the substrate are represented with white dots. Each dot is a spiral center in subsequent frames of the HS-AFM movie. B: Scatterplot of the spiral centers as shown in A. Spiral centers have been clustered using a kmeans approach (number of clusters = number of spirals) with three spatial coordinates used as variables. C: Boxplot of the spiral centers as described in A and B, with all the spiral centers binned into two distinct populations. A kmeans clustering of spiral centers into two clusters using only the height value of the spiral center as the clustering variable yields similarly accurate results.
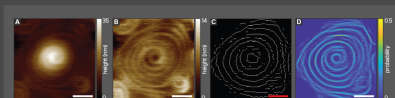
Stability of individual Snf7 assemblies centered on protrusions. A: HS-AFM topograph of a single, large Snf7 assembly with center coinciding with the center of a protrusion of the support. The spiral is surrounded by smaller adjacent spirals that are not centered on top of a protrusion. B: A Gaussian has been fit to the data shown in A and the obtained fit has been subtracted from the raw HS-AFM topograph. C: Binarization of data shown in A obtained by a radial peak search approach. D: The peaks found using the binarization approach have been summed up for each frame in the HS-AFM stack and divided by the number of stacks. The resulting image shows the probability of finding a filament peak for each pixel in the stack. The results shown here demonstrate that Snf7 spirals undergo relatively little remodelling once polymerization is complete, even when polymerizing in an out-of-plane conformation because of the topography of the underlying substrate. Scale bars: 50 nm.

CONCLUSIONS

- Snf7 polymerizes efficiently on nanopatterned substrate displaying a variety of different curvatures

- Snf7 polymerizes and saturates the lipid bilayer surface in minutes; nucleation and polymerization proceeds simultaneously throughout the substrate with no observable preference for any specific curvature

- Snf7 assemblies tend to separate into two distinct populations, with spiral centers found majoritarily either in the bottom of the substrate or the top of the protrusions.

- Ultimate topography of mature, stable Snf7 assemblies is determined by the underlying substrate.

REFERENCES

[1] Teis D et al. Dev Cell. 2008 Oct 14;15(4):578–89;
[2] Lee IH et al. Proc Natl Acad Sci U S A. 2015 Dec 29; 112(52): 15892–15897.
[3] Chiaruttini N et al. Cell. 2015 Nov 5;163(4):866–79;
[4] Mierzwa B et al. Nat Cell Biol. 2017 Jul;19(7):787–798.
[5] Ando T et al. Prog Surf Sci. 2008 Nov;83(7–9):337–437.

AUTHORS

Simon Scheuring
Professor of Physiology and Biophysics in Anesthesiology
Weill Cornell Medicine, 1300 York Avenue, New York, NY 10065, USA
email: sis2019@med.cornell.edu

Nebojsa Jukic
Graduate Student at Weill Cornell Graduate School of Medical Sciences
Weill Cornell Medicine, 1300 York Avenue, New York, NY 10065, USA
email: nej2011@med.cornell.edu

Alma P. Perrino
Postdoctoral researcher at the Department of Anesthesiology
Weill Cornell Medicine, 1300 York Avenue, New York, NY 10065, USA
email: aep2004@med.cornell.edu

1. Weill Cornell Medicine, Department of Physiology & Biophysics; New York, USA
2. Weill Cornell Medicine, Department of Anesthesiology; New York, USA

ScheuringLab   bio-afm-lab.com   @ScheuringLab

FORCE-INDUCED CONFORMATIONAL CHANGES IN PIEZO1

Yi-Chih Lin[1,#], Yusong R Guo[2,#], Atsushi Miyagi[1], Jesper Levring[2],
Roderick MacKinnon[2,*] and Simon Scheuring[1,*]

[1] Department of Anesthesiology, Department of Physiology and Biophysics, Weill Cornell Medicine, New York, United States
[2] Laboratory of Molecular Neurobiology and Biophysics, Howard Hughes Medical Institute, The Rockefeller University, New York, United States
#Equal contribution
*Correspondence to: Roderick MacKinnon (mackinn@mail.rockefeller.edu) and Simon Scheuring (sis2019@med.cornell.edu)

Bio-AFM-Lab
http://bio-afm-lab.com
ScheuringLab
@ScheuringLab

Abstract

Piezo1 is a mechanosensitive channel that converts applied force into electrical signals. Partial molecular structures show that Piezo1 is a bowl-shaped trimer with extended arms. Here we use cryo-electron microscopy to show that Piezo1 adopts different degrees of curvature of different sizes. We also use high-speed atomic force microscopy to analyse the deformability of Piezo1 under force in membranes on a mica surface, and show that Piezo1 can be flattened reversibly into the membrane plane. By approximating the absolute force applied, we estimate a range of values for the mechanical spring constant of Piezo1. Both methods of microscopy demonstrate that Piezo1 can deform its shape towards a planar structure. This deformation could explain how lateral membrane tension can be converted into a conformation-dependent change in free energy to gate the Piezo1 channel in response to mechanical perturbations.

Architecture and proposed activation mechanisms of mechano-sensitive channel Piezo1
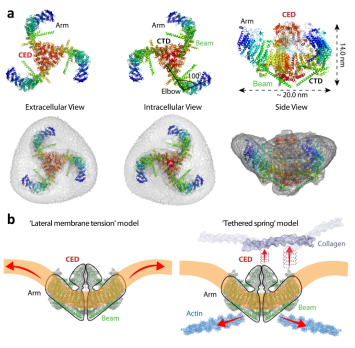
Figure 1. (a) Top, bottom and side views of Piezo1 (PDB 6B3R) in cartoon representation (top) and embedded in the micelle density map (EMD-7042) contoured at 6σ: CED: C-terminal extracellular domain, CTD: C-terminal domain. (b) Proposed models of Piezo1 channel activation. Left: Lateral membrane tension model: Changes in membrane properties, e.g. tension or curvature, will lead to a gating force applied onto the Piezo1 channel. Right: Tethered spring model: The Piezo1 channel is activated through interactions with the cytoskeleton or the extracellular matrix. Red arrows indicate force application.

Reconstitution of Piezo1 channels in vesicles exhibit various orientations in cryo-EM micrographs
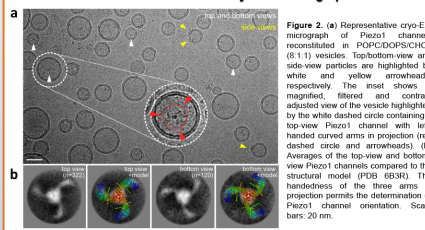
Figure 2. (a) Representative cryo-EM micrograph of Piezo1 channels reconstituted in POPC/DOPS/CHOL (8:1:1) vesicles. Top/bottom-view and side-view particles are highlighted by white and yellow arrowheads, respectively. The inset shows a magnified, filtered and contrast adjusted view of the vesicle highlighted by the white dashed circle containing a top-view Piezo1 channel with left-handed curved arms in projection (red dashed circle and arrowheads). (b) Averages of the top-view and bottom-view Piezo1 channels compared to the structural model (PDB 6B3R). The handedness of the three arms in projection permits the determination of Piezo1 channel orientation. Scale bars: 20 nm.

Piezo1 channels become flatter in large vesicles
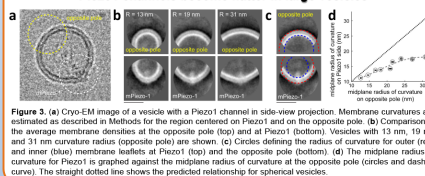
Figure 3. (a) Cryo-EM image of a vesicle with a Piezo1 channel in side-view projection. Membrane curvatures are estimated as described in Methods for the region centered on Piezo1 and on the opposite pole. (b) Comparison of the average membrane densities at the opposite pole (top) and at Piezo1 (bottom). Vesicles with 13 nm, 19 nm and 31 nm curvature radius (opposite pole) are shown. (c) Circles defining the radius of curvature for outer (red) and inner (blue) membrane leaflets at Piezo1 (top) and the opposite pole (bottom). (d) The midplane radius of curvature for Piezo1 is graphed against the midplane radius of curvature at the opposite pole (circles and dashed curve). The straight dotted line shows the predicted relationship for spherical vesicles.

High-Speed Atomic Force Microscopy (HS-AFM) of Piezo1 in supported membranes
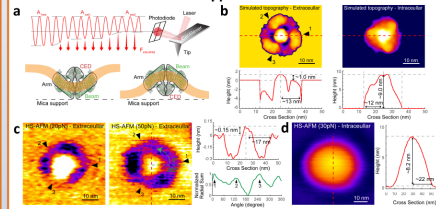

Figure 4. (a) Schematic diagram of force-controlled HS-AFM imaging of membrane-embedded Piezo1. The ratio A_{set}/A_{free} (A_{set} is the setpoint and A_{free} is the free oscillation amplitude of the cantilever, respectively) defines the average applied force $\langle F_{HS-AFM}\rangle$ during imaging. (b) Top: Simulated topographies of Piezo1 in the detergent micelle (see Figure 1a) viewed from the extracellular (left) and the intracellular (right) faces. The continuous membrane was set as a uniform height level extending from the most peripheral resolved TM helices. The three black arrowheads indicate the position of the three arms of Piezo1. Bottom: Height section profiles of the simulated topographies. From the extracellular side, the channel is expected to appear bowl-shaped with a central plug that maximally protrudes by ~1nm from the periphery and the membrane plane, while the intracellular side structure protrudes ~5nm above the bilayer at the 3-fold axis. (c, d) HS-AFM images at specific $\langle F_{HS-AFM}\rangle$ of Piezo1 viewed from the extracellular ((c), –20 pN and –50 pN) and intracellular ((d), –30 pN) faces. Right: Section profiles (red traces) of the topographies. Extracellular face: three arms of Piezo1 are observed within the deep ring area, as highlighted by the radial profile with ~120° periodicity (green trace). The extracellular face is characterized by a central plug surrounded by a bowl with negative height, i.e. at a level below the surrounding bilayer. The intracellular face shows a featureless dome.

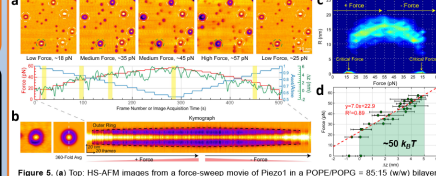### Mechanical response of Piezo1 to applied force

Figure 5. (a) Top: HS-AFM images from a force-sweep movie of Piezo1 in a POPE/POPG = 85:15 (w/w) bilayer. Each image is an average over 10 frames acquired at a specific loading force (5 yellow shaded areas below). Bottom: Force (red), A_{set}/A_{free} ratio (blue) and Z-piezo displacement (green) as function of frame acquisition time. A_{free}~1.5 nm. Representative of ≥11 independent experiments from ≥5 different Piezo1 samples. (b) Example of lateral expansion analysis. Each single molecule (left) is 360-fold symmetry averaged (middle) and a kymograph (right) across the center of Piezo1 calculated (white dashed line). The kymograph (representative of ≥100 particles) highlights the outer radius (halo) expansion (black dashed line) as a function of force. (c) Normalized probability density map of outer ring radius (R) as a function of force. 100 Piezo1 particles from 11 movies acquired on ≥5 different samples. The symmetric distribution of R shows the structural reversibility upon force increase and decrease. A critical force F_c~18 pN is required during HS-AFM operation. (d) Applied force as a function of the sample displacement towards the AFM tip. The linear regression (red dashed line, disregarding the zero-force and negative Δz data points) provides the stiffness constant K~7.0 pN/nm and the work exerted by the HS-AFM (green-shaded area) for stressing a spring-like Piezo1 based on our proposed dome-flattening model. Data are mean ± s.d. with n≥10.

Conclusions:

Based on our cryo-EM and HS-AFM results, we conclude that Piezo1 can undergo a reversible, flattening deformation when force is applied. The HS-AFM experiments apply force normal to the membrane surface. If tethers can attach to the channel in a cellular setting then similarly directed forces could gate Piezo1. If lateral membrane tension is the primary gating stimulus, then equation 1 presents a way to think about the energetic equivalence to a normal force, such as that applied by the HS-AFM tip.

$$\Delta G = \Delta G(\gamma = 0) - \gamma \Delta A \qquad (equation\ 1)$$

ΔG: the free energy difference between the flat and curved conformations
γ: lateral membrane tension
$\Delta G(\gamma = 0)$: the free energy difference between the flat and curved conformations in the absence of lateral tension
ΔA: Projected area difference between flat and curved conformations

---

Millisecond time resolution of GltPh dynamics by HS-AFM line scanning

Tina R.Matin[1], George R Heath[1], Gerard Huysmans[2], Olga Boudker[2,3], Simon Scheuring[1,2]

1. Department of Anesthesiology, Weill Cornell Medicine, New York, NY 10065;
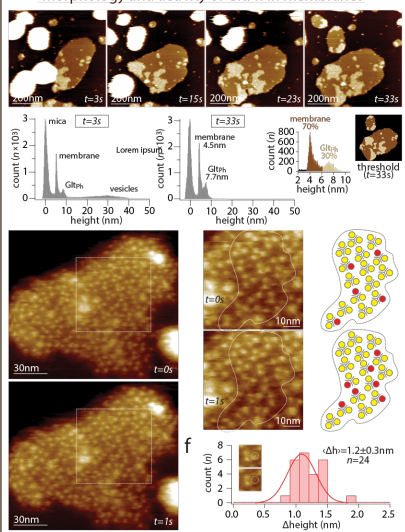2. Department of Physiology and Biophysics, Weill Cornell Medicine, New York, NY 10065;
3. Howard Hughes Medical Institute, Weill Cornell Medicine, New York, NY 10065;
*Correspondence to: sis2019@med.cornell.edu

Bio-AFM-Lab

Abstract

Mammalian glutamate transporter proteins play the crucial role in removing excitatory neurotransmitters from the synaptic cleft. Malfunction of Glutamate transporters is identified in various neurological disorders such as cerebral stroke, epilepsy, Alzheimer's disease, dementia, Huntington's disease, amyotrophic lateral sclerosis (ALS) and malignant glioma. During the past decade, our understanding of the structure and function of these proteins have evolved profoundly from studying a prokaryotic glutamate transporter homolog (GltPh). Here, we report the development and use of novel high-speed atomic force microscopy (HS-AFM) based techniques that reach millisecond time resolution, and explored previously undetectable short-lived transport states in unlabeled membrane reconstituted GltPh. We find that GltPh exhibits much faster dynamics than previously thought.

Morphology and activity of GltPh in membranes

High-speed AFM line scanning (HS-AFM-LS): millisecond time resolution

Individual traces of protomers

HS-AFM-LS contours GltPh protomers at different height levels

Dynamics of elevator domain based on two state model

High-resolution X-ray structures in various conformational states

Weill Cornell Medicine
Anesthesiology

# ESCRT-III spirals are loaded springs that govern spontaneous membrane deformation

Alma P. Perrino, Nebojsa Jukic, Simon Scheuring

Department of Anesthesiology, Weill Cornell Medicine, New York, NY 10065;
Department of Physiology and Biophysics, Weill Cornell Medicine, New York, NY 10065;
*Correspondence to: sis2019@med.cornell.edu

Bio-AFM-Lab
Weill Cornell Medicine
Anesthesiology

Abstract

The endosomal sorting complex required for transport-III (ESCRT-III) system is crucial in many cellular processes that imply membrane deformation and fission, where the ESCRT-III proteins are in the cytoplasm and the membrane bud faces away from the cytoplasm. The ESCRT-III subunits polymerize and form filaments that assemble in high-order structures like spirals on flat membranes or helices in cylindrical membrane tubules. High-speed atomic force microscopy (HS-AFM) has provided information about the polymerization growth, the dynamics and subunit turnover of ESCRT-III spirals on supported lipid bilayers on mica. Here, we use Polydimethylsiloxane (PDMS), a polymer whose elasticity ranges from 100kPa to 20MPa, as the substrate for supported lipid bilayers. After formation of a homogeneous lipid bilayer on PDMS, we supply ESCRT-III (Snf7) and observe and analyze the structural dynamics of ESCRT-III on such soft supports. Our novel data show that on the soft substrate the spirals reduce their inter-filament distance and concentrate into smaller disks. Eventually the inner ring undergoes a transition downwards deforming the bilayer and the substrate beneath the spiral, in analogy to the native function of ESCRT-III, providing direct proof of the 'loaded spiral model'

Substrate preparation
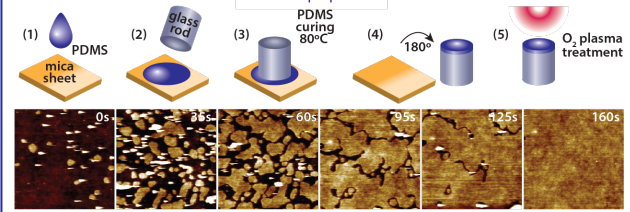
Inner ring transition
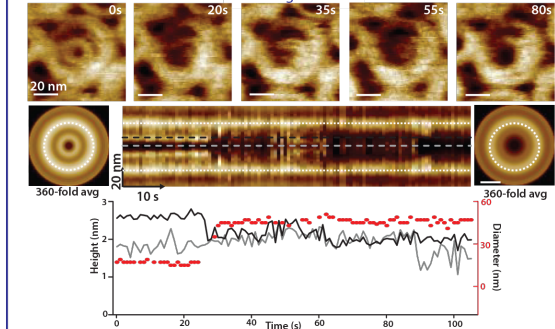
A transition of the inner ring of Snf7 spirals has been observed for the first time at molecular level by AFM. This transition can be assumed as a stochastic process triggered by Snf7 polymerization. The spiral releases the energy accumulated during polymerization. The deformation of the bilayer is of, at least, 1 nm in depth.

Snf 7 polymerization

HS-AFM images of Snf7 following polymerization allow us to observe the dynamics of the spirals for long periods of time on the same area.

The area covered by a single spiral, the radii of inner and outer ring and the interfilament distance are analyzed as a function of time.

On a soft substrate that mimics the elasticity of the cell membrane, Snf7 spirals concentrate in smaller disks reducing their area as well as their interfilament distance.

Substrates comparison

Clathrin-coated pits form from elastically loaded clathrin lattices

Grigory Tagiltsev[1,2] and Simon Scheuring[1,2]

introduction

Clathrin-mediated endocytosis (CME) is the major endocytosis pathway for the specific internalization of large compounds, growth factors and receptors, and in synaptic regulation. Formation of internalized vesicles from the flat plasma membrane is accompanied by maturation of cytoplasmic clathrin-coats that englobe the endocytic membrane area.

How clathrin-coats mature to accommodate the energetically costly topological changes and the mechanistic role of clathrin coats during CME are still largely unknown.

two proposed models

1. Constant radius of curvature

2. Constant clathrin coat area

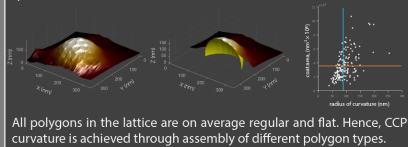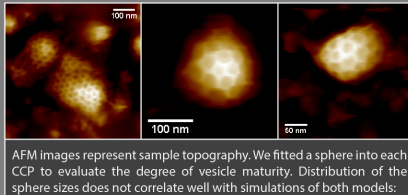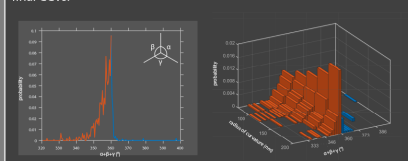? Real CCP maturation mechanism remains unknonw
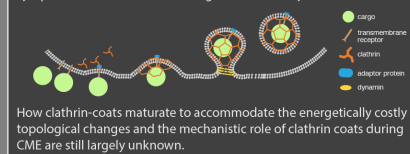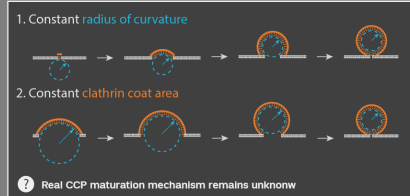
methods

High-speed atomic force microscopy (HS-AFM) permits observation of structural dynamics in biological processes. To study the CCP budding by HS-AFM, we use plasma membranes prepared by cell unroofing.

results

AFM images represent sample topography. We fitted a sphere into each CCP to evaluate the degree of vesicle maturity. Distribution of the sphere sizes does not correlate well with simulations of both models:
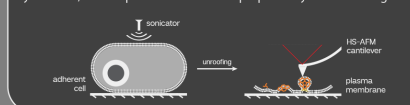
All polygons in the lattice are on average regular and flat. Hence, CCP curvature is achieved through assembly of different polygon types.
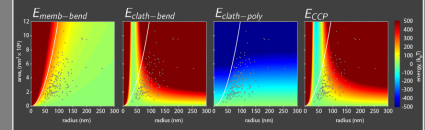
Sum of the three inter-arm angles of clathrin triskelia is a direct measure of local curvature. Clathrin in CCPs had several recurrent angular conformations, with inter-arm angle sums equal to various geometrically relevant closed polyhedra that architecturally resemble final CCVs.
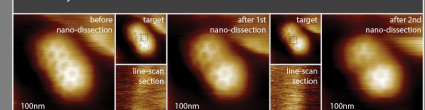
new model

$$E_{CCP} = \underbrace{\frac{A\kappa_{memb}}{2}\left(\frac{1}{R}\right)^2}_{E_{memb-bend}} + \underbrace{\frac{A\kappa_{memb}}{2}\left(\frac{1}{R} - \frac{1}{R_{clath}}\right)^2}_{E_{clath-bend}} - \underbrace{a\left(A - 0.015 \times 2\pi\sqrt{\frac{A^2}{R} - \frac{A^3}{(2\pi R)^2}}\right)}_{E_{clath-poly}}$$

CCP nano-dissecton:
Each nano-dissection releases spatial constraints maintained by the polymerized clathrin lattice, which upon nano-dissection are released, and the lattice adopted an energetically more favorable state due to its elastically loaded network action.

conclusion

- Previously proposed models of CCP maturation do not fully describe CCP maturation process.

- We propose a new model of CCP maturation based on clathrin behaving as a loaded spring.

affiliations

1 - Weill Cornell Medicine, Department of Physiology & Biophysics, 1300 York Avenue, 10065 New York, NY
2 - Weill Cornell Medicine, Department of Anesthesiology, 1300 York Avenue, 10065 New York, NY

Email:
sis2019@med.cornell.edu (Simon Scheuring)
grt2006@med.cornell.edu (Grigory Tagiltsev)

Follows us online:
http://bio-afm-lab.com
ScheuringLab @ScheuringLab

49

Determining the contribution of ryanodine receptors to action potential-driven calcium efflux from the endoplasmic reticulum in cortical neurons
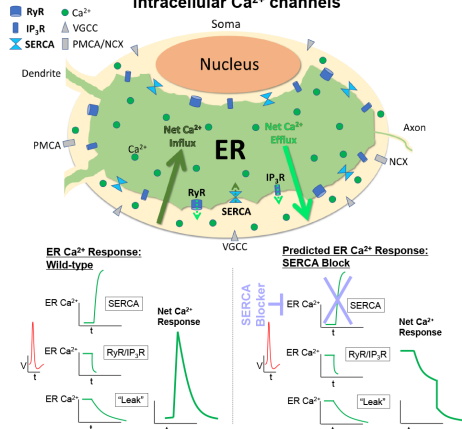
Weill Cornell Medicine
Anesthesiology

Daniel Cook[1], Ryan Farrell[2], Timothy Ryan[3]

Department of Anesthesiology[1] and Biochemistry,[3] Weill Cornell Medicine, New York, NY
Rockefeller University[2], New York, NY

Introduction: Calcium ions (Ca^{2+}) are critical to cellular physiology. Calcium in the cytosol is regulated, in part, by the endoplasmic reticulum (ER), which is the largest intracellular store of Ca^{2+} and has Ca^{2+} concentrations ~1000 times cytoplasmic levels.[1] In neurons of the central nervous system (CNS), the ER extends throughout the soma, dendrites, and axons, and the ER can tune pre- and post-synaptic function.[2,3] ER Ca^{2+} levels are determined by sarco(endo)plasmic reticulum ATPases (SERCAs), which pump Ca^{2+} into the ER, and ryanodine and IP_3 receptors (RyRs and IP_3Rs, respectively), that allow Ca^{2+} release from the ER into the cytosol, though other "leak" pathways may contribute to ER Ca^{2+} efflux.[1] The impact of RyRs on ER Ca^{2+} dynamics in neurons of the CNS is not well defined. Recently developed genetically-encoded, fluorescent calcium indicators targeted to the ER allow ER Ca^{2+} levels and fluxes to be precisely measured with microscopy in primary neuronal cultures from neonatal rats.[2]

Objective: Determine the contribution of RyRs to action-potential driven ER Ca^{2+} flux in cortical neurons.

ER Ca^{2+} levels set by competing influx and efflux through intracellular Ca^{2+} channels

Legend: RyR, IP_3R, SERCA, Ca^{2+}, VGCC, PMCA/NCX

Soma
Nucleus
Dendrite
Net Ca^{2+} Influx
Net Ca^{2+} Efflux
ER
PMCA
Ca^{2+}
Axon
NCX
RyR
IP_3R
SERCA
VGCC

ER Ca^{2+} Response: Wild-type
ER Ca^{2+} | SERCA | Net Ca^{2+} Response
ER Ca^{2+} | RyR/IP_3R
ER Ca^{2+} | "Leak"

Predicted ER Ca^{2+} Response: SERCA Block
SERCA Blocker
ER Ca^{2+} | SERCA | Net Ca^{2+} Response
ER Ca^{2+} | RyR/IP_3R
ER Ca^{2+} | "Leak"

Figure 1. *Top*: Schematic of ER Ca^{2+} levels in neuron of the CNS balanced by influx through SERCA and efflux from RyR, IP_3R, and a "leak" channel. *Bottom*: An action potential (AP, red trace) initiates competing ER Ca^{2+} pathways that sum to a net flux (*left*) from cytosol to ER. With SERCA blockade (*right*), we hypothesize observing AP-driven efflux.

References
1. Verkhratsky, A. Physiol. Rev. 85, 201–79 (2004).
2. de Juan-Sanz, J. et al. Neuron 93, 867–81 (2017).
3. 7. Segal, M., Korkotian, E. & Huntley, G. W. Front. Neuroanat. 8, 1–7 (2014).

Cytosolic and ER-targeted genetically-encoded Ca^{2+} indicators reveal intracellular Ca^{2+} dynamics

50 AP, 50 Hz
ER-GCaMP6-150-Halo
Cytosolic-jRCaMP1b
$\Delta F/F_0$ 0.75 0.50
10 s
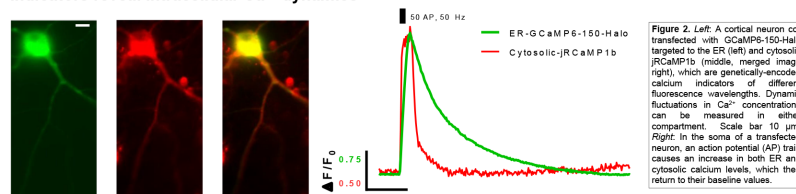
Figure 2. *Left*: A cortical neuron co-transfected with GCaMP6-150-Halo targeted to the ER (left) and cytosolic jRCaMP1b (middle, merged image right), which are genetically-encoded calcium indicators of different fluorescence wavelengths. Dynamic fluctuations in Ca^{2+} concentrations can be measured in either compartment. Scale bar 10 μm. *Right*: In the soma of a transfected neuron, an action potential (AP) train causes an increase in both ER and cytosolic calcium levels, which then return to their baseline values.

Pharmacologic inhibition of SERCA reveals AP-driven Ca^{2+} efflux from ER
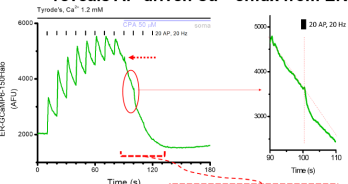

Figure 3. *Top*: A cortical neuron was stimulated with 20 action potentials (AP, 20 Hz) every 10 s while perfusing the SERCA inhibitor cyclopiazonic acid (CPA). After CPA onset, AP-driven influx is blocked (dashed arrow), revealing stimulation-driven efflux (ring). *Inset*: Acute change in slope of trace with a single AP train (corresponding to the ring). *Bottom*: 1st derivative analysis of the region highlighted by the bracket, with spikes representing acute changes in the slope due to AP-driven ER Ca^{2+} efflux. Ring corresponds to part of trace shown in inset above.

Inhibition of RyR prevents AP-stimulated Ca^{2+} efflux from ER

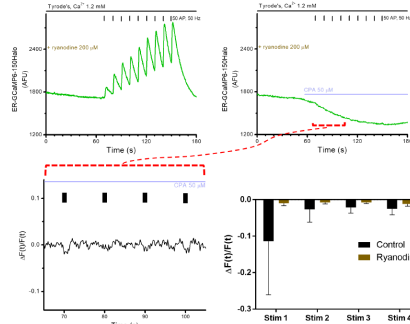
Control
Ryanodine
Stim 1 Stim 2 Stim 3 Stim 4

Figure 4. *Top left*: A cortical neuron was pre-treated for 1 h with 200 μM ryanodine, inhibiting RyRs. Stimulating with 50 action potentials (50 Hz) every 10 s caused a net increase in ER Ca^{2+}, with upward spikes for each AP train. Repeating this protocol after 1 min in CPA (*top right*) blocked ER Ca^{2+} entry. After RyR inhibition, acute AP-driven decreases in ER Ca^{2+} are abolished (compare to Figure 3). *Bottom left*: 1st derivative analysis of bracketed region from CPA trace does not show abrupt slope changes (compare to Figure 3). *Bottom right*: Average responses of peaks in 1st derivative spikes in control and ryanodine pre-treated neurons (control n = 3, ryanodine n = 6, mean ± SD).

Conclusions:

- ER-targeted GCaMPs in cortical neurons reveal changes in ER Ca^{2+} levels that are driven by cytosolic Ca^{2+} influx generated by APs.

- Blocking SERCA channels with CPA allows quantification of isolated AP-driven efflux.

- RyRs are primarily responsible for AP-driven Ca^{2+} efflux in the soma of cortical neurons, but a separate, AP-independent ER "leak" pathway also exists.

Clinical Research Studies

1. **Two dose neuraxial morphine for prevention of postdural puncture headache (NEMO for PDPH)**
   PI: *Jaime Aaronson, MD*
   Protocol #: 1509016603
   Multi- Institutional randomized, control trial to determine the efficacy of two doses of neuraxial (either epidural or intrathecal) preservative –free morphine (PFM) to prevent headache after ADP in patients. In collaboration with Columbia University Medical Center.

2. **ROTEM(R) sigma External Matrix Comparison Study: Venous versus Arterial Citrated Whole Blood Samples**
   PI: *Hugh Hemmings, MD, PhD*
   Protocol #: 1704018119
   The objective of this comparison study using matched venous and arterial citrated whole blood samples will be performed to evaluate the difference in test results for venous and arterial blood using assays currently available with the ROTEM sigma analyzer. Sponsored by Instrumentation Laboratory.

3. **A Post-Market, Multicenter, Prospective, Randomized, Crossover Clinical Trial Comparing 10 kHz Spinal Cord Stimulation (HF10 Therapy) Combined with Conventional Medical Management to Conventional Medical Management Alone in the Treatment of Chronic, Intractable, Neuropathic Limb Pain (the "Study")**
   PI: *Neel Mehta, MD*
   Protocol #: 1704018119
   The purpose of this post-market study is to document comparative safety, clinical effectiveness, and cost-effectiveness of the addition of 10 kHz Spinal Cord Stimulation (HF10 therapy) to Conventional Medical Management (CMM) compared with CMM alone in subjects with chronic, intractable, neuropathic lower limb pain due to diabetic neuropathy (Painful Diabetic Neuropathy or PDN). This study is a multi-center, prospective, randomized comparison of the two treatments. Sponsored by Nevro Company.

4. **PROtective ventilation with high versus low PEEP during one-lung ventilation for THORacic surgery - PROTHOR: A randomized control trial**
   PI: *Matthew Murrell, MD, PhD*
   Protocol #: 1701017890
   Multi-center, randomized controlled trial investigating the use of a higher or lower PEEP strategy in reducing postoperative pulmonary complications in patients undergoing thoracic surgery with one lung ventilation. In collaboration with Technische Universität Dresden.

5. **ConsCIOUS2: A Prospective Study of the Isolated Forearm Technique Commands, Long-term Sequalae and Electroencephalogram Correlates Following Laryngoscopy and Intubation in Patients 18-40 Years of Age**
   PI: *Kane Pyror, MD*
   Protocol #: 1706018306
   Multi-center center confirming and extending the results of ConSCIOUS1 with a primary aim of confirming that the incidence of Isolated Forearm Technique responsiveness is approximately 10% in 18-40 year-old patients. In collaboration with University of Wisconsin-Madison.

6. **Optimisation of Perioperative Cardiovascular Management to Improve Surgical Outcome II (OPTIMISE II) Trial**
PI: *Kane Pryor, MD*
Protocol #: 1804019164
An open, international, multi-center, randomized controlled trial of cardiac output-guided fluid therapy with low dose inotrope infusion compared to standard of care in subjects undergoing major elective gastrointestinal surgery. Sponsored by Queen Mary University of London.

7. **Mitral Apparatus Tissue Characterization for Prediction of Anesthesia-induced changes and mid-term success after surgical and percutaneous Mitral Valve Repair**
PI: *Lisa Q. Rong, MD*
Protocol #: 1801018920
This is a prospective study of 150 subjects with documented mitral regurgitation undergoing elective scheduled percutaneous or surgical mitral valve repair. The study will evaluate pre-procedural echo-cardiogram and cardiac magnetic resonance results, intraoperative echocardiogram results and 6 month post-operative echocardiogram results. It will test novel echo technologies to detect presence and extent of MI in the mitral apparatus as a strategy to aid intra-operative decision-making for patients undergoing MR repair. We aim to validate intra-operative echo derived LV strain as an index of mitral apparatus infarct burden. Sponsored by Foundation for Anesthesia Education and Research.

8. **Non-Invasive Monitoring of Brain Activity in Altered Conscious States**
PI: *Seyed A. Safavynia, MD, PhD*
Protocol #: 1801018908
This study will use functional near-infrared spectroscopy (fNIRS) and electroencephalography (EEG) to monitor brain activity in delirious and lucid states during recovery from general anesthesia. By analyzing hemodynamic and electrical activity within the brain, we will quantify differences in cerebral hemodynamics and cortical connectivity during episodes of PACU delirium. This study is sponsored by the Foundation for Anesthesia Education and Research and the Charles A. Frueauff Foundation.

9. **A Randomized Controlled Trial of Regional Versus General Anesthesia for Promoting Independence After Hip Fracture (REGAIN TRIAL)**
PI: *Tiffany Tedore, MD*
Protocol #: 1511016763
Multicenter, randomized clinical trial of two standard of care approaches to anesthesia (spinal vs. general) for hip fracture surgery. Will assess recovery of ambulation at approximately 60 days. In collaboration with the University of Pennsylvannia, sponsored by PCORI.

Chart, Observational, & Survey Studies

1. **Retrospective review of opioid, Tylenol and ibuprofen intake after Cesarean Delivery**
   PI: *Jaime Aaronson, MD*
   Protocol #: 1708018477
   A retrospective quality chart review evaluating the effects of a new initiative that has been implemented across all NYP locations. This will involve evaluating in-hospital pain medicine intake (opioids, acetaminophen, NSAIDs) to all women delivering by a cesarean section at Columbia University Medical Center, Allen Hospital, Weill Cornell and Lower Manhattan Hospitals. In collaboration with Columbia University Medical Center.

2. **Women Physicians Initiative Symposium**
   PI: *Ruth Gotian, EdD MS*
   Protocol #: 1907020515
   This retrospective chart review aims to assess the utility of pre-procedural MRI in evaluating gaps in ligamentum Flavum in planning for cervical epidural steroid injections. In collaboration with NewYork-Presbyterian Hospital and Columbia University Medical Center.

3. **International Nutrition Survey 2018**
   PI: *Natalia Ivascu, MD*
   Protocol #: 1905020062
   The purpose of the study is to evaluate current nutrition practices in the ICU setting, and use comparative information from a global variety of sites to develop strategies for improvement of nutrition practices. The study aims to evaluate and monitor nutrition performance by focusing on different groups of critically ill patients as part of an on-going improvement strategy to improve nutrition care and clinical outcomes. This study is in colaboration with Queen's University at Kingston.

4. **Utility of MRI in Assessing Gaps in Ligamentum Flavum in Planning for Cervical Epidural Steroid Injection**
   PI: *Jatin Joshi, MD*
   Protocol #: 1703018099
   This study will assess the utility of pre-procedural MRI in evaluating gaps in ligamentum flavum in planning for cervical epidural steroid injections. Our goal is to evaluate the rate of midline gaps in the ligamentum flavum in the lower cervical spine region that can be identified by MRI and compare to existing cadaveric data.

5. **Maternal Temperature Monitoring During Cesarean Delivery Using A Temperature Capturing Foley Catheter**
   PI: *Klaus Kjaer, MD, MBA*
   Protocol #: 1807019402
   This descriptive retrospective-observational study will assess the intraoperative core temperatures of parturients who had scheduled, elective Cesarean sections to identify thermal dysregulation due to use of neuraxial anesthesia.

6. **Rate Of General Anesthesia Use for Cesarean Delivery Among Anesthesiologists with and without Fellowship Training in Obstetric Anesthesia**
   PI: *Klaus Kjaer, MD, MBA*
   Protocol #: 1703018074
   Retrospective chart review to determine whether obstetric anesthesia fellowship-trained attending anesthesiologists are more or less likely to provide general anesthesia for non-routine cesarean deliveries compared to non-fellowship trained staff.

7. **Utility of repeat MRI imaging in lumbar radiculopathy**
   PI: *Neel Mehta, MD*
   Protocol #: 1808019549
   Our study would like to specifically assess how repeat MRI imaging affects the course of care for patients. We would like to determine whether significant changes are seen in patient's MRI when a clinician decides they warrant repeat imaging. We would also like to understand the reasons for ordering repeat imaging and whether this imaging leads to further interventions or surgeries.

8. **Evaluation of Patient Satisfaction Following Cholecystectomy**
   PI: *Kane Pryor, MD*
   Protocol #: 1705018203
   This is a prospective, interventional study to investigate the effects of musical and noise-cancelling intervention on patient satisfaction, quality of recovery, and self-reported pain after surgery. We hypothesize that if patients are provided with classical music via active phase-reversal noise-cancelling headphones, they will express greater satisfaction (short- and long-term), improved quality of recovery, and lower self-reported pain than those who receive no intervention or noise cancellation alone.

9. **Echocardiographic Predictors of Recurrent Aortic Valve Insufficiency After Valve Sparing Aortic Surgery**
   PI: *Lisa Q. Rong, MD*
   Protocol #: 1604017133
   Retrospective review study to identify potential echocardiographic predictors of recurrent aortic valve insufficiency in patients who have undergone valve sparing aortic root surgery.

10. **Characterization of the changes in aortic strain and aortic valve pathology in ascending aortic surgery**
    PI: *Lisa Q. Rong, MD*
    Protocol #: 1806019370
    This study aims to evaluate the changes in wall tension and aortic strain of the descending aorta after an ascending aortic graft is placed using Transesophageal Echocardiogram imaging.

11. **Anesthesia Related Factors Affecting Parental Satisfaction in Pediatric Ambulatory Surgery**
    PI: *Aarti Sharma, MD, MBBS*
    Protocol #: 1512016819
    Utilizing a survey questionnaire comprising 6 satisfaction questions and a comment section to gather information about a parents' satisfaction with the care provided for the child before, during, and after surgery.

12. **Intraoperative Measurement of Cardiac Output During Cardiac Surgery: Which TEE Method Is Best?**
    PI: *Christopher Tam, MD*
    Protocol #: 1612017772
    Comparing the cardiac output measurements between TEE and PAC thermodilution technique and assess intra- and inter-observer reproducibility for quantifying left ventricle stroke acquired by TEE. In collaboration with the University of Toronto.

13. **The Association between Obesity, Pain Severity, Pain Interference, and Opioid Consumption**
    PI: *Lisa Witkin, MD*
    Protocol #: 1701017853
    Analyzing data collected from a longitudinal observational cohort of chronic pain outpatients seen in WCM pain medicine clinic, studying the association of obesity as a risk factor for pain outcomes, as a predictor of opioid consumption, and as a predictor of high risk opioid use.

Registry Studies

1. **RELIEF: A Global Registry to Evaluate Long-Term Effectiveness of Neurostimulation Therapy for Pain**
   PI: *Shakil Ahmed, MD*
   Protocol #: 1309014281
   This study is a prospective, multi-center, global registry of Boston Scientific Corporation (BSC) neurostimulation systems for pain created to provide a broad evidence base to assess long-term clinical and economic outcomes of BSC neurostimulation systems in a large number of subjects representing real-world use patterns. Sponsored by Boston Scientific Corporation.

2. **Weill Cornell Center for Human Rights Registry**
   PI: *Gunisha Kaur, MD, MA*
   Protocol #: 1810019677
   This study aims to create a database for clients seeking services at the Weill Cornell Center of Human Rights (WCCHR).

3. **Pediatric Craniofacial Surgery Perioperative Registry (PCSPR)**
   PI: *Jennifer Lee, MD*
   Protocol #: 1504016130
   Multi-center registry to capture information relating to the perioperative course and management of children undergoing craniofacial reconstructive surgery. The aggregate multi-institutional data set will be used for benchmarking for national quality improvement efforts. In collaboration with the Children's Hospital of Philadelphia.

4. **Spinal Cord Stimulator Implant Registry**
   PI: *Neel Mehta, MD*
   Protocol #: 1811019714
   We propose the creation of a registry that looks to collect longitudinal data from the approx 300-400 patients pre- and post-implantation of SCS currently treated by the Pain Management clinic. We intend to present collect over the lifetime of the device and include factors like trends comparing efficacy against various diagnoses, opioid use and pain scores.

5. **Pediatric Difficult Intubation (PeDI) Registry - Improving Safety and Quality of Airway Management in Children with Difficult Airways**
   PI: *Jasmine Patel, MD*
   Protocol #: 1602016988
   Observational, multi-center study data collection to establish a registry that will allow participating institutions to assess the outcomes of care of children with Difficult Direct Laryngoscopy (DDL) and to facilitate comparison to the other institutions' difficult airway management practices and outcomes. In collaboration with the Children's Hospital of Philadelphia.

6. **Anesthesiology Education Research Registry**
   PI: *Kane Pryor, MD*
   Protocol #: 1403014915
   To design and establish a registry to assess the utility of various metrics in predicting anesthesiology resident performance outcomes.

7. **Perioperative Transesophageal Echocardiography Registry**
   PI: *Lisa Q. Rong, MD*
   Protocol #: 1708018484
   The goal of this study is to establish a retrospective and prospective pre-, intra-, and postoperative anesthesia echocardiography data registry for subjects who have received anesthesia services for cardiac surgery with intraoperative transesophageal echocardiography at New York-Presbyterian Hospital/Weill Cornell Medical College since 2010.

8. **Chronic Pain Registry**
   PI: *Lisa Witkin, MD*
   Protocol #: 1705018203
   To establish a retrospective chronic pain patient data registry for patients with chronic pain, and to use the patient data registry, Practice Based Evidence (PBE), and Clinical Practice Improvement (CPI) methodology to identify specific pain management interventions that are most effective for specific patient types with chronic pain.

9. **The Development and Implementation of a Collaborative Health Outcomes Information Registry for the Weill Cornell Multidisciplinary Spine Center**
   PI: *Lisa Witkin, MD*
   Protocol #: 1701017897
   This study aims to develop and implement a patient-reported outcomes data collection system for the Weill Cornell Center for Comprehensive Spine Care. Ideally, this will allow ongoing treatment to be determined by the patients' response and progress and can improve evidence-based medicine guidance of treatment. Sponsored by the Applebaum Foundation.

Global Health Studies

1. **Assessing PTSD in Refugee Trauma Survivors in a Developing Country Using a Validated Survey**
   PI: *Gunisha Kaur, MD, MA*
   Protocol #: 1711018772
   This study will screen the female survivors of the 1984 Sikh Massacre in the Widow Colony in Delhi, India for Post-Traumatic Stress Disorder (PTSD) and Major Depressive Disorder).

2. **The Implementation Of A Novel Pain-Screening Tool In The Diagnoses Of Pain Symptoms And Syndromes In Refugee Torture Survivors**
   PI: *Gunisha Kaur, MD, MA*
   Protocol #: 1608017472
   We are evaluating refugee torture survivors who are receiving services at the Weill Cornell Center for Human Rights. There are two research questions in this study: if the current standard of care results in the under or missed diagnosis of pain and pain syndromes, and if a validated pain screening tool can supplement the current standard protocol used in the assessments of survivors of torture. This investigation was funded by NIH grant KL2TR002385 of the Clinical and Translational Science Center at Weill Cornell Medicine.

3. **The New Generation Of Anesthesiologists: The Rise Of Global Consciousness Through Residency Education**
   PI: *Gunisha Kaur, MD, MA*
   Protocol #: 1512016839
   This study evaluates the impact of a global health experience on a physician's global awareness via survey method.

4. **A Novel Model Of Global Health Education in Anesthesiology**
   PI: *Gunisha Kaur, MD, MA*
   Protocol #: 1702017955
   This FAER funded project assesses the value of a digital, interactive, multimedia touch curriculum on anthropologically centered global heath with trainees. The study has resulted in the creation of an innovative textbook on global health for physicians treating foreign born patients both in the United States and abroad.

5. **Sexual Health Knowledge Survey: Comparing Female Refugees to the General Population**
   PI: *Sheida Tabaie, MD*
   Protocol #: 1806019368
   This study aims to investigate whether or not a sexual health knowledge deficit exists among female refugees and whether or not the implementation of a sexual health education curriculum designed specifically for female refugees will close this knowledge deficit. Funded by the Weill Cornell Medicine Clinical and Translational Science Center.

Education Studies

1. **Experiential Curriculum for Communication and Professionalism in Anesthesiology**
   PI: *June Chan, MD*
   Protocol #: 1807019387
   This study is a retrospective analysis of data collected during the course of established curricular activities mandated by the Weill Cornell Anesthesiology Education division to evaluate its trainees.

2. **Leveraging Effective Learning by Identifying Learning Styles**
   PI: *Ruth Gotian, EdD, MS*
   Protocol #: 1904020246
   This will be a prospective analysis of survey data that will be collected to evaluate a new learning intervention being implemented in the Department of Anesthesiology at WCM.

Center for Perioperative Outcomes Studies

1. **Multicenter Perioperative Outcomes Group (MPOG) and Anesthesiology Performance Improvement And Reporting Exchange (ASPIRE) Performance Site**
   PI: *Hugh C. Hemmings Jr., MD, PhD, FRCA*
   Protocol #: 120812817
   The Multicenter Perioperative Outcomes Group (MPOG) is a consortium of anesthesiology departments of academic medical centers with electronic perioperative information systems. The purpose of MPOG is to allow multi-institutional collaboration for the purpose of accelerating outcomes research and quality improvement in perioperative medicine.

2. **Analysis Of Pain-Related Hospital Consumer Assessment Of Healthcare Providers And Systems (Hcahps) Free Text Responses**
   PI: *Neel D. Mehta, MD*
   Protocol #: 1709018575
   A retrospective review linking key elements of the Electronic Health Record (EHR) to HCAHPS Survey data, specifically the pain-related free-text responses of adult patients who have completed the HCAHPS survey's free response section from April 2016-Dec 2017. We aim to develop a program that will translate survey responses into actionable suggestions to address shortcomings in pain treatment by linking to demographic, medication, and co-morbid variables.

3. **Validation Of Administrative Coding Of Accidental Dural Punctures In A Parturient Population**
   PI: *Kane Pryor, MD*
   Protocol #: 1905020208
   There is a lack of literature that assesses the validity of current administrative coding of anesthetic complications, including complications related to obstetric anesthesia. This retrospective study will validate the coding of one of the most common complications of obstetric anesthesia, the accidental dural puncture during epidural placement, in an administrative database.

4. **Data Registry**
   PI: *Zachary Turnbull, MD, MBA, MS*
   Protocol #: 1208012815
   The Research Data Repository establishes a retrospective and prospective pre-, intra-, and postoperative anesthesiology data registry for patients who have received anesthesia services at New York-Presbyterian Hospital/Weill Cornell Medical College since 2001.

5. **Examining Trends in Emergency and Non-Emergency American Society of Anesthesiologists (ASA) Status and Associations with Postoperative Outcomes and Mortality**
   PI: *Zachary Turnbull, MD, MBA, MS*
   Protocol #: 1802019001
   This study will identify the difference in mortality rate of American Society of Anesthesiologists Physical Status (ASA PS) 5 and 5E (Emergency) patients at 48 hours and 30 days following surgery, the distribution of patients across discharge locations, and the length of stay by ASA PS classification and procedure type in a large dataset.

6. **Outcomes Research Utilizing the HCUP State Inpatient Sample**
   PI: *Zachary Turnbull, MD, MBA, MS*
   Protocol #: 1308014181
   Outcomes research studies are performed using existing Health Cost and Utilization Project (HCUP) State Inpatient Databases (SID), an existing publicly available de-identified database. Projects are ongoing with multiple research questions being investigated by the CPO and collaborators.

7. **Outcomes Research Utilizing The Multicenter Perioperative Outcomes Group (MPOG) Database**
PI: *Zachary Turnbull, MD, MBA, MS*
Protocol #: 1812019849
Outcomes research studies are performed using data from the Multicenter Perioperative Outcomes Group (MPOG), a comprehensive perioperative patient registry that consists of more than 50 hospitals across 18 states and 2 countries. Projects are ongoing with multiple research questions being investigated by the CPO and collaborators.

8. **Perioperative Factors And Postoperative Acute Kidney Injury Outcomes**
PI: *Zachary Turnbull, MD, MBA, MS*
Protocol #: 1905020208
This study aims to identify profiles of perioperative factors, both intraoperative and in the immediate postoperative period, to better understand differences in the perioperative management of intra-abdominal surgery patients and its association with postoperative acute kidney injury (AKI). This study will in conducted in collaboration with Columbia University Irving Medical Center.

9. **Resident Care Logs: An Accurate Reflection of Training?**
PI: *Zachary Turnbull, MD, MBA, MS*
Protocol #: 1602016986
ACGME case log data is used in assessing residents' procedural competencies, specific case type experiences, and to help determine future resident operating room assignments. The aim of this study is to highlight the potential for inaccuracies in the ACGME self-reported data and to implement an automated email reminder system that generates required ACGME specific case information from our anesthesia information management systems (AIMS) to improve upon these inaccuracies and reduce case-logging burden.

Upcoming Studies

1. **Factors Affecting Post Procedure Immobilization in Retinoblastoma Patients Receiving Intra-arterial Chemotherapy**
   PI: *Yang Long, MD*
   Protocol #: 1906020385
   This retrospective chart review will determine if certain medications given intraoperatively can affect length of immobilization and prevent use of rescue medications postoperatively in pediatric patients receiving intra-arterial chemotherapy for the treatment of intraocular retinoblastoma.

2. **Long-Term Real-World Outcomes Study on Patients Implanted with a Neurostimulator**
   PI: *Neel Mehta, MD*
   Protocol #: 1908020621
   The REALITY study is a prospective, multi-center, open label investigation conducted to gain a broader understanding of how Abbott's neurostimulation systems are being used in the real-world setting. It will serve the dual purpose of collecting long-term safety and effectiveness of these devices, and obtaining information about the different patient populations who are using them. Sponsored by Abbott.

3. **The Effects of Truncal Blocks in Donor Nephrectomies**
   PI: *Tiffany Tedore, MD*
   Protocol #: 1907020411
   This study intends to create two groups for comparison of outcomes: those who have undergone a donor nephrectomy with a truncal block and those who have undergone a donor nephrectomy without.

4. **Self-Management of Chronic Pain Using PainDrainer**
   PI: *Neel Mehta, MD*
   Protocol #: 1904020168
   The proposed clinical investigation is a single-arm open concept trial (SAC) to evaluate if PainDrainer, a digital pain coach based on artificial intelligence (AI), will improve the self-management of chronic pain and increase quality of life. In collaboration with Lund University.

5. **Carotid Doppler Imaging Correlation with Pulmonary Artery Catheters As A Marker For Fluid Responsiveness**
   PI: *James Osorio, MD*
   Protocol #: Pending
   The objective of this study is to evaluate the use of carotid doppler imaging, specifically measuring carotid blood flow, corrected carotid flow time, and respiratory variation in peak carotid velocity and evaluate if these measures can be used as a reliable marker for fluid responsiveness when compared to the use of a Pulmonary Artery catheters in mechanically ventilated, postoperative cardiac surgery patients.

6. **A Phase 2 Randomized Double-Blind, Placebo-Controlled Study to Evaluate the Safety and Efficacy of a Single Intrathecal Preoperative Administration of Brivoligide Injection in Patients with a Pain Catastrophizing Scale Score ≥16 Undergoing Mastectomy with Immediate Tissue Expander or Implant Placement**
   PI: *Mohammed Piracha , MD*
   Protocol #: Pending
   This is a multi-center, randomized, double-blind, placebo-controlled study to evaluate the safety and efficacy of brivilogide injection adminstered intrathecally before surgery in patients with a Pain Catastrophizing Scale (PCS) score of greater than 16 undergoing mastectomy with immediate tissue expander or implant placement. Sponsored by Adynxx.

Recruitment Completed Studies

1. **Airway Challenges in Patients with Retinoblastoma Caused by Chromosome 13q Deletions**
   PI: *Casey Chai, MD*
   Protocol #: 1805019237
   Retrospective chart review that studied patients with retinoblastoma caused by chromosome 13q deletion. Patients with 13q deletion retinoblastoma often need frequent anesthetics for exams and interventions, so anesthesiologists should be cognizant of their potential risk of difficult intubation, which may be related to the degree of genetic deletion and craniofacial dysmorphism. In collaboration with Memorial Sloan Kettering Cancer Center.

2. **ROTEM Sigma Performance Evaluation- Method Comparison with Predicate Device and Reference Intervals**
   PI: *Hugh C. Hemmings Jr., MD, PhD, FRCA*
   Protocol #: 1406015207
   Performance evaluation of the new ROTEM sigma coagulation analyzer relative to the current ROTEM delta thromboelastometry system. Sponsored by Instrumentation Laboratory.

3. **PRotective Ventilation with Higher versus Lower PEEP during General Anesthesia for S urgery in OBESE Patients**
   PI: *Peter Goldstein, MD*
   Protocol #: 1701017891
   Multi-center, randomized control trial investigating the use of a higher or lower PEEP strategy in reducing postoperative pulmonary complications in obese patients undergoing surgery with general anesthesia. In collaboration with Technische Universität Dresden.

4. **Early vs Late Stroke after Cardiac Surgery: Variability in Location and Outcome**
   PI: *Natalia Ivascu, MD*
   Protocol #: 1504016129
   This is a retrospective chart review looking at cardiac surgery patients and the association between timing of stroke onset and anatomic location of CVA.

5. **Prospective, Randomized Study Of Multicolumn Implantable Lead Stimulation For Pre-dominant Low Back Pain (PROMISE)**
   PI: *Neel Mehta, MD*
   Protocol #: 1209013020
   Prospective, multi-center, randomized, open-label, parallel-group design to compare Medtronic neuro-stimulation systems to optimal medical management in treating patients with chronic pain.

6. **Spinal Cord Stimulator Education During Pain Fellowship: Unmet Training Needs and Factors that Impact Future Practice**
   PI: *Neel Mehta, M.D.*
   Protocol #: 1507016431
   Examining how current ACGME accredited pain fellowships are educating their fellows about spinal cord stimulators (SCS) in order to identify unmet training needs for teaching about SCS, assess SCS training practices in current and past fellows, and measure opinions about the role of industry in SCS training.

7. **Anesthesia Ready Time for Hemodialysis Patients Undergoing Cardiac Surgery**
   PI: *James Osorio, MD*
   Protocol #: 1701017927
   Retrospective chart review evaluating "anesthesia ready time." We hypothesize that line placement (i.e. central, arterial) in renal failure patients on hemodialysis is time consuming, and therefore the "anesthesia ready time" will be longer for hemodialysis patients having cardiac surgery relative to other critically-ill patients.

8. **The Effect of intravenous Anesthetics on Fear Learning and Memory**
   PI: *Kane Pyror, MD*
   Protocol #: 0710009434
   130 healthy adult volunteers were given a very low dose of an anesthetic drug intravenously. While receiving the drug, subjects performed a series of memory tests and a fear conditioning experiment set up like a very simple computer game. To create the fear response, subjects occasionally received a mildly uncomfortable shock to their arm. The subject is able to determine the highest level of shock that they will receive. This study was conducted to learn how the drugs affect the way people process fear and emotion. This knowledge might one day be used in the treatment of psychiatric disorders.

9. **The Influence Of Anesthetic Depth On Patient Outcome After Major Surgery (The BALANCED Anesthesia Study)**
   PI: *Kane Pryor, MD*
   Protocol #: 1405015113
   Prospective, randomized clinical trial of 'deep' versus 'light' anesthesia to examine whether anesthetic depth alters perioperative outcome.

10. **The Prevention of Delirium and Complications Associated with Surgical Treatments (PODCAST) Clinical Trial**
    PI: *Kane Pryor, MD*
    Protocol #: 1209013008
    This is a multi-institutional, randomized control study that tests whether a low dose of ketamine can prevent post-operative pain and delirium.

11. **Neuroimaging The Effect Of Intravenous Anesthetics On Amygdala-Dependent Memory Processes**
    PI: *Kane Pryor, MD*
    Protocol #: 0710008933
    An fMRI study to establish whether intravenous anesthetics cause a common change in amygdala and hippocampal function during memory processes, or whether the effects on these brain structures are dissociable.

12. **Restrictive versus Liberal Fluid Therapy in Major Abdominal Surgery 'RELIEF' Study**
    PI: *Kane Pryor, MD*
    Protocol #: 1405015112
    Multicenter, randomized clinical trial assigning subjects to "Restrictive" and "Liberal" IV fluid regimens. Fluid is regulated from the start of surgery until 24 hours post-op, after which disability-free survival is tracked for one year.

13. **Comparison of 2D and 3D Doppler-derived cardiac output to the pulmonary artery catheter**
    PI: *Lisa Qia Rong, MD*
    Protocol #: 1708018434
    This study aims to compare the determination of stroke volume (SV) and cardiac output (CO) by two dimensional (2D) and three dimensional (3D) methods with the gold standard of pulmonary artery (PA) catheter-derived SV and CO during cardiac surgery.

14. **Effects of Methylene Blue on Pulse Oximetry and Spinal NIRS in Thoracoabdominal Surgery**
    PI: *Lisa Q. Rong, MD*
    Protocol #: 1703018032
    Retrospective chart review of the effects of methylene blue on both pulse oximetry and spinal NIRS. This study will expand on the current literature describing the ability of dyes, such as methylene blue, to cause erroneous oxygen saturation readings

15. **The Effect Of Early Extubation On Post-Operative Outcomes In Patients Undergoing Transfemoral Aortic Valve Replacement**
PI: *Nikolaos Skubas, MD, FACC, FASE, DSc*
Protocol #: 1601016899
Retrospective analysis of patients who underwent a TAVR and NYP-WCMC after January 2015. The purpose is to determine the association between early extubation and length of stay in patients undergoing transcatheter aortic valve replacement for aortic stenosis.

16. **Dose-Response Relationships For Hemidiaphragmatic Paresis Following Ultrasound-Guided Supraclavicular Brachial Plexus Blockade**
PI: *Tiffany Tedore MD*
Protocol #: 1609017547
Clinical trial investigating the dose-response relationship between local anesthetic volume and ipsilateral hemidiaphragmatic paresis (HDP) in patients getting ultrasound guided supraclavicular brachial plexus block.

17. **The Utilization Of Mobile Phone Technology To Quantitatively Assess Functional Outcomes Of Chronic Pain Patients- A Feasibility Study**
PI: *Lisa Witkin, MD*
Protocol #: 1409010349
Assessing the feasibility and value of using smart phone applications to collect objective, quantitative functional data from patients under active treatment for chronic pain.